Role of Protein Kinase R in metabolic homeostasis.

A thesis submitted for the degree of

Doctor of Philosophy

By

Agnieszka Pindel

Supervisors:

Dr. Anthony Sadler

Prof. Bryan Williams

Centre for Cancer Research

Monash Institute of Medical Research

Faculty of Medicine, Nursing and Health Sciences

2013

MONASH INSTITUTE OF MEDICAL RESEARCH

MONASH University

TABLE OF CONTENTS

DECLARATION **6**

NOTICE I **7**

NOTICE II **7**

ACKNOWLEDGEMENTS **8**

PUBLICATIONS AND ATTENDED CONFERENCES **10**

SECTION I LIST OF PUBLICATIONS 10
SECTION II LIST OF ORAL PRESENTATIONS 10
SECTION III LIST OF POSTER PRESENTATIONS 11
SECTION IV LIST OF AWARDS 12

ABSTRACT **13**

ABBREVIATIONS **15**

CHAPTER 1 LITERATURE REVIEW **20**

1.1. METABOLIC DISEASE 21
1.2. PHYSIOLOGICAL CONTROL OF ENERGY HOMEOSTASIS 23
1.3. GLUCONEOGENESIS 24
1.4. METABOLIC ENERGY SYSTEMS 26
1.4.1. Tricarboxylic acid cycle *27*
1.4.2. Oxidative phosphorylation *27*
1.4.3. Fatty acid oxidation *28*
1.4.4. NAD^+ and NADH redox carriers *29*
1.4.5. Pentose phosphate pathway *30*
1.5. PI3K/AKT INSULIN SIGNALLING PATHWAY 31
1.6. AMPK AND MTOR SIGNALLING IN REGULATION OF METABOLIC HOMEOSTASIS 33
1.6.1. The role of AMPK in lipogenesis *34*
1.6.2. The role of AMPK in gluconeogenesis *36*
1.7. INFLAMMATION IN METABOLIC DISEASE 37
1.8. PROTEIN TRANSLATION IN ENERGY HOMEOSTASIS 39
1.8.1. The role of eIF2α kinases in the pathogenesis of the metabolic syndrome *41*
1.8.2. The role of PERK in the unfolded protein response *43*
1.8.3. The role of PKR in cell signalling responses *44*
1.9. CONCLUSION 46
1.10. REFERENCES 47

CHAPTER 2 METHODS **56**

2.1 ANIMAL HANDLING 58
2.1.1 Mice *58*
2.1.2 High fat diet and standard chow diet feeding *58*
2.1.3 Glucose tolerance, insulin tolerance and pyruvate tolerance tests *58*
2.1.4 Animal sedation, blood draw by cardiac puncture and organ collection *59*

2.1.5 Blood plasma analysis *59*
2.1.6 Dual energy x-ray scans (DEXA) *59*
2.1.7 Temperature and activity measurements *59*
2.1.8 Ex vivo explants *60*
2.1.9 Intraperitoneal leptin injection *60*
2.2 TISSUE CULTURE 60
2.2.1 Cell culture maintenance *60*
2.2.2 Freezing cells *61*
2.2.3 Viable cell count *61*
2.2.4 Primary spleen macrophage preparation *61*
2.2.5 Primary peritoneal macrophage preparation *62*
2.2.6 In vitro stimulation experiments *62*
2.3 MEASUREMENT OF OXYGEN CONSUMPTION 63
2.4 NAD/NADH QUANTIFICATION 63
2.5 RNA PREPARATION 64
2.5.1 RNA extraction from cells *64*
2.5.2 DNAse treatment of RNA *64*
2.5.3 First strand cDNA synthesis *65*
2.5.4 Quantitative Real time-PCR *65*
2.6 DNA PREPARATION 65
2.6.1 DNA purification *65*
2.6.2 Polymerase Chain Reaction (PCR) *66*
2.6.3 SDS page gel electrophoresis *66*
2.7 PROTEIN PREPARATION 67
2.7.1 Protein extraction from cells *67*
2.7.2 Protein extraction from tissues *67*
2.7.3 Protein concentration assay *67*
2.8 WESTERN BLOTTING 68
2.8.1 Western blot *68*
2.8.2 Western blot band quantification *68*
2.9 ENZYME LINKED IMMUNOSORBENT ASSAY (ELISA) 68
2.10 IMMUNOHISTOCHEMISTRY 70
2.10.1 Immunostaining for insulin *70*
2.10.2 Formalin tissue fixation and embedding. *70*
2.10.3 Oil-red-O staining *70*
2.10.4 Haematoxylin and eosin staining *70*
2.10.5 Quantification of adipocyte and islets of langerhans size. *71*
2.10 STATISTICAL ANALYSIS 71
2.11 SOLUTION RECIPES 71
2.12 REFERENCES 74

CHAPTER 3 THE ROLE OF PKR IN DIET INDUCED OBESITY AND CARDIOVASCULAR DISEASE 75
3.1 INTRODUCTION 76
3.2 RATIONALE 77
3.3 HYPOTHESIS, AIMS AND METHODS 78
3.4 RESULTS 79

ABLATION OF PKR INCREASES DIET INDUCED WEIGHT GAIN 79
3.4.1 PKR regulates weight gain, adipocyte size and adiposity in response to a high fat diet. 79
3.4.2 PKR does not modulate baseline thermogenesis in BAT or affect physical activity. 79
LOSS OF PKR PROMOTES DIABETES INDUCING EVENTS 80
3.4.3 PKR improves insulin sensitivity, hepatic glucose output and glucose tolerance. 80
3.4.4 Ablation of PKR reduces Langerhans islet size. 81
PKR ALTERS BLOOD LIPID COMPOSITION AND SUSCEPTIBILITY TO FATTY LIVER DISEASE 82
3.4.5 PKR alters plasma lipoprotein profiles. 82
3.4.6 PKR alters expression of DGAT2 required for triglyceride synthesis. 83
3.4.7 Characterisation of apoE:PKR knockout mice in response to high fat diet. 83
ROLE OF PKRs KINASE AND ADAPTOR FUNCTION IN WEIGHT GAIN AND GLUCOSE HOMEOSTASIS 85
3.4.8 K271R heterozygote and homozygote mice have differential responses to a high fat diet. 85
3.4.9 Lack of PKR kinase activity does not affect glucose homeostasis. 85
3.4.10 Lack of PKR kinase activity alters islet size. 86
3.4.11 Lack of PKR kinase activity does not affect blood plasma lipoprotein composition. 87

3.5 DISCUSSION 87

3.6 CONCLUSION 97

3.7 REFERENCES 98

CHAPTER 4 THE ROLE OF PKR IN ENERGY HOMEOSTASIS 101

4.1 INTRODUCTION 102

4.2 RATIONALE 105

4.3 HYPOTHESIS, AIMS AND METHODS 105

4.4 RESULTS 107

PKR REGULATES GLUCONEOGENESIS 107
4.4.1 PKR regulates expression of the gluconeogenic enzyme glucose-6-phosphatase. 107
4.4.2 PKR regulates the expression of glucose-6-phosphate dehydrogenase. 109
LACK OF PKR DISRUPTS MITOCHONDRIAL BIOENERGETICS 110
4.4.3 PKR deficiency suppresses mitochondrial proton leakage and increases ATP synthesis. 110
4.4.4 PKR does not affect leptin signalling. 113
LACK OF PKR IMPAIRS INSULIN SIGNALLING 113
4.4.5 Lack of functional PKR dampens the insulin response in 3T3 MEFs, by reducing expression of IRS2. 113
4.4.6 Lack of functional PKR suppresses p70S6K and enhances Akt phosphorylation. 114
4.4.7 PKR in mTOR signalling 115
4.4.8 Loss of PKR reduces expression of PP2A and enhances Akt phosphorylation. 116
4.4.9 PKR does not affect splicing of the UPR protein XBP1. 117
PKR REGULATES AMPK SIGNALLING IN A TISSUE SPECIFIC MANNER 117
4.4.10 PKR does not modulate AMPK signalling in response to high fat diet feeding. 117
4.4.11 PKR alters expression of SREBP1C. 118
4.4.12 Fasting increases phosphorylation of acetyl-CoA carboxylase in the liver of high fat diet fed mice lacking PKR. 119
PKR REGULATES STERILE INFLAMMATORY RESPONSES 119
4.4.13 PKR does not regulate circulating levels of cytokines in response to high fat diet. 119
4.4.14 IL-6 transignalling. 120

4.4.15 PKR regulates inflammasome mediated signalling. 120

4.5 DISCUSSION 122

4.6 CONCLUSION 131

4.7 REFERENCES 132

CHAPTER 5 DISCUSSION 137

5.1 GENERAL DISCUSSION 138

5.2 CONCLUSION 144

5.3 REFERENCES 145

APPENDICIES 142

APPENDIX I ACCEPTED MANUSCRIPT GENERATED FROM THIS THESIS. 142

APPENDIX II RESULTS FROM HONOURS THESIS. 143

APPENDIX III RESULTS FROM HONOURS THESIS. 144

APPENDIX IV WESTERN BLOT ANALYSIS OF AMPK ACTIVATION. 145

APPENDIX V WESTERN BLOT ANALYSIS OF INSULIN SIGNALLING *IN VITRO.* 146

APPENDIX VI WESTERN BLOT ANALYSIS OF INSULIN SIGNALLING *IN VITRO.* 147

APPENDIX VII GENOTYPING OF CELL LINES. 148

APPENDIX VIII *EX VIVO* TISSUE EXPLANTS RESULTS. 149

APPENDIX IX INFLAMMASOME ACTIVATION IN SMO CELL LINES. 150

APPENDIX X INFLAMMASOME ACTIVATION IN RAW CELL LINES. 151

APPENDIX XI INFLAMMASOME ACTIVATION IN RAW CELL LINES. 152

APPENDIX XII DIET COMPOSITION 153

DECLARATION

This thesis contains no material which has been accepted for the award of any other degree or diploma in any university or other institution, and to the best of my knowledge, contains no material previously published or written by another person, except where due reference is made in the text of the thesis. Where the work in the thesis is part of joint research or publication, the relative contributions of the respective persons are listed in the text.

Agnieszka Pindel

Centre for Cancer Research

Monash Institute of Medical Research

Faculty of Medicine, Nursing and Health Sciences

NOTICE I

NOTICE II

ACKNOWLEDGEMENTS

One of the pleasures of completing this journey is to remember the people who have helped and supported me along this long but fulfilling road. I take this opportunity to acknowledge them and extend my sincerest gratitude.

Foremost I would like to express my deepest appreciation to my supervisors Doctor Anthony Sadler and Professor Bryan Williams for Your endless support, valuable advice and encouragement throughout the duration of this thesis. You have not only provided me with the necessary foundation to complete my PhD but have encouraged me to think independently and have strongly influenced the way I approach science. I would especially like to thank Tony for continually sharing Your knowledge and enthusiasm, with Your guidance and encouragement I was able to overcome many difficulties, I am forever grateful.

Besides my supervisors I would like to thank other members of my laboratory group for making my time in the lab enjoyable and for your insightful comments and at times hard questions, which have all shaped the outcome of my thesis journey. I am particularly grateful to Dr. Howard Lim for allowing me to refer to his unpublished work in this thesis. I would also like to acknowledge the great help that Dr. Olivier Latchoumanin has been in helping me perform a number of western blots, his generous assistance is acknowledged throughout.

This thesis was seen through to completion with the help and support of numerous other people including Dr. Pablo Enriori from the Department of Physiology at Monash University. Pablo's friendly nature, expertise and enthusiasm were critical to the completion of a number key experiments. I also take this opportunity to sincerely thank Associate Professor Peter Tipping and Anh Cao from the Monash Medical Center for their valuable assistance in the preparation of the atherosclerosis project.

Last but not least I thank my family and friends for their unconditional support, constant interest and love at each turn of my PhD journey. I extend a heartfelt thanks to my friends Gemma, Verity, Larissa, Peeta and Candice for supporting me along this journey. I consider myself lucky to have friends like You by my side. I warmly thank my PhD "twin"

Lauren Kerr for being a kind and generous friend. You have been an amazing support, inspiration and motivation, there is no doubt in my mind that surviving I would not have been able to survive the PhD life without You. I sincerely thank another fellow PhD student, Alex Wilding. Your knowledge is vast and beyond any comprehension, I thank You for making this PhD enjoyable and particularly for all Your technical support and challenging discussions. Lastly, I extend my deepest respect to my mum Mariola for being the most unselfish and hard-working woman I know, my dad Roman for his endless encouragement and tremendous sacrifices and my sister Karolina for her continued patience and care. I also thank my wonderful grandparents Teresa and Władek for effortlessly dedicating themselves to our family, for this and much more, I am forever in their debt. It is to my family that I dedicate this thesis.

PUBLICATIONS AND ATTENDED CONFERENCES

Section I List of publications

Pindel A and Sadler A (2011). "The role of protein kinase R in the interferon response." J Interferon Cytokine Res 31(1): 59-70.

Lancaster G, Kowalski G, Sadler A, Nicholls H, Bruce C, Weir J, Winbanks C, Whitham M, **Pindel A**, Paul Gregorevic P, Meikle P, Williams B and Febbraio M (2012). "Deletion of the dsRNA-dependent protein kinase (PKR) prevents saturated fatty acid induced inflammation in vitro, but promotes obesity and insulin resistance in vivo." Cell Metabolism. – *Submission pending.*

Section II List of oral presentations

Part of the work in this thesis was presented as oral presentations at the following conferences:

2010, Chicago, ISICR conference

The role of PKR in obesity and related disease. Presenting author – Dr. A. Sadler

2010, Melbourne, Three minute thesis

The role of PKR in obesity and related disease. Presenting author - A. Pindel

2011, Melbourne, VIIN Young Investigator Symposium

Investigating a role for PKR in obesity related disease. Presenting author - A. Pindel

2011, Melbourne, MIMR Postgraduate Symposium

Role of Protein Kinase R in obesity related disease. Presenting author – A. Pindel

2012, Melbourne, ASMR student research symposium

Role of Protein Kinase R in obesity related disease. Presenting author – A. Pindel

2012, Germany, Heidelberg, Invited speaker at DKFZ

The role of Protein Kinase R in metabolic homeostasis. Presenting author – A. Pindel

2012, Germany, Bonn, Invited speaker at The Cologne Institute of Genetics

The role of Protein Kinase R in metabolic homeostasis. Presenting author – A. Pindel

2012, Melbourne, MIMR Postgraduate symposium

The role of Protein Kinase R in metabolic homeostasis. Presenting author – A. Pindel

2012, Melbourne, An interview with Robyn Williams for The Science Show, ABC Radio National

Link to online podcast "The proteins which regulate obesity":

http://www.abc.net.au/radionational/programs/scienceshow/the-proteins-which-regulate-obesity/4401700

Section III List of poster presentations

Part of the work in this thesis was presented as posters at the following conferences:

2011, Melbourne, Heart Foundation Conference

The role of PKR in obesity and related disease. Presenting author - A. Pindel

2011, Melbourne, The first frontiers in obesity and diabetes conference

The role of PKR in obesity and related disease. Presenting author - A. Pindel

2012, Germany EMBL Diabetes and obesity conference

The role of Protein Kinase R in metabolic homeostasis. Presenting author – A. Pindel

Section IV List of awards

2011 Awarded $300 by Life Technologies at the MIMR postgraduate student symposium.

2012 Awarded a Monash Research Graduate School student travel grant.

ABSTRACT

Obesity related conditions, predominantly cardiovascular disease and diabetes constitute the most significant burden to healthcare in much of the western world. The physiological response to excess nutrients influences the health consequence of obesity. Hence regulation of cellular processes that maintain energy homeostasis, such as protein translation, are critical to the pathogenesis of metabolic disease. The Protein Kinase R (PKR) participates in cell signalling and plays a key role in the maintenance of protein translation by regulating the activity of the eukaryotic initiation factor 2-alpha (eIF2α). We hypothesized that metabolic sensing via PKR and its substrate, eIF2α, would initiate a general stress response to high fat diets that then modulates obesity-related diseases. This study provides the first evidence supportive of a critical role for PKR in regulating metabolic and inflammatory responses to ameliorate diet-induced obesity and ensuing pathologies.

PKR ameliorates weight gain and subcutaneous fat mass deposition in response to a high fat diet. However, the detected decrease in locomotor activity and BAT temperature in mice ablated for PKR was found to not be statistically significant. Loss of PKR also perturbs major lipid signalling pathways, resulting in augmented expression of fatty acid synthase (FASN) and diacylglycerol transferase 2 (DGAT2), both of which induce triglyceride synthesis and likely contribute to adipose tissue expansion. Indeed, mice ablated for PKR are hyperlipidemic as reflected by increased serum concentration of triglycerides, decreased concentration of low-density lipoprotein (LDL) and an unfavourable ration of high to low density lipoprotein (HDL/LDL). The consequence of this altered lipid metabolism is explored by measuring the effect of PKR deficiency on obesity associated cardiovascular disease in the apolipoprotein E (apoE) deficient mouse as a model for atherosclerosis. Ablating PKR from mice also deficient in apoE exacerbates diet-induced atherosclerosis, confirming that PKR plays a key role in disease development.

We also show that PKR maintains pancreatic islet size and normal glucose homeostasis. Ablation of PKR increases expression of the gluconeogenic enzyme glucose-6-phosphatase (G6pase) in the liver accounting for increased hepatic glucose production and glucose intolerance. We also establish that PKR deficiency *in vitro* suppresses expression of the insulin receptor substrate 2 (IRS2) and consequently disrupts insulin signalling by

reducing phosphorylation of p70S6K. In contrast to a recent report by Nakamura et al, that PKR promotes diet-induced obesity by increasing inflammation and suppressing insulin signalling by phosphorylation of IRS1, we see no PKR-dependent regulation of classic inflammatory cytokines IL-6 and TNF-α. Instead, in the absence of PKR heightens secretion of IL-1β from the pancreas, which has previously been reported to associate with pancreatic islet cell damage and disturbed glucose homeostasis. The mechanism likely to explain this effect is PKR-mediated inflammasome activation; however further research is required to confirm this mode of action.

Collectively these findings demonstrate that PKR is protective against diet-induced weight gain and the pathogenesis of metabolic disease. These results fit in with the principle function of PKR to relieve stress by inducing the integrated stress response.

ABBREVIATIONS

α-MSH	α-melanocyte stimulating hormone
βL	β-Lapachone
ACC	Acetyl-CoA carboxylase
AgRP	Agouti related peptide
Akt	Protein kinase B
ALP	Alkaline phosphatase
ALT	Alanine transaminase
AMP	Adenosine monophosphate
AMPK	AMP-activated protein kinase
ApoE	Apolipoprotein E
ASC	Apoptosis associated speck like protein containing a CARD domain
ATF	Activating transcription factor
ATGL	Adipose triglyceride lipase
ATP	Adenosine 5'triphosphate
AUC	Area under curve
BAT	Brown adipose tissue
cAMP	Cyclic AMP
CAMKK	Ca^{2+}/calmodulin-dependent protein kinase kinase
CART	Cocaine and amphetamine-regulated transcript
C/EBP	CCAAT/-Enhancer Binding Protein
CHD	Coronary heart disease
CHOP	CCAAT/-enhancer-binding protein homologous protein
CHORE	Carbohydrate responsive element
COX	Cytochrome C oxidase
CPT1	Carnitine palmitoyltransferase 1
CRE	cAMP response element
CREB	cAMP response element binding protein
CRP	C-reactive protein

CRTC2	CREB regulated transcription co-activator 2
CVD	Cardiovascular disease
DG	Diacylglycerol
DGAT2	Diacylglycerol transferase
DHAP	Dihydroxyacetone phosphate
DIO	Diet induced obesity
eIF2α	Eukaryotic initiation factor 2-alpha
eIF4E	Eukaryotic translation initiation factor 4E
ER	Endoplasmic reticulum
ETC	Electron transport chain
FAD	Flavin adenine nucleotide
FAO	Fatty acid oxidation
FBpase	Fructose-bisphosphatase
FFA	Free fatty acids
FOXO1	Forkhead box protein O1
G6pase	Glucose 6-phosphatase
G6PD	Glucose 6-phosphate dehydrogenase
GCN2	General control nonrepressed 2
GDH	Glutamate dehydrogenase
GLAP	Glyceraldehyde phosphate
GRU	Glucocorticoid regulatory unit
GSKβ	Glycogen synthase kinase 3-beta
GTT	Glucose tolerance test
H&E	Hematoxylin and eosin
HDL	High density lipoprotein
HFD	High fat diet
HRI	Heme regulated inhibitor
ICAM	Intracellular adhesion molecule
IFN	Interferon
IκB	Inhibitor of kappa B

IKKε	I kappaB kinase epsilon
IL	Interleukin
IL-1β	Interleukin 1-beta
IR	Insulin receptor
IRE	Insulin response element
IRS	Insulin receptor substrate
ITT	Insulin tolerance test
JAK	Janus kinase
JNK	C-Jun kinase
LDH	Lactate dehydrogenase
LDL	Low density lipoprotein
LDL-R	Low density lipoprotein receptor
LepR	Leptin receptor
LKB1	Liver kinase B1
L-PK	Liver pyruvate kinase
MCAD	Medium chain acyl co-A dehydrogenase
MEF	Mouse embryonic fibroblasts
MMP	Matrix metalloproteinase
MO25	Mouse protein 25
mTOR	Mammalian target of rapamycin
MTT	Microsomal triglyceride transfer protein
NAD	Nicotinamide adenine dinucleotide
NAFLD	Non-alcoholic fatty liver disease
NAD	Nicotinamide adenine dinucleotide
NF-κB	Nuclear factor-kappa B
NLRP	Nucleotide-binding oligomerization domain, Leucine rich Repeat and Pyrin domain containing
NPY	Neuropeptide Y
NR	Nicotinamide riboside
NRF1	Nuclear respiratory factor 1
NQ1	NADH:quinone oxidoreductase 1

oxLDL	Oxidised low density lipoprotein
OXPHOS	Oxidative phosphorylation
PC	Pyruvate carboxylase
PDC	Pyruvate dehydrogenase complex
PDK4	Pyruvate dehydrogenase kinase 4
PEP	Phosphoenol pyruvate
PEPCK	Phosphoenol pyruvate carboxykinase
PERK	PKR-like ER localized kinase
PFK	Phosphofructokinase
PGC1α	Peroxisome proliferator-activated receptor gamma co-activator 1α
PI3K	Phosphoinositide 3-kinase
PIP_2	Phosphatidylinositol 4,5-bisphosphate
PIP_3	Phosphatidylinositol 3,4,5-triphosphate
PKR	Protein Kinase R
PKR null	Protein Kinase R deficient
POMC	Pro-opiomelanocortin
PP2A	Protein phosphatase 2 A
PP2C	Protein phosphatase 2 C
PPARγ	Peroxisome proliferator-activated receptor gamma
PPP	Pentose phosphate pathway
PRAS40	Proline rich Akt substrate 40
PTEN	Phosphatase and tensin homolog
PTT	Pyruvate tolerance test
RBM	RNA-binding domain
RHEB	Ras homologue enriched in brain
ROS	Reactive oxygen species
SIRT1	Sirtuin1
SMC	Smooth muscle cells
SMØ	Spleen macrophage
SOCS3	Suppressor of cytokine signalling 3

SREBP1C	Sterol-regulatory element binding protein 1C
STAT3	Signal transducer and activator of transcription 3
STRAD	STE-related adaptor protein
TG	Triglyceride
TCA	Tricarboxylic acid cycle
TEM	Transmission electron microscopy
TLR	Toll like receptor
TNFα	Tumour necrosis factor alpha
TSC	Tuberous sclerosis complex
UCP	Uncoupling protein 1
UPR	Unfolded protein response
XBP	X-box binding protein
WAT	White adipose tissue
WB	Western blot
WRS	Wolcott Rallison syndrome
WT	Wild type

A

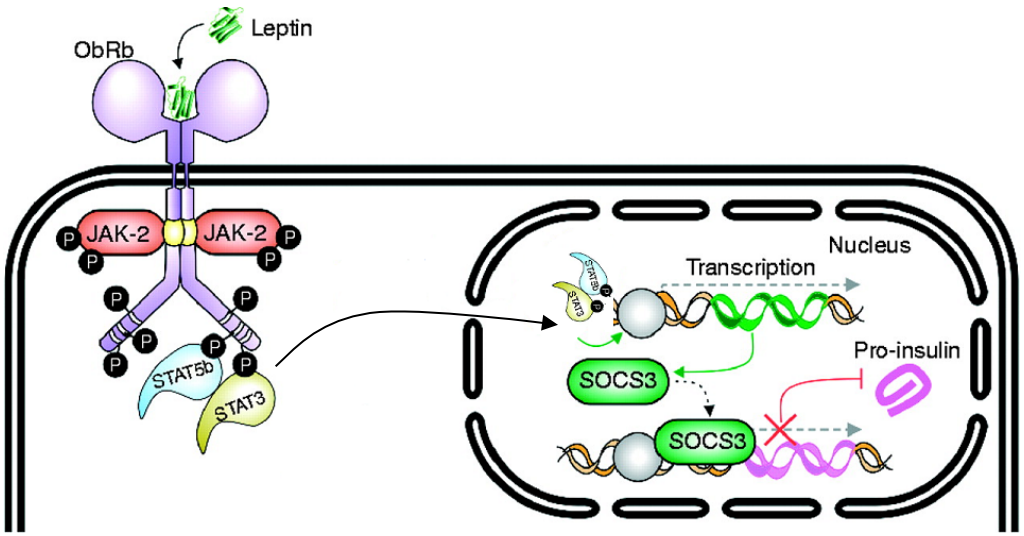
Leptin
ObRb
JAK-2
JAK-2
P
STAT5b
STAT3
Nucleus
Transcription
Pro-insulin
SOCS3
SOCS3

B

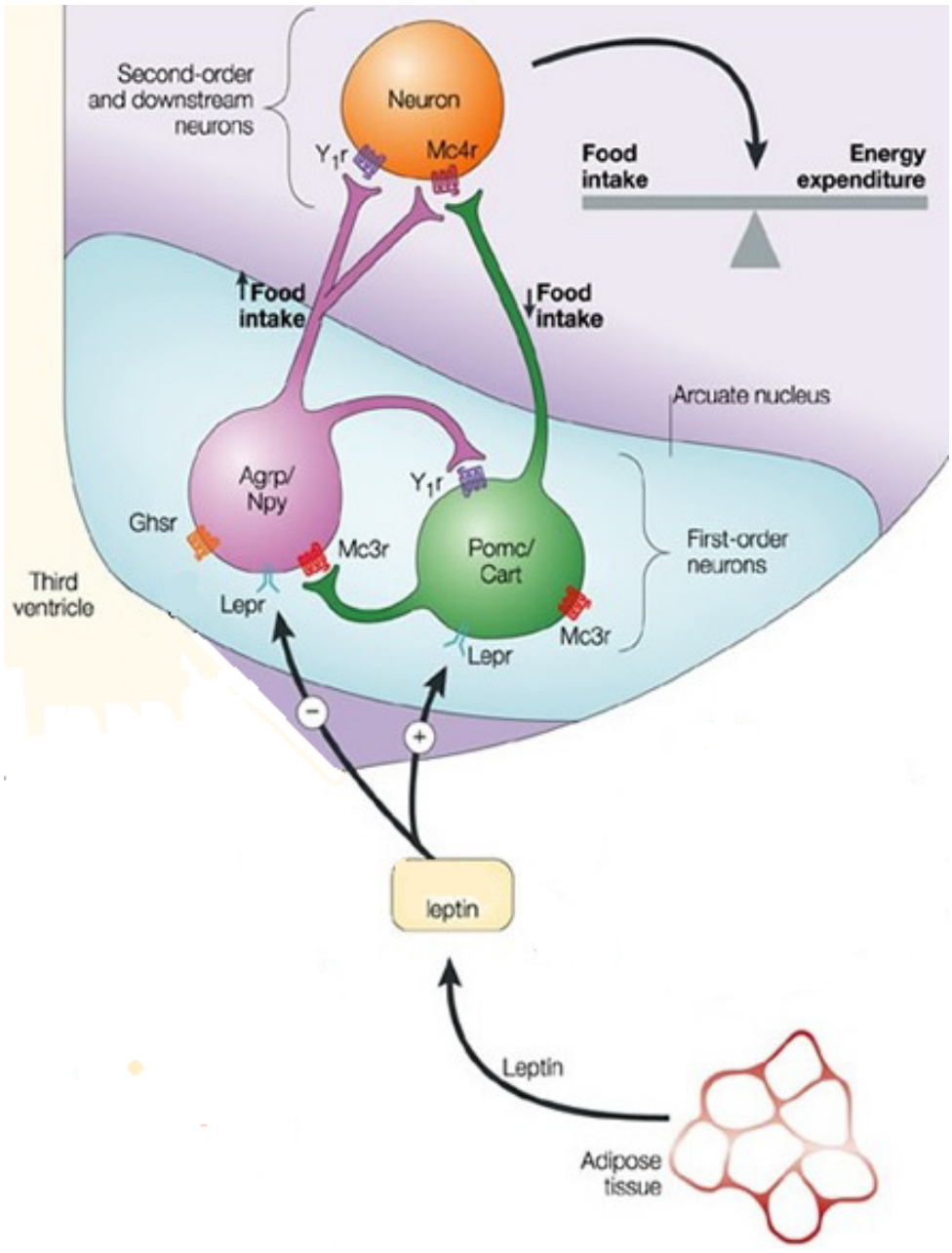
Second-order and downstream neurons
Neuron
Y1r
Mc4r
Food intake
Energy expenditure
↑Food intake
↓Food intake
Arcuate nucleus
Agrp/ Npy
Ghsr
Mc3r
Lepr
Third ventricle
Y1r
Pomc/ Cart
First-order neurons
Mc3r
Lepr
leptin
Leptin
Adipose tissue

Figure 1A. Leptin JAK/STAT3 signaling cascade.

The major actions of leptin are mediated by the JAK2/STAT3 signalling pathway in the arcuate nucleus of the hypothalamus. Leptin binds to the leptin receptor mediating its homodimerization and interaction with JAK kinases. JAK2 is consequently autophosphorylated and recruits STAT proteins to the membrane. JAK mediates STAT3 phosphorylation and dimerization which allows it to disassociate from the leptin receptor complex and translocate to the nucleus to induce gene transcription. One of the best characterised target genes for STAT3 is SOCS3. Figure adapted from Marroqui, Gonzalez et al. 2012.

Figure 1B. Leptin signalling in the hypothalamus.

Leptin is synthesised by white adipose tissue and binds to AgRP/NPY and POMC/CART neurons that express the leptin receptor (LepR). Leptin binding to the AgRP/NPY neurons inhibits the release of orexigenic signals and suppresses appetite. Whereas binding of leptin to the POMC/CART neurons releases the anorexigenic signal α-MSH which promotes food intake. Figure adapted from Barsh and Schwartz 2002.

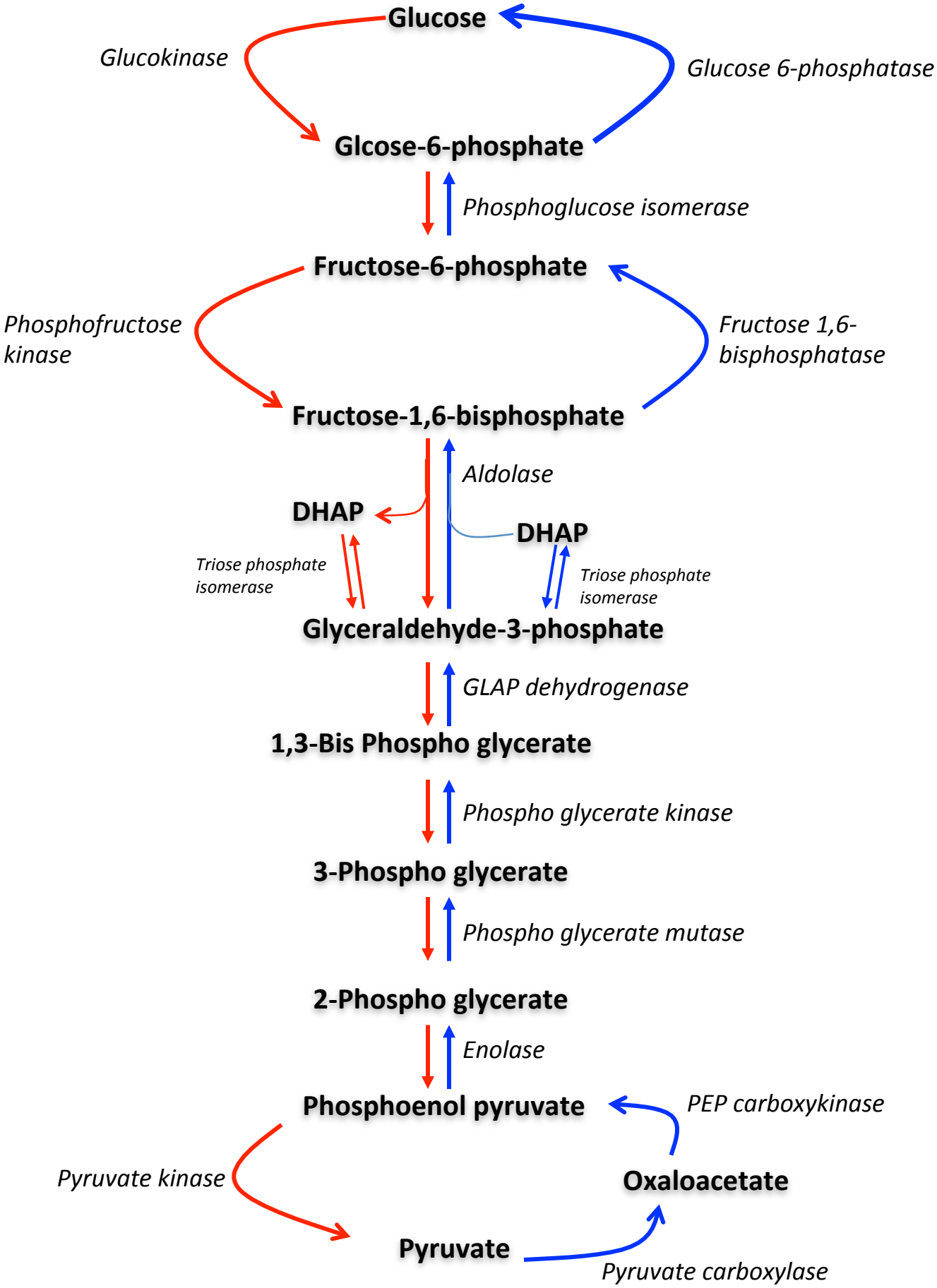
Glucose
Glucokinase
Glucose 6-phosphatase
Glcose-6-phosphate
Phosphoglucose isomerase
Fructose-6-phosphate
Phosphofructose kinase
Fructose 1,6-bisphosphatase
Fructose-1,6-bisphosphate
Aldolase
DHAP
DHAP
Triose phosphate isomerase
Triose phosphate isomerase
Glyceraldehyde-3-phosphate
GLAP dehydrogenase
1,3-Bis Phospho glycerate
Phospho glycerate kinase
3-Phospho glycerate
Phospho glycerate mutase
2-Phospho glycerate
Enolase
Phosphoenol pyruvate
PEP carboxykinase
Pyruvate kinase
Oxaloacetate
Pyruvate
Pyruvate carboxylase

Figure 2. Gluconeogenesis.

Gluconeogenesis is a metabolic pathway that mediates the conversion of pyruvate into glucose. The first committed step of gluconeogenesis is the PC mediated carboxylation of pyruvate to oxaloacetate in the mitochondria. The following six reactions that lead to the production of fructose-1-6-bisphosphate are reverse of the reactions involved in glycolysis. The final stage of gluconeogenesis is different to glycolysis because different enzymes are involved. In glycolysis fructose-1,6-bisphosphatase catalyzes the carboxylation of fructose-1,6-bisphosphate to fructose-6-phosphate which is in turn converted to glucose-6-phosphate by phosphoisomerase. The final step entails glucose-6-phosphatase mediated dephosphorylation of glucose-6-phosphate to create free glucose. Whereas the first step of the glycolytic pathway is facilitated by glucokinase which phosphorylates glucose to produce glucose-6-phosphate. Glucose-6-phosphate is then converted to fructose-6-phosphate by the phosphoglucose isomerase. Phosphofructokinase (PFK1) catalyzes the rate limiting step of glycolysis and phosphorylates fructose-6-phosphate to produce fructose 1,6 bisphosphate.

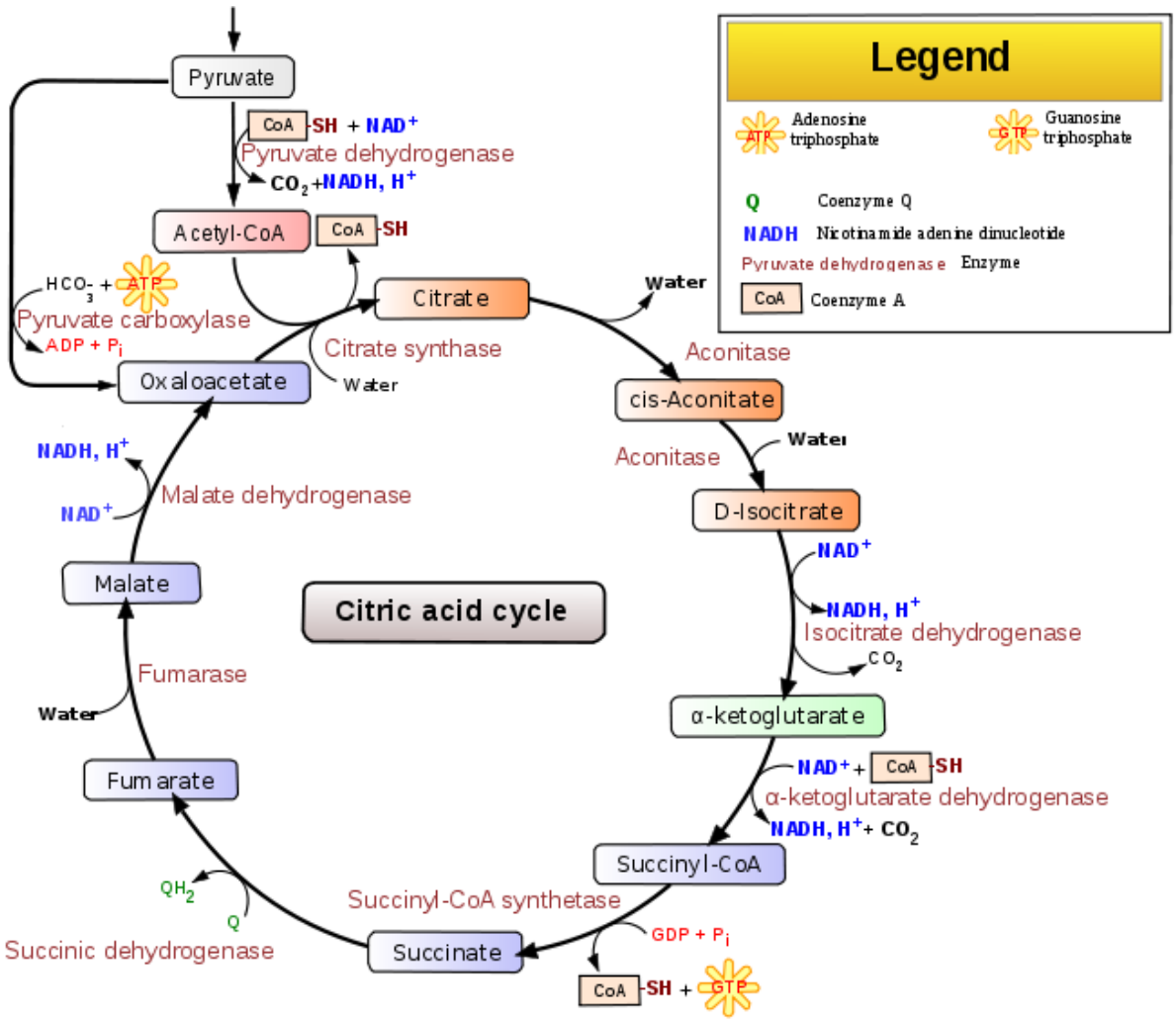

Figure 3. The tricarboxylic acid cycle.

The TCA cycle occurs in the mitochondria and is a key component of aerobic respiration because it produces essential intermediates for OXPHOS. The initial step of the TCA cycle requires pyruvate to be decarboxylated by the pyruvate dehydrogenase complex (PDC) to form acetyl-coA which feeds into the TCA cycle and is condensed by citrate synthase to form citrate. The next eight reactions are catalysed as shown. Oxidation of two pyruvate molecules produces 4 CO_2, 2 ATP, 6 NADH and 2$FADH_2$. Figure adapted from Wikipedia 2008.

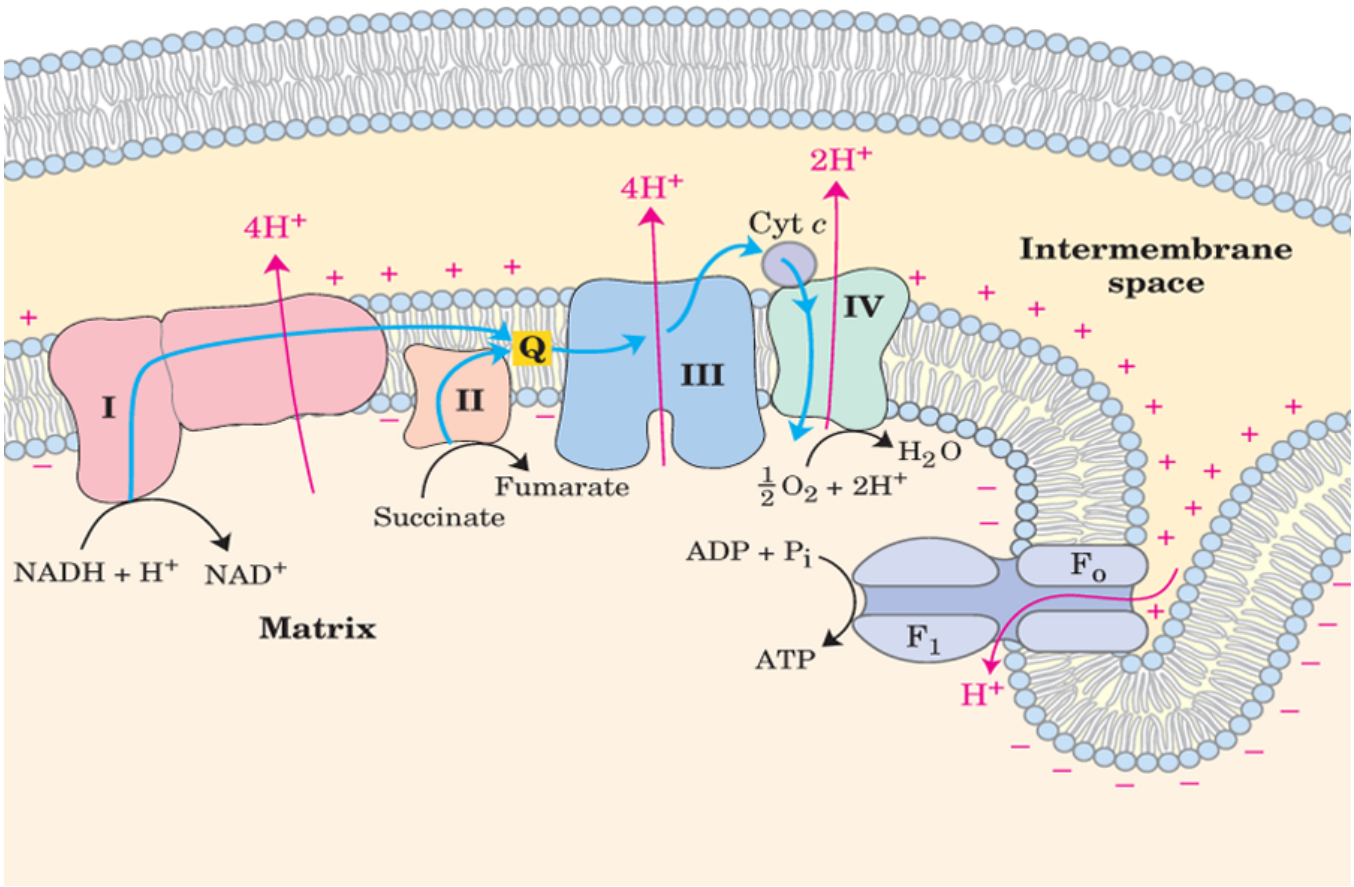
4H+
4H+
2H+
Cyt c
Intermembrane space
I
II
Q
III
IV
Succinate
Fumarate
½ O2 + 2H+
H2O
NADH + H+
NAD+
Matrix
ADP + Pi
ATP
Fo
F1
H+

Figure 4. Oxidative phosphorylation and the electron transport chain.

The electron transport chain is located in the inner mitochondrial membrane. It consists of four membrane embedded enzyme complexes that shuttle electrons to create an electrochemical gradient that is used by ATP synthase to create ATP. The coenzymes NADH and FADH2, produced by glycolysis and the TCA cycle, are entry points for OXPHOS. NADH is oxidized to NAD by NADH dehydrogenase, which concurrently transfers 2 electrons to coenzyme Q and pumps 4 hydrogen ions across the inner membrane. Complex II consisting of succinate dehydrogenase, receives free electrons from FADH2 and transfers them to coenzyme Q without acting as a proton pump. Cytochrome C reductase (complex III) accepts electrons from coenzyme Q produced by complex I and II and transfers them to cytochrome C while pumping 4 hydrogen ions across the membrane. Cytochrome C transfers electrons from complex III to the final complex, cytochrome c oxidase which transfers 4 electrons to O_2 to form H_2O.

Reference http://inoxx.net/?tag=electron-transport-chain

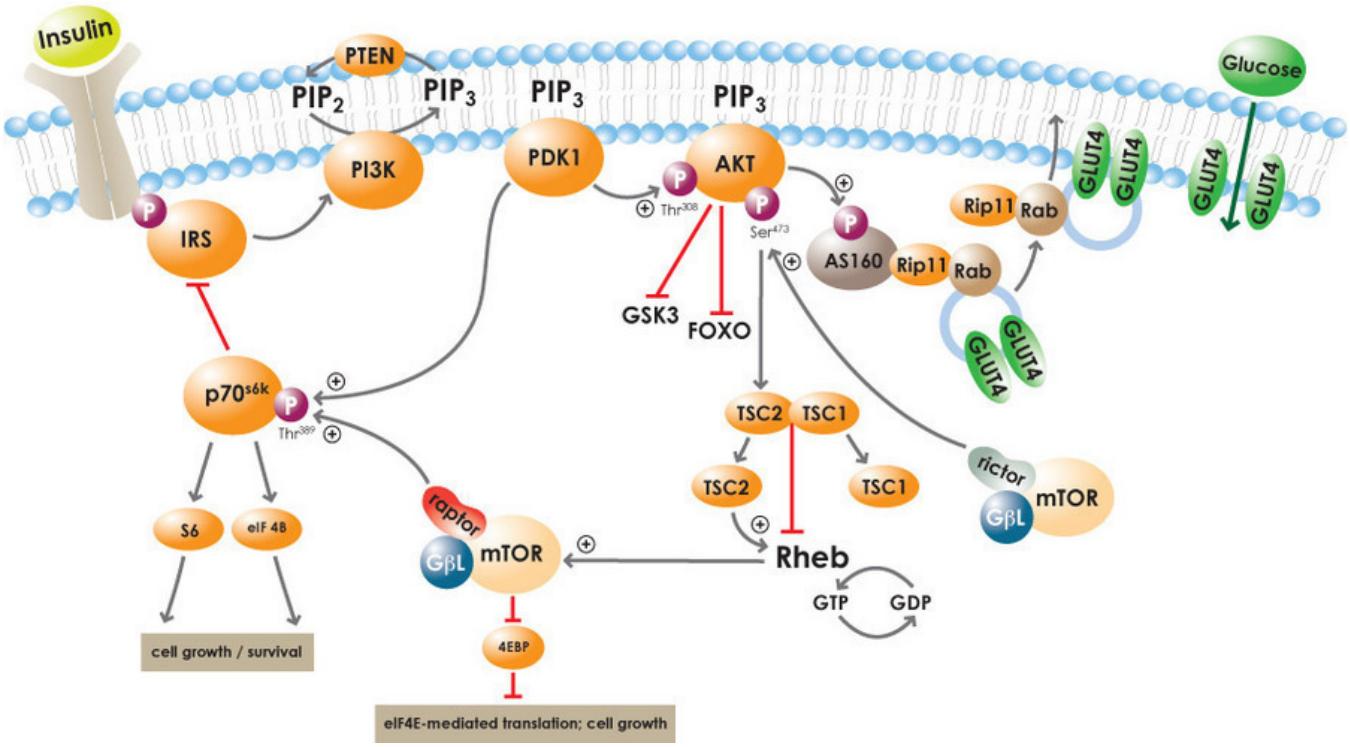
Insulin
PTEN
PIP2
PIP3
PIP3
PIP3
PI3K
PDK1
AKT
IRS
Thr308
Ser473
Glucose
GLUT4
GLUT4
GLUT4
GLUT4
Rip11
Rab
AS160
Rip11
Rab
GLUT4
GLUT4
GSK3
FOXO
p70s6k
Thr389
TSC2
TSC1
TSC2
TSC1
rictor
mTOR
GβL
raptor
mTOR
GβL
Rheb
GTP
GDP
S6
eIF 4B
4EBP
cell growth / survival
eIF4E-mediated translation; cell growth

Figure 5. PI3K/Akt signalling

Insulin binds to the membrane embedded tyrosine kinase insulin receptor (IR) causing its autophosphorylation and tyrosine phosphorylation of insulin receptor substrates (IRS). Tyrosine phosphorylated IRS binds to the regulatory subunit p85, of class I phosphoinositide 3 kinase (PI3K), which in turn phosphorylates the 3'hydroxyl group of membrane bound phosphatidylinositol 4,5-biphosphate to produce phosphatidylinositol 3,4,5-triphosphate (PIP_3) (Taha and Klip 1999). Serine phosphorylation of IRS and dephosphorylation by protein tyrosine phosphatase 1 (PTP1) inhibits insulin signalling. PIP_3 then recruits pleckstrin homology (PH) domain containing molecules such as phoinositide-dependent protein kinase (PDK1) and Akt to the plasma membrane. Binding of PIP3 to Akt releases its catalytic domain allowing it to be phosphorylated by PDK1 on threonine residue 308 and serine 473 by PDK2 (Alessi and Cohen 1998; Yang, Tschopp et al. 2004). Activated Akt inhibits its major downstream targets GSK3β, FOXO1, PRAS 40 (Manning and Cantley 2007). Akt enhances the activity of mTOR by preventing formation of the Gtpase activating protein TSC1/TSC2 and allowing Rheb mediated activation of mTORC1. In turn, mTORC1 phosphorylates p70S6K. Enhancing protein translation and attenuating insulin signalling in a negative feedback loop. p70S6K phosphorylates IRS on serine residue 307 which in turn downregulates expression of IRS1 and suppresses Akt mediated translocation of GLUT4 to the cell membrane and prevents glucose uptake. PTEN provides negative feedback to the PI3K/Akt pathway by converting PIP_3 to PIP_2, this prevents recruitment of PDK and Akt to the plasma membrane. Figure adapted from May 2012.

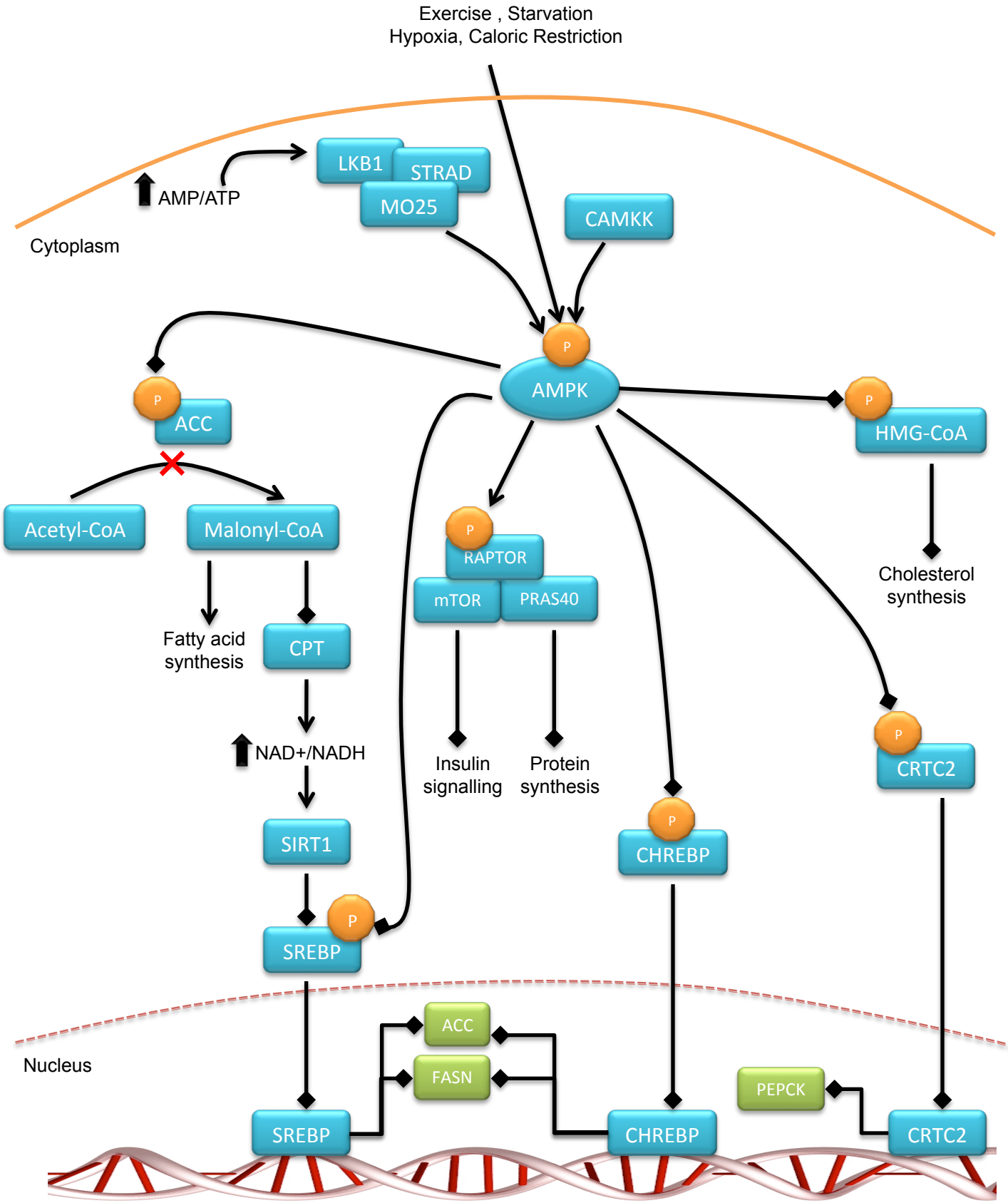
Exercise , Starvation
Hypoxia, Caloric Restriction
AMP/ATP
LKB1
STRAD
MO25
CAMKK
Cytoplasm
P
AMPK
P
ACC
P
HMG-CoA
Acetyl-CoA
Malonyl-CoA
Cholesterol
synthesis
P
RAPTOR
mTOR
PRAS40
Fatty acid
synthesis
CPT
Insulin
signalling
Protein
synthesis
P
CRTC2
NAD+/NADH
P
CHREBP
SIRT1
P
SREBP
Nucleus
ACC
FASN
PEPCK
SREBP
CHREBP
CRTC2

Figure 6. AMPK signalling.

AMPK is activated by metabolic stress signals that increase cellular concentration of AMP. These signals include low glucose levels, starvation, ischemia, hypoxia and physical exercise. Binding of AMP to AMPK exposes its phosphorylation sites allowing it to be phosphorylated by two main upstream kinases CAMKK and the LKB1 complex. Phosphorylation of AMPK inhibits the activity of its main downstream target acetyl co-A carboxylase (ACC). Inactive ACC cannot facilitate the production of malonyl-CoA thereby inhibiting fatty acid synthesis. Abundance of Malonyl-CoA normally suppresses CPT-mediated shuttling of fatty acids to mitochondria for β-oxidation. However when ACC is phosphorylated the concentration of malonyl-CoA is decreased which promotes β-oxidation and an increase in the NAD/NADH ratio. SirT is activated by this increase and deacetylates and inhibits the activity of SREBP which is also directly phosphorylated and inhibited by AMPK. AMPK also phosphorylates the mTORC2 complex to influence protein synthesis and insulin signalling. It also suppresses the transcriptional activity of SREBP1C and ChREBP thus preventing transcription of lipogenic, and gluconeogenic genes including FASN and ACC. Lastly AMPK also modulates cholesterol synthesis by inhibiting the activity of HMG-CoA reductase.

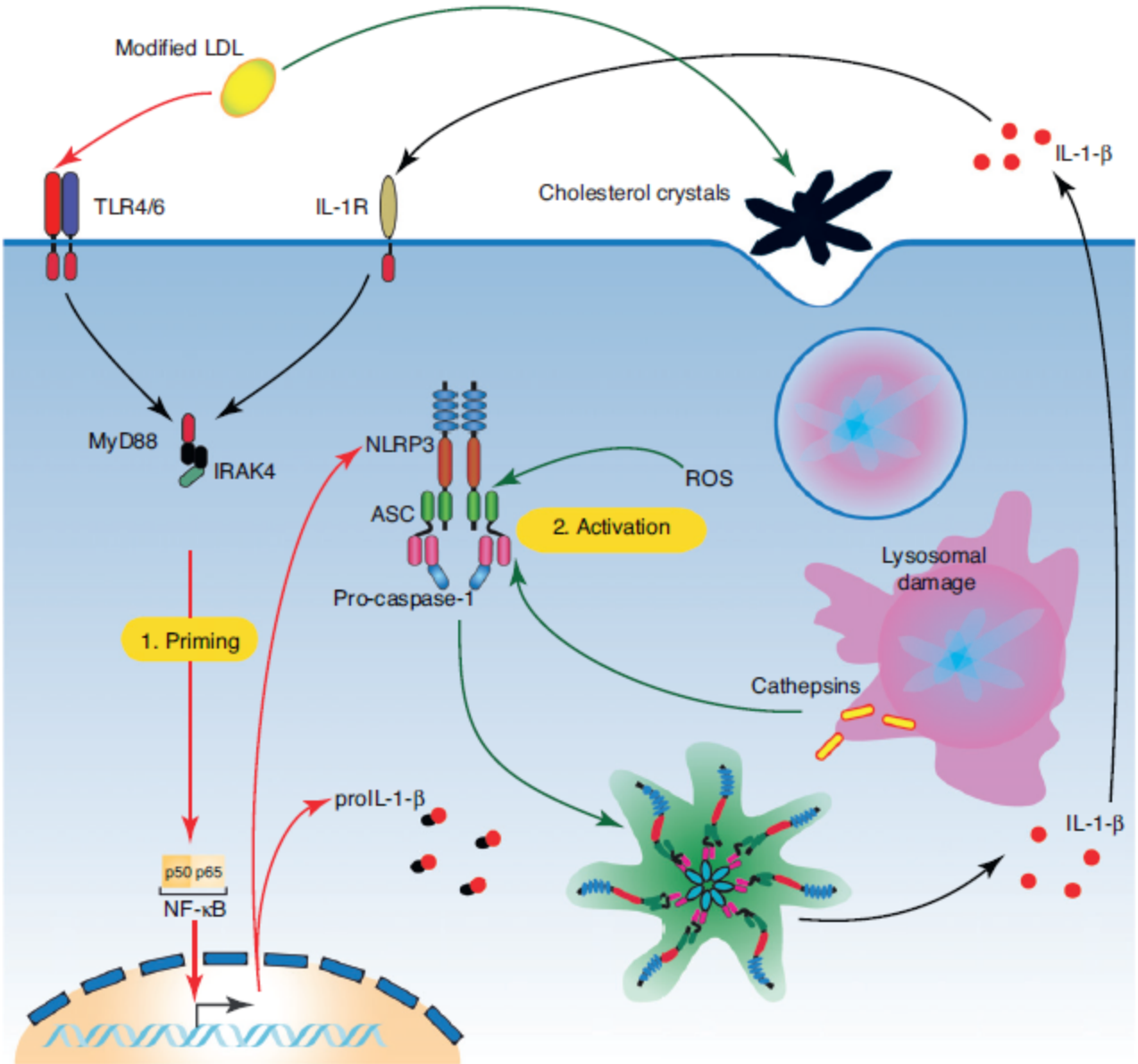
Modified LDL
TLR4/6
IL-1R
Cholesterol crystals
IL-1-β
MyD88
IRAK4
NLRP3
ASC
Pro-caspase-1
ROS
2. Activation
Lysosomal damage
Cathepsins
1. Priming
p50 p65
NF-κB
proIL-1-β
IL-1-β

Figure 7. Inflammasome activation.

Metabolic danger signals such as pro-inflammatory cytokines, free fatty acids and low density lipoproteins are recognized by the pattern recognition factors TLR2, -4 and -6. This priming signal facilitates the translocation of NF-κB to the nucleus to induce transcription of genes encoding for NLRP3, ASC, caspase-1 and the cytokines IL-1β and IL-18. A second activating signal triggers Inflammasome oligomerization. The activating signals include reactive oxygen species, cholesterol crystals and cathepsin B which is released from damaged phagolysosomes. Assembly of the inflammasome induces cleavage of pro-caspase 1 into its active form. Biologically active caspase-1 then proteolytically cleaves pro-IL1β and secretes the mature form of IL-1β. Figure adapted from De Nardo and Latz 2011.

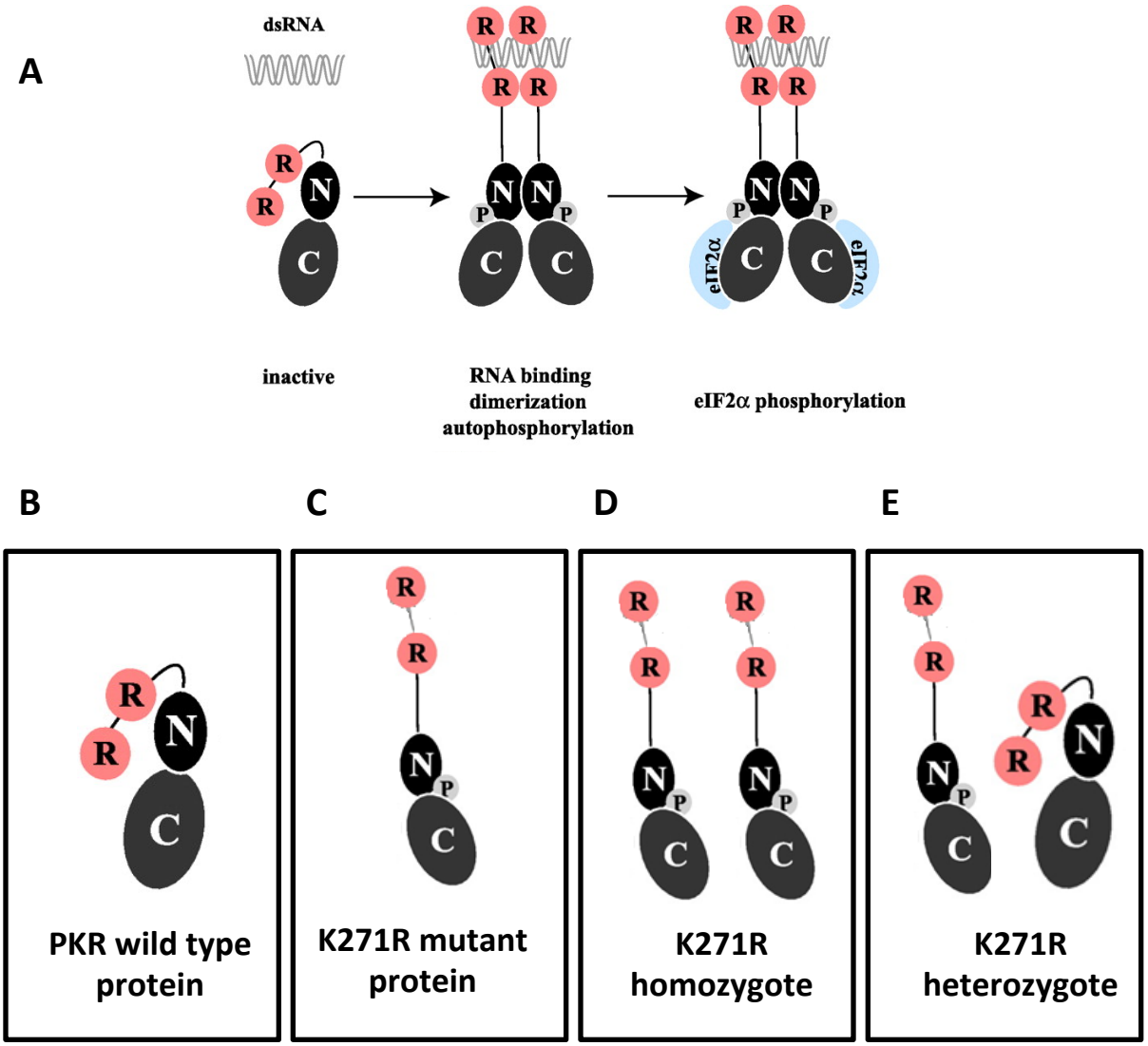

Figure 8. Structure and function of the K271R protein.

A Structure of an inactive PKR molecule. RNA-binding domains fold over the C-terminal kinase domain to inhibit PKR activity. In the presence of RNA, PKR unfolds and is able to autophosphorylate and dimerize with another PKR molecule. **B** Inactive wild type PKR protein exists in a 'closed' conformation. **C** The K271R mutation alters the conformation of the PKR protein an 'open' state allowing it to participate in signalling via its RNA binding domains which are exposed. **D** The K271R homozygote mouse has two copies of the K271R protein and is therefore able to participate in signalling. **E** The K271R heterozygote mouse has one wild type and one mutant copy of the PKR protein and therefore has half of the ability of the K271R homozygote mouse to signal and also may retain some residual kinase activity. Alternatively the wild type PKR protein may interact with the K271R mutant protein in a dominant negative fashion. R- RNA-binding domain, C- C-terminus, N- N-terminus, P-phosphorylated.

CHAPTER 2 METHODS

CHAPTER 2 METHODS 56

2.1 ANIMAL HANDLING 58
2.1.1 Mice 58
2.1.2 High fat diet and standard chow diet feeding 58
2.1.3 Glucose tolerance, insulin tolerance and pyruvate tolerance tests 58
2.1.4 Animal sedation, blood draw by cardiac puncture and organ collection. 59
2.1.5 Blood plasma analysis 59
2.1.6 Dual energy x-ray scans (DEXA) 59
2.1.7 Temperature and activity measurements 59
2.1.8 Ex vivo explants 60
2.1.9 Intraperitoneal leptin injection 60
2.2 TISSUE CULTURE 60
2.2.1 Cell culture maintenance 60
2.2.2 Freezing cells 61
2.2.3 Viable cell count 61
2.2.4 Primary spleen macrophage preparation 61
2.2.5 Primary peritoneal macrophage preparation 62
2.2.6 In vitro stimulation experiments 62
2.3 MEASUREMENT OF OXYGEN CONSUMPTION 63
2.4 NAD/NADH QUANTIFICATION 63
2.5 RNA PREPARATION 64
2.5.1 RNA extraction from cells 64
2.5.2 DNAse treatment of RNA 64
2.5.3 First strand cDNA synthesis 65
2.5.4 Quantitative Real time-PCR 65
2.6 DNA PREPARATION 65
2.6.1 DNA purification 65
2.6.2 Polymerase Chain Reaction (PCR) 66
2.6.3 SDS page gel electrophoresis 66
2.7 PROTEIN PREPARATION 67
2.7.1 Protein extraction from cells 67
2.7.2 Protein extraction from tissues 67
2.7.3 Protein concentration assay 67
2.8 WESTERN BLOTTING 68
2.8.1 Western blot 68
2.8.2 Western blot band quantification 68
2.9 ENZYME LINKED IMMUNOSORBENT ASSAY (ELISA) 68
2.10 IMMUNOHISTOCHEMISTRY 70
2.10.1 Immunostaining for insulin 70
2.10.2 Formalin tissue fixation and embedding. 70
2.10.3 Oil-red-O staining 70
2.10.4 Haematoxylin and eosin staining 70
2.10.5 Quantification of adipocyte and islets of langherhans size. 71
2.10 STATISTICAL ANALYSIS 71

2.11 SOLUTION RECIPES 71
2.12 REFERENCES 74

2.1 ANIMAL HANDLING

2.1.1 Mice

Animals were housed under specific pathogen-free conditions and maintained on a 12-hour light and 12-hour dark cycle and constant temperature of 23±2°C. Apolipoprotein E knockout (apoE KO) animals were obtained from Associate Professor Peter Tipping from the Monash Medical Center, Melbourne. The apoE KO mouse was created as previously described, and was then crossbred with the PKR knockout mouse to produce the apoE:PKR double knockout mouse (Plump, Smith et al. 1992). The PKR knockout animal was created as previously described and backcrossed onto the C57Bl6 strain (Yang, Reis et al. 1995).

2.1.2 High fat diet and standard chow diet feeding

8 to 10 week old mice were fed either a 22% fat, 0.15% cholesterol semi-pure atherogenic rodent diet (Specialty feeds, SF00-219) or a standard chow diet (Specialty feeds, standard mouse and rat cubes) for the duration of 10 weeks. Composition of each diet can be found in appendix XII. Mice were weighed weekly and assessed for fat and lean mass body composition by DEXA (see section 2.1.6) at the completion of the 10 week HFD feeding period. The animals were then sacrificed by sedation and decapitation. Blood plasma was collected by cardiac puncture (explained further in 2.1.4). The heart, liver, abdominal adipose tissue and leg muscle were collected immediately and snap frozen in liquid nitrogen. Tissue samples were stored at -80°C.

2.1.3 Glucose tolerance, insulin tolerance and pyruvate tolerance tests

All tolerance tests were performed at the completion of the 10-week chow or HFD feeding period. Animals were fasted overnight (16 hours), and injected intraperitoneally with 1g/kg body weight of glucose (Sigma, G7528-250g), 0.75U/kg body weight of insulin (Novo Nordisk Pharmaceutical, Actrapid) or 2g/kg body weight of sodium pyruvate (Sigma, P2256-25g). Blood was collected from the saphenous vein and glucose concentration was measured using a glucometer (Accu-chek, Roche Diagnostic Corp.) at 0, 15, 30, 60, and 120 min after

peritoneal glucose injection. See section 2.17 for preparation of insulin, glucose and pyruvate solutions.

2.1.4 Animal sedation, blood draw by cardiac puncture and organ collection.

Mice were sedated with avertin (0.4mg/g of body weight) and sedation checked by the toe pinch reflex method. Blood was drawn using a 25-gauge needle and 1ml syringe. Animals were laid on their back and the needle inserted at the bottom of the sternum and parallel to the spine, aiming for the left eye.

2.1.5 Blood plasma analysis

Blood collected by cardiac puncture was allowed to coagulate overnight at 4°C. The following morning the sample was spun at 1300g for 10 minutes to separate red blood cells from the serum. Serum was carefully removed and stored at -80°C for future analyses. Blood plasma samples were diluted 1:3 in saline and analysis was performed at the Department of Pathology. Total cholesterol, HDL, LDL, triglyceride, ALP and ALT levels were measured by standard commercial enzymatic assays using a Beckman Coulter LX20PRO Analyser, with reagents and calibration supplied by Beckman Coulter Diagnostics Australia.

2.1.6 Dual energy x-ray scans (DEXA)

At the completion of the 10-week high fat diet mice were sedated and assessed for body fat and lean body mass by dual energy x-ray absorptiometry scans (Lunar PIXImus II, GE Medical Systems, Madison, WI)

2.1.7 Temperature and activity measurements

6-8 week old mice were anesthetised by inhalation with fluorane or sedated by injection with avertin. To measure temperature and physical activity G2 e-mitters (Mini-Mitter, Bend, OR) were surgically implanted into the interscapular region and securely sutured to a brown adipose tissue pad. Mice were allowed to recover for a day after the surgery and brown adipose tissue temperature was recorded every minute for the next 4 to 5 days using the

ER-4000 energizer/receivers and VitalView data acquisition software (Mini-Mitter). Mice were fed either a 20% high fat diet or chow diet for the duration of data collection.

2.1.8 Ex vivo explants

8-week old mice were fed a high fat diet for 5 weeks after which they were sacrificed. The liver, adipose tissue and pancreas were isolated in a PC2 fume hood. A 2cm piece of each tissue was placed in a 12 well plate filled with 1ml of DMEM supplemented with 10% FCS, the rest of the tissue was snap frozen for protein or RNA extraction. The tissues were incubated overnight at 37°C. The next day media was removed and analysed by ELISA for IL-1β secretion. The tissue was weighed and discarded. Concentration of IL-1β was expressed relative to weight of tissue.

2.1.9 Intraperitoneal leptin injection

Beginning at 8 weeks of age mice were fed a 20% HFD for the duration of 12 weeks. The animals were then starved for 6 hours after which they were injected intraperitoneally with PBS or 1mg/kg body weight of human leptin. 45 minutes post injection the animals were sacrificed and the brain and hypothalamus were rapidly collected and snap frozen. Hypothalamus was homogenized in 1ml RIPA buffer (appendix).

2.2 TISSUE CULTURE

2.2.1 Cell culture maintenance

15ml centrifuge tube	Corning, 4300791
50ml centrifuge tube	Corning, 430829
5cm tissue culture dish (60mmx15mm)	Falcon, 353002
10cm tissue culture dish (100mmx20mm)	Corning, 430167
6 well tissue culture plate	Falcon, 353046
12 well tissue culture plate	Falcon, 353043
48 well tissue culture plate	Falcon, 353078

Wild type and PKR null immortalized spleen macrophages (SmØ) were already established in the lab (Chakrabarti, Sadler et al. 2008). Mouse embryonic fibroblasts (MEFs) and immortalised spleen macrophages were cultured at 37d°C, 5% CO_2 in Dulbecco's Modified Eagle Medium (DMEM) (Gibco, 11965) supplemented with 10% fetal bovine or calf serum. The cells were grown in either 10 or 5cm dishes and passaged every 2 to 3 days to a 1:10 ratio. For confluent cultures, media was removed; cells were washed with 5ml of phosphate buffered saline (PBS) (Sigma, D8662) and left to stand for a minute. PBS was removed and cells were trypsinized for 5 minutes with TrypLE Express (Gibco, 12604).

2.2.2 Freezing cells

For a confluent culture, media was aspirated; cells were washed with PBS and trypsinized for 5 minutes with TrypLE Express. Cells were resuspended in DMEM and spun down for 4 minutes at 1200rpm. Media was aspirated and the cell pellet was reconstituted in 1ml of freeze media and transferred to a 1.5ml cryotube. The cryotube was immediately placed in a freeze boy and frozen down at -80C. Freeze media: 20% FCS, 0.05% DMSO and 79.95% DMEM.

2.2.3 Viable cell count

After trypsinization cells were resuspended in DMEM. 10µl of resuspended cells was mixed with 30µl of trypan blue. Introduce 10µl of cell suspension under the cover slip placed on top of a haemocytometer (Sigma-Aldrich, Z359629-1EA). Dead stain purple, live cells are characterised by 'halos'. The number of viable cells was counted in four large corner squares of the haemocytometer grid and multiplied by 10,000 to obtain the number of cells in the original cell suspension.

2.2.4 Primary spleen macrophage preparation

Isolation of primary spleen macrophages was performed in sterile conditions in a laminar flow hood. Animals were anesthetised and decapitated by neck dislodgement. The spleen was removed and washed in PBS and transferred to a clean petri dish filled with 5ml DMEM 10% FCS and finely ground using rough slides. The cells were dispensed into a 12 well plate

and allowed to attach overnight. Next day the media was aspirated, the cells were washed with PBS and replaced with fresh DMEM 10% FCS.

2.2.5 Primary peritoneal macrophage preparation

Isolation of primary peritoneal macrophages was performed in sterile conditions in a laminar flow hood. Animals were anesthetised and decapitated by neck dislodgement. A small abdominal incision was made and the skin was pulled back exposing the intraperitoneal cavity. Up to 10ml of cold RPMI (Gibco, 11875) was then injected into the intraperitoneal cavity. The mouse was shaken and massaged to promote detachment of peritoneal macrophages from the cavity lining. RPMI media was removed, placed into a tube and spun down for 4 minutes at 12,00RPM. The cells were washed, reconstituted in RPMI supplemented with 10% FCS and 1X penicillin streptomycin (Gibco, 15070) antibiotics and seeded overnight in a 12 well plate. Next day the media was aspirated and the cells washed with PBS and replaced with fresh RPMI 10% FCS.

2.2.6 *In vitro* stimulation experiments

Resuspended cells were seeded into 6, 12, 24 or 48-well plates at required density. Cells were allowed to attach overnight at 37ºC and used only at 70% confluency. Next day the media was aspired, the cells were washed with PBS to remove any non-adherent cells and fresh media was added. The cells were then serum starved for 2 hours after which they were stimulated with appropriate treatments or inhibitors. In some instances the cells were serum starved over night (19 hours). After specified serum starvation the cells were treated with either rapamycin (Selleck Chemical, S1039) or okadaic acid (Santa Cruz, sc-3513). 100% ethanol or DMSO was used as controls. Rapamycin and okadaic acid treatment periods are specified in the figure legends. Following appropriate treatment the cells were then stimulated with insulin at varied concentrations and time points. At the completion of the experiment supernatant from each well was collected and frozen at -20ºC for ELISA. The remaining cells were washed with PBS and then lysed with an alkaline cell lysis buffer and frozen at -20ºC for western blot analysis.

2.3 MEASUREMENT OF OXYGEN CONSUMPTION

Oxygen consumption was determined by high-resolution respirometry (Oxygraph-2k; Oroboros Instruments, Innsbruck, Austria). MEFs were counted and resuspended in Hanks Balanced Salt Solution (HBSS) at 10million cells/ml to determine the O_2 consumption rate. Measurements were taken at 37°C. Data was collected using DatLab software (Oroboros Instruments).

Oligomycin was added to inhibit ATP synthesis; antimycin (2 µM) was used to determine non-mitochondrial oxygen consumption; FCCP (0.05 µM) was added to study maximal activity of the electron transport chain.

2.4 NAD/NADH QUANTIFICATION

To measure concentration of NAD/NADH a Biovision kit was used (Biovision, K337-100). The assay was carried out as specified in the kit instructions. Cells were grown in a 10cm dish and harvested at 80% confluence. Media was aspired, cells were washed with cold PBS after which 800µl of extraction buffer was added, followed by 10 minute freeze-thaw cycles. Cells were scraped and the protein lysate was sheared using 27-gauge needle and 1ml syringe (BD, 302100). The samples were then filtered through 10kD spin column filters (Biovision, 1997-25) at 13000RPM for 30 minutes. The supernatants were stored on ice until required. Using a 1/10 dilution of the sample a BCA protein concentration assay was performed. 1.2mg/ml of protein lysate was loaded per well in a 96 well plate. Similar cell preparation was performed for the NADP/NADP quantification assay. However supernatant samples were not filtered through the 10kD columns.

2.5 RNA PREPARATION

2.5.1 RNA extraction from cells

For RNA extraction 2ml grinding tubes (Mo Bio laboratories, 13119-500) filled with 1.4mm zirconium oxide beads were used (Bertin Technologies, 03961-1-103). 50-100mg of tissue was homogenized in 1ml of TRIzol reagent (Invitrogen, 15596-018) using the Precellys 24 (Bertin technologoies) lysis and homogenizing automated equipment at 6500RPM for 2x20 seconds with a 5 second delay between sessions. The samples were then incubated for 5 minutes at RT, mixed with 0.2ml of chloroform (Sigma, C2432-500ml), shaken vigorously and incubated at RT for 3 minutes. The samples were centrifuged at 12,000g for 15 minutes at 4^{o}C, after which the aqueous phase was transferred to a fresh tube and the chloroform wash was repeated again. The samples were then mixed with 0.5ml of isopropyl alcohol, incubated at RT for 10 minutes and centrifuged at 12,000xg for 10 minutes at 4^{o}C. The supernatant was carefully removed not to disturb the pellet. The RNA pellet was washed with 1ml of 75% ethanol, gently vortexed and centrifuged at 7,500g for 5 minutes at 4^{o}C. The ethanol wash was repeated twice after which the supernatant was removed, the RNA pellet was air dried for 5 minutes and dissolved in 40µl of RNAse-free water (Gibco, 10977-015) by pipetting up and down.

2.5.2 DNAse treatment of RNA

RNA was DNAse treated with RQ1 RNase-Free DNase (Promega, M6101).

DNA digestion mix consisted of:

RNA in water	1–8µl
RQ1 RNase-Free DNase 10X Reaction Buffer	1µl
RQ1 RNase-Free DNase	1u/µg RNA

Nuclease-free water to a final volume of 10µl.

The digestion mix was incubated at 37°C for 30 minutes. To terminate the reaction (inactivate DNase) 1µl of RQ1 DNase stop solution was added and incubated at 65°C for 10 minutes. Samples were then stored at -80°C.

2.5.3 First strand cDNA synthesis

First strand cDNA was synthesised using SuperScript™ II RT kit (Invitrogen, 18080-044).
Add 1 µl of 50µM Oligo(dT), 300ng random primers, 200ng to 1µg total RNA, 1 µL dNTP Mix (10 mM of each dATP, dGTP,dCTP, dTTP) and top up with sterile, distilled water to make 12µl. This mixture was heated to 65°C for 5 minutes, then chilled on ice for 1 minute. The contents of the tube were collected by brief centrifugation and the following components were added 4µl 5X First-Strand Buffer, 1µl 0.1 M DTT and 1µl RNaseOUT™ (40 units/µL), and 1µl SuperScript™ II RT. The contents of the tube were mixed gently and incubated at 25°C for 5 min, followed by incubation at 50°C for 60 minutes. The reaction was inactivated by heating at 70°C for 15 minutes.

2.5.4 Quantitative Real time-PCR

RT-PCR was performed using the SYBR greener qPCR SuperMix (Invitrogen, 11761-100). All data were normalized to 18S or the indicated in-house gene and quantitative measures were obtained using the $\Delta\Delta C_T$ method.
RT-PCR master mix: SYBR GreenER 10µl, RNA template 1µl, Forward oligonucleotide 1µl (10µM), reverse oligonucleotide 1µl (10µM), distilled H_2O 7µl to make 20 µl.

2.6 DNA PREPARATION

2.6.1 DNA purification

The automated purification of genomic DNA from mouse-tail clippings was performed using the Maxwell® 16 DNA purification Kit (Promega, AS1030,) and the Maxwell® 16 Instrument. DNA purification was carried out as specified in the Promega instruction book.

2.6.2 Polymerase Chain Reaction (PCR)

DNA was amplified by PCR using the My Cycler instrument (Biorad). Master mix components: 10µl of 2XGotaq Green Master mix (Promega, M7122), 250nm of each forward and reverse primers, 100ng of DNA template, topped up to 20µl with DNase/RNase free H_2O.

	PKR	**NEO**	**K271R**
2X Gotaq Green master mix	10µl	10µl	10µl
DNA template	1ul	1ul	1ul
Forward primer	1ul (10µM)	0.8ul (10µM)	4ul (1µM)
Reverse primer	1ul (10µM)	0.8ul (10µM)	4ul (1µM)
H2O	7ul	7.4ul	1ul

PCR cycling conditions to amplify PKR and NEO products:

1st step 95°C for 4 mins

2nd step 95°C for 30s, 62°C for 30s and 72°C for 30s repeated for 35 cycles

3rd step 72°C for 4 min

PCR cycling conditions to amplify K271R product:

1st step 95°C for 4 mins

2nd step 95°C for 30s, 55°C for 30s and 72°C for 60s repeated for 35 cycles

3rd step 20°C

2.6.3 SDS page gel electrophoresis

PCR samples were separated on a 1.5% agarose (Bioline, BIO-4-1025) gel, supplemented with 2% SybrSafe DNA gel stain (Invitrogen, 533102). 20µl/well of sample were loaded and 3µl of'1Kb Plus' DNA ladder solution (Invitrogen, 10787-018), to enable sizing of the bands produced from the samples. The gel was electrophoresed for approximately 60 minutes at

100 volts in SDS buffer (appendix 2). DNA bands were visualised using the Invitrogen Safe Imager and photographed using the Biodoc-IT System (UVP).

2.7 PROTEIN PREPARATION

2.7.1 Protein extraction from cells

Media was removed, cells were washed with PBS and depending on the size of the well (100-200µl) cell lysis buffer was added. The cells were then subjected to a 20-minute freeze and 20-minute thaw cycle whilst rocking. The lysed cells were then scraped and sonicated or sheared using hyperbaric needles.

2.7.2 Protein extraction from tissues

Protein was extracted from muscle, liver, adipose and heart. 2ml-grinding tubes (Mo Bio laboratories, 13119-500) filled with 1.4mm zirconium oxide beads were used (Bertin Technologies, 03961-1-103). 50-100mg of tissue was homogenized in 1ml of cell lysis buffer using the Precellys 24 (Bertin technologoies) lysis and homogenizing automated equipment at 6500RPM for 2x20 seconds with a 5 second delay between sessions. The samples were then centrifuged at 13RPM for 20minutes at 4°C. The protein concentration of the supernatant was determined using a protein assay kit.

2.7.3 Protein concentration assay

Pierce BCA protein assay kit (Thermo scientific, 23335). 2mg/ml of BSA was used at the top standard in this assay. Lysed protein samples were diluted 1/10 in distilled H_2O and 25µl/well of sample was loaded in duplicates in a 96-well plate (Thermo scientific, 442404). 200µl/well of working reagent was added and the plate was incubated at 37°C for 30 minutes. Absorbance was read at 630nm (FLUOstar optima, BMG labtech). The working reagent consists of 50-part solution A and 1 part solution B.

2.8 WESTERN BLOTTING

2.8.1 Western blot

5%, 10%, 12% or 15% SDS gel was prepared using 1.5mm cassettes (Invitrogen, NC2015) and 1.5mm combs. Protein samples were diluted with 4X Sample loading buffer and denatured at 100°C for 4 minutes. Up to 40µl of sample was loaded per well and the band size was distinguished by loading 4µl/well of the molecular weight marker (RPN800E, GE Healthcare). The gel was electrophoresed in 1X TG-SDS running buffer at 50 volts for the first 30 minutes and 130 volts until the blue dye front migrated off the gel.

For protein transfer the following assembly was required: 3 sponges, 3 whatman papers, gel, membrane (soaked in ethanol for 30 seconds) (Immobilon-FL, Millipore,), 3 whatman papers and 3 sponges. Proteins were transferred in 1X transfer buffer at 25 volts for 120 minutes. The membrane was then washed with TBS and blocked in odyssey blocking buffer (Li-Cor biosciences, 927-40000) for 1 hour and probed with primary antibody diluted in odyssey blocking buffer (either overnight at 4°C or for 2 hours at room temperature (RT) depending on specifications). After incubation the membrane was washed with TBS and incubated with the appropriate secondary antibody for 1 hour at RT. The membrane was then washed with TBS and scanned at appropriate channel. The gel was stained with commassie blue for 1 hour and destained overnight with destaining buffer.

2.8.2 Western blot band quantification

Protein amounts from all samples were assessed using the BCA-kit followed by protein concentration normalization before all western blot experiments.

2.9 ENZYME LINKED IMMUNOSORBENT ASSAY (ELISA)

96-well Nunc Maxisorb plates were used for all ELISAs (Thermo scientific, 442404)

Mouse IL-6	R&D systems,
Mouse TNF-α ELISA set II kit	BD OptEIA, 558534
Mouse IL-1β ELISA kit	BD OptEIA, 559603

Mouse monoclonal CRP	Abcam, ab50861
Mouse Leptin	R&D Systems, MOB00

96 well plates were coated with 100µl/well of primary antibody (Refer to table for antibody dilutions) diluted in carbonate buffer pH 9.6. The plate was sealed and incubated overnight at 4^{o}C. Wells were emptied and washed 3 times with 300µl/well wash Buffer (0.05% Tween-20 in PBS). To remove any residual buffer the plate was inverted and blotted on absorbent paper.

Plates were then blocked with either assay diluent 200µl/well and slowly rocked at room temperature (RT) for 2 hours. The wells were then aspired and washed as described above. Standard and sample dilutions, prepared earlier, were loaded (100µl/well) into appropriate wells and incubated overnight at 4ºC or for 2 hours at RT.

The wells were then aspired, washed 3 times and incubated with 100µl/well diluted biotinylated SaV-HRP conjugated detection antibody for 3 hours at RT (Refer to table for antibody dilutions). The plate was then washed 3 times and incubated with 100µl of TMB substrate (3,3'-5.5' tetramethlybenzidine liquid substrate; Sigma) in the dark for 30 minutes or until colour developed. When appropriate colour developed the reaction was stopped with 100 µl/well of stop solution (H_2SO_4). The absorbance was read at 450nm (FLUOstar optima, BMG labtech) within 5 minutes of ceasing the reaction.

	CRP	**IL-6**	**IL-1β**	**TNF-α**	**Leptin**
Primary antibody	1:500	2µg/ml	1:500	1:500	1:500
Detection antibody	1:500	0.4µg/ml	1:500	1:500	1:500
SAv-HRP	1:500	1:500	1:500	1:500	1:500

2.10 IMMUNOHISTOCHEMISTRY

2.10.1 Immunostaining for insulin

The immunohistochemistry protocol for paraffin embedded sections to detect insulin in pancreatic sections can be found online www.cellsignalling.com. Rabbit anti-insulin #4590, cell signalling.

2.10.2 Formalin tissue fixation and embedding.

2cm liver pieces were fixed in 10% formalin and embedded in OCT. Frozen livers were sectioned at 5-microns.

2.10.3 Oil-red-O staining

Oil-red-O stains for fats and lipids in frozen tissue sections. Working oil-red-O consists of equal parts of stock oil-red-O (Sigma, O0625) and 30% Isopropyl alcohol (Ajax Finechem, 425-2.5L GL). Oil-red-o and 30% isopropyl alcohol were mixed and allowed to stand for 15 minutes. Slides were first rinsed with distilled water, placed in 30% Isopropyl Alcohol for 5 minutes followed by working oil-red-O for 15 minutes. The slides were then removed from working oil-red-, dipped in 30% isopropyl Alcohol and rinsed with distilled water. Harris Hematoxylin was then applied for 1 minute, followed by a rinse in distilled water. The slides were finally mounted in glycerin jelly (Ajax Finechem, 242-500ml).

2.10.4 Haematoxylin and eosin staining

Formalin fixed, paraffin embedded or frozen sections were stained with H&E. Sections were rinsed with distilled water, nuclei stained with hematoxylin for 4 minutes, rinsed in running tap water, slides quickly dipped into 0.3% acid alcohol to differentiate, rinsed in tap water then quickly dipped in Scott's tap water followed by another tap water rinse. Slides were stained with eosin for 2 minutes, dehydrated, cleared and mounted.

2.10.5 Quantification of adipocyte and islets of langerhans size.

Adipocyte size was quantified manually using ImageJ software. Pancreas slides were scanned using the Aperio Scanscope Digital slide scanner, and size of islets of Langerhans was assessed manually using the Aperio ImageScope software.

2.10 STATISTICAL ANALYSIS

All statistical analysis was performed using the unpaired T- test except for weight gain data which was analysed using linear regression (GraphPad Prism 5) or Area under curve.

2.11 SOLUTION RECIPES

Isopropanol	Ajax Finechem, 425-2.5L GL
Ethanol	Merck, 45748
Methanol	Merck, 44364

Alkaline cell lysis buffer

50mM Tris-HCl ph7.4, 150mM NaCl, 50mM beta-glycerophosphate, 0.1mM EDTA, 10% glycerol, 1% Triton x100. Add PMSF 1/100, Protease inhibitor cocktail 1/50, tyrosine inhibitor 1/50 and 1 phosphatase pill per 10ml of lysis buffer.

Coomassie (RT):

To make 1L: add 500ml methanol, 100ml acetic acid glacial, 400ml milliQ water and 2g Coomassie Blue R-250 (Bio-Rad).

Destaining buffer (RT):

To make 1L: add 800ml water, 100ml EtOH and 100ml acetic acid glacial.

Glucose solution

Dissolve 0.625g of D-glucose (Sigma, G-7528) in 10ml of saline (0.9% NaCl, Pfizer) and incubate overnight at room temperature. Final concentration of solution 0.0625g/ml. Inject body weight (g) multiplied by 16. For example: body weight 30g, 30g x 16 = 480µl of glucose.

Insulin preparation

Add 75µl of 100mU/µl insulin (Novo Nordisk Pharmaceuticals, Actrapid) to 10ml saline (Pfizer) to make 0.75mU/µl. Inject

Want 0.75U/kg.

Lower buffer (4X)

Add 1.5M Tris-base, 0.4% SDS in 1L MiliQ water. Adjust pH to 8.8.

Pyruvate solution

Dissolve 1.25g of sodium pyruvate (sigma, P2256-25g)) in 10ml saline (Pfizer) to make 0.125g/ml.

Inject 2g pyruvate/kg body weight (0.002g/g) To be Injected: body weight X 16 = µl

Sample loading buffer (4X)

2ml SDS 20%, 1.25ml glycerol, 1ml Stacking buffer pH 6.8, 0.2g DTT, 6.25ml MilliQ water and Bromophenol blue powder.

SDS-gel

	2 gels at 5%	**2 gels at 7.5%**	**2 gels at 10%**
Water	12.5ml	10.95ml	9.95ml
Lower buffer 4X pH8.8	5ml	5ml	5ml
Acryl bis 40%	2.5ml	3.9ml	5ml
Ammonium persulfate (APS)	125µl	125µl	125µl
Temed	15µl	15µl	15µl

Ammonium persulfate preparation: 0.200g of APS in 1ml of milliQ water.

Stacking gel mix for two gels: add 6.03ml water, 950µl upper buffer 4X pH 6.8, 970µl Acryl-bis 40%, 75µl Ammonium persulfate and 10µl Temed. Fill 2/3 of the cassette with SDS-gel mix, then pour 1/3 of water on top and allow to set. After setting pour the excess water off, add stacking gel mix, insert comb and allow to set.

Transfer buffer 10X

15.35g TrisHCl , 18.5g Tris-base, 144g Glycine make up to 1L with milliQ water.

To make 1L of 1X transfer buffer add 100ml 10X Transfer Buffer, 200 ml EtOH or MetOH, 700ml MilliQ water.

TBS 20X

0.05% TTBS 1X

To make 1L: add 50ml TBS 20X, 950ml MilliQ water and 500µl Tween.

Tyrosine phosphatase inhibitor

Mix 50µl sodium orthovanadate, 95µl H_2O_2 and 355µl miliQ water.

Upper buffer (4X)

Tris 0.5M, SDS 0.4%, pH 6.8.

2.12 REFERENCES

Chakrabarti, A., A. J. Sadler, et al. (2008). "Protein Kinase R-dependent Regulation of Interleukin-10 in Response to Double-stranded RNA." J Biol Chem **283**(37): 25132-25139.

Plump, A. S., J. D. Smith, et al. (1992). "Severe hypercholesterolemia and atherosclerosis in apolipoprotein E-deficient mice created by homologous recombination in ES cells." Cell **71**(2): 343-353.

Yang, Y. L., L. F. Reis, et al. (1995). "Deficient signaling in mice devoid of double-stranded RNA-dependent protein kinase." EMBO J **14**(24): 6095-6106.

CHAPTER 3 THE ROLE OF PKR IN DIET INDUCED OBESITY AND CARDIOVASCULAR DISEASE.

CHAPTER 3 THE ROLE OF PKR IN DIET INDUCED OBESITY AND CARDIOVASCULAR DISEASE..... 75

3.1 INTRODUCTION 76

3.2 RATIONALE 77

3.3 HYPOTHESIS, AIMS AND METHODS 78

3.4 RESULTS 79

ABLATION OF PKR INCREASES DIET INDUCED WEIGHT GAIN 79

3.4.1 PKR regulates weight gain, adipocyte size and adiposity in response to a high fat diet. 79

3.4.2 PKR modulates activity and baseline thermogenesis in BAT. 79

LOSS OF PKR PROMOTES DIABETES INDUCING EVENTS 80

3.4.3 PKR improves insulin sensitivity, hepatic glucose output and glucose tolerance. 80

3.4.4 Ablation of PKR reduces Langerhans islet size. 81

PKR ALTERS BLOOD LIPID COMPOSITION AND SUSCEPTIBILITY TO FATTY LIVER DISEASE 82

3.4.5 PKR alters plasma lipoprotein profiles. 82

3.4.6 PKR alters expression of DGAT2 required for triglyceride synthesis. 83

3.4.7 Characterisation of apoE:PKR knockout mice in response to high fat diet. 83

ROLE OF PKRs KINASE AND ADAPTOR FUNCTION IN WEIGHT GAIN AND GLUCOSE HOMEOSTASIS 85

3.4.8 K271R heterozygote and homozygote mice have differential responses to a high fat diet. 85

3.4.9 Lack of PKR kinase activity does not affect glucose homeostasis. 85

3.4.10 Lack of PKR kinase activity alters islet size. 86

3.4.11 Lack of PKR kinase activity does not affect blood plasma lipoprotein composition. 87

3.5 DISCUSSION 87

3.6 CONCLUSION 97

3.7 REFERENCES 98

3.1 INTRODUCTION

It has become clear that immune and inflammatory mechanisms modulate metabolic processes and play a key role in the development and progression of metabolic disease (Lumeng and Saltiel 2011). This notion is supported by a large number of compelling experiments and clinical data that correlate the risk of developing atherosclerosis and ensuing cardiovascular disease with the presence of auto-immune and pro-inflammatory diseases, such as arthritis and diabetes (Grant 2005; Solomon, Goodson et al. 2006). In addition, ablation of specific inflammatory proteins such as toll-like receptor 2 (TLR2), I kappa B kinase-ε (IKKε) or c-Jun kinase 2 (JNK2) has been shown to provide protection against the development of diet induced metabolic and cardiovascular disease (CVD) (Chiang, Bazuine et al. 2009; Belgardt, Mauer et al. 2010; Himes and Smith 2010). CVD refers to the numerous conditions that affect the heart and blood vessels. The most common pathological process leading to CVD is atherosclerosis, which is the narrowing and hardening of the medium and large-sized arteries due to plaque build-up (Falk 2006). Until recently atherosclerosis was characterised as a passive disorder of lipid deposition within the arterial wall (Steinberg 1987). However, more recent evidence indicates that atherosclerosis is a dynamic process, crucially modulated by the inflammatory immune response (Stokes, Cooper et al. 2002). Accordingly, potential targets to ameliorate atherosclerosis include a range of inflammatory pathways. In light of the established role for protein kinase R (PKR) in inflammation and the notion that immune inflammatory mechanisms play a key role in the development of metabolic disease, as part of my honour study I investigated the role for PKR in the pathogenesis of atherosclerosis (Pindel 2008; Pindel and Sadler 2011).

For the purpose of these experiments I used the transgenic apolipoprotein E deficient (apoE) mouse model for atherosclerosis because C57Bl6 animals when fed an atherogenic diet do not develop atherosclerotic lesions (Piedrahita, Zhang et al. 1992). ApoE facilitates excretion of cholesterol rich lipoproteins by binding to the hepatic low density lipoprotein (LDL) receptor which plays a critical role in the degradation and elimination of excess cholesterol (Greenow, Pearce et al. 2005). Accordingly, ablation of the apoE gene results in heightened cholesterol levels and a condition that mimics many aspects of human

atherosclerosis (Plump, Smith et al. 1992). To be able to measure the consequence of PKR-dependent cell signalling on diet-induced atherogenesis, the PKR knockout mice were crossbred with apoE deficient mice to create the double apoE:PKR knockout mice. This experiment demonstrated that rather than being pro-atherogenic, as would be predicted by a pro-inflammatory role, PKR reduced cardiovascular disease. Moreover, the apoE:PKR knockout mice had significantly increased weight gain, elevated blood levels of LDL/HDL ratio and reduced triglyceride levels in comparison to control apoE knockout mice when fed a high fat diet (Appendix II and III). These intriguing observations, pointing to an unexpected consequence of PKR in metabolic control, formed the substance for this thesis.

3.2 RATIONALE

PKR phosphorylates eIF2α to restrain global protein synthesis. Previous work has reported that phosphorylation of eIF2α is an important biological response involved in modulating the development of the metabolic syndrome. In addition, PKR participates in cell signalling to modulate inflammation and has been shown to regulate the activity of NF-κB and JNK, which are implicated in the development obesity related inflammation and insulin resistance (Gregor et al., 2009, Goh et al., 2000, Hsu et al., 2004). In view of these two roles of PKR, and the realisation that crosstalk between immune and metabolic signalling pathways is linked to the pathogenesis of the metabolic syndrome, I hypothesise that PKR constitutes such a link. I expect that stresses elicited by a high fat diet will regulate the activity of PKR. Indeed, palmitic acid has been reported to directly inhibit PKR. Hence, PKR, with a second eIF2α kinase PERK (which is activated by the unfolded protein response), present as plausible responders to metabolic stress. The activating ligands for the other eIF2α kinases, HRI and GCN2, low heme concentrations in red blood cells and amino acid deficiency, respectively, are unlikely triggers in a high calorie diet. Importantly, PERK has not been demonstrated to play as significant of a role in cell signalling as PKR. Recognition of the mechanism by which PKR modulates metabolic syndrome could identify novel targets for the treatment of metabolic disease.

3.3 HYPOTHESIS, AIMS AND METHODS

Hypothesis

I hypothesize that metabolic sensing via PKR initiates a general stress response to high fat diets that alleviates metabolic disease burden.

Aims

The physiological responses of; WT, PKR knockout, PKR kinase-dead (K271R) knock-in mice, apoE knockout and the double apoE:PKR knockout mice to high fat diet, in comparison to standard chow feeding, was measured to determine a role for PKR in regulating metabolic outcomes. These transgenic mice were compared for:

I. Weight gain and body mass composition;

II. Glucose homeostasis by measuring glucose output and glucose tolerance;

III. Pancreatic structure and function;

IV. The development of hyperlipidemia and blood lipid and lipoprotein composition, and;

V. The development of NAFLD, hepatic triglyceride accumulation and liver function;

Methods

The PKR knockout mouse was created by targeted disruption of exons 2-4 in the N-terminal region of the PKR gene (N-PKR knockout) as previously described (Yang, Reis et al. 1995). PKR knockout mice were backcrossed on a C57Bl6 background. As part of my honour thesis PKR knockout mice were crossbred with apoE deficient mice to create the double apoE:PKR knockout mice. Eight week old WT, PKR knockout, apoE knockout, apoE:PKR knockout mice were fed either a standard chow or a high fat 'atherogenic' diet (SF00-219 composition 22% fat, 19% protein, 0.15% cholesterol) for 10 weeks as a diet induced obesity model and the responses in these animals were compared.

3.4 RESULTS

ABLATION OF PKR INCREASES DIET INDUCED WEIGHT GAIN

3.4.1 PKR regulates weight gain, adipocyte size and adiposity in response to a high fat diet.

Previous studies have established that mice deficient for PKR have comparable weight gain to wild type mice in response to a chow diet. Consistent with these reports I demonstrate in figure 3.1A that chow diet fed PKR WT (n=6) and PKR knockout (n=7) mice have similar weight gain. However, in response to a high fat diet PKR knockout mice gain significantly (*p=0.023) more weight compared to wild type littermates (Fig. 3.1B). The equations for the lines of best fit for PKR WT and PKR knockout mice are as follows: 01.30g±0.13g and 1.73g±0.10g indicating a significant difference in weight gain.

Density measures, by dual energy X-ray absorptiometry (DEXA) analysis, show that the loss of PKR promotes adiposity compared to wild type mice (15.29±0.85g and 11.58g±1.80g, respectively; *p=0.044), with fat accounting for 36.79±1.37% of total body mass in PKR knockout mice and only 29.81±2.26% in wild type mice (Fig.3.2B and C). This analysis confirms that weight gain in these animals manifests as a result of increased adiposity rather than changes in lean body mass (PKR WT 26.12g±0.50g and PKR knockout 26.07g±0.33 lean body mass, respectively; p=0.9364) (Fig.3.2A). The role for PKR in modulating adipogenesis is further substantiated by the observation that mice ablated for PKR have enlarged subcutaneous adipocytes compared to wild type mice as quantified by Image J (*p=0.0001) (Fig.3.3A and B). Taken together these findings implicate PKR in regulating expansion of adipose tissue depots and consequent weight gain in response to high fat diets.

3.4.2 PKR does not modulate baseline thermogenesis in BAT or affect physical activity.

Thermogenesis is a mitochondrial specific process that uncouples oxidative phosphorylation from ATP synthesis and releases energy in the form of heat. Thermogenesis is a crucial component regulating energy balance in small mammals. Therefore I sought to

measure thermogenic activity by calorimetric analysis of brown adipose tissue temperature. For the purpose of this experiment I used 8-week old PKR WT and knockout mice that were fed a high fat diet for the duration of the calorimetric analysis. Given that mice are nocturnal animals I observed a corresponding increase in BAT temperature and locomotor activity during the dark period of the day (shaded area of the graph). Notably Figure 3.4A demonstrates that high fat diet fed PKR knockout mice have reduced BAT temperature in the dark and light period compared to wild type mice, however this difference is not statistically significant as assessed by area under curve (AUC) analysis (Fig.3.4B).

Similarly, measurement of physical activity revealed that, in response to high fat diet during both the dark and light cycle, mice ablated for PKR are less active compared to wild type mice, however this difference is not statistically significant as analysed by AUC (Fig.3.4C and D). In conjunction with these findings chow feeding has no effect on BAT-mediated thermogenesis or physical activity (Fig.3.5A-C). Collectively these results suggest that PKR does not appear to modulate activity or BAT temperature by stresses elicited by high fat diets, however this notion requires further investigation to determine whether dietary components, such as fatty acids or lipids, induce phosphorylation of PKR and its downstream target eIF2**α.**

LOSS OF PKR PROMOTES DIABETES INDUCING EVENTS

3.4.3 PKR improves insulin sensitivity, hepatic glucose output and glucose tolerance.

The observed increased weight gain observed in mice carrying a mutation of the PKR gene, EIF2ak2, is known to be associate with insulin resistance and type 2 diabetes. Hence I investigated the physiological role for PKR in glucose homeostasis by performing glucose tolerance tests. High fat diet and chow diet fed PKR WT and knockout mice were starved overnight and challenged with glucose the following morning. Statistical comparison of glucose levels at specific time points (Fig3.6A) and area under curve analysis (Fig3.6B) shows that chow diet fed WT and PKR knockout mice have similar glucose tolerance ($p=0.0732$). In addition, these two groups of animals had comparable fasted blood glucose concentration (Fig.3.6C).

In contrast, mice lacking PKR on a high fat diet have delayed blood glucose clearance post glucose stimulation, by analysis at specific time points and by area under curve analysis (Fig.3.7A and B). Additionally, mice ablated for PKR, fed a high fat diet, had significantly (*p=0.0146) increased fasting blood glucose levels (Fig.3.7C). Taken together these observations demonstrate that loss of PKR triggers disturbances in glucose homeostasis, causing glucose intolerance, in response to a high fat diet.

3.4.4 Ablation of PKR reduces Langerhans islet size.

Blood glucose homeostasis is primarily maintained by the insulin hormone, which is produced by β-cells located within islets of Langerhans. Destruction of β-cells, resulting in reduced islet size and number, is a pathogenic feature of insulin resistance and an underlying cause of type 1 diabetes. Therefore I sought to morphologically assess the structure of the pancreas for islet damage by H&E staining. Islets of Langerhans stain a lighter pink and appear as rounded structures that are surrounded by acinar cells stained in a darker purple (Fig.3.8A). Both WT and PKR knockout mice have normal pancreatic morphology. The islets of Langerhans appear free of immune cell infiltration and there is no evident defragmentation of the nucleus indicative of apoptosis (Fig.3.9A-H). There is also no noticeable degranulation of acinar cells demonstrating that the exocrine portion of the pancreas is not atrophic (Fig.3.9I-P). However figures 3.9 Q and R show mild pancreatic fatty infiltration in mice ablated for PKR. Although the pancreatic structure is morphologically indistinguishable between the animal cohorts, our results demonstrate that mice devoid of PKR have significantly smaller islets of Langerhans compared to wild type mice (Fig.3.8B). The responses of a PKR kinase dead K271R mouse to high fat diets, shown in fig 3.8, 3.9 and 3.10 for K271R mice are discussed further in section 3.4.10. Staining of frozen pancreatic sections for insulin showed that β-cells of both PKR WT and PKR knockout mice are functional and capable of producing insulin (Fig.3.10). However this assessment is not quantitative, so does not provide information about the amount of insulin produced by β-cells. Therefore it is unclear whether the modest reduction in the size of the islets results in an insulin insufficiency that could account for the impaired glucose homeostasis. I have not adequately ruled out alternative explanations, such as that insulin resistance rather than

insulin production, could account for impaired glucose homeostasis. Additional causes for the altered glucose homeostasis are explored below.

PKR ALTERS BLOOD LIPID COMPOSITION AND SUSCEPTIBILITY TO FATTY LIVER DISEASE

3.4.5 PKR alters plasma lipoprotein profiles.

Obesity is reported to associate with heightened levels of lipids and lipoproteins, which on its own is an independent risk factor for cardiovascular disease and atherosclerosis. To address the question whether diet induced weight gain in mice ablated for PKR is associated with atherogenic dyslipidemia, I evaluated circulating levels of lipid and lipoprotein. Circulating concentration of triglycerides is two-fold higher (*p=0.0196) in PKR knockout mice compared to wild type (Fig.3.11B). These mice also have significantly decreased plasma levels of LDL (p*0.0363) and LDL/HDL ratio (*p=0.0177) (Fig.3.15 D and E). Although cholesterol levels in mice ablated for PKR are 15.9% higher compared to the WT, figure 3.11A shows that this difference is not significantly different (PKR WT 9.66±0.85mmol/L, PKR knockout 11.20±0.91mmol/L). There is no detectable change in circulating concentration of HDL between wild type or PKR knockout mice. Collectively these findings suggest that lack of PKR disrupts lipid-signalling pathways causing dyslipidemia.

Elevated plasma triglyceride levels are reported to associate with fatty liver disease, therefore I sought to establish whether this phenotype correlates with hepatic steatosis in mice ablated for PKR. Following ten weeks of high fat diet feeding PKR knockout mice have significantly paler and yellower livers, which is indicative of excess lipid accumulation. Correspondingly, quantification of lipid levels by oil red-O staining shows mice deficient for PKR have significantly greater hepatic lipid accumulation (*p=0.0120) (Fig 3.12A and B). These findings suggest that mice ablated for PKR have an increased risk of fatty liver disease, likely due to elevated plasma triglyceride levels. In light of the association between fatty liver disease and insulin resistance, it is plausible to speculate that hepatic lipid deposition contributes to disturbances in glucose homeostasis (Seppala-Lindroos, Vehkavaara et al. 2002; Samuel, Liu et al. 2004).

3.4.6 PKR alters expression of DGAT2 required for triglyceride synthesis.

To investigate mechanisms that could account for the increased weight gain and dyslipidemia observed in mice deficient for PKR I evaluated expression of enzymes involved in triglyceride synthesis and fatty acid oxidation. Medium chain acyl-coA dehydrogenase (MCAD) initialises the first step of β-oxidation (however it is not the rate limiting enzyme of the pathway), whereas microsomal triglyceride transfer protein (MTTP) and diacylglycerol acyltransferase-2 (DGAT) are required for lipoprotein and triglyceride synthesis, respectively. Figure 3.13A shows that hepatic expression of DGAT2 is significantly (*p=0.0209) decreased in mice ablated for PKR in comparison to wild type mice, however its expression in WAT is similar between the animal cohorts (Fig.3.13B). Increased expression of DGAT2 in the liver of mice ablated for PKR may contribute to enhanced synthesis and accumulation of triglycerides in this tissue. Expression of MTTP or MCAD in liver or adipose tissue is similar between the animal cohorts, suggesting that reactions catalysed by these enzymes are equivalent. It is important to note that this study does not comprehensively evaluate the expression of the rate limiting enzymes involved in these pathways, also the sample size used in figure 3.13B is inadequate, therefore it is difficult to rule out the contribution of fatty acid oxidation and lipoprotein synthesis to adipose tissue expansion and fatty liver disease in mice devoid of PKR. Hence future studies should assess the expression of the rate-limiting enzymes CPT1 and SCD1.

3.4.7 Characterisation of apoE:PKR knockout mice in response to high fat diet.

Consistent with data in single PKR knockout mice, I demonstrate that high fat diet fed mice ablated for apoE:PKR gain significantly more weight than apoE knockout controls (Fig.3.14A,*p=0.0199). These mice also have delayed clearance of glucose from the blood as shown by increased concentration of glucose 120 minutes post glucose injection after 5 weeks of high fat diet feeding (Fig.3.15A). Although apoE:PKR knockout mice have only minor non-significant (Fig.3.15B) perturbations in glucose homeostasis, they have significantly lower fasting blood glucose concentration in comparison to apoE knockout

controls (Fig.3.15C,*p=0.0099). This phenotype is only observed during fasting, because postprandial glucose levels are comparable in both experimental mouse cohorts (Fig.3.15D).

Consistent with results obtained in single PKR knockout mice, 40 weeks of chow feeding had no impact on weight gain (p=0.2696) (Fig.3.14B). Also, there was no significant difference in the total blood glucose concentration during a GTT between apoE knockout and apoE:PKR knockout mice (Fig.3.16A). However, similarly to high fat diet fed mice, fasted blood glucose concentration was significantly lower in apoE:PKR knockout mice after 30 (*p=0.0273) and 40 (*p=0.0086) weeks of chow diet feeding in comparison to control mice (Fig.3.16C and D). To establish whether these mice are insulin sensitive I performed an insulin tolerance test. Glucose clearance was equivalent in both mouse cohorts (Fig.3.16E). These findings suggest that apoE:PKR knockout animals have lower glycemia (hypoglycemia) not as a result of enhanced insulin sensitivity but perhaps due to decreased gluconeogenesis, or alternatively increased glucose breakdown.

As part of my honours thesis I assessed concentration of plasma lipoproteins in apoE:PKR ablated mice fed a high fat diet (Appendix II and III). These results showed that loss of PKR, on the apoE knockout background, significantly reduced concentration of blood triglycerides and increased concentration of circulating LDLs, compared to the apoE knockout mouse. This differs from the single PKR knockout mouse, presumably due to the altered transport of lipid in the apoE knockout background. I speculated that enhanced triglyceride deposition in the liver could account for reduced circulating triglyceride concentration. However hepatic oil red-O staining intensity in apoE:PKR knockout and apoE knockout mice is similar, suggestive of comparable hepatic lipid deposition (Fig.3.17A and B). The extent of liver damage, assessed by measuring circulating levels of liver injury biomarkers ALP and ALT, demonstrate only moderately, but not significantly, elevated liver damage in the apoE:PKR knockout mice (Fig.3.17C and D). Collectively, these findings confirm that deletion of PKR, on the apoE deficient background, promotes weight gain and disrupts glucose homeostasis, hence confirming our hypothesis that PKR plays an important role in modulating metabolic disease outcome caused by high fat diets.

ROLE OF PKRs KINASE AND ADAPTOR FUNCTION IN WEIGHT GAIN AND GLUCOSE HOMEOSTASIS

3.4.8 K271R heterozygote and homozygote mice have differential responses to a high fat diet.

Mice both homozygote and heterozygote for the altered gene expressing the K271R mutation were fed a high fat diet for 10 weeks. In keeping with findings from PKR knockout mouse, K271R heterozygotes gained significantly more weight in comparison to WT mice (*p=0.0002) (Fig.3.18A). Unexpectedly, the K271R homozygote mice have similar weight gain as PKR wild type mice (p=0.4669), and significantly less than the heterozygous animals (*p=0.0174) (Fig.3.18B). The equations for the lines of best fit for weight gain for WT mice are 1.17g±0.09g, K271R heterozygote 1.68g±0.10g and K271R homozygote 1.28g±0.18 indicating that weight gain is greatest in K271R heterozygote mice. This finding demonstrates that the kinase function of PKR is dispensable for modulating diet-induced weight gain and adiposity. We can only speculate that the difference between the heterozygous and homozygous K271R mice might be due to the different levels of the proteins in the two mice. PKR autoregulates its own translation and considerably higher levels PKR are apparent in the homozygous compared to the heterozygous mouse. It was previously demonstrated that the kinase dead human PKR (K296R) retained cell-signalling capacity but was attenuated compared to the WT protein (Gil, Esteban, 2001).

3.4.9 Lack of PKR kinase activity does not affect glucose homeostasis.

Given that high fat diet fed PKR knockout mice are glucose intolerant, I wanted to establish the requirement for the catalytic activity of PKR in the maintenance of glucose homeostasis. Similarly to PKR knockout mice, I observed that K271R heterozygote mice have significantly increased fasting blood glucose levels (*p=0.0145) when compared to WT or K271R homozygote mice (3.19C). In addition, K271R heterozygote mice have consistently elevated blood glucose concentration throughout the GTT, with a major difference seen 90 minutes post glucose injection (Fig.3.19A). Although these findings suggest that K271R

heterozygote mice have delayed blood glucose clearance, AUC analysis shows that total blood glucose concentration is statistically similar to wild type mice (Fig.3.19B, p=0.0771). In keeping with the weight gain results, K271R homozygote mice have comparable blood glucose concentration to WT mice when analysed by AUC or by time point comparison. These results demonstrate that mice heterozygote for the K271R mutation have disturbed glucose homeostasis and resultant fasting hyperglycaemia, compared to WT or K271R homozygote mice.

3.4.10 Lack of PKR kinase activity alters islet size.

PKR knockout mice are glucose intolerant and have smaller islets of Langerhans. Hence, I hypothesised that the glucose intolerant mice devoid of catalytically active PKR would have a similar defect. As shown previously, morphological assessment of pancreas from K271R homozygote and heterozygote mice did not reveal any significant differences in pancreatic structure of islets of Langerhans (Fig.3.8). Pancreas sections stained with H&E show normal confined islets with no significant evidence of immune cell infiltration or apoptosis (Fig.3.9). The exocrine portion of the pancreas between wild type, K271R heterozygote or homozygote mice, is also morphologically indistinguishable (Fig.3.9). Furthermore, immunostaining of pancreas sections for insulin demonstrated that both K271R homozygote and heterozygote mice have functional insulin producing β-cells (Fig.3.10). However, the K271R homozygote mice have significantly smaller islets compared to wild type or K271R heterozygote mice (Fig.3.8B). This finding is surprising because the homozygous animal did not appear to be glucose intolerant and it does not align with the observed glucose intolerance of the K271R heterozygote mice. Taken together these results suggest that the kinase function of PKR may be required to maintain the structure of islets of Langerhans because the K271R heterozygote and wild type mice, both of which express some catalytically active PKR, are protected from islet damage. Also, the observed reduction in islet size, seen in both the null and homozygous mutant PKR mice, does not account for the defect in glucose homeostasis in null or heterozygous PKR K271R mice.

3.4.11 Lack of PKR kinase activity does not affect blood plasma lipoprotein composition.

To address the question of whether increased weight gain associates with dyslipidemia, I assessed levels of circulating lipids and lipoproteins. Figure 3.20A-E demonstrates that plasma levels of cholesterol, triglycerides, LDL, HDL and LDL/HDL ratio is similar in K271R homozygote and K271R heterozygote mice compared to wild type mice fed a high fat diet. Hence, the lack of PKR kinase activity does not account for altered blood lipid chemistry. Instead it appears that hyperlipidemia is driven by the non-kinase function of PKR.

Further plasma assessment revealed that the level of the circulating biomarker of liver injury, ALP, is significantly increased in K271R heterozgoyte mice compared to WT (*p=0.0066) and K271R homozygote (*p=0.0176) animals (Fig.3.21A). There is no difference in ALP blood concentration between K271R homozygote and WT mice. Concentration of circulating ALT is similar between K271R homozygote (59.57±17.49mmol/L) and WT animals (96.33±22.06mmol/L) and K271R heterozygote (205.7±68.09mmol/L) and WT animals (Fig.3.21B). However K271R heterozygote mice have greater concentration of ALT compared to K271R homozygote mice (*p=0.0407). From these findings it is plausible to speculate that catalytically active PKR protects against liver injury and the consequent release of the liver injury biomarker ALP. Liver injury is linked to insulin resistance and dysregulation of glucose homeostasis. Therefore enhanced liver injury, rather than islet insufficiency, may account for impaired glucose homeostasis in K271R heterozygote mice.

3.5 DISCUSSION

Taken together these findings implicate a novel role for PKR in modulating responses to a high fat diet. The results in this chapter demonstrate that mice devoid of functional PKR have an increased susceptibility to high fat diet induced obesity and glucose intolerance. Since there is no measurable metabolic defect in chow fed mice and given the role of PKR as a cytosolic sensor, it is reasonable to speculate that PKR may sense dietary nutrients in order to trigger signalling pathways that regulate metabolic homeostasis. This speculation is

supported by recent evidence that demonstrates PKR to be activated by palmitate (Carvalho-Fillh et al., 2012).

Perhaps the most significant finding of this study is that loss of PKR promotes weight gain entirely as a result of increased adiposity. This finding lead me to speculate that reduced thermogenesis and suppressed energy expenditure could account for this phenotype. Contrary to the expected outcome, the difference in mean BAT temperature or physical activity of high fat diet or chow fed PKR knockout and wild type mice was deemed insignificant by area under curve analysis. Collectively these findings suggest that ablation of PKR does not diminish the capacity to expend energy from BAT in the form of heat does not suppress physical activity. Although this analysis didn't reveal a statistically significant difference, other studies have shown that a reduction of BAT temperature by 1°C has a significant consequence on weight gain (Lockie, Heppner et al. 2012). However the scale of difference in mean BAT temperature between PKR knockout and wild type mice was less than 1°C (PKR knockout 37.24°C and 37.73°C for wild type mice) therefore not likely to account for the difference in the body weight between WT and PKR null mice.

A limitation of this experiment is that WT and PKR ablated mice were fed a high fat diet only for the duration of the calorimetric analysis, which lasted 3-4 days. At this time there was no primary difference in weight gain between the mouse cohorts, likely preventing the detection of a significant difference in energy expenditure, secondarily to increased weight gain. Future studies should assess BAT temperature after 10 weeks of high fat diet feeding. We should also take into consideration that during this experiment our animals were single-housed, whereas mice fed the 10-week high fat diet (results from chapter 3) were housed at higher density. This is relevant because the greater the number of animals housed in a cage, the lower is their need for BAT thermogenesis, and this is demonstrated by reduced expression of UCP1 (Himms-Hagen and Villemure 1992). Lastly, the room temperature at which the animals were housed could have affected the outcome of the experiment as previous reports have shown that evaluating thermogenesis at temperatures below thermoneutrality may prevent the detection of differences in the basal metabolic rate of mice. A more accurate means of assessing the contribution of

thermogenesis to energy expenditure might be gained by measuring BAT temperature in response to a cold tolerance test at 4°C (Pisani, Djedaini et al. 2011; Bostrom, Wu et al. 2012). However, one limitation of such a study is that the metabolic rate after cold adaption may increase as a result of elevated shivering rather than thermogenesis. Therefore we propose that future experiments should examine metabolism at thermoneutrality (30°C). An alternate non-invasive method for measuring energy expenditure in the mouse is performed by indirect calorimetry using metabolic chambers. This equipment measures a number of variables including O_2 consumption and CO_2 production, food intake and physical activity to provide valuable information about the energy state of the mouse.

In conjunction with results obtained in single PKR knockout mice, high fat diet fed apoE:PKR knockout mice are also susceptible to weight gain. Notably, the magnitude of weight gain of apoE:PKR knockout mice is less than that seen in single PKR knockout mice, for the reason that ablation of apoE has been shown to be protective against diet induced adiposity (Schreyer, Vick et al. 2002; Hofmann, Perez-Tilve et al. 2008; Karavia, Papachristou et al. 2011). Nevertheless, lack of functional PKR appears to overcome the protective effects of apoE deficiency to promote diet induced weight gain.

It is conceivable that once adipocytes of mice deficient for PKR reach their capacity for storing fat, the surplus lipids are shunted toward ectopic fat storage resulting in fatty liver disease. In accordance with this hypothesis, mice devoid of PKR have significantly increased blood concentration of triglycerides and greater hepatic lipid deposition compared to wild type animals. Previous reports have shown that over-expression of the enzyme DGAT2 in adipocytes promotes triglyceride synthesis resulting in increased blood TG concentration and weight gain. Contrary to the expected outcome, expression of DGAT2 is significantly reduced in the liver of high fat diet fed PKR knockout mice, this finding suggests that PKR-mediated regulation of lipogenesis in the liver is independent of DGAT2. Opposing the observation in liver, expression of DGAT2 is notably, but not significantly elevated in WAT of PKR ablated mice. Transcript levels of DGAT2 are regulated by the transcription factor CEBPβ, whose expression in turn is moderated by PKR (Calkhoven, Muller et al. 2000; Payne, Au et al. 2007). Therefore it was speculated that PKR could suppress liver-specific

transcription of DGAT2 in a CEBPβ dependent manner. However, we show that DGAT2 expression is induced independent of PKRs kinase function, which is essential for translational control of CEBPβ, therefore the proposed mechanism seems less likely to account for PKR-mediated DGAT2 expression.

Besides the established role for DGAT2 in modulating triglyceride synthesis, previous reports have demonstrated that loss of DGAT2 in mice causes dry, cracked skin that lacks elasticity (Stone, Myers et al. 2004). Consistent with this data, high fat diet fed apoE:PKR knockout mice often presented with dry, irritated and inflamed epidermis (data not shown), substantiating a PKR-dependent role in regulation of DGAT2 expression. Collectively these findings implicate PKR in moderating metabolic signalling pathways that govern triglyceride synthesis and transport. Principally I propose that deposition of circulating triglycerides, rather than *de novo* lipogenesis in the liver, is the primary mechanism that explains fatty liver disease in these mice.

The level of lipid in the livers of apoE and apoE:PKR mice fed a high fat diet was comparable and the levels of plasma triglycerides were lower, not higher, in the double knockout mouse. The difference in weight between the apoE and apoE:PKR double knockout mouse demonstrates that modification of lipoprotein profiles alone is not a predisposing factor for obesity in PKR knockout mice since chow fed apoE:PKR knockout animals gain the same weight as apoE knockout mice although they are hyperlipidemic. Instead I speculated that the response to the high fat diet induces primary weight gain, which then modulates secondary metabolic outcomes and disrupts lipoprotein profiles.

In addition to the aforementioned mechanisms, increased concentration of circulating triglycerides could in part be explained by enhanced LDL lipolysis. This speculation is based on the observation that mice devoid of PKR have significantly decreased circulating levels of LDL compared to wild type mice. We expect that augmented hydrolysis of LDLs, rather than defects in LDL assembly or transport, would account for this reduction because expression of the LDL transport protein MTTP is equivalent in PKR knockout and wild type mice.

Consistent with the increased weight gain of high fat diet fed mice ablated for PKR, examination of glucose homeostasis revealed that they are also glucose intolerant and hyperglycemic in the fasted state due to enhanced glucose output. Importantly, glucose tolerance and fasting glucose concentration was comparable in mice fed a chow diet, confirming that the PKR-dependent effects are specifically modulated by the high fat diet. To further explore the contribution of PKR in regulating diabetes, more rigorous measures entailing glucose and insulin clamps are being conducted by our collaborators.

Previous studies have reported that deletion of the eIF2α kinase PERK causes hyperglycemia and diabetes as a result of pancreatic β-cell death and atrophy of the exocrine pancreas caused by ER stress (Harding et al., 2000). This phenotype is unique to animals ablated for PERK as deletion of PKR, GCN2 or HRI has not previously been associated with β-cell death or damage of pancreatic islets of Langerhans (Yang, Reis et al. 1995; Abraham, Stojdl et al. 1999; Guo and Cavener 2007). Accordingly, histopathological examination of the pancreas revealed that WT and PKR knockout mice fed a high fat diet have a morphologically normal exocrine pancreas and islets of Langerhans, devoid of immune cell infiltration and apoptotic cells. Examination of tissue sections by eye however is not a substantial means of assessing cell apoptosis, therefore firm conclusions about cell death cannot be drawn from this type of analysis. To gauge a more quantitative measure of cell death, pancreatic sections should be stained with terminal deoxynucleotidyl transferase dUTP nick end labeling (TUNEL), which detects fragmented DNA.

Furthermore PKR wild type and knockout mice appear to have functional, insulin producing β-cells as demonstrated by comparative insulin staining. An apparent, feature of the exocrine pancreas of mice ablated for PKR was adipocyte infiltration. However, given that this pathology is not common in all PKR knockout mice it most likely does have a significant consequence on the physiological function of the pancreas. Nevertheless, this finding confirms that lack of functional PKR enhances ectopic fat storage.

The primary observation from this analysis was that loss of PKR significantly associated with reduced islet size. Due to time constraints I was unable to thoroughly assess

the cause for the reduction in islet size. However, given that the staining intensity for insulin appears comparable in both animal cohorts, it is conceivable that β-cell destruction does not account for reduced islet size; alternatively the death of α-cells could be a contributing factor. Therefore future studies should measure the number and evaluate the function of pancreatic α-cells by either immunostaining pancreatic sections for glucagon or by measuring circulating concentration of glucagon. It is important to note that I have not adequately ruled out the possibility that insulin resistance, rather than islet insufficiency, accounts for impaired glucose homeostasis in PKR knockout mice. This could be determined by measuring the blood concentration of insulin during a glucose tolerance test. Unfortunately I was unable to collect adequate volumes of blood by cheek puncture during a GTT to perform an insulin ELISA.

Similarly to single PKR ablated mice, apoE:PKR knockout mice fed a high fat diet for 5 weeks have delayed clearance of glucose from the blood in comparison to apoE knockout controls. However, contrasting the findings in PKR knockout mice, apoE:PKR knockout mice have significantly lower fasted blood glucose concentration compared to apoE knockout controls. Surprisingly apoE:PKR knockout mice fed a 30 and 40 week chow diet also have fasting hypoglycemia, despite an absence of glucose intolerance. The apparent divergence in glucose tolerance between apoE:PKR knockout and single PKR knockout mice may be explained for by the protective effects of apoE deficiency. Previous reports show that ablation of apoE improves glucose tolerance, which may provide an adequate explanation for the reduction in glucose defects in apoE:PKR knockout mice compared to PKR knockout mice (Schreyer, Vick et al. 2002; Hofmann, Perez-Tilve et al. 2008). There are a number of other potential explanations for these findings. First, given that weight gain of the apoE:PKR knockout mice does not reflect the weight gain of PKR knockout mice, I would expect suppressed development of secondary metabolic outcomes, accordingly accounting for a reduced difference in glucose sensitivity between apoE:PKR knockout and apoE knockout mice.

Secondly, it may be plausible to speculate that glucagon release is suppressed in mice deficient for PKR. Glucagon plays a central role in glucose homeostasis because it

promotes the conversion of glycogen into glucose, hence loss of glucagon producing α-cells from islets of Langerhans or suppressed ability to secrete glucagon in apoE/PKR knockout mice presents a plausible mechanism explaining fasting hyperglycemia. Glucagon release is also suppressed by free fatty acids and although I did not assess the blood concentration of FFA, I speculate that apoE:PKR deficient mice to have increased rates of lipolysis because they have reduced blood TG levels, which would consequently correlate with elevated concentration of free fatty acids. Confirming this speculation, postprandial glucose levels of apoE:PKR deficient mice is comparable to that of apoE knockout mice, likely because of similar rates of lipolysis in the fed state.

Otherwise heterozygous activating mutations of the glucokinase gene which are known to cause fasting hyperinsulinemic hypoglycemia, may provide a plausible explanation for differences in glucose tolerance between apoE:PKR and PKR knockout mice (Christesen, Jacobsen et al. 2002; Osbak, Colclough et al. 2009). Such mutations stimulate glucokinase activity causing hyperinsulinemia and resultant hypoglycemia. Future studies should identify whether fasting hypoglycemia correlates with elevated levels of insulin caused by activating mutations of the glucokinase gene. Notably, mutations in the glucokinase gene in addition to causing hypoglycemia also provoke the development of diabetes, therefore providing a justification for the involvement of glucokinase in the apoE:PKR knockout and PKR knockout mice to differentially modulate glucose homeostasis. Importantly, variations in fasted blood glucose levels can also be accounted for by experiment design, because blood glucose concentration of apoE:PKR knockout mice is measured after 5 weeks of HFD and after 10 weeks in single PKR knockout mice, possibly capturing separate progressive events.

Collectively, these findings implicate PKR in the pathogenesis of the metabolic syndrome in response to high fat diets. Importantly these findings demonstrate that primary weight gain caused by high fat diets culminates in secondary responses that impair glucose sensitivity and promote dyslipidemia. Furthermore, PKR modulates protective responses to high fat diet by altering the expression of genes involved in major metabolic biochemical pathways for triglyceride synthesis. Overall, PKR is protective against diet-induced pathologies.

The K271R homozygote animal is created by a single point mutation of the lysine residue 271 to an arginine to create a kinase dead PKR mutant protein. As alluded to in chapter 1 the K271R homozygote animal may retain some capacity to participate in cell signalling events because of its conformation that exposes the RNA-binding domains. For these reasons, in addition to exploring the physiological responses of K271R homozygote mice to high fat diet, I also assessed the responses of K271R heterozygote mice.

The conformity in the responses between the WT and K271R homozygous mice demonstrates that the kinase function is dispensable for the PKR-dependent protection from high fat diet induced weight gain and dyslipidemia. It remains difficult to definitively account for the function of PKR, because if the protein functions solely as a scaffold then the K271R heterozygote mice should also have phenocopied the WT animal. Instead, this mouse showed significantly greater weight gain compared to either K271R homozygote or wild type animals in response to high fat diet feeding. Rather, the weight gain of the K271R heterozygote mice is comparable to that of PKR knockout mice, suggesting that PKR governs similar signalling events in these animal models to modulate the development of metabolic disease. Consistent with results observed in PKR knockout mice, K271R heterozygote mice are hyperglycaemic after fasting and have elevated total blood glucose concentration during a GTT, compared to wild type or K271R homozygote mice, suggesting delayed glucose clearance. Notably, the K271R homozygote mice have an intermediary effect on blood glucose concentration, suggesting that the partial ability of the mutant PKR protein to signal via its RBD protects against the development of glucose intolerance. The result showing that K271R homozygote mice have smaller islets of Langerhans suggests that a change in islet size does not account for glucose intolerance. Hence it is likely that reduced islet size in PKR knockout mice does not account for the change in glucose tolerance or weight gain. Moreover, the K271R heterozygote mouse has normal islets of Langerhans but became obese on a high fat diet. It has previously been established that the K271R mutant protein homodimerizes with the WT PKR protein to inhibit the kinase activity of the WT PKR in a dominant negative fashion (Fig.3.22E). Based on this, I expect there to be only limited amounts of catalytically active PKR in the K271R heterozygote animal. However, it cannot be

excluded that the remaining catalytic activity is of some physiological consequence. An additional complicating factor in these experiments is that the levels of PKR expressed by the different mice (PKR WT, knockout, K271R heterozygote and homozygote) are not equivalent, as PKR regulates its own expression level via control of translation. Preliminary work from my lab suggests that the K271R homozygous mouse has significantly more PKR protein than the heterozygous or wild type mouse. The heightened levels of kinase dead PKR in the K271R homozygous mice may account for the disparate effects between the heterozygous and homozygous K271R mice. Collectively these findings suggest that absence of PKR causes severe glucose intolerance and weight gain, which is not resolved by intermediary levels of expression of kinase dead PKR, but that can be rescued by high level expression of kinase dead PKR.

A report has argued that deletion of exons 2-4 in the N-terminal region of the PKR gene to create the PKR knockout mice, results in the transcription of a small PKR transcript that retains some kinase activity (Baltzis, Li et al. 2002). Our laboratory has not been able to confirm these findings. If true, it is plausible that the K271R heterozygote mouse might replicate the effect of incompletely ablating PKR by replicating low-level kinase activity. How a reduced level of kinase activity, compared to the WT animal, exacerbates weight gain, while complete ablation of kinase activity (in the homozygous K271R mouse) is difficult to explain. The mechanism responsible for reduced islet size in the K271R homozygote mouse, without affecting glucose homeostasis is still largely unknown and requires further investigation. Nonetheless, this rescue is not complete due to the difference in islet size between K271R homozygote and wild type mice. Therefore it appears that the partial loss of both PKRs adaptor function, which inhibits signalling, mediated via protein-protein interactions, and kinase activity, contributes to the pathogenesis of obesity and glucose intolerance.

Interestingly, a report published by Nakamura et al (2010) during my studies shows an opposing function for PKR in diet induced obesity and diabetes compared to the role I establish for PKR in this thesis. Contrasting our results they show that wild type mice are obese, hyperinsulinemic and glucose intolerant compared to mice lacking functional PKR.

There are several differences between our study and that of Nakamura (2010). Nakamura et al, used an alternate animal mouse model of PKR deficiency, created through deletion of exon 12 in the C-terminal domain of the PKR gene (Abraham, Stojdl et al. 1999). This animal produces a small PKR transcript that encodes the N-terminus of PKR that is translated to produce normal levels of PKR dsRNA binding domain (Baltzis, Li et al. 2002). A number of studies have demonstrated contrasting physiological responses of these C-PKR and N-PKR targeted animal. This may equate to some extent to our observations with the WT, PKR ablated and heterozygous versus homozygous K271R transgenic mice, with the latter mice also expressing the RNA-binding domains of PKR. Hence, the N-terminal RNA-binding domains could account for the unexpected variance between the different transgenic mice. A number of studies have demonstrated that homologous RNA-binding domains from different proteins interact. PKR has been demonstrated to inhibit several proteins in this manner. Inhibition of other proteins that encode RNA-binding domains might explain some of these discrepancies, and the relative level of protein expression could account for the difference between the heterozygous and homozygous K271R mice.

Other differences between my study and Nakamura's (2010) include the genetic backgrounds. In our experiments we used the isogenic C57Bl6J mice, versus a mixed background Balbc:129Sv used in the Nakamura et al study. C57Bl6J mice are more prone to weight gain, hyperglycemia, hyperinsulinemia and the development of diabetes in comparison to the 129SV strain (Kulkarni, Almind et al. 2003). Genome wide scans have also revealed that C57bl6 mice have increased expression of protein kinase C-delta, which is a region on chromosome 14 linked to insulin resistance and hyperinsulinemia (Almind and Kahn 2004; Bezy, Tran et al. 2011). Alternatively environmental factors may also explain some of these discrepancies. Growing evidence suggests that gut microbiota composition plays an important role in diet induced obesity, insulin resistance and glucose intolerance. The mechanism by which this occurs is still largely unclear (Backhed 2011). The gut microbiota harvests energy from foods and plays an important role in nutrient absorption. Interestingly, transplation of obese-gut microbiota into germ-free mice significantly

increases their adiposity, clearly identifying the importance of gut microbiota in the pathogenesis of obesity (Cani, Osto et al. 2012; Tremaroli and Backhed 2012).

3.6 CONCLUSION

The findings in this chapter demonstrate that PKR protects against the development of high fat diet induced metabolic disease by modulating whole body metabolic homeostasis. The beneficial effects of PKR are in part to inhibit DGAT2-mediated triglyceride synthesis and to suppress adipose tissue hypertrophy. PKR is also implicated in modulating efficient blood glucose clearance and the maintenance of functional islets of Langerhans in response to high fat diets. Importantly, the discovery that the kinase activity of PKR is dispensable to modulate weight gain but required for normal development of the islets of the pancreas is intriguing. The next chapter focuses on elucidating the PKR dependent mechanism responsible for regulating homeostasis.

3.7 REFERENCES

Abraham, N., D. F. Stojdl, et al. (1999). "Characterization of transgenic mice with targeted disruption of the catalytic domain of the double-stranded RNA-dependent protein kinase, PKR." J Biol Chem **274**(9): 5953-5962.

Almind, K. and C. R. Kahn (2004). "Genetic determinants of energy expenditure and insulin resistance in diet-induced obesity in mice." Diabetes **53**(12): 3274-3285.

Backhed, F. (2011). "Programming of host metabolism by the gut microbiota." Ann Nutr Metab **58 Suppl 2**: 44-52.

Baltzis, D., S. Li, et al. (2002). "Functional characterization of pkr gene products expressed in cells from mice with a targeted deletion of the N terminus or C terminus domain of PKR." J Biol Chem **277**(41): 38364-38372.

Belgardt, B. F., J. Mauer, et al. (2010). "Hypothalamic and pituitary c-Jun N-terminal kinase 1 signaling coordinately regulates glucose metabolism." Proc Natl Acad Sci U S A **107**(13): 6028-6033.

Bezy, O., T. T. Tran, et al. (2011). "PKCdelta regulates hepatic insulin sensitivity and hepatosteatosis in mice and humans." J Clin Invest **121**(6): 2504-2517.

Bonnet, M. C., R. Weil, et al. (2000). "PKR stimulates NF-kappaB irrespective of its kinase function by interacting with the IkappaB kinase complex." Mol Cell Biol **20**(13): 4532-4542.

Bostrom, P., J. Wu, et al. (2012). "A PGC1-alpha-dependent myokine that drives brown-fat-like development of white fat and thermogenesis." Nature **481**(7382): 463-468.

Calkhoven, C. F., C. Muller, et al. (2000). "Translational control of C/EBPalpha and C/EBPbeta isoform expression." Genes Dev **14**(15): 1920-1932.

Cani, P. D., M. Osto, et al. (2012). "Involvement of gut microbiota in the development of low-grade inflammation and type 2 diabetes associated with obesity." Gut Microbes **3**(4): 279-288.

Chiang, S. H., M. Bazuine, et al. (2009). "The protein kinase IKKepsilon regulates energy balance in obese mice." Cell **138**(5): 961-975.

Christesen, H. B., B. B. Jacobsen, et al. (2002). "The second activating glucokinase mutation (A456V): implications for glucose homeostasis and diabetes therapy." Diabetes **51**(4): 1240-1246.

Chu, W. M., D. Ostertag, et al. (1999). "JNK2 and IKKbeta are required for activating the innate response to viral infection." Immunity **11**(6): 721-731.

Falk, E. (2006). "Pathogenesis of atherosclerosis." J Am Coll Cardiol **47**(8 Suppl): C7-12.

Gil, J., J. Alcami, et al. (2000). "Activation of NF-kappa B by the dsRNA-dependent protein kinase, PKR involves the I kappa B kinase complex." Oncogene **19**(11): 1369-1378.

Grant, P. J. (2005). "Inflammatory, atherothrombotic aspects of type 2 diabetes." Curr Med Res Opin **21 Suppl 1**: S5-12.

Greenow, K., N. J. Pearce, et al. (2005). "The key role of apolipoprotein E in atherosclerosis." J Mol Med **83**(5): 329-342.

Guo, F. and D. R. Cavener (2007). "The GCN2 eIF2alpha kinase regulates fatty-acid homeostasis in the liver during deprivation of an essential amino acid." Cell Metab **5**(2): 103-114.

Himes, R. W. and C. W. Smith (2010). "Tlr2 is critical for diet-induced metabolic syndrome in a murine model." FASEB J **24**(3): 731-739.

Himms-Hagen, J. and C. Villemure (1992). "Number of mice per cage influences uncoupling protein content of brown adipose tissue." Proc Soc Exp Biol Med **200**(4): 502-506.

Hofmann, S. M., D. Perez-Tilve, et al. (2008). "Defective lipid delivery modulates glucose tolerance and metabolic response to diet in apolipoprotein E-deficient mice." Diabetes **57**(1): 5-12.

Karavia, E. A., D. J. Papachristou, et al. (2011). "Deficiency in apolipoprotein E has a protective effect on diet-induced nonalcoholic fatty liver disease in mice." FEBS J **278**(17): 3119-3129.

Kulkarni, R. N., K. Almind, et al. (2003). "Impact of genetic background on development of hyperinsulinemia and diabetes in insulin receptor/insulin receptor substrate-1 double heterozygous mice." Diabetes **52**(6): 1528-1534.

Lockie, S. H., K. M. Heppner, et al. (2012). "Direct control of brown adipose tissue thermogenesis by central nervous system glucagon-like peptide-1 receptor signaling." Diabetes **61**(11): 2753-2762.

Lumeng, C. N. and A. R. Saltiel (2011). "Inflammatory links between obesity and metabolic disease." J Clin Invest **121**(6): 2111-2117.

Osbak, K. K., K. Colclough, et al. (2009). "Update on mutations in glucokinase (GCK), which cause maturity-onset diabetes of the young, permanent neonatal diabetes, and hyperinsulinemic hypoglycemia." Hum Mutat **30**(11): 1512-1526.

Payne, V. A., W. S. Au, et al. (2007). "Sequential regulation of diacylglycerol acyltransferase 2 expression by CAAT/enhancer-binding protein beta (C/EBPbeta) and C/EBPalpha during adipogenesis." J Biol Chem **282**(29): 21005-21014.

Piedrahita, J. A., S. H. Zhang, et al. (1992). "Generation of mice carrying a mutant apolipoprotein E gene inactivated by gene targeting in embryonic stem cells." Proc Natl Acad Sci U S A **89**(10): 4471-4475.

Pindel, A. (2008). "Investigating a role for PKR in atherosclerosis." Monash University.

Pindel, A. and A. Sadler (2011). "The role of protein kinase R in the interferon response." J Interferon Cytokine Res **31**(1): 59-70.

Pisani, D. F., M. Djedaini, et al. (2011). "Differentiation of Human Adipose-Derived Stem Cells into "Brite" (Brown-in-White) Adipocytes." Front Endocrinol (Lausanne) **2**: 87.

Plump, A. S., J. D. Smith, et al. (1992). "Severe hypercholesterolemia and atherosclerosis in apolipoprotein E-deficient mice created by homologous recombination in ES cells." Cell **71**(2): 343-353.

Sadler, A. J. (2010). "Orchestration of the activation of protein kinase R by the RNA-binding motif." J Interferon Cytokine Res **30**(4): 195-204.

Samuel, V. T., Z. X. Liu, et al. (2004). "Mechanism of hepatic insulin resistance in non-alcoholic fatty liver disease." J Biol Chem **279**(31): 32345-32353.

Schreyer, S. A., C. Vick, et al. (2002). "LDL receptor but not apolipoprotein E deficiency increases diet-induced obesity and diabetes in mice." Am J Physiol Endocrinol Metab **282**(1): E207-214.

Seppala-Lindroos, A., S. Vehkavaara, et al. (2002). "Fat accumulation in the liver is associated with defects in insulin suppression of glucose production and serum free fatty acids independent of obesity in normal men." J Clin Endocrinol Metab **87**(7): 3023-3028.

Solomon, D. H., N. J. Goodson, et al. (2006). "Patterns of cardiovascular risk in rheumatoid arthritis." Ann Rheum Dis **65**(12): 1608-1612.

Steinberg, D. (1987). "Lipoproteins and the pathogenesis of atherosclerosis." Circulation **76**(3): 508-514.

Stokes, K. Y., D. Cooper, et al. (2002). "Hypercholesterolemia promotes inflammation and microvascular dysfunction: role of nitric oxide and superoxide." Free Radic Biol Med **33**(8): 1026-1036.

Stone, S. J., H. M. Myers, et al. (2004). "Lipopenia and skin barrier abnormalities in DGAT2-deficient mice." J Biol Chem **279**(12): 11767-11776.

Tremaroli, V. and F. Backhed (2012). "Functional interactions between the gut microbiota and host metabolism." Nature **489**(7415): 242-249.

Yang, Y. L., L. F. Reis, et al. (1995). "Deficient signaling in mice devoid of double-stranded RNA-dependent protein kinase." EMBO J **14**(24): 6095-6106.

Zamanian-Daryoush, M., T. H. Mogensen, et al. (2000). "NF-kappaB activation by double-stranded-RNA-activated protein kinase (PKR) is mediated through NF-kappaB-inducing kinase and IkappaB kinase." Mol Cell Biol **20**(4): 1278-1290.

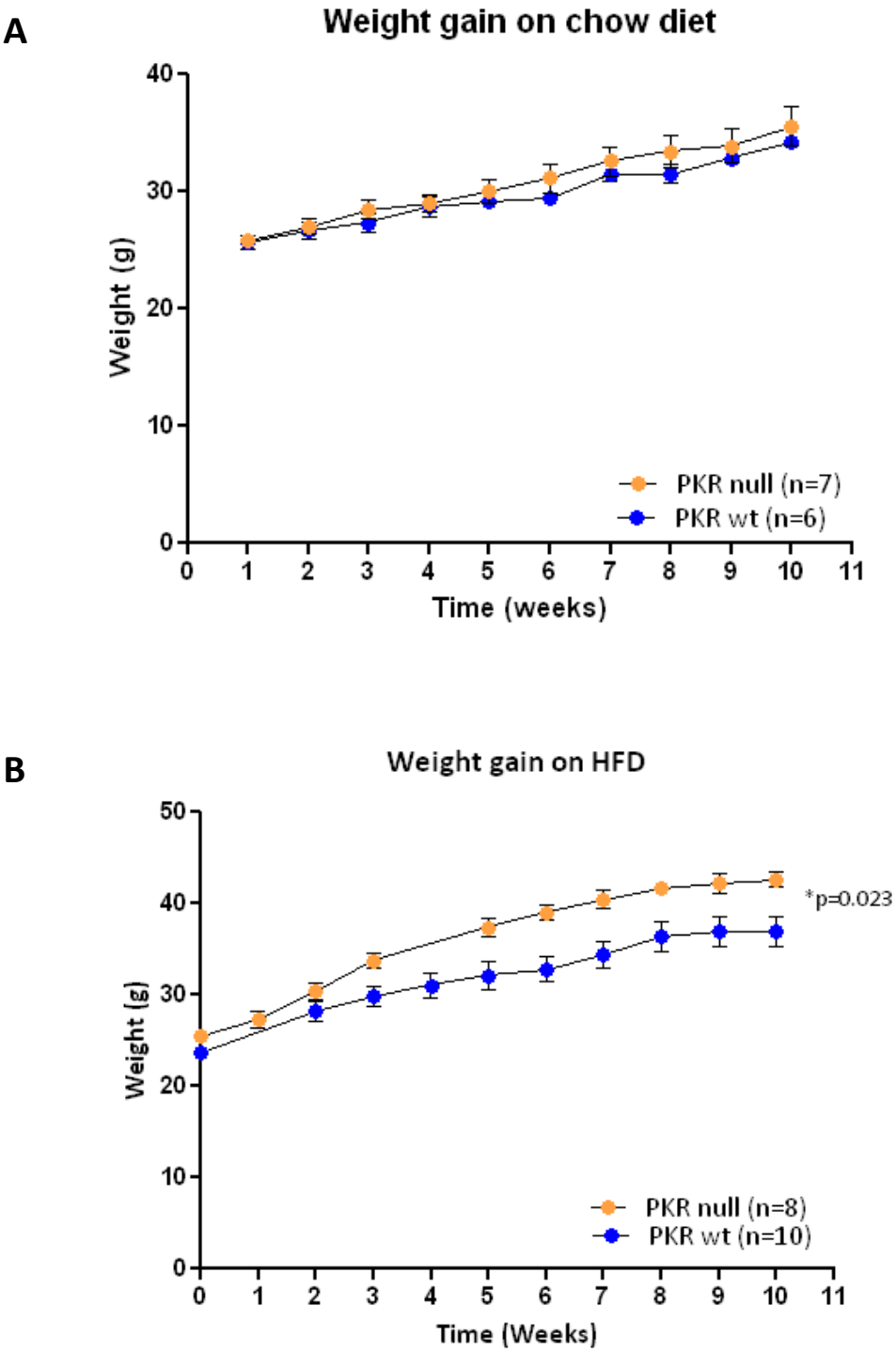

Figure 3.1 Weight gain of PKR wt and null mice fed a high fat or chow diet.

Weight gain of **A** Eight week old PKR wt (n=6) and PKR null (n=7) mice fed a chow diet for ten weeks, **B** Eight week old PKR wt (n=10) and null (n=8) mice fed a high fat diet for ten weeks. Statistical analysis: linear regression, mean±SEM. *Statistically significant.

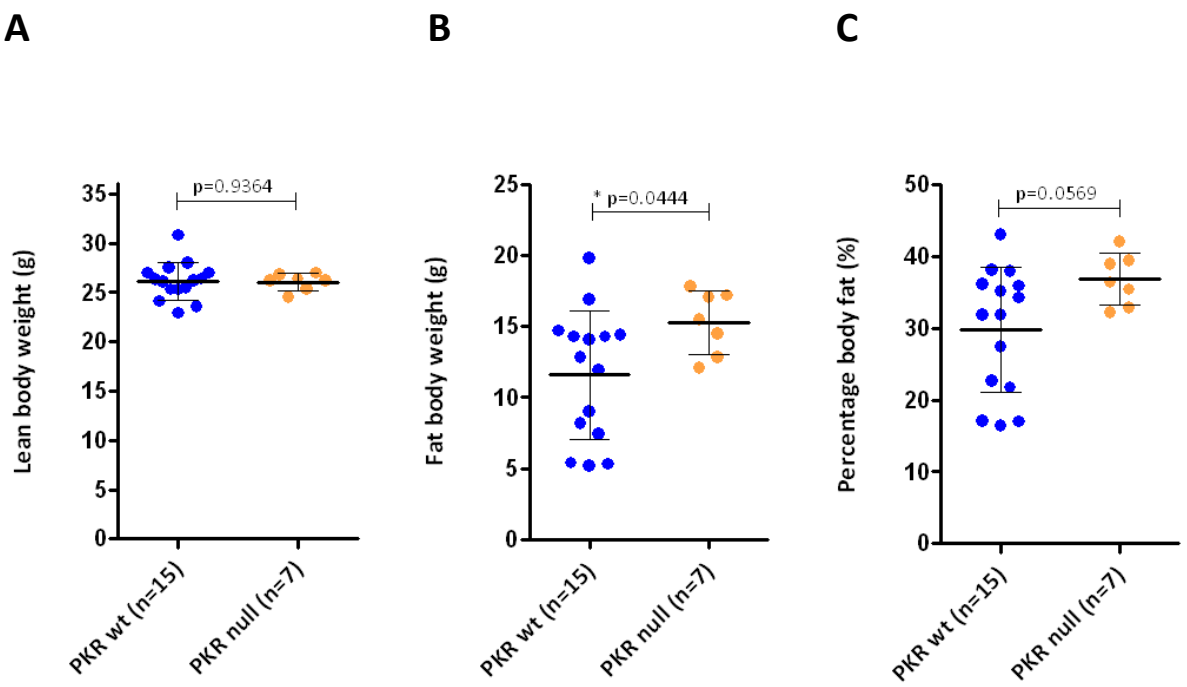

Figure 3.2 Body mass composition of PKR wt and null mice fed a high fat diet.

Data compiled from DEXA scans of PKR wt (n=15) and null (n=7) mice fed a high fat diet for ten weeks showing **A** lean body weight (g) (p=0.9364), **B** fat body weight (g) (*p=0.044) and **C** total percentage (%) of body fat (p=0.057). Statistical analysis Mann-Whitney U-test, mean±SD. *Statistically significant.

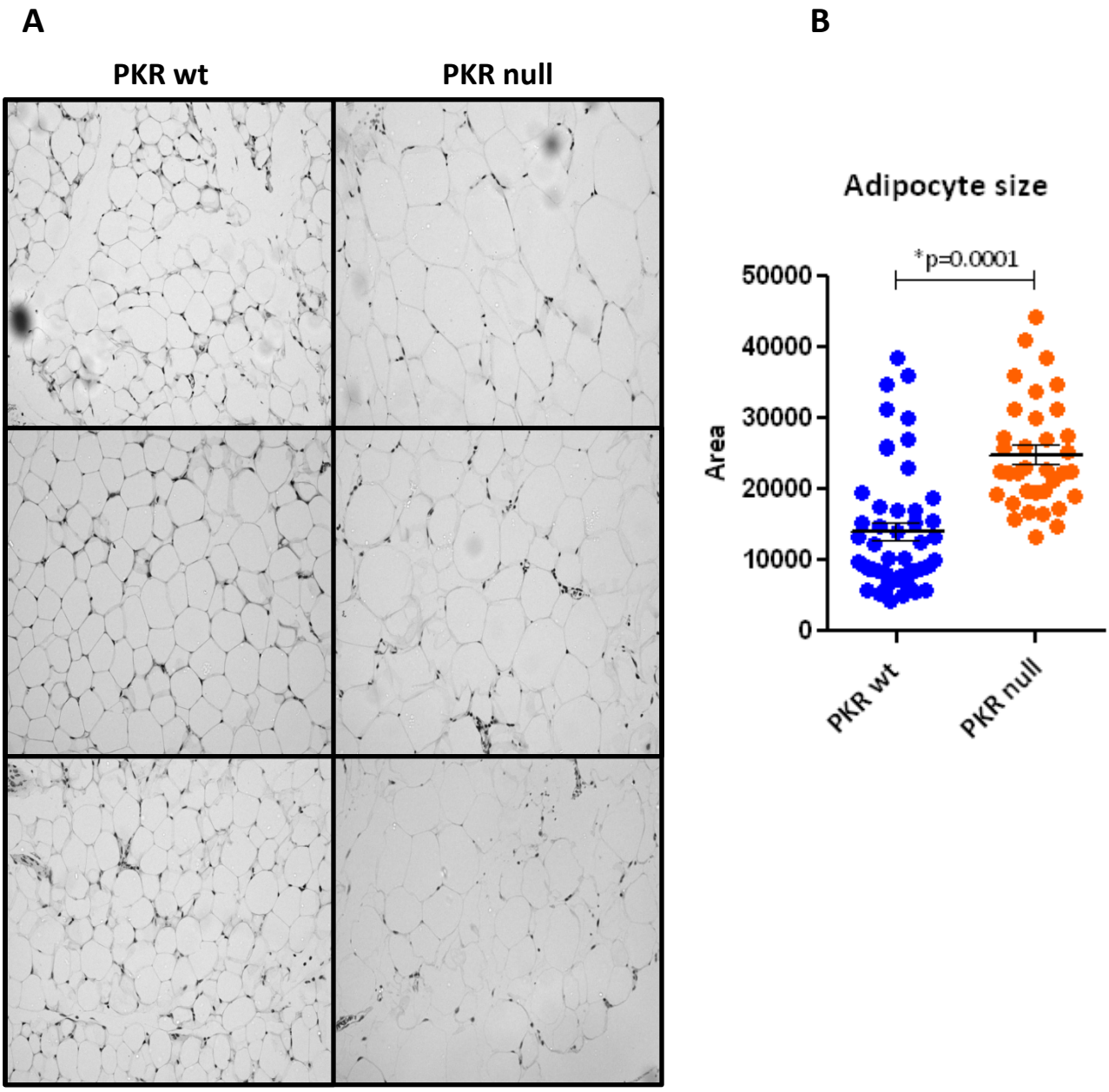

Figure 3.3 White adipose tissue sections from PKR wt and null mice fed a high fat diet.

A Frozen white adipose tissue sections (5µM), fixed in 10% formalin. Sections from three representative wt and PKR null mice, **B** adipocyte size quantification (Image J). Statistical analysis: unpaired T-test, mean±SEM.*Statistically significant.

A

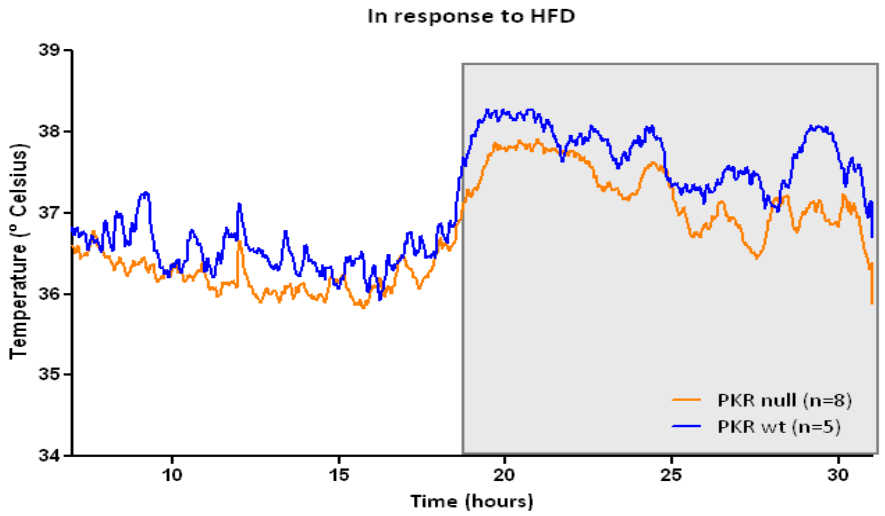
In response to HFD
Temperature (° Celsius)
39
38
37
36
35
34
10
15
20
25
30
Time (hours)
PKR null (n=8)
PKR wt (n=5)

B

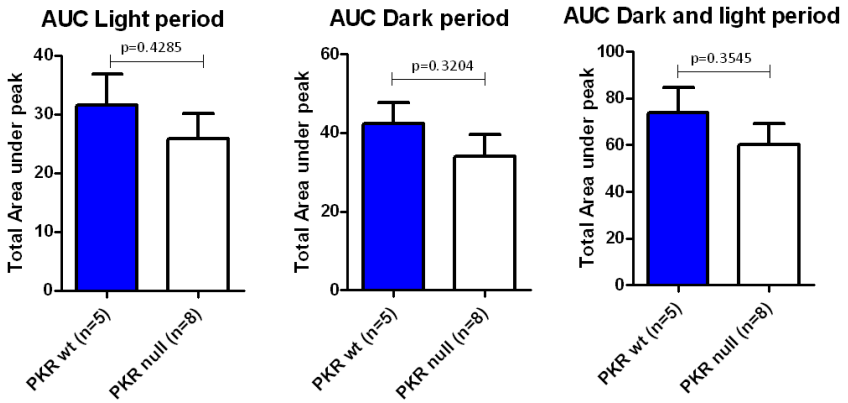
AUC Light period
p=0.4285
Total Area under peak
40
30
20
10
0
PKR wt (n=5)
PKR null (n=8)
AUC Dark period
p=0.3204
60
40
20
0
AUC Dark and light period
p=0.3545
100
80
60
40
20
0

C

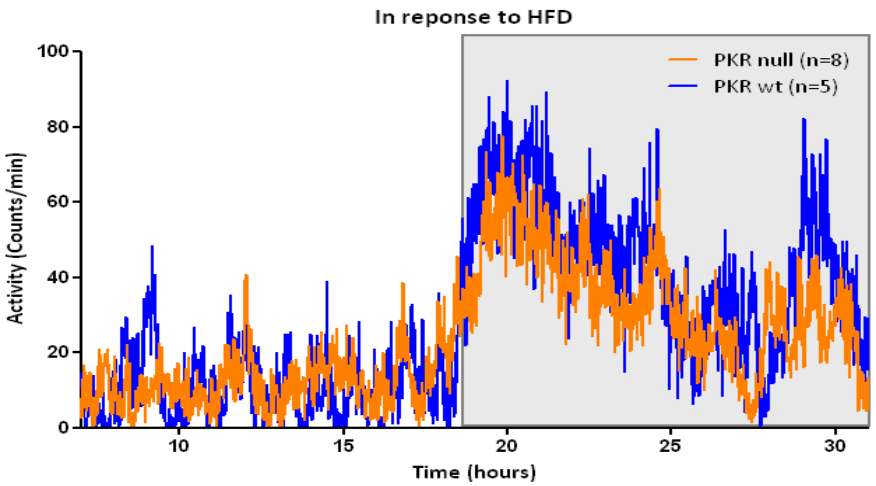
In reponse to HFD
PKR null (n=8)
PKR wt (n=5)
Activity (Counts/min)
100
80
60
40
20
0
10
15
20
25
30
Time (hours)

D

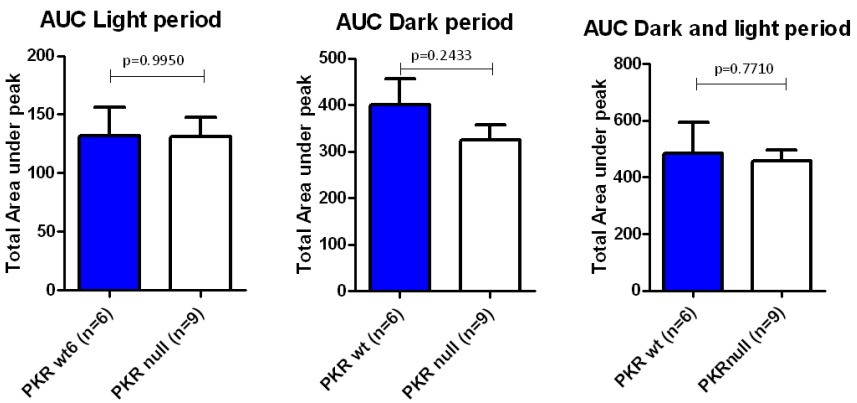
AUC Light period
p=0.9950
Total Area under peak
200
150
100
50
0
PKR wt6 (n=6)
PKR null (n=9)
AUC Dark period
p=0.2433
500
400
300
200
100
0
AUC Dark and light period
p=0.7710
800
600
400
200
0
PKR wt (n=6)
PKRnull (n=9)

Figure 3.4 Temperature and physical activity in PKR wt and null mice in response to high fat diet.

A BAT temperature over 24 hours, **B** AUC for dark period, light period and over 24 hours for BAT thermogenesis , **C** locomotor activity over 24 hours, **D** AUC for dark period, light period and 24 hours for locomotor activity. Gray area represents the dark period. Statistical analysis: area under curve, results are mean ± SEM.

A

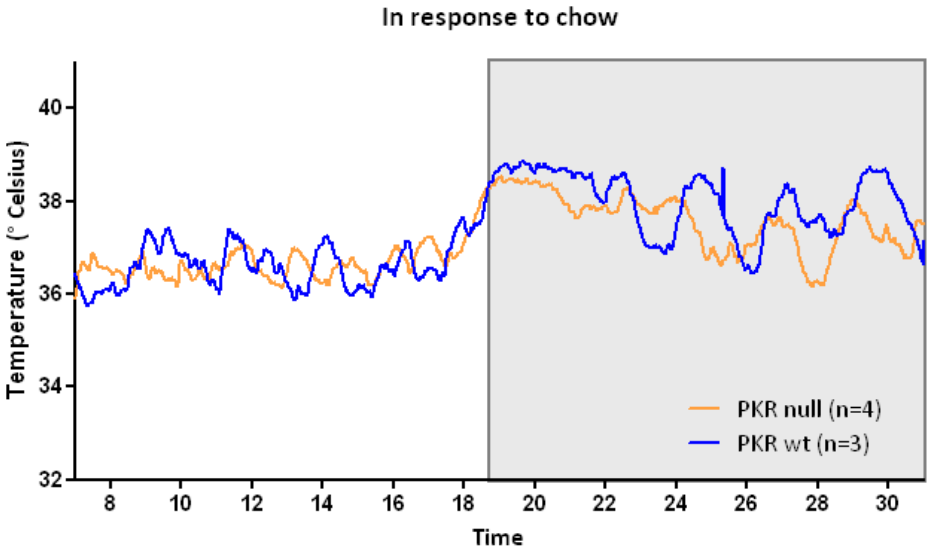
In response to chow
Temperature (° Celsius)
40
38
36
34
32
8
10
12
14
16
18
20
22
24
26
28
30
Time
PKR null (n=4)
PKR wt (n=3)

B

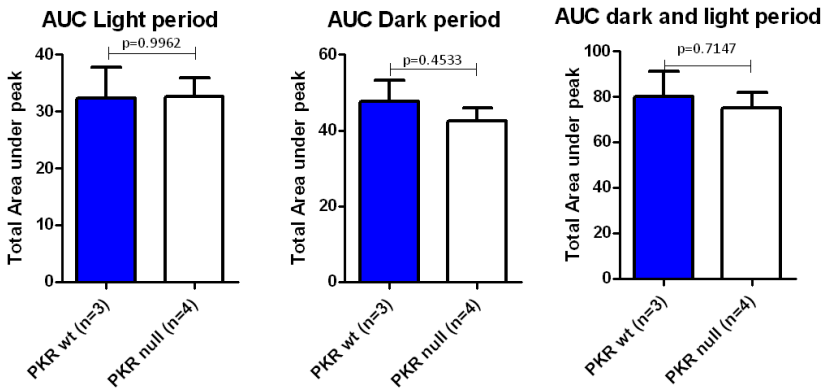
AUC Light period
p=0.9962
Total Area under peak
40
30
20
10
0
PKR wt (n=3)
PKR null (n=4)
AUC Dark period
p=0.4533
60
40
20
0
AUC dark and light period
p=0.7147
100
80
60
40
20
0

C

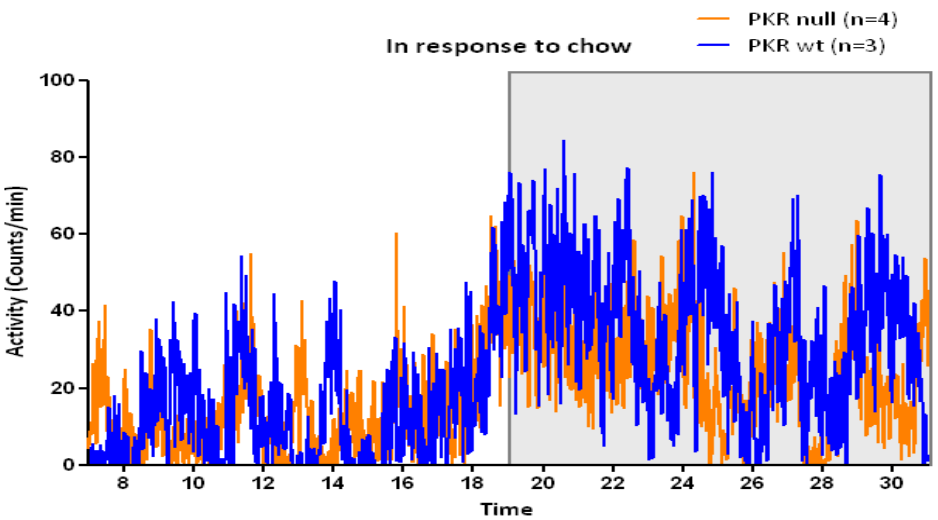
In response to chow
PKR null (n=4)
PKR wt (n=3)
Activity (Counts/min)
100
80
60
40
20
0
8
10
12
14
16
18
20
22
24
26
28
30
Time

D

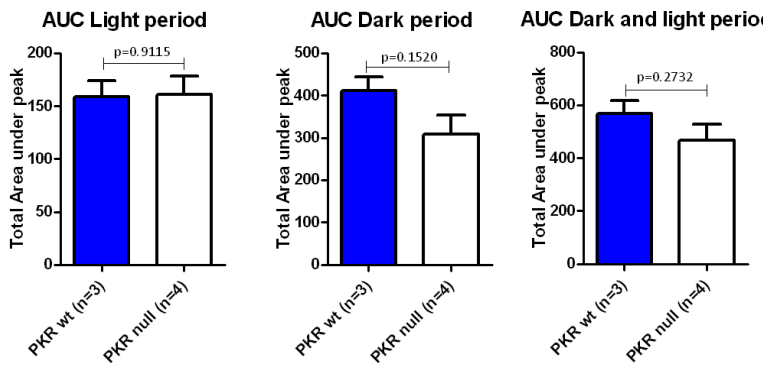
AUC Light period
p=0.9115
Total Area under peak
200
150
100
50
0
PKR wt (n=3)
PKR null (n=4)
AUC Dark period
p=0.1520
500
400
300
200
100
0
AUC Dark and light period
p=0.2732
800
600
400
200
0

Figure 3.5 Temperature and physical activity in PKR wt and null mice in response to chow diet.

A BAT temperature over 24 hours, **B** AUC for dark period, light period and over 24 hours for BAT thermogenesis , **C** locomotor activity over 24 hours, **D** AUC for dark period, light period and 24 hours for locomotor activity. Gray area represents the dark period. Statistical analysis: area under curve, results are mean ± SEM.

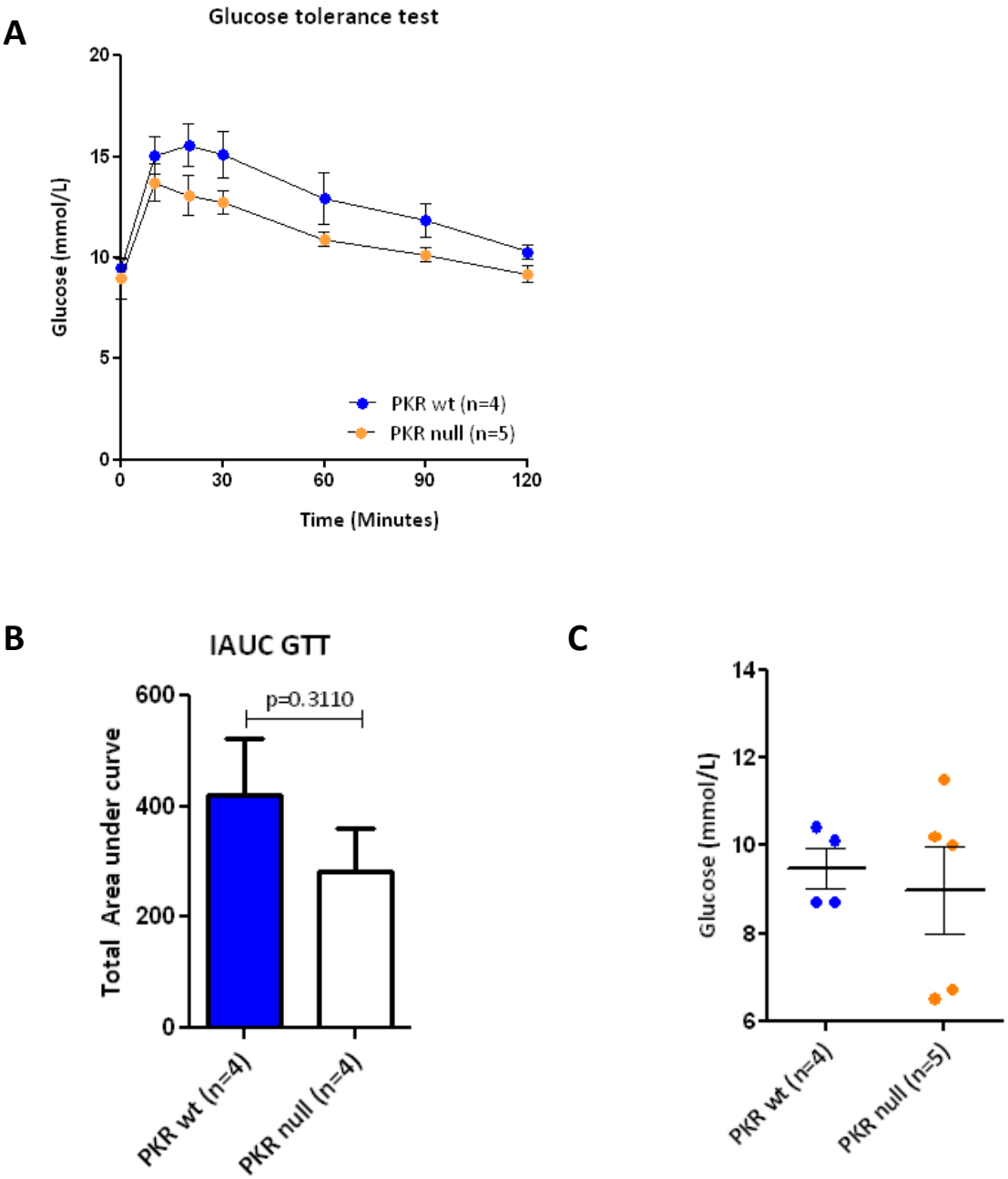

Figure 3.6 Glucose tolerance test in response to chow diet.

A Glucose tolerance of PKR wt (n=4) and PKR null (n=5) animals fed a chow diet for ten weeks. Statistical analysis of GTT time points comparing wt and PKR null mice: 0min p=0.6941, 10min p=0.3375, 20min p=0.1321, 30min p=0.0867, 60min p=0.1362, 90min p=0.0780, 120min p=0.089. **B** bar graph representing the total area under curve analysed for a GTT analysed by IAUCC. **C** blood glucose concentration measured after 16 hours of fasting in PKR wt (n=4) and PKR null (n=5) animals fed a chow diet for 10 weeks. Statistical analysis: unpaired T-test, mean±SEM.*Statistically significant.

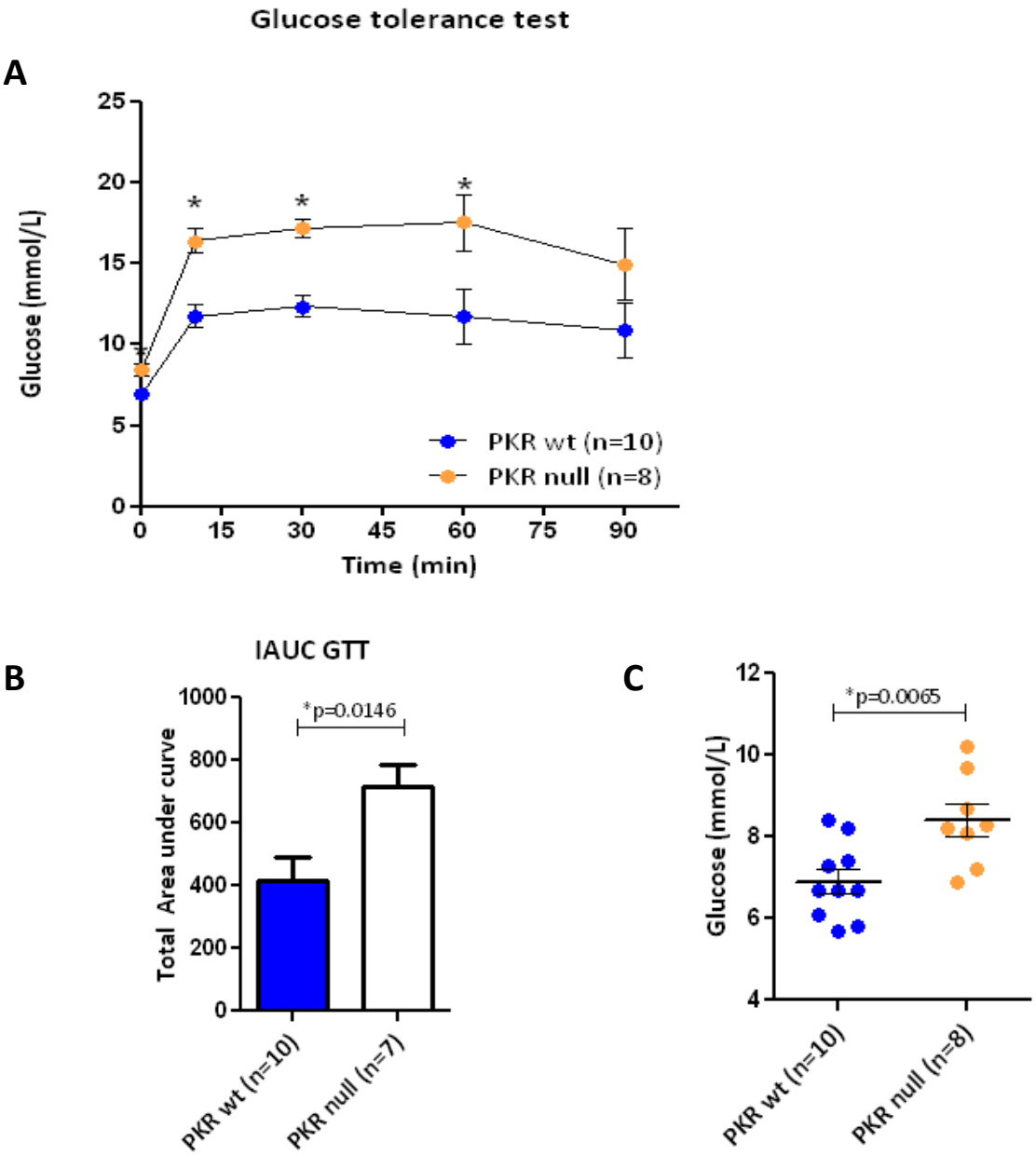

Figure 3.7 Glucose tolerance test in response to high fat diet.

A Glucose tolerance test of wt (n=10) and PKR null (n=8) animals fed a chow diet for ten weeks. Statistical analysis of GTT time points comparing PKR wt and PKR null mice: *0min p=0.0.0065, *10min p=0.0005, *30min p=0.0001, *60min p=0.0.0326, 90min p=0.1543. **B** incremental area under curve analysis for GTT (p=0.0146). **C** blood glucose concentration 16 hours post fasting in PKR wt (n=10) and PKR null (n=8) animals fed a high fat diet for 10 weeks (p=0.0065). Statistical analysis: unpaired T-test, mean±SEM.*Statistically significant.

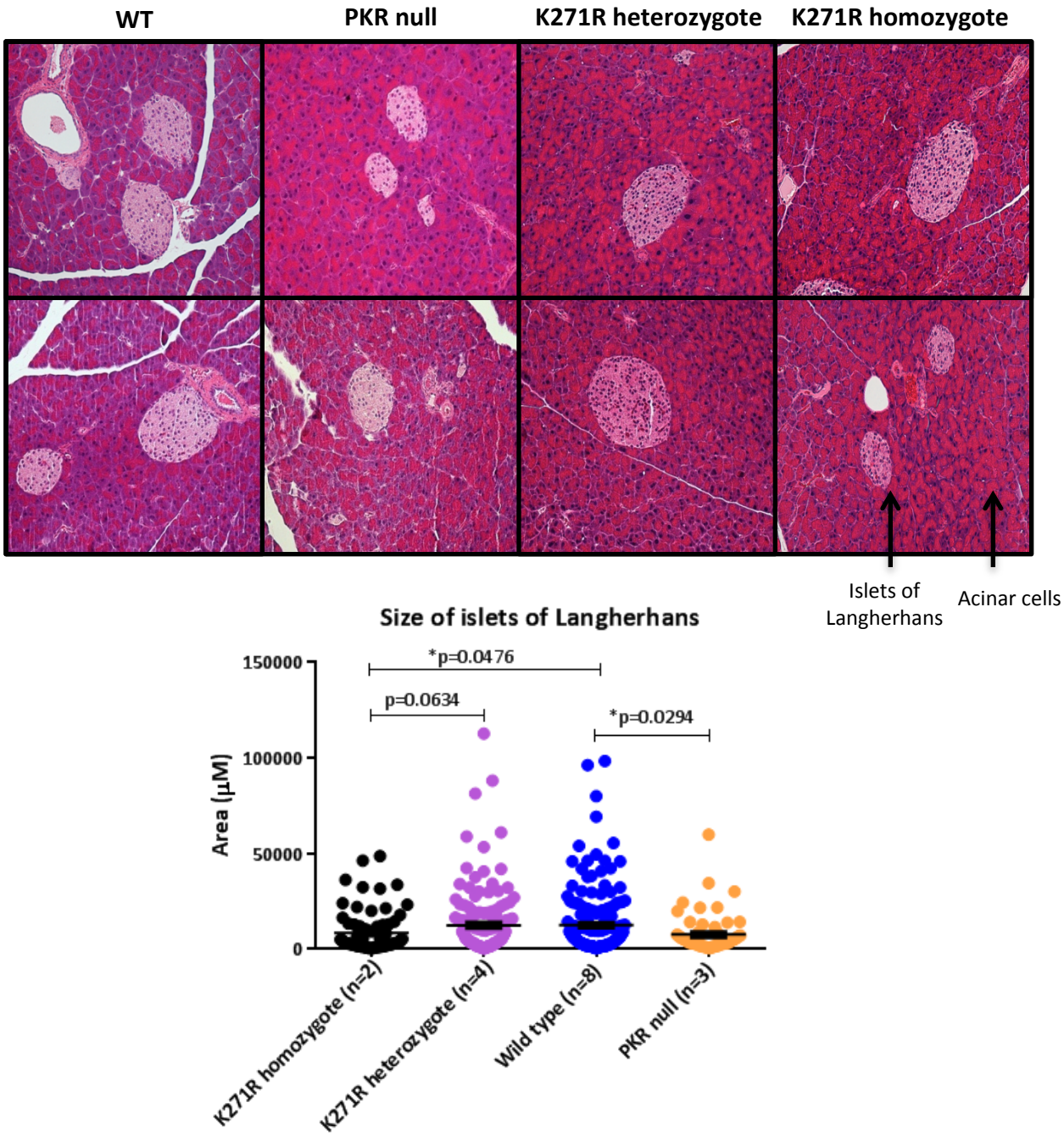

Figure 3.8 Pancreatic β-cell morphology in Wt and PKR null, or mutant mice fed a high fat diet.

Paraffin sections (5µM) of pancreas from PKR wt and null animals fed a high fat diet for ten weeks. **A** H&E stained pancreas sections, magnification 10X, showing round and undisrupted islets of Langerhans stained in lighter pink, surrounded by acinar cells, **B** quantification of islet size expressed as area (µM) (Aperio, ImageScope software).

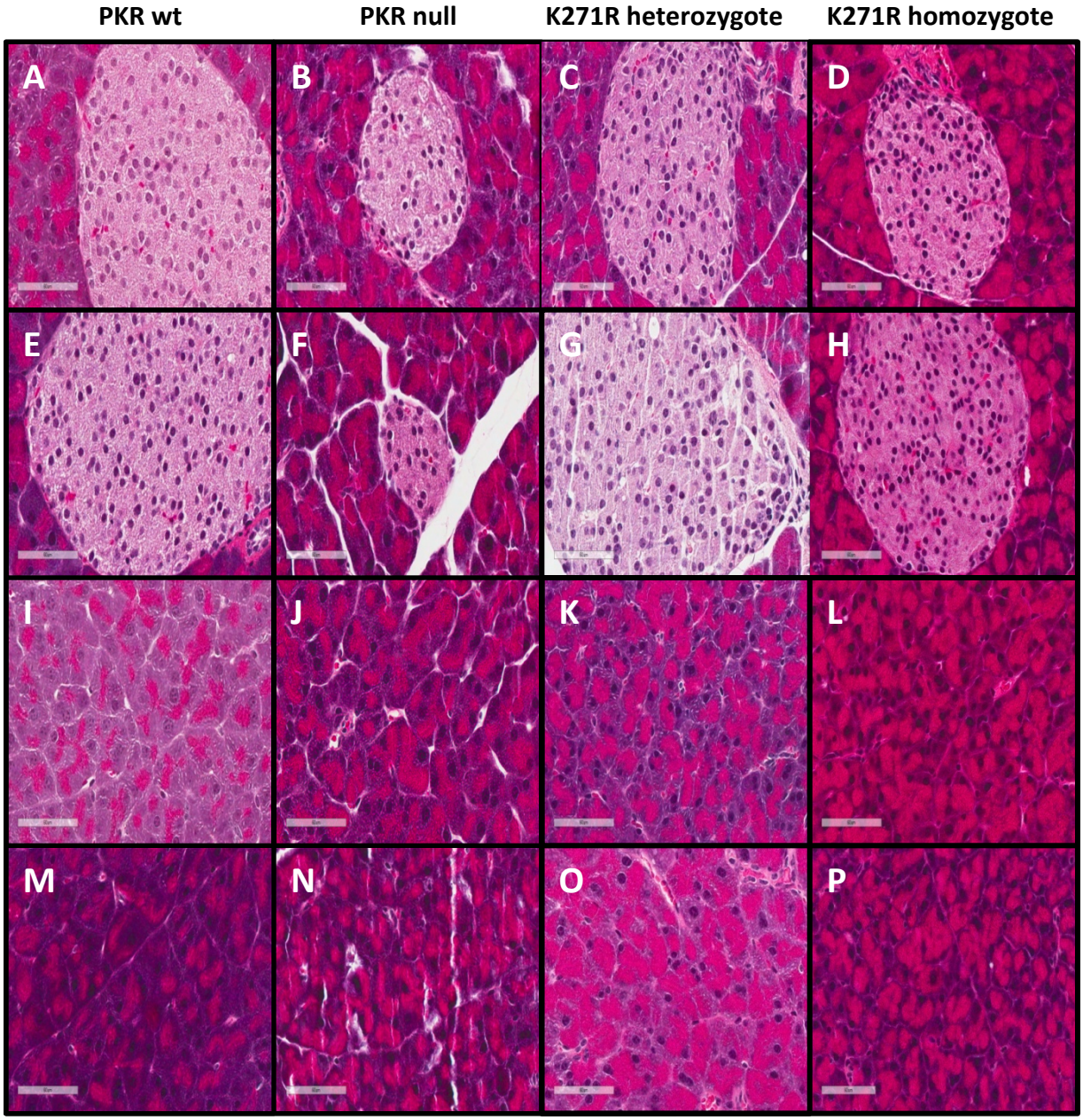
PKR wt
PKR null
K271R heterozygote
K271R homozygote
A
B
C
D
E
F
G
H
I
J
K
L
M
N
O
P

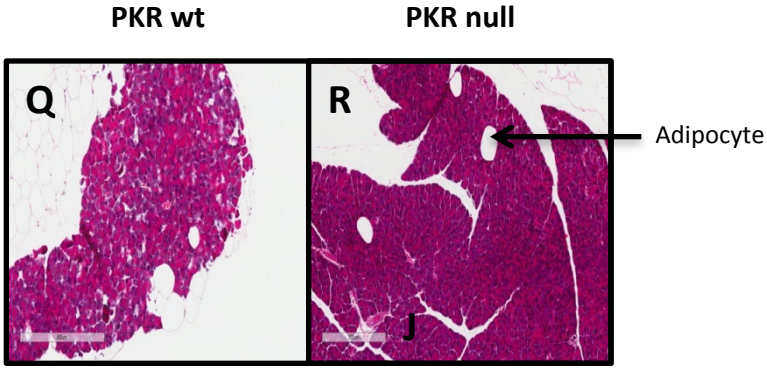
PKR wt
PKR null
Q
R
Adipocyte
J

Figure 3.9 Pancreatic β-cell morphology in wt, PKR null and mutant mice fed a high fat diet.

H&E stained paraffin sections (5μM) of pancreas from PKR wt and null or kinase-dead (mutant K271R) animals fed a high fat diet for ten weeks. **A-H** 40X magnification of islets of Langerhans, **I-P** 40X, magnification of acinar cells and **Q** and **R** the replacement of some acinar cells by adipocytes in PKR null mice.

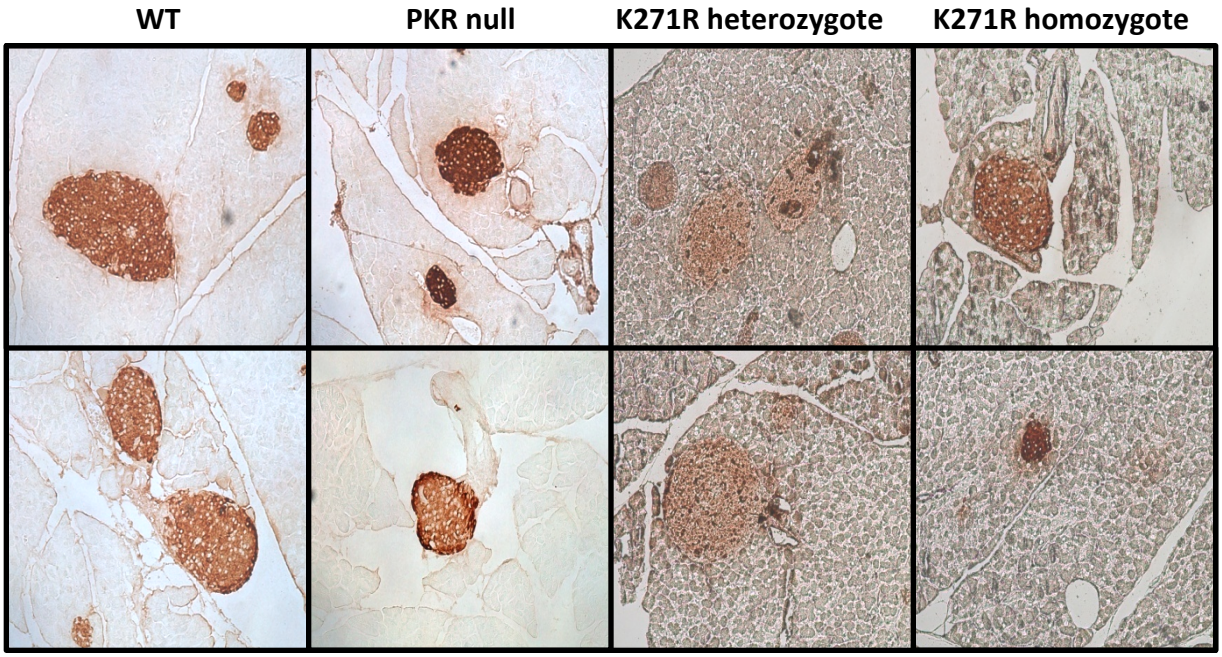

Figure 3.10 Pancreatic insulin production in islets of Langerhans of wt and PKR null or mutant mice fed a high fat diet.

Paraffin sections (5µM) of pancreas from PKR wt, null or kinase dead mutant animals fed a high fat diet for ten weeks. Islets of Langherhans are immunostained for insulin.

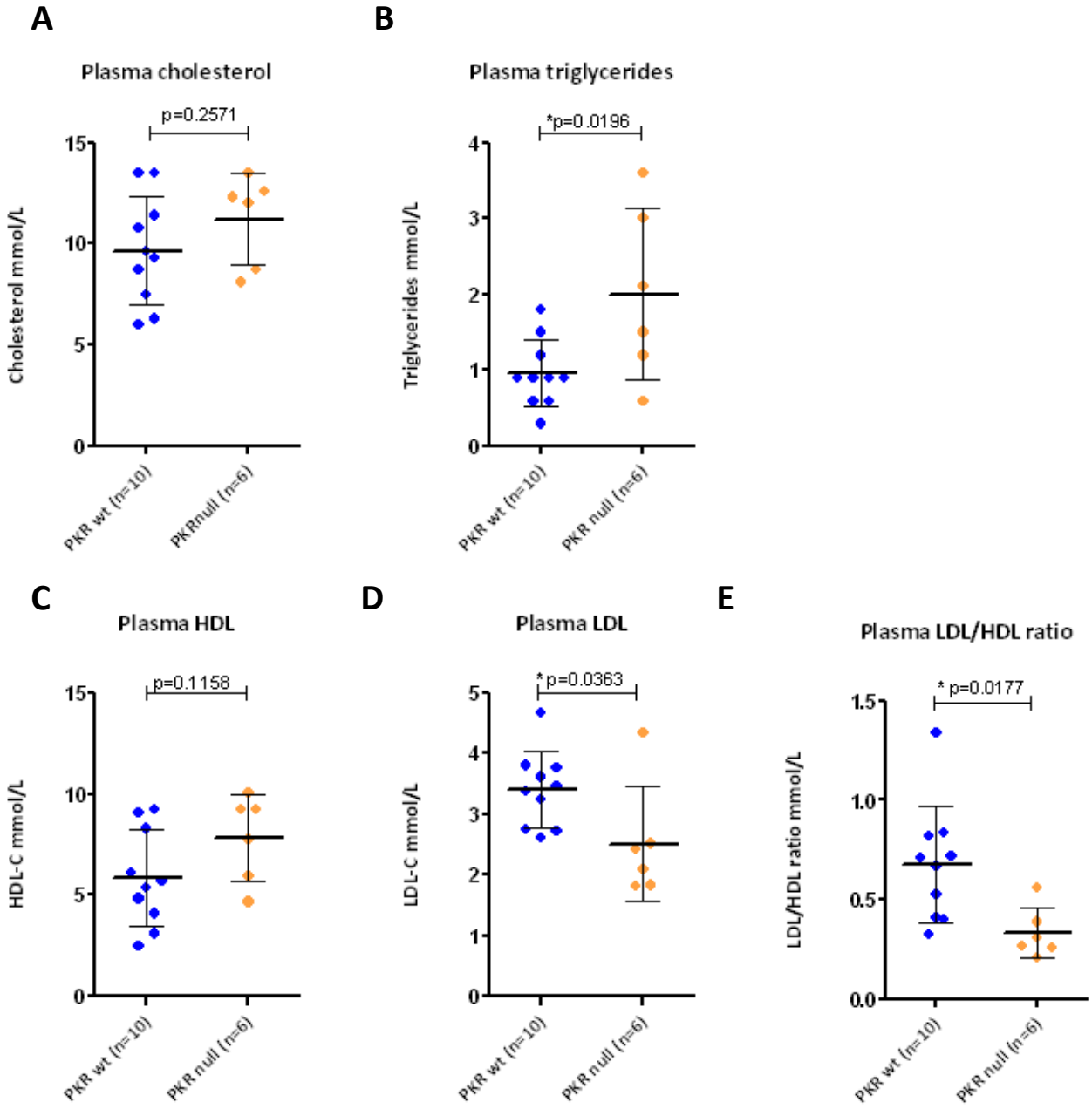

Figure 3.11 Blood lipid and lipoprotein composition of wt and PKR null mice fed a high fat diet.

Blood concentration of **A** cholesterol, **B** triglyceride, **C** HDL, **D** LDL and **E** the HDL/LDL ratio. Statistical analysis: unpaired T-test, Mean±SD. *Statistically significant.

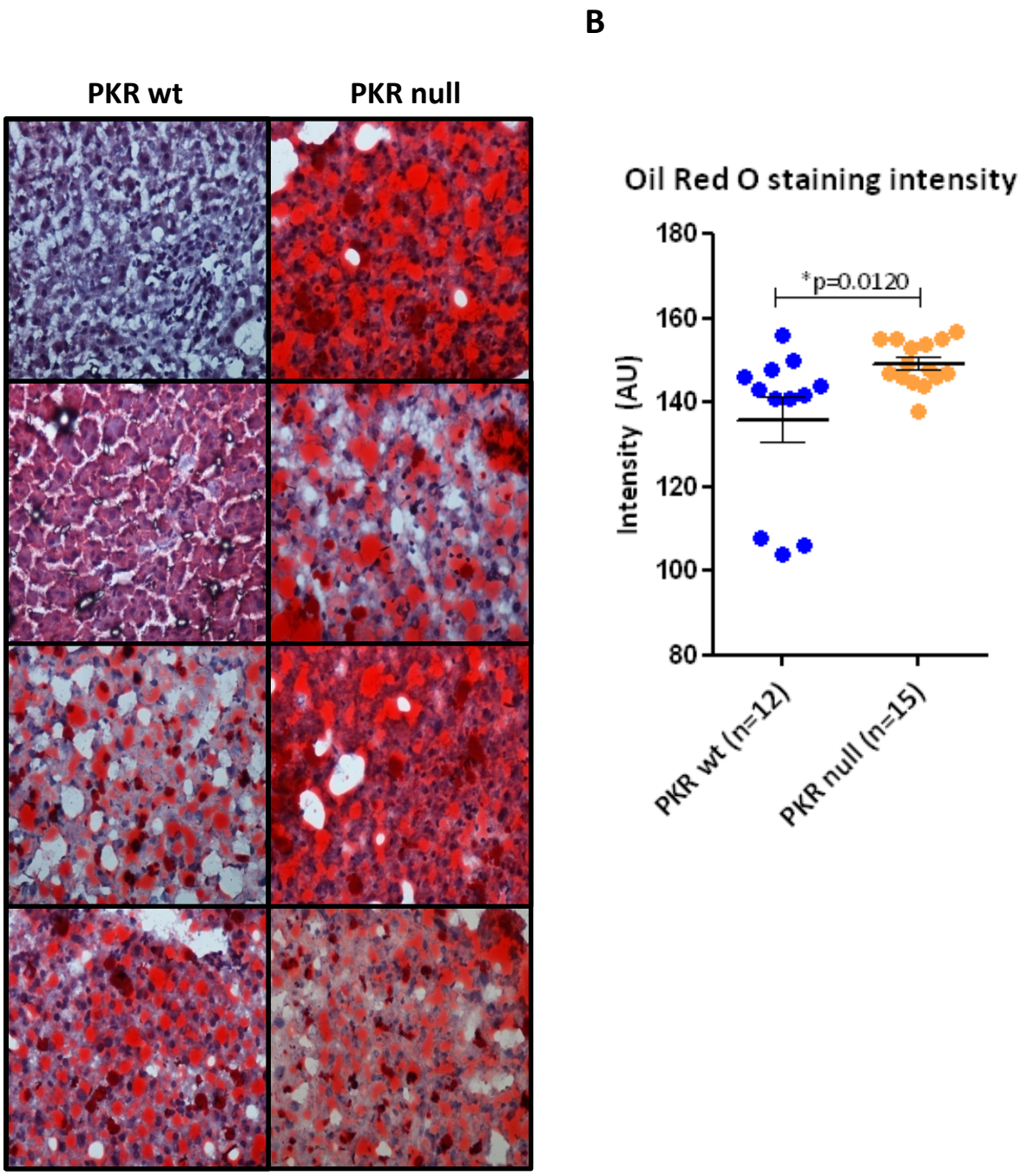

Figure 3.12 Hepatic lipid accumulation in Wt and PKR null mice fed a high fat diet for 10 weeks.

A Frozen liver sections (5µm) stained with Oil red-O from wt (n=4) and PKR null (n=4) animals fed a high fat diet, **B** quantification of Oil red-O staining in liver (using ImageJ). Statistical analysis: unpaired T-test, Mean±SEM. *Statistically significant.

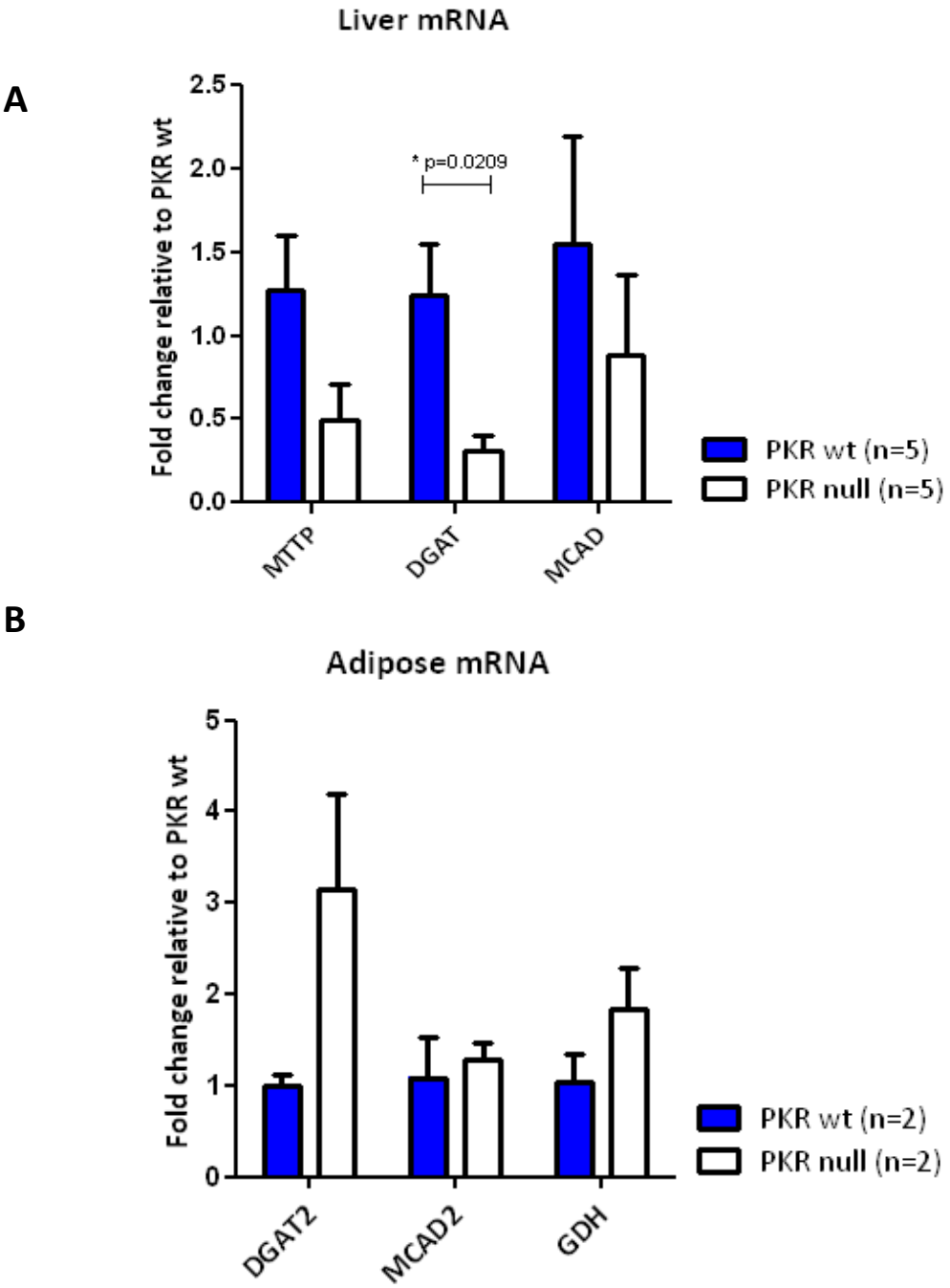

Figure 3.13 Hepatic expression of fatty acid synthesis and lipid transport genes in response to high fat diet.

A mRNA levels of MTTP, DGAT and MCAD analysed by QRT-PCR in liver tissue of PKR wt (n=5) and PKR null (n=5) mice fed a high fat diet. Results are expressed as fold change relative to PKR wt. Expression of target genes was compared to the internal control 18s. **B** mRNA levels of DGAT2, MCAD2 and GDH analysed by QRT-PCR in white adipose tissue of PKR wt (n=2) and PKR null (n=2) mice fed a high fat diet for 10 weeks. Results are expressed as fold change relative to PKR wt. Expression of target genes was compared to the internal control β-actin. Statistical analysis: unpaired T-test, mean ± SEM. * Statistically significant.

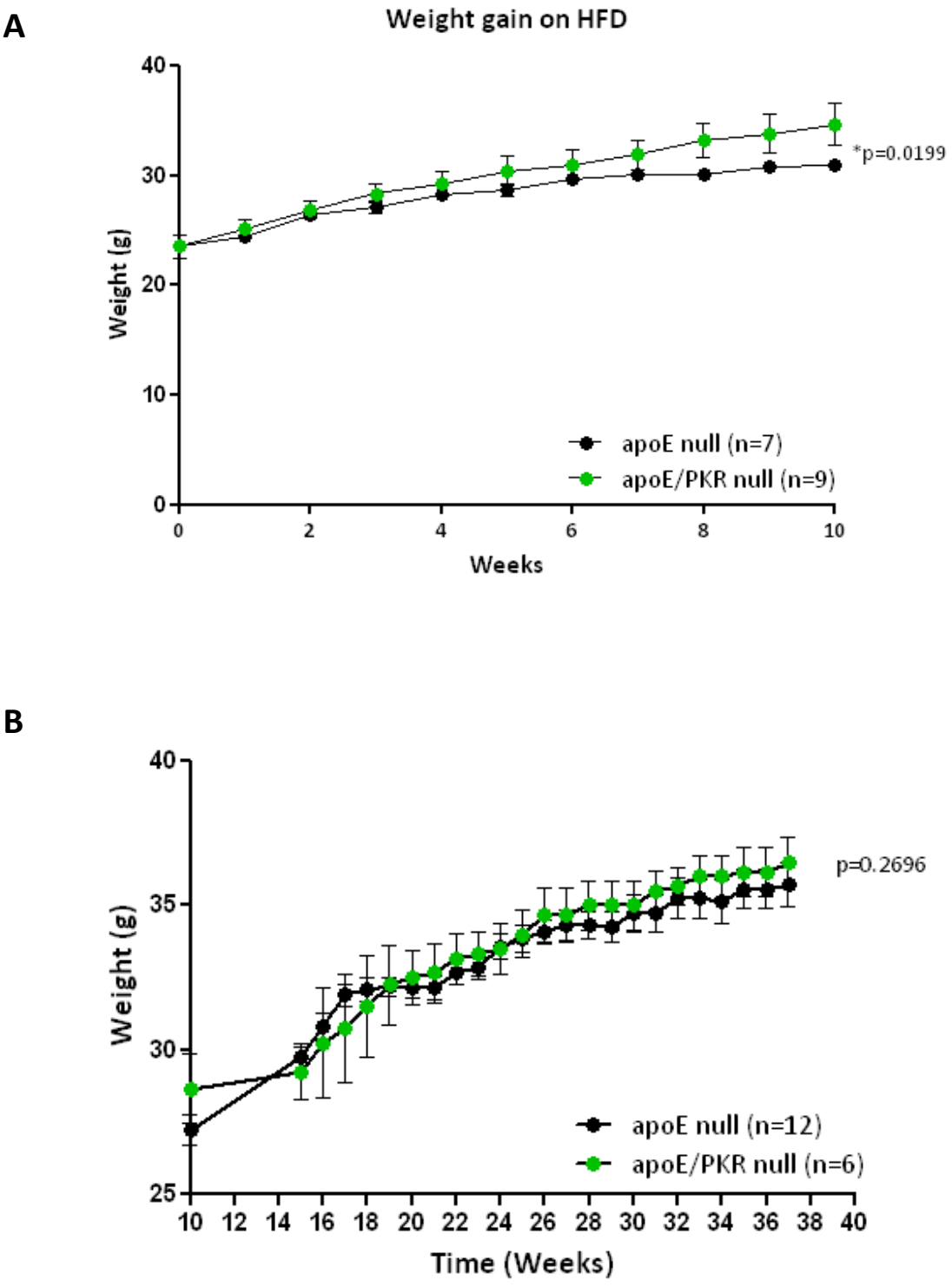

Figure 3.14 Weight gain of apoE knockout and apoE:PKR knockout mice fed a high fat or chow diet.

Weight gain of **A** apoE:PKR null (n=9) and apoE null (n=7) mice fed a high fat diet for ten weeks and **B** apoE:PKR null (n=12) and apoE null (n=6) mice fed a chow diet for 40 weeks. Weight was recorded weekly. Statistical analysis: linear regression, mean±SEM. *Statistically significant. Statistical analysis: linear regression, mean±SEM.

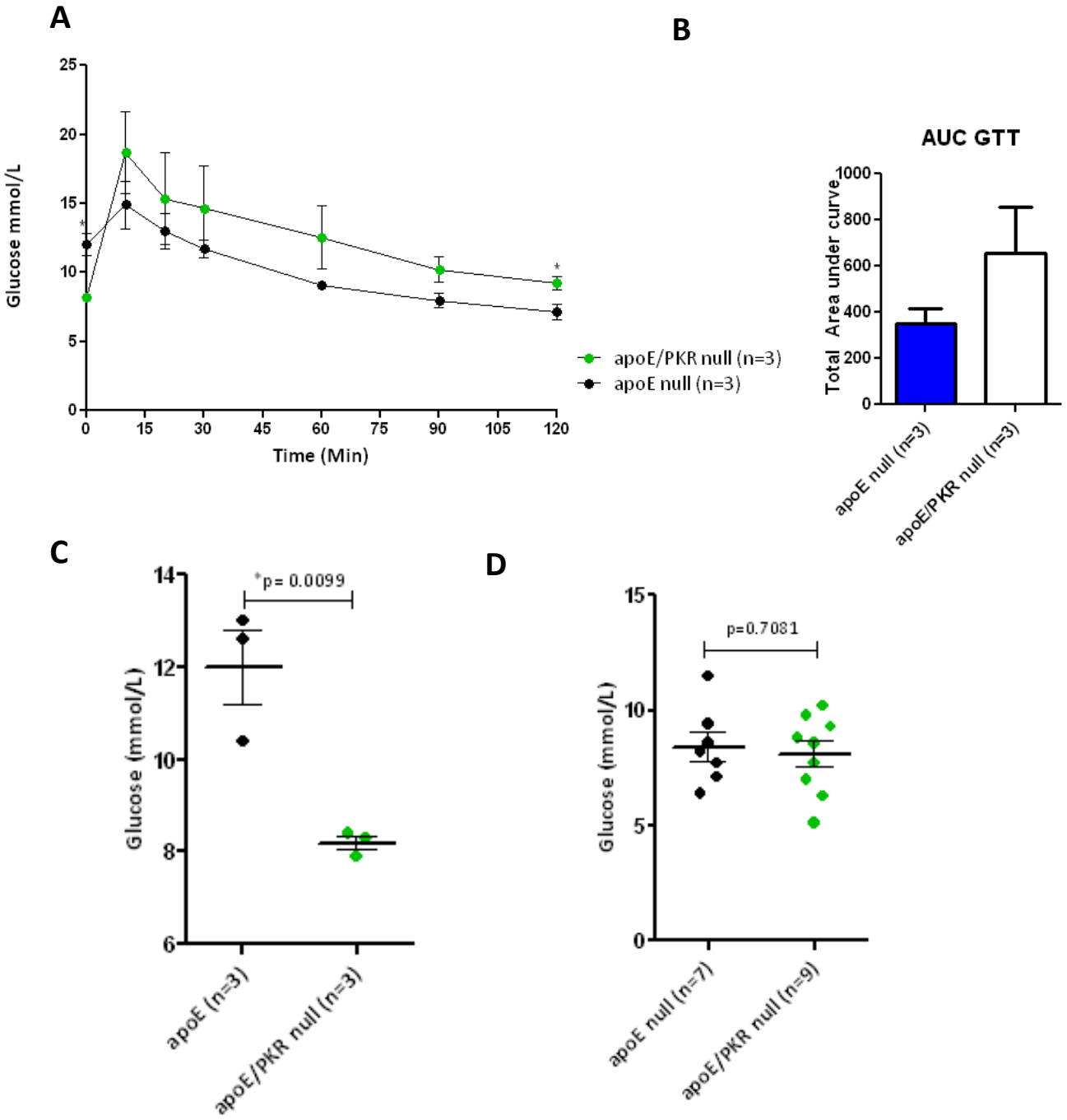

Figure 3.15 Glucose homeostasis in response to a high fat diet.

A Blood glucose concentration during a GTT after a 5 week HFD. Statistical analysis of GTT time points comparing apoE null and apoE:PKR null mice: *0min, p=0.0099, 10min p=0.3353, 20min p=0.5444, 30min p=0.3973, 60min p=0.1962, 90min p=0.0957, *120min p=0.0462. **B** AUC for GTT after a 5 week HFD, **C** Fasted blood concentration after 5 weeks of HFD, **D** Postprandial blood glucose levels after 10 weeks of HFD Statistical analysis: unpaired T-test, mean ± SEM. * Statistically significant.

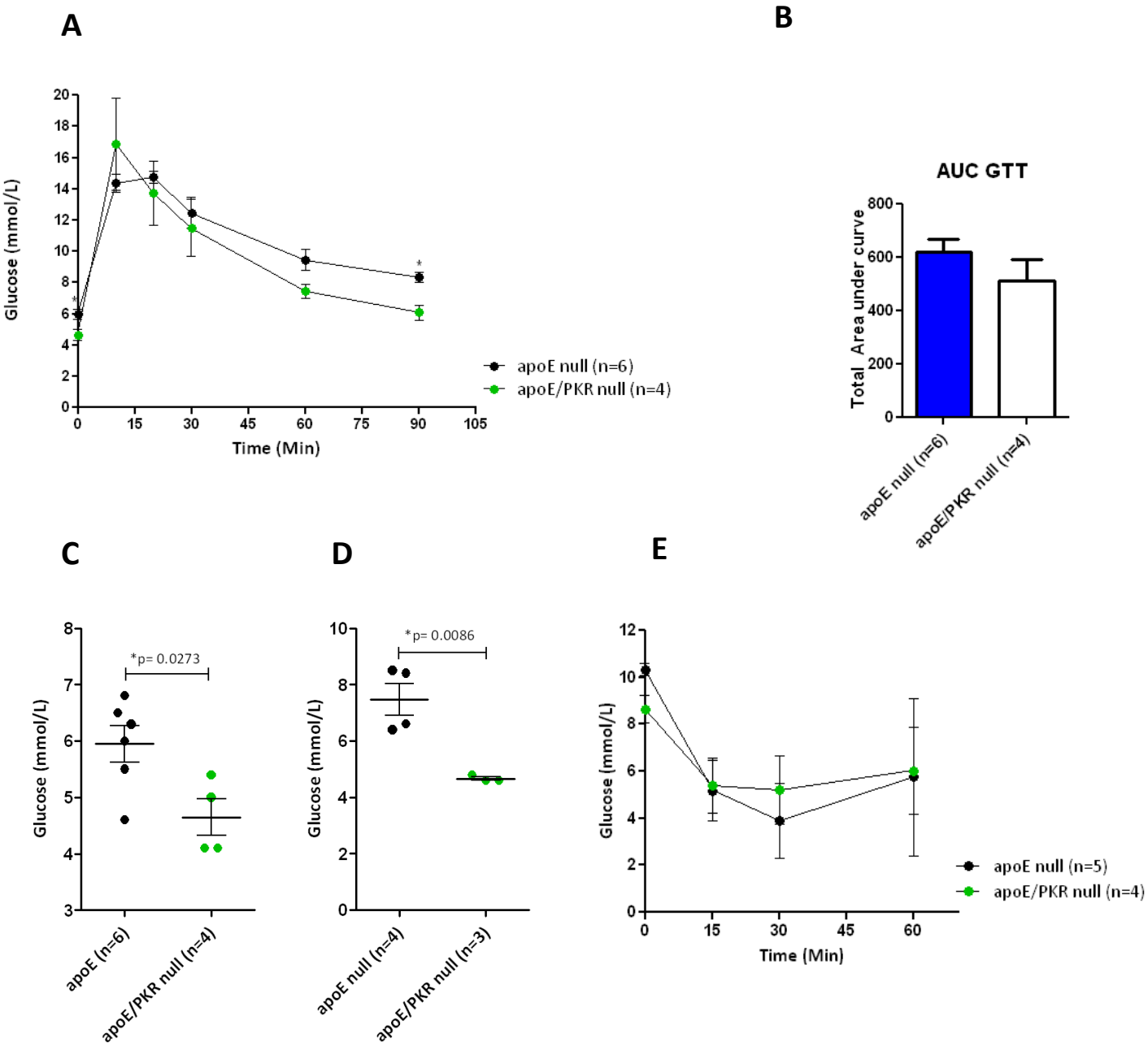

Figure 3.16 Glucose and insulin homeostasis in response to a chow diet.

A Blood glucose levels during a GTT performed after a 30 week chow diet. Statistical analysis of GTT time points comparing apoE null and apoE:PKR null mice: *0min p=0.0271, 10min p=0.3388, 20min 0.5444, 30min 0.6323, 60min 0.0691, *90min 0.0034, **B** AUC for GTT after a 30 week chow diet, **C** fasted blood glucose concentration after a 30 week chow diet, **D** fasted blood glucose concentration after a 40 week chow diet and **E** Blood glucose concentration during an ITT, after a 30 week chow diet. Statistical analysis of GTT time points comparing apoE null and apoE:PKR null mice: 0min, p=0.6128, 15min p=0.7571, 30min p=0.9201, 60min p=0.9403. Statistical analysis: unpaired T- test, mean ±SEM. *Statistically significant.

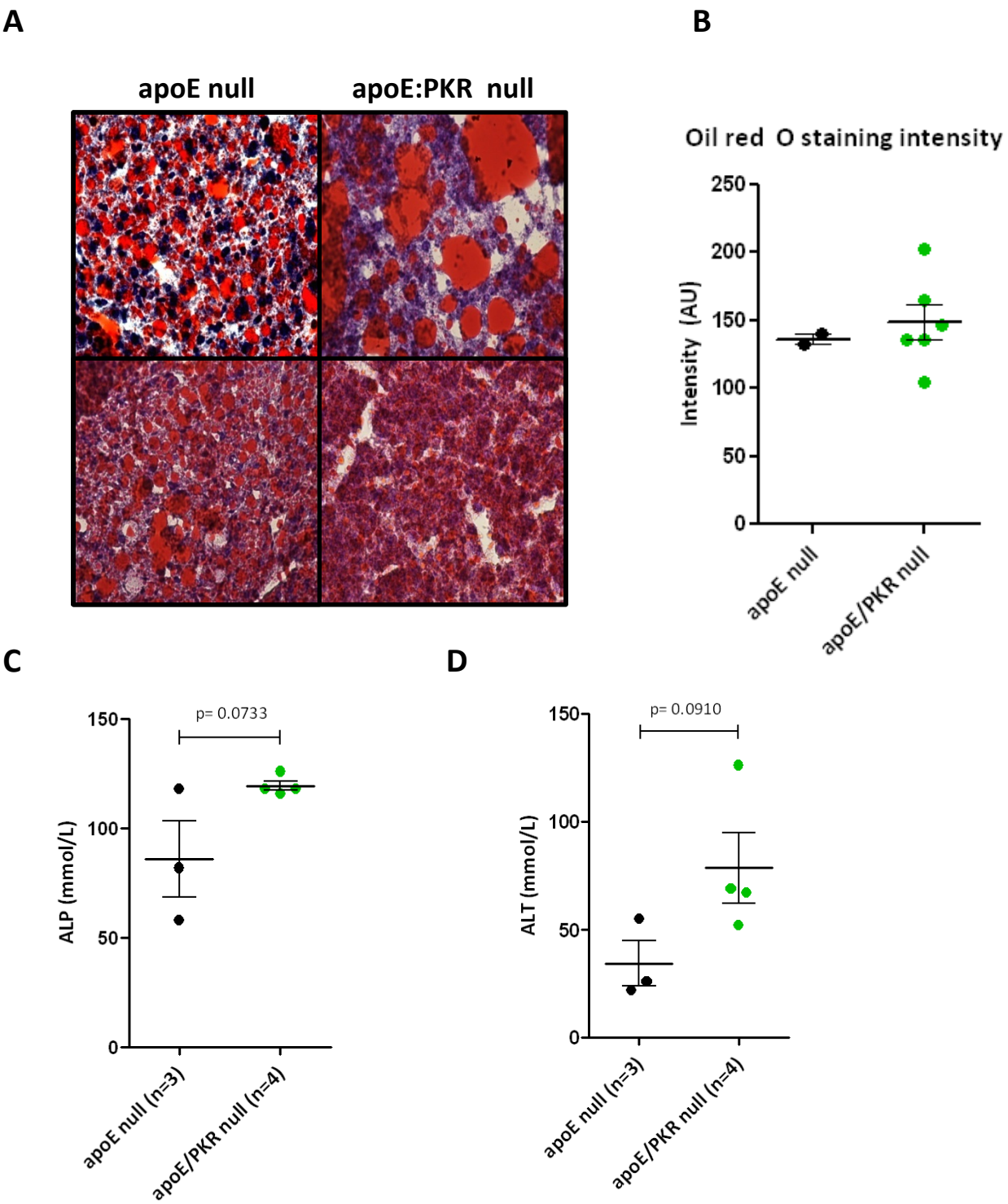

Figure 3.17 Hepatic triglyceride accumulation and concentration of ALP and ALT in apoE null and apoE:PKR null mice fed a high fat diet for 10 weeks.

A Frozen liver sections (5µm) stained with Oil red-O from wt (n=4) and PKR null (n=4) animals fed a high fat diet, **B** quantification of Oil red-O staining in liver (ImageJ). Blood concentration of **C** ALP (p=0.0733) and **D** ALT in apoE:PKR null and apoE null mice fed a week high fat diet. Statistical analysis: unpaired T-test, Mean±SEM. *Statistically significant.

A

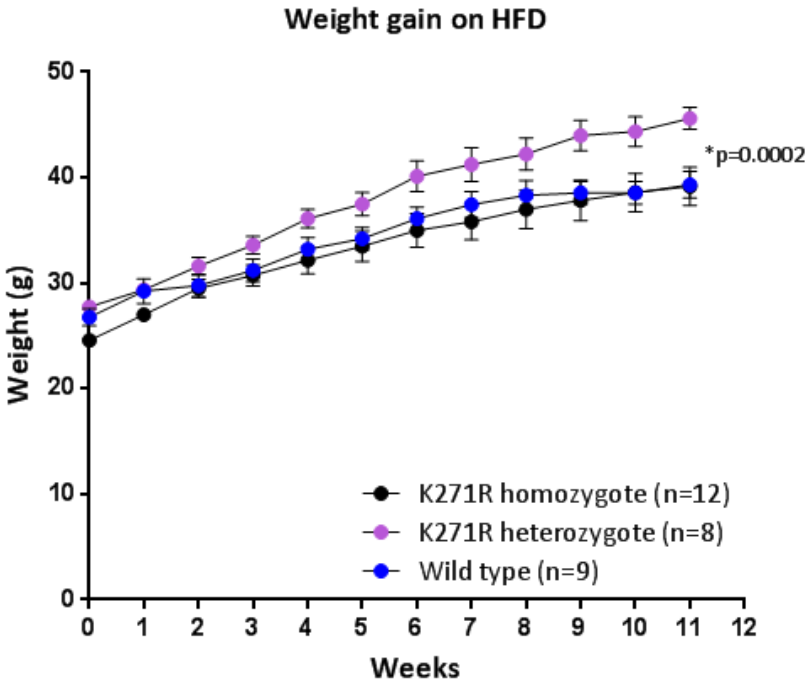

B

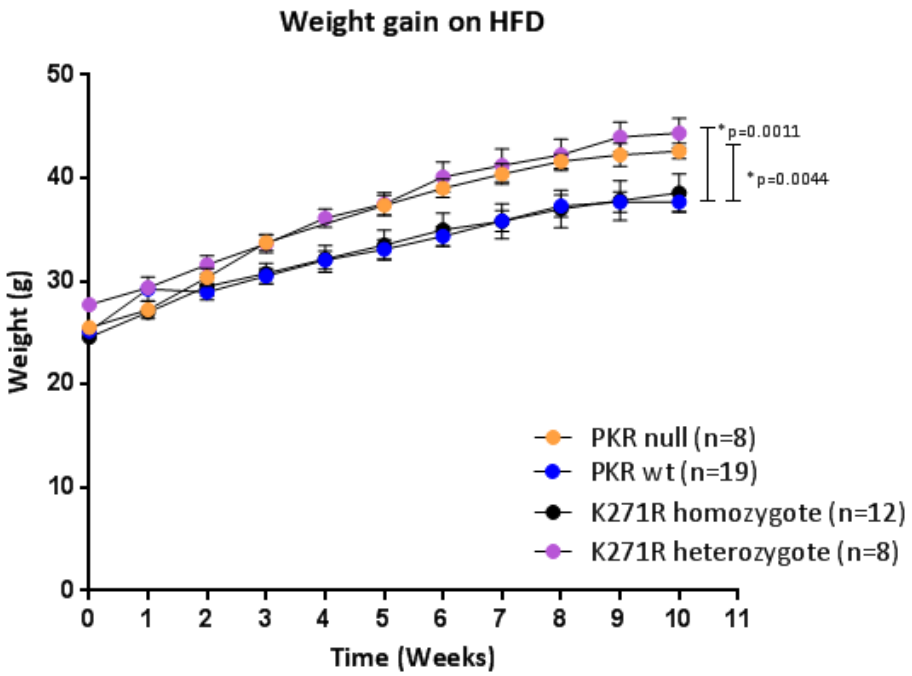

Figure 3.18 Weight gain of wt, K271R homozygote and K271R heterozygote animals fed a high fat diet.

Weight gain of **A** wt (n=9), K271R heterozygote (n=8) and K271R homozygote (n=12) mice fed a high fat diet for 10 weeks and **B** of wt (n=9), K271R homozygote, K271R heterozygote and PKR null (n=8) mice fed a high fat diet for 10 weeks, combined data. Statistical analysis: linear regression, mean±SD. *Statistically significant.

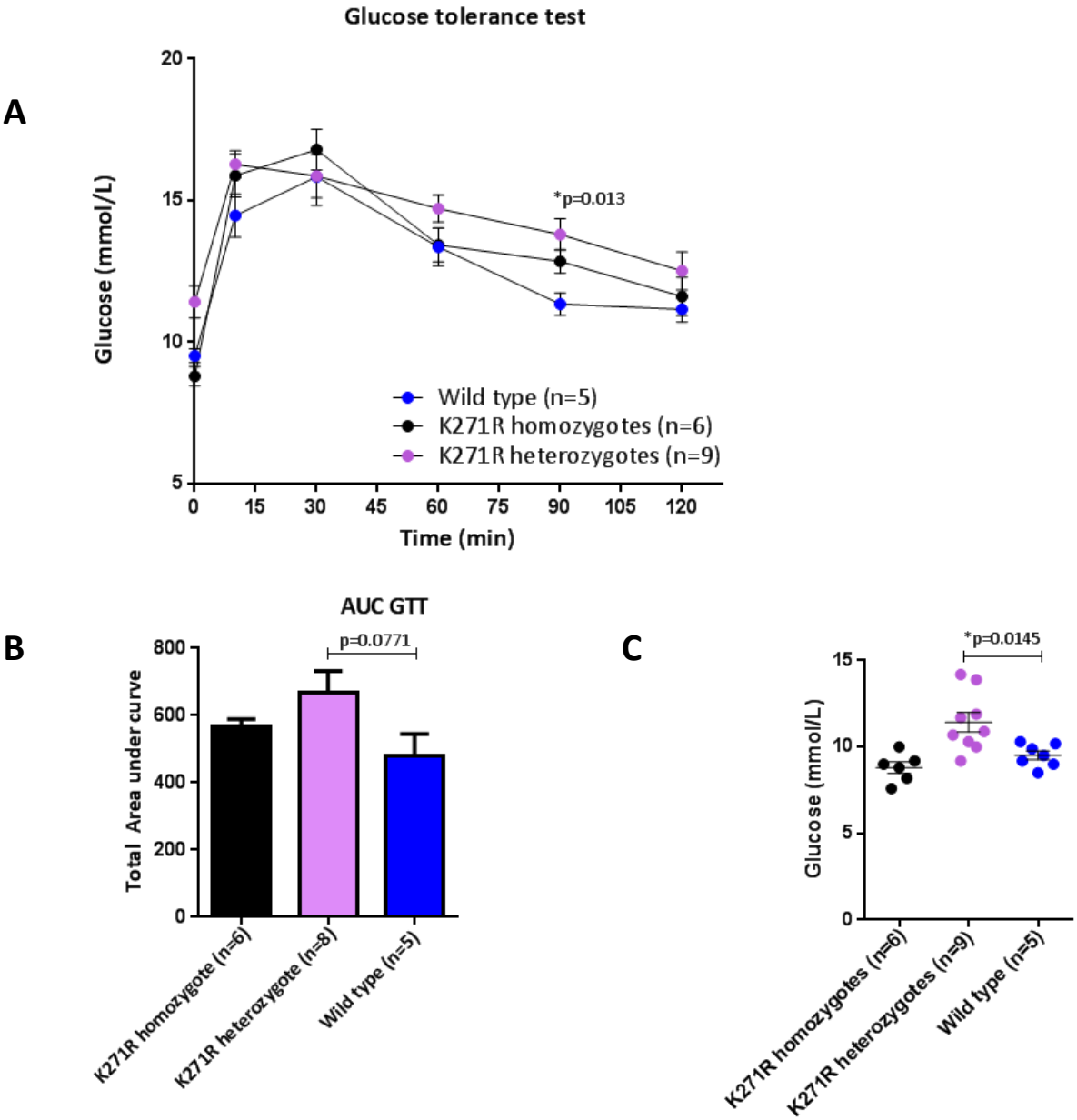

Figure 3.19 Blood glucose levels during a glucose tolerance test in response to a high fat diet.

A Glucose tolerance test of K271R heterozygote (n=9), K271R homozygote (n=6) and PKR wild type (n=5) mice fed a high fat diet. Statistical analysis of GTT time points comparing K271R homozygote and wild type mice: 0min p=0.1118, 10min p=0.2171, 30min p=0.4493, 60min 0.9362, *90min p=0.0359, 120min p=0.6038. Statistical analysis of GTT time points comparing K271R heterozygote andwild type mice: *0min p=0.0504, 10min p=0.1531, 60min p=0.0.1576, *90min p=0.0122, 120min p=0.4374, **B** AUC for GTT, **C** Fasting blood glucose concentration in K271R heterozygote (n=9), K271R homozygote (n=9) and wild type (n=5) animals fed a high fat diet for 10 weeks (*p=0.0145), Statistical analysis: Unpaired T-test, Mean±SEM and area under curve, mean ± SEM. * Statistically significant

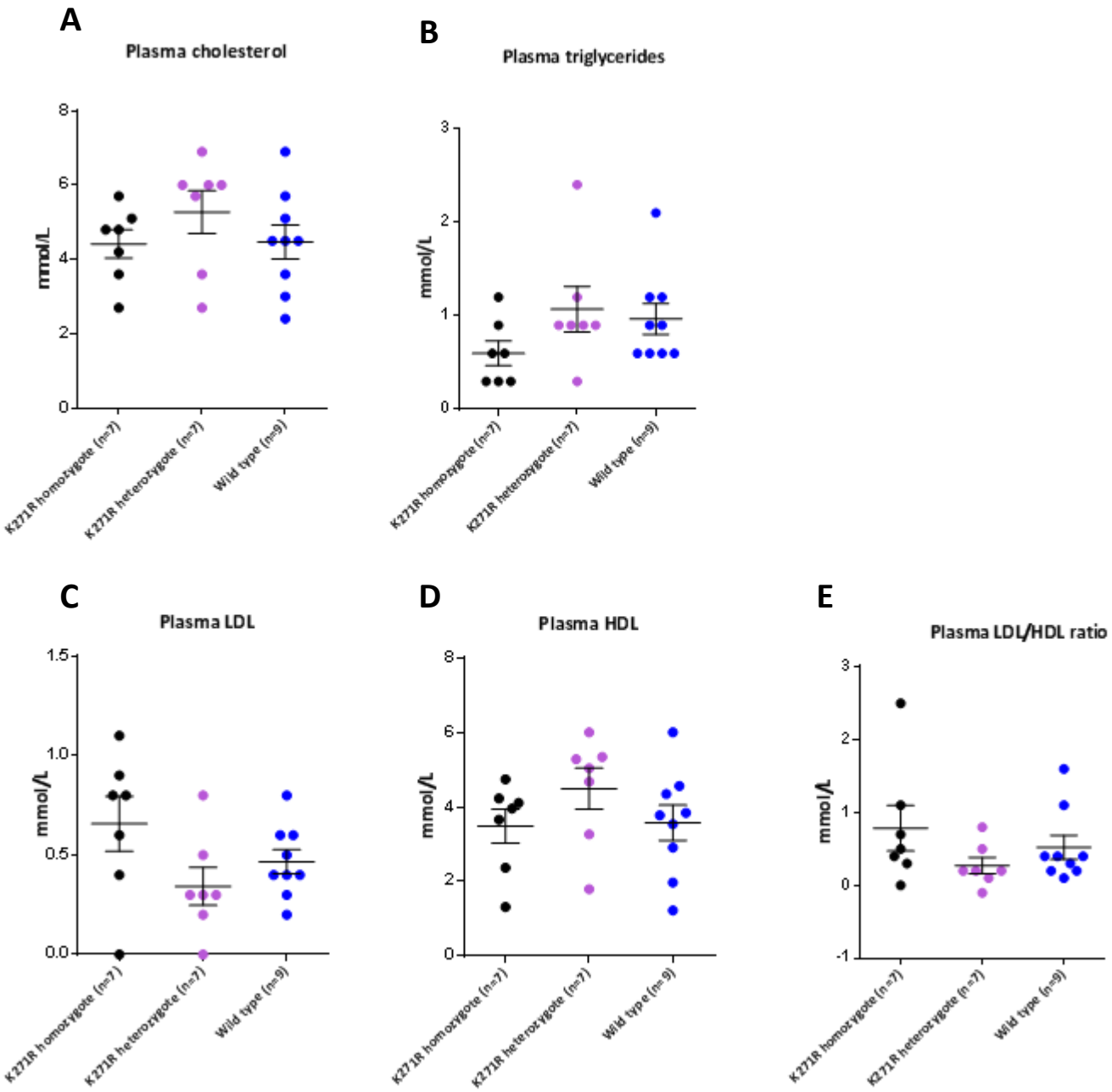

Figure 3.20 Blood lipid and lipoprotein composition after high fat diet feeding.

Plasma from K271R heterozygote (n=7), K271R homozygote (n=7) and wild type (n=5) fed a high fat diet for ten weeks was analysed for **A** cholesterol, **B** triglyceride, **C** LDL, **D** HDL and **E** LDL/HDL ratio were assessed in Statistical analysis: Unpaired T-test, Mean±SEM.* Statistically significant

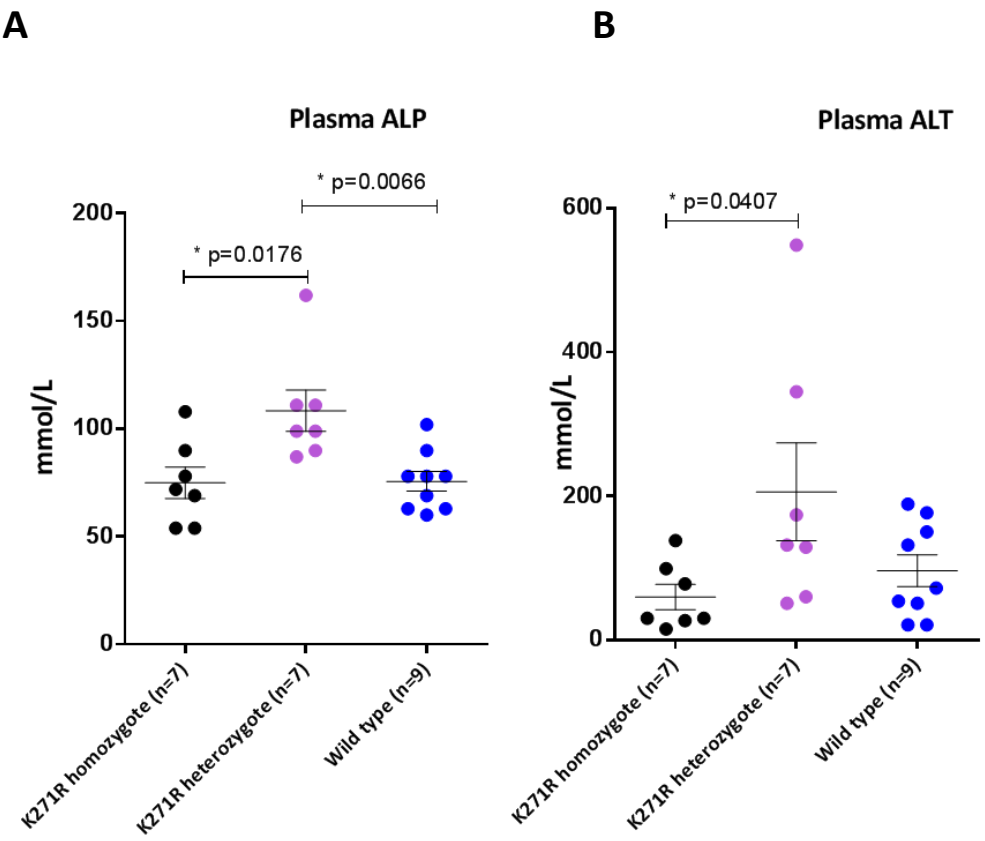

Figure 3.21 Circulating concentration of ALT and ALP in response to high fat diet.

Circulating concentration of **A** ALP and **B** ALT in K271R homozygote (n=7), K271R heterozygote (n=7) and wild type (n=9) mice fed a high fat diet for 10 weeks. Statistical analysis: Unpaired T-test, Mean±SEM. *Statistically significant.

CHAPTER 4 THE ROLE OF PKR IN ENERGY HOMEOSTASIS

CHAPTER 4 THE ROLE OF PKR IN ENERGY HOMEOSTASIS 101

4.1 INTRODUCTION 102

4.2 RATIONALE 105

4.3 HYPOTHESIS, AIMS AND METHODS 105

4.4 RESULTS 107

PKR REGULATES GLUCONEOGENESIS AND THE PENTOSE PHOSPHATE PATHWAY 107

4.4.1 PKR regulates expression of the glucogenic enzyme glucose-6-phosphatase. 107

4.4.2 PKR affects the pentose phosphate pathway. 109

LACK OF PKR DISRUPTS MITOCHONDRIAL BIOENERGETICS 110

4.4.3 PKR deficiency suppresses mitochondrial proton leakage and increases ATP synthesis. 110

4.4.4 PKR does not affect leptin signalling. 113

LACK OF PKR IMPAIRS INSULIN SIGNALLING 113

4.4.5 Lack of functional PKR dampens the insulin response in 3T3 MEFS, by reducing expression of IRS2. 113

4.4.6 Lack of functional PKR suppresses p70S6K and enhances Akt phosphorylation. 114

4.4.7 PKR in mTOR signalling 115

4.4.8 PKR reduces expression of PP2A thus negatively affecting Akt phosphorylation. 116

4.4.9 PKR does not affect splicing of the UPR protein XBP1. 117

PKR REGULATES AMPK SIGNALLING IN A TISSUE SPECIFIC MANNER 117

4.4.10 PKR modulates AMPK signalling in response to high fat diet feeding. 117

4.4.11 PKR alters expression of SREBP1C. 118

4.4.12 Fasting increases phosphorylation of acetyl-CoA carboxylase in the liver of high fat diet fed mice lacking PKR. 119

PKR REGULATES STERILE INFLAMMATORY RESPONSES 119

4.4.13 PKR does not regulate circulating levels of cytokines in response to high fat diet. 119

4.4.14 IL-6 transignalling. 120

4.4.15 PKR regulates inflammasome mediated signaling. 120

4.5 DISCUSSION 122

4.6 CONCLUSION 131

4.7 REFERENCES 132

4.1 INTRODUCTION

To account for the effect of PKR in reducing diet-induced obesity I sought to identify cellular processes that were altered, between WT and PKR mutant cells and mice. These studies focus on the mitochondria, as the primary organelle for metabolism, and cell signalling pathways that regulate energy homeostasis and the pathogenesis of obesity.

The main function of the mitochondria is to produce ATP through the oxygen consuming process of OXPHOS and to facilitate thermogenesis (Jung, Shetty et al. 1979). Adaptive (non-shivering) thermogenesis plays a key role in the maintenance of murine body temperature and energy expenditure in response to changes in temperature and diet. Thermogenesis occurs specifically in the mitochondria of brown adipose tissue and is driven by a transmembrane hydrogen ion transporter called uncoupling protein 1 (UCP1). UCP1 uncouples substrate oxidation from ATP synthesis and dissipates the energy as heat (Klingenberg and Huang 1999). Brown adipose tissue is highly innervated by the sympathetic nervous system (SNS). Exposure to cold stimulates the SNS to release norepinephrine, which interacts with β3-adrenergic receptors (β3-AR) to promote the activity of adipose triglyceride lipase (ATGL) enzyme. ATGL mediates the conversion of triglycerides to free fatty acids that induce BAT-specific expression of UCP1 (Winkler and Klingenberg 1994; Enerback, Jacobsson et al. 1997; Deiuliis, Liu et al. 2010). Accordingly, treatment with β3-AR agonists reduces adiposity by increasing energy expenditure (Grujic, Susulic et al. 1997). In light of the role of mitochondria in processes that regulate energy homeostasis, mitochondrial dysfunction has profound effects on whole body energy balance and is closely related to the pathophysiology of metabolic disease. Because of the suggested role for PKR in regulating weight, in this chapter I investigated the effect of genetic influences on levels of UCP1 and mitochondrial bioenergetics in this chapter.

Although energy imbalance is a key reason for obesity, disturbances in levels of endocrine hormones are also a predisposing factor. In particular dysregulation of blood glucose and insulin concentration has a critical consequence on the pathogenesis of obesity. Gluconeogenesis is primarily regulated by the endocrine hormone insulin, which alters

expression of PEPCK and G6pase by modulating the activity of the PI3K/Akt signalling network. The rationale for assessing the requirement for PKR in modulating insulin regulated signalling pathways is substantiated by a recent report that found eIF2ak2 kinases act upstream of the PI3K signaling cascade (Kazemi, Mounir et al. 2007).

In addition, preliminary experiments conducted by Dr Anthony Sadler indicate that PKR directly modulates the pentose phosphate pathway. This finding, together with the observation that PKR ablated mice are glucose intolerant, prompted me to assess levels of gluconeogenic enzymes in the mouse.

Furthermore, metabolic actions of insulin extend beyond regulation of glucose homeostasis and have also been shown to activate the major energy regulator AMPK, demonstrating that crosstalk between energy sensing systems and those that regulate cellular homeostasis are important for regulating whole body energy homeostasis (Ueno, Carvalheira et al. 2005; Liu, Gauthier et al. 2010). As was alluded to in chapter one, mechanisms that control protein translation play a key role in metabolic regulation. Previous studies have demonstrated the eIF2AK2 kinases modulate mTOR signaling. This was first shown for GCN2, which improves insulin sensitivity by decreasing mTOR signaling in response to leucine deprivation. More latterly PKR has been shown to suppress mTOR signaling in a p53 dependent manner in a mouse model of Alzheimer's disease (Morel, Couturier et al. 2009; Xiao, Huang et al. 2011). Therefore, I sought to assess whether the mTOR pathway is altered in WT compared to PKR ablated cells to account for diet induced weight gain and adiposity.

To date there is no direct association between PKR and AMPK. However, one report demonstrates that phosphorylation of AMPK associates with increased phosphorylation of PKR and eIF2α in obese Zucker rats (Katta, Kakarla et al. 2012). This provides a tentative molecular link between these signaling pathways. The consequence of abnormal AMPK-mediated signaling is central to defects in lipid metabolism and gluconeogenesis and significantly contributes to the development of metabolic disorders (Hardie, 2008). Therefore, I focused on evaluating the activation of these two energy-sensing pathways based on already established links with PKR.

In addition to being disturbed by impairments of metabolic processes, energy homeostasis can also be indirectly influenced by inflammation. The link between inflammation and obesity was first proposed by Hotamisligil et al (1993), who demonstrated that obesity correlates with increased levels of the pro-inflammatory cytokine TNFα (Hotamisligil, Shargill et al. 1993). Expression of TNFα has subsequently been shown to disrupt insulin signalling, leading to insulin resistance (Hotamisligil, Shargill et al. 1993; Hotamisligil, Peraldi et al. 1996). Inflammation is the biological response of an organism to harmful stimuli that threaten to compromise cell integrity and cellular homeostasis. The rapid engagement of the acute phase response of inflammation involves activation of macrophages that then produce inflammatory cytokines IL-6, IL-1, TNFα and acute phase proteins including C-reactive Protein (CRP), which act to clear the infection site. CRP acts in a positive feedback loop to promote inflammation by increasing expression of TNFα and IL-1 from macrophages (Galve-de Rochemonteix, Wiktorowicz et al. 1993). CRP is an important circulating biomarker of cardiovascular disease, because it has strong predictive value for atherothrombic outcomes. CRP is also a biomarker for type 2 diabetes. The failure of the immune system to acutely resolve infection results in chronic low-grade inflammation, which is now established as a characteristic feature of obesity (Bastard, Maachi et al. 2006; de Heredia, Gomez-Martinez et al. 2012). PKR modulates inflammatory responses by activating, most notably, NF-κB to induce cytokines linked with inflammation in obese conditions (Deb, Haque et al. 2001; Meusel, Kehoe et al. 2002; Chakrabarti, Sadler et al. 2008; Pindel and Sadler 2011). Hence it is plausible that PKR could ameliorate weight gain by altering the expression of inflammatory cytokines.

The process of sterile inflammation, mediated by the multi-protein inflammasome, has become recognised as a key modulator of inflammation associated with obesity. Sterile inflammation is triggered by metabolic stimuli such as ceramide, fatty acids and cholesterol crystals that act as a first signal to stimulate TLR receptors to synthesise pro-IL-1β and NLRP3. The fatty acid palmitate and lipid substances such as ceramides have been demonstrated to modulate PKR. Additionally, cell-signalling pathways triggered by, for instance, the TLR receptors and transcription factors that regulate the inflammatory response have been demonstrated to indirectly activate PKR. The evident overlap of

metabolic molecules that induce PKR and NLRP3 lead us to speculate that an important interplay between these two inflammatory effectors may exist. To date one report has identified that PKR acts as an upstream sensor and is essential for NLRP3 activation (Lu, Nakamura et al. 2012).

4.2 RATIONALE

Rationale

The preceding results demonstrate that ablation of PKR promotes weight gain, adiposity, glucose intolerance, hyperglycaemia and NAFLD in response to high fat diets. Therefore the objective of this study is to identify PKR-dependent molecular mechanisms that modulate the development of the metabolic syndrome in response to high fat diets. Because of the established role for PKR in regulating the activity of cell signalling proteins, we propose that PKR directly modulates key metabolic processes and indirectly affects metabolism through regulation of the activity of major energy sensing pathways, or ameliorates the metabolic syndrome through modulation of sterile inflammation.

4.3 HYPOTHESIS, AIMS AND METHODS

Hypothesis

We hypothesise that PKR modulates metabolic signalling or activates energy systems to ameliorate weight gain and the development of metabolic disease.

Aims

Protein components of cell signalling pathways will be compared between tissues taken from WT and PKR knockout mice fed a high fat diet, and between cells extracted from WT and PKR knockout animals treated with metabolic stimuli. These experiments aim to assess:

I. The levels of key hepatic gluconeogenic and glycolytic enzymes that may cause glucose intolerance in PKR ablated mice;

II. Cellular oxygen consumption and mitochondrial bioenergetics to determine the effect of PKR on mitochondrial proton leakage and OXPHOS function;

III. The insulin-mediated PI3K/Akt responses *in vitro*;

IV. Levels of AMPK signalling protein mediators;

V. Levels of inflammatory cytokines in response to diet;

VI. Inflammasome components and secretion of IL-1β in a modified *in vitro* explant model.

VII. The requirement for inflammasome activation and IL-1β secretion in regulating weight gain.

Methods

To investigate signalling *in vitro* I used a modified PKR ablated 3T3 primary mouse embryonic fibroblast cell line isolated from C57Bl6/J mice. The Bac7 and Bac10 cells were isolated as previously described by Yang et al, using the 3T3 protocol (Yang, Reis et al. 1995). The original derivation method for these and primary MEFs is described in a PhD thesis written by Zan Xu from the Department of Genetics at the Case Western Reserve University, Cleveland, Ohio, USA (Xu and Williams, 1998). The MEFs were transfected with a bacterial artificial chromosome (BAC) carrying the whole human *eIF2kα2* (which encode PKR) genetic loci. MEFs denoted Bac7 express a functional human PKR, whereas MEFs denoted Bac10 contain the construct but do not express PKR (Cheung et al., 1999). The use of this isogenic cell line and method of derivation has been previously reported in these studies (Chakrabarti et al., 2008; Deb et al., 2001; Sadler et al., 2009). I also used primary WT, PKR ablated, and K271R transgenic MEFs and these cells immortalized with the Simian virus, SV40 large T-antigen (referred to as SV40 within the text). Immortalized (with the viral myc and ras genes) spleen macrophages (SMOs) were isolated from WT and PKR knockout mice

previously established in the lab (Chakrabarti, Sadler et al. 2008). Correct expression of PKR in these cell lines was assessed by western blot analysis (Appendix VIIIA) and QRT-PCR analysis (Appendix VIIIB).

4.4 RESULTS

PKR REGULATES GLUCONEOGENESIS

4.4.1 PKR regulates expression of the gluconeogenic enzyme glucose-6-phosphatase.

Disturbances in gluconeogenic and glycolytic processes are two pathogenic mechanisms underlying type 2 diabetes and insulin resistance. My results so far demonstrate that mice devoid of PKR are glucose intolerant and have fasting hyperglycemia in comparison to wild type mice. These findings prompted me to determine whether changes in mRNA levels of key gluconeogenic enzymes PEPCK, FBpase and G6pase could be responsible for the impaired glucose homeostasis. As shown in figure 4.1A, the expression of G6pase is significantly elevated in the liver of mice ablated for PKR compared to WT controls (*p=0.0365). There is no difference in the hepatic expression of PEPCK or FBpase enzymes that catalyse the early reactions of gluconeogenesis. This suggests that in PKR knockout mice gluconeogenesis is specifically enhanced in the terminal stage of the process. Expression of G6pase in skeletal muscle is similar in PKR knockout and wild type mice keeping in with the fact that this tissue is not a major site for gluconeogenesis (Fig.4.1B). Surprisingly, in light of the altered mRNA levels of G6Pase, no change could be detected in the levels of hepatic G6pase protein in WT and PKR knockout mice (Fig.4.1C and D). However, the anti-G6Pase antibody used performed poorly in our hands, and so did not allow an accurate measure of G6Pase levels. These findings suggest that part of the mechanism by which PKR improves glucose homeostasis is by regulating the expression of G6pase.

Further investigation reveals that loss of PKR induces hepatic expression of G6pase in a manner that positively associates with the severity of glucose intolerance. This

phenomenon is most prominent in K271R heterozygote mice in which high levels of the G6pase mRNA associate with a suppressed GTT response, compared to K271R homozygote and WT mice which have relatively normal glucose tolerance and, correspondingly, lower levels of the hepatic G6pase transcript (Fig.4.1E, *p=0.0078). Expression of PEPCK and FBpase in the liver of K271R homozygote mice is comparable to that of wild type mice (Fig.4.7F). In accordance with this conjecture, mice ablated for apoE:PKR and apoE have similar expression of G6pase, PEPCK and FBpase and comparable glucose output (Fig.4.1G). This discovery is consistent with our speculation that deletion of apoE suppresses weight gain and the development of secondary metabolic outcomes when compared to single PKR ablated mice.

Next I sought to determine whether suppressed glucose breakdown could account for increased blood glucose concentration in mice deficient for PKR. I demonstrate that expression of the glycolytic enzymes hexokinase-1 and hexokinase-3, which initiate the first step of glycogen synthesis and glycolysis, and expression of phosphofructokinase 1 (PFK), which is a major regulatory enzyme of the pathway, are comparable in the livers of WT and PKR ablated mice suggesting that the glycolytic reactions catalysed by these enzymes are equivalent in both animal cohorts (Fig.4.1H).

Another physiological measure of gluconeogenesis is provided by the pyruvate tolerance test (PTT). The PTT assesses the capacity of the liver to convert pyruvate to glucose, therefore WT and PKR ablated mice were subjected to a PTT. This experiment reveals that loss of PKR increases hepatic glucose output at 10 and 120 minutes after pyruvate administration, which is indicative of enhanced hepatic glucose output (Fig.4.2A). In spite of the observation that AUC for the PTT was similar in PKR knockout and wild type mice (Fig.4.2B), blood glucose concentrations remained high 120 minutes post pyruvate injection suggestive of sustained glucose production.

Together these findings demonstrate a change in a key enzyme that increases the synthesis of glucose, with no countering change in key enzymes of central metabolic pathways that reduce glucose levels; thereby identifying a mechanism for the defect in glucose homeostasis that leads to the hyperglycaemia observed in mice ablated for PKR.

However, the analysis, described next, identifies a possible alternative mechanism that could account for reduced glucose concentration.

4.4.2 PKR regulates the expression of glucose-6-phosphate dehydrogenase.

Preliminary work performed by Dr. Anthony Sadler from our laboratory has suggested that PKR may affect the pentose phosphate pathway. These experiments have shown that the PKR-dependent effects on the PPP were relieved by overexpression of transketolase, an enzyme that catalyzes the non-oxidative phase in the pathway. This finding is relevant because the PPP is an alternate process to glycolysis for the oxidation of glucose. Therefore I sought to assess expression of enzymes within the pentose phosphate pathway.

The rate-limiting step of the PPP is catalysed by the glucose-6-phosphate dehydrogenase (G6PD) enzyme, which is stimulated by NADP+. G6PD plays a major role in producing NADPH that is critical for reductive reactions especially lipogenesis and adipogenesis Expression of G6PD is reported to be elevated during obesity and is linked to impaired lipid metabolism and insulin resistance, a phenotype that is seen in the PKR ablated mice (Park, Rho et al. 2005). Figure 4.2C demonstrates that hepatic expression of G6PD is significantly (*p=0.0299) elevated in PKR knockouts compared to WT mice. This could indicate that loss of PKR enhances the capacity to breakdown glucose, which could potentially counter the earlier results. As this is in discord with the hyperglycaemia observed in the PKR ablated mice, it is presumed that insufficient glucose is degraded via this pathway to normalize glucose levels. Hence, PKR-dependent metabolic changes that associate with increased blood glucose concentration dominate the phenotype. Importantly a recent report demonstrates that over-expression of G6PD associates with insulin resistance, hence it is plausible to speculate that PKR-dependent regulation of G6PD provides a mechanism responsible for modulating glucose homeostasis (Wang, Zhao et al. 2012)

In addition to G6PD, the other key producers of NADPH are isocitrate dehydrogenase (IDH) and malic enzyme 1 (ME1), which are part of the TCA cycle. Consistent with the observation that G6PD is increased in mice ablated for PKR, hepatic expression of ME1, IDH1

and IDH2 is also somewhat elevated, although this effect does not reach statistical significance (Fig.4.2C). Based on these results I speculated that mice lacking PKR would produce large amounts of the NADPH cofactor, which is required for two key cellular processes, lipid synthesis and OXPHOS, to produce energy in the form of ATP. To investigate this notion I assessed cellular levels of NAD, NADH, NADP and NADPH in Bac7 and Bac10 MEFs. However, the percentage of NADH and NADPH that makes up the total NAD pool is similar in Bac7 and Bac10 MEFs (Fig.4.2D and E). Hence, there is no apparent PKR-dependent difference in NADH and NADPH concentrations *in vitro*. Caution has to be exercised in interpreting these results as putative differences in the outputs from the pentose phosphate pathway predicted *in vivo* may not be apparent *in vitro*. It is plausible that a high demand for lipid and ATP synthesis in immortalized cultured cells could consume the cofactors NADH and NADPH, making this difference between PKR knockout and WT mice undetectable. An alternative approach to assess the functionality of mitochondria in WT and PKR ablated cell lines is conducted below.

LACK OF PKR DISRUPTS MITOCHONDRIAL BIOENERGETICS

4.4.3 PKR deficiency suppresses mitochondrial proton leakage and increases ATP synthesis.

The findings presented so far have implicated PKR in regulating weight in response to high fat diets, demonstrating that PKR plays a critical role in the maintenance of energy homeostasis. These findings encouraged me to investigate the contribution of thermogenic uncoupling and mitochondrial specific ATP synthesis to the overall energy status of the animal. Although area under curve analysis didn't reveal a statistically significant difference in thermogenesis, expression of the uncoupling protein 1 (UCP1) in white adipose tissue was significantly suppressed (Fig.4.3A, *p=0.0087) high fat diet fed PKR knockout mice. The predicted outcome of decreased expression of UCP1 in WAT is reduced thermogenesis and low energy expenditure, which is in accordance with increased weight gain seen in mice ablated for PKR.

Diffusion of ions and molecules across the mitochondrial membrane is also facilitated by the membrane embedded voltage-dependent anion channel (VDAC) protein, which forms a complex with other proteins to allow mitochondrial uncoupling. Expression of VDAC protein in the liver is similar in PKR ablated and WT mice confirming that decreased expression of UCP1, rather than VDAC, is in part responsible for suppressed mitochondrial proton leakage in mice deficient for PKR (Fig.4.3B).

Oxidative phosphorylation within the mitochondria is driven by the electron transport chain, which consists of 5 multi-protein complexes. I assessed protein and mRNA expression of these complexes because defects in electron transport chain associate with severe energy imbalances and obesity. Figure 4.3C shows that hepatic mRNA levels of NADH dehydrogenase (complex I), ATP synthase (Complex V) and the TCA cycle enzymes cytochrome C and isocitrate dehydrogenase are lower in mice devoid of PKR, however this difference is not statistically significant. Consistent with these data, mitochondrial protein levels of cytochrome c oxidase (complex IV) are unchanged in the liver, muscle or heart of PKR WT and knockout mice suggesting that PKR does not affect expression of OXPHOS enzymes (Fig.4.3D). Further investigation should assess the enzymatic activity of these complexes to ensure there is no unexpected change that could contribute to mitochondrial dysfunction.

Another means of assessing cellular energy expenditure and mitochondrial function is to measure oxygen consumption using the oxygraph respirometry machinery. Figure 4.4A shows that spleen macrophages lacking PKR have a significantly higher basal respiration rate (*p=0.0286) than PKR expressing cells. This is of consequence because a higher respiration rate is a hallmark feature of obese individuals. Treatment with the ATPase inhibitor (complex I) oligomycin prevents generation of a proton gradient and shows respiration that is due to other respiratory pathways such as proton leakage. Accordingly, I established that proton leak accounts for 20.53% of basal oxygen consumption in PKR knockout SMOs, which is significantly less (*p=0.0488) compared to 32.28% in wild type SMOs (Fig.4.4A and B). Consistent with these data, ATP synthesis accounts for 79.47% of basal oxygen consumption in PKR knockout SMOs compared to 67.72% in wild type SMOs (Fig.4.4B). These results

demonstrate that elevated ATP synthesis in cells lacking PKR may account for increased basal respiration (*p=0.0488). FCCP uncouples oxidative phosphorylation from ATP synthesis, by allowing proton leakage across the membrane and demonstrates the maximal oxidative capacity of the cell. The maximal mitochondrial oxidative capacity of PKR knockout SMOs (48.46% above basal oxygen consumption) is lower than that of wild type cells (58.88% above basal oxygen consumption), however, this difference is not statistically significant (Fig.4.4B). Treatment with antimycin (inhibitor of complex III) demonstrates that non-mitochondrial oxygen consumption is similar in PKR wild type and knockout MEFs.

I also assessed oxygen consumption in 3T3-immortalised MEFs. Results from these experiments duplicate those obtained in SMOs, in that cells devoid of PKR (BAC10) have increased basal oxygen consumption compared to wild type cells (BAC7), however this difference was not assessed to be statistically significant (Fig.4.4C). Furthermore, MEFs devoid of PKR have notably increased ATP synthesis and suppressed proton leakage (*p=0.0058 and *p=0.0159, respectively) (Fig.4.4C and D). Consistent with results obtained in spleen macrophages, non-mitochondrial oxygen consumption is similar in both PKR knockout and wild type MEFs. Unfortunately despite many attempts to optimise FCCP conditions in 3T3 MEFs I was unable to successfully uncouple OXPHOS in these immortalised cell lines, therefore the data presented in figure 4.2C does not provide information about the maximal oxidative capacity of the cell.

Taken together these findings demonstrate that ablation of PKR promotes oxidative phosphorylation coupled to ATP production and significantly reduces the expression of UCP1 thereby decreasing the contribution of mitochondrial uncoupling to energy expenditure. These findings also support the notion that in PKR knockout cells enhanced ATP production may consume excess NADH or NADPH produced by the G6PD enzyme, thereby preventing detection of a significant difference in concentration of these cofactors. Hence it is likely that mice devoid of PKR have an altered metabolic profile due to augmentation of OXPHOS and mitochondrial uncoupling, in addition to the detected alteration in the G6PD.

4.4.4 PKR does not affect leptin signalling.

The positive association between leptin concentration and obesity is long established (Montague, Farooqi et al. 1997). Therefore I measured if PKR-mediated regulation of weight gain associates with altered expression of leptin. Both chow and high fat diet fed apoE:PKR knockout and apoE knockout mice have similar blood leptin concentrations (Fig.4.5A and B). It has to be noted that weight gain of apoE:PKR ablated mice is not as pronounced as that seen in single PKR knockout mice, likely reducing the capacity to detect a difference in leptin levels.

Next I assessed activation of the leptin signalling cascade by measuring the phosphorylation status of STAT3 in the hypothalamus and liver of single PKR knockout and wild type mice fed a high fat diet. Experiments to drive phosphorylation of STAT3 by administering leptin show no response suggesting that the intraperitoneal route of leptin administration is not effective, or alternatively there was a technical difficulty in detecting the *in vivo* phosphorylation of STAT3. (Fig.4.5C and D). As there was no conspicuous difference in the levels of leptin between the apoE and apoE:PKR knockout mice I did not pursue this pathway. Future studies could better assess STAT3 phosphorylation in the hypothalamus after a, more appropriate, cerebrovascular leptin challenge. However, our preliminary data do not suggest that a defect in leptin signalling accounts for the PKR-dependent diet-induced weight gain.

LACK OF PKR IMPAIRS INSULIN SIGNALLING

4.4.5 Lack of functional PKR dampens the insulin response in 3T3 MEFs, by reducing expression of IRS2.

Given that mice ablated for PKR are glucose intolerant, and in line with the role of PKR in modulating the activity of JNK and mTOR signalling, I speculated that ablation of PKR could interfere with insulin induced PI3K/Akt signalling because attenuation of the insulin signalling cascade associates with development of type 2 diabetes (Iordanov, Paranjape et al. 2000; Morel, Couturier et al. 2009). First I determined the concentration of insulin that

was required to induce PI3K signalling *in vitro*. Bac7 MEFs were treated with 1µM or 100nm insulin for 15 or 70 minutes. Figure 4.6A shows that phosphorylation of p70S6K is greatest 70 minutes after stimulation with 1uM insulin compared to a 15 minute insulin stimulation and non-treated cells. Therefore, to assess insulin-mediated responses in subsequent experiments I used 1µM of insulin for 60 minutes.

Metabolic stress caused by excess nutrients or hyperinsulinemia is reported to suppress insulin signalling by promoting the internalization and down regulation of the insulin receptor (IR). Accordingly, proteosomal degradation of the insulin receptor associates with insulin resistance, obesity and diabetes (Garvey, Olefsky et al. 1986; Tiwari, Halagappa et al. 2007; Zhou, Zhang et al. 2009). Figure 4.6B and C demonstrates that protein expression of insulin receptor-β (IRβ) is similar in WT, PKR knockout and K271R homozygote primary and 3T3 MEFs with or without insulin stimulation (Confirmed in primary MEFs in Appendix VI B). Interestingly, protein expression of the essential insulin mediator, insulin receptor substrate-2 (IRS2), is markedly decreased in 3T3 and primary MEFs lacking PKR (Fig.4.7A-C and appendix VI A), although, expression of the *irs2* mRNA is similar in WAT of PKR knockout and WT mice (Fig.4.7D).

Recent evidence suggests that AMPK is activated by insulin to regulate the activity of PI3K/Akt and modulate insulin signalling (Liu, Gauthier et al. 2010; Chopra, Li et al. 2012). Therefore, I assessed activation of AMPK in response to insulin stimulation. Insulin has no effect on AMPK phosphorylation in 3T3 and primary MEFs lacking or expressing PKR (Fig.4.7A and B). These finding suggests that ablation of PKR does not influence degradation of the insulin receptor but, instead, reduces protein expression of IRS2 independently of insulin-induced AMPK phosphorylation. This would be expected to impair insulin signalling.

4.4.6 Lack of functional PKR suppresses p70S6K and enhances Akt phosphorylation.

I anticipated that reduced expression of IRS2 in cells lacking PKR would attenuate downstream signalling, which would be evidenced as a reduction of p70S6K and Akt phosphorylation. I assessed insulin-mediated phosphorylation of p70S6K in 3T3 MEFs over a time course of 180 minutes (Fig.4.8A). Phosphorylation of p70S6K is greatest at 30 and 60

minutes after insulin stimulation in WT MEFs. This response is significantly dampened in PKR knockout MEFs, corroborating that PKR modulates insulin signalling (confirmed in appendix V A-C). To further test this notion, I assessed phosphorylation of a downstream target of PI3K, the translational repressor 4EBP1 (Gingras, Kennedy et al. 1998). However, no difference in insulin-mediated phosphorylation of 4EBP1 is detected in WT and PKR ablated cells (Fig.4.8B). To establish that downstream regulation of p70S6K is dependent on PKR, I assessed phosphorylation of p70S6K in NmuMNG cells after treatment with a PKR inhibitor, 2-aminopurine (2AP). In keeping with the preceding data, inhibition of PKR suppressed p70S6K phosphorylation, confirming that this is a PKR dependent mechanism (Fig.4.8C).

The expected outcome of attenuated phosphorylation of p70S6K in MEFs ablated for PKR is decreased phosphorylation of Akt. Phosphorylation of Akt was assessed at serine residue 473 because this residue needs to be phosphorylated to allow full activation of the Akt protein. I demonstrated that MEFs lacking PKR have elevated levels of basally phosphorylated Akt (Fig.4.8D), however there is no change in phosphorylation of Akt in response to insulin stimulation compared to wild type MEFs. This finding is confirmed by another western blot shown in appendix V B. It has been proposed that rapamycin mediated inhibition of mTOR induces Akt phosphorylation in a PI3K dependent manner but paradoxically suppresses phosphorylation of p70S6K and 4EBP1, providing a plausible explanation for our findings (Sun, Rosenberg et al. 2005).

4.4.7 PKR in mTOR signalling

Since phosphorylation of p70S6K is suppressed in MEFs deleted for PKR I speculated that reduced mTOR signalling could account for these differences. Therefore, I addressed the role of mTOR in phosphorylation of p70S6K in response to insulin and rapamycin treatment in SV40 MEFs. To identify an effective concentration of rapamycin required to inhibit phosphorylation of the downstream mTOR effector p70S6K, WT spleen macrophages were treated with 10nm or 100nm rapamycin for 30, 60 or 120 minutes (Fig.4.9A). Phosphorylation of p70S6K was effectively suppressed by all treatments and a dose of 100nm of rapamycin for 1 hour is used in subsequent experiments. Figure 4.9B shows that in WT and PKR ablated MEFs phosphorylation of p70S6K is induced in response to insulin

and consequently inhibited with rapamycin treatment when compared to DMSO (the carrier solute) treated cells. Furthermore, stimulating cells with insulin following rapamycin treatment does not induce phosphorylation of p70S6K suggesting that insulin-mediated activation of p70S6K could rely on mTOR signalling.

Intriguingly, rapamycin treatment had the same effect on 4EBP1 in Bac7 and Bac10 3T3 MEFs (Fig.4.9C). Previous reports have established that rapamycin specifically inhibits the mTOR complex 1 but not mTORC2. This is of consequence as regulation of 4EBP1 is reported to be independent of mTORC1, therefore rapamycin mediated suppression of mTORC1 is able to suppress phosphorylation of p70S6K but not 4EBP1 providing a plausible explanation for the lack of change in phosphorylation (Nawroth, Stellwagen et al. 2011).

4.4.8 Loss of PKR reduces expression of PP2A and enhances Akt phosphorylation.

Another mechanism that is critical in modulating phosphorylation of Akt is mediated by the serine/threonine phosphatase PP2A. PP2A is a negative regulator of insulin signalling because it dephosphorylates Akt rendering it inactive (Ugi, Imamura et al. 2004). PKR has been identified to induce PP2A activity by inhibitory phosphorylation of the PP2A regulator B56α (Xu and Williams 2000). Therefore, I sought to assess protein levels of PP2A in response to insulin treatment. I observed that basal expression of the PP2A protein is similar in primary MEFs lacking and expressing PKR and that insulin stimulation has no effect on PP2A expression (Fig.4.10 A and B and appendix VI B). Interestingly, protein levels of PP2A in the liver of high fat diet fed mice ablated for PKR are significantly reduced in comparison to wild type mice (Fig.4.10A and B, *p=0.0077) demonstrating that PKR may modulate expression of PP2A. One shortfall of this experiment is that I did not assess whether loss of PKR affects PP2A activity and consequent Akt phosphorylation. Hence it would be beneficial to perform a PP2A activity assay or *in vitro* signalling experiment to investigate the effect of PP2A inhibition on Akt phosphorylation. This hypothesis remains to be elucidated but constitutes a potential mechanism by which PKR could modulate Akt activity.

4.4.9 PKR does not affect splicing of the UPR protein XBP1.

ER stress is reported as a common pathological feature of obesity and it induces the UPR response, which is the principal event required for activation of another eIF2α kinase, PERK. XBP1 is a transcription factor that is activated during the UPR response. Therefore, I assessed the stasis of XBP1 to gauge the involvement of the UPR, and by proxy PERK, in liver and muscle tissue from WT and PKR knockout mice fed a high fat diet. This data suggest that the UPR is not induced because both WT and PKR knockout mice have similar levels of the spliced (activated) form of XBP1 in the liver and muscle, suggesting that PERK is also not activated in this instance (Fig.4.11A-D). I also assessed WAT specific expression of molecular chaperones induced during the UPR. HSP90AA is somewhat elevated in WAT from mice ablated for PKR compared to WT mice. Expression of the other chaperones, HSP90Ab and HSP90β, is unchanged in WAT and liver (Fig.4.11E and F). This is an important finding as it demonstrates that our experimental conditions do not involve the other eIF2α kinase, PERK.

PKR REGULATES AMPK SIGNALLING IN A TISSUE SPECIFIC MANNER

4.4.10 PKR does not modulate AMPK signalling in response to high fat diet feeding.

Disturbances of the AMPK-signalling network significantly influence energy homeostasis. Hence I assessed activation of the AMPK cascade *in vivo* in response to a chow and high fat diet to evaluate whether mice lacking PKR have perturbed signalling. The results show that phosphorylation of AMPK and its downstream target ACC, as well as protein levels of FASN are equivalent in the liver of high fat diet fed WT and PKR ablated mice (Fig.4.12A-F). There is no significant difference in transcript levels of LKB1, ACC, FASN or the metabolic enzyme lipoprotein lipase in muscle or liver tissue of PKR knockout and WT mice (Fig.4.13A and B). The difference seen in the mRNA level of SREBP1C (Fig.4.13A) is discussed below in section 4.13. These findings suggest that PKR does not modulate activation of AMPK in response to high fat diets.

To investigate the consequence of PKR ablation on AMPK signalling in apoE ablated mice single western blots were performed. In accordance with findings from single PKR knockout mice, expression of ACC and FASN in muscle and liver is similar between apoE and apoE:PKR knockout mice as are mRNA levels of LKB1, ACC or FASN (Appendix IV A-C). Intriguingly expression of FASN is notably elevated in WAT of high fat diet fed apoE:PKR knockout mice (Appendix IV B). Although these findings rely on single observations, a WAT specific increase in FASN expression is noteworthy as it could in part explain the increased adipocyte size and weight gain observed in apoE:PKR knockout mice.

Furthermore initial findings from apoE:PKR ablated animals show that on the apoE ablated background activation of AMPK and ACC may occur in a tissue-specific pattern (Appendix IV B and D). These findings point toward a tentative role for PKR in posttranslational modulation of AMPK signalling on the apoE ablated background. However how PKR modulates this signalling cascade is still largely unknown but it is presumably a consequence of altered lipid transport. The conclusion drawn from these findings in apoE ablated mice are highly speculative and require further investigation to conclusively confirm a role for PKR in regulation of FASN.

4.4.11 PKR alters expression of SREBP1C.

SREBP1C is a regulatory element binding protein that induces transcription of genes involved in fatty acid synthesis such as ACC, FASN and SCD-1. To assess a role for PKR in regulating fatty acid synthesis in response to a high fat diet I measured expression of SREBP1C in WT and PKR ablated mice. I expected expression of SREBP1C to be similar because there is no change in transcription of SREBP1C target genes. However, opposing this speculation, hepatic expression of SREBP1C is significantly reduced in mice lacking PKR (Fig.4.13A, *p=0.0217). The PKR-dependent mechanism that governs expression of SREBP1C is uncertain however a family of transcription factors known to regulate expression of SREBP1C, are regulated by eIF2α phosphorylation.

4.4.12 Fasting increases phosphorylation of acetyl-CoA carboxylase in the liver of high fat diet fed mice lacking PKR.

Given that AMPK is activated by nutrient deprivation, I reasoned that differences in in AMPK or ACC phosphorylation might better be detected in response to fasting. Therefore, I fasted PKR deficient and WT mice overnight and then allowed them to re-feed on the high fat diet for 2 or 4 hours. In line with the expected result, fasting (0 hour time point) caused marked phosphorylation of ACC in the liver and heart of WT mice (Fig4.15A and B). This response was attenuated by re-feeding. Interestingly, phosphorylation of ACC was unchanged in mice ablated for PKR in response to fasting or re-feeding when compared to WT mice (Fig.4.15A and B). It is important to note that only one animal was sacrificed for each time point; therefore the data presented here is only speculative and needs further investigation. Phosphorylation of ACC is representative of fatty acid oxidation and suppressed lipid synthesis; therefore this mechanism could contribute to the protective effects offered by PKR expression against the development of diet-induced disease.

PKR REGULATES STERILE INFLAMMATORY RESPONSES

4.4.13 PKR does not regulate circulating levels of cytokines in response to high fat diet.

Since metabolic inflammatory responses are asserted to promote the development of obesity, I sought to assess levels of the circulating pro-inflammatory cytokines TNFα, IL-6 and CRP in mice fed a high fat diet. There is no detectable difference for any of the assessed cytokines between PKR WT and knockout mice (Fig4.16A-D). Consistent with these data hepatic gene expression of IL-6, IL-1β, IL-12, CXCL10 and IL-10 is unchanged, as is expression of IL-6, IL-1β and IL-12 in the muscle of PKR WT and knockout mice (Fig.4.17A and B). These results suggest that PKR does not regulate the production or expression of classical inflammatory cytokines in response to a high fat diet.

4.4.14 IL-6 transignalling.

PKR is known to indirectly regulate mRNA levels of Interleukin-6 (IL-6) (Goh, deVeer et al. 2000). IL-6 modulates a range of biological activities including immune and inflammatory responses and plays a key role in chronic inflammation underlying a number of disease states including rheumatoid arthritis and colon cancer (Kopf, Baumann et al. 1994; van der Poll and van Deventer 1998; Wei, Kuo et al. 2001; Scheller, Ohnesorge et al. 2006). IL-6 is normally expressed by hepatocytes and leukocytes and initiates classical signalling by binding to a membrane bound IL-6 receptor complex consisting of the IL-6 receptor and a constitutively expressed gp130 signal transducing protein. In addition to the classical role of IL-6 in inflammation, IL-6 participates in trans-signalling to drive inflammation in tissues other than the liver (Scheller, Ohnesorge et al. 2006). The shift to trans-signalling is believed to be a good indication of the chronic inflammatory status of an individual. The membrane bound IL-6 receptor becomes proteolytically cleaved by the metalloproteinase ADAM17 to create a soluble form of the receptor (sIL-6R). sIL-6R then translocates to distant organ sites where it associates with gp130 and induces IL-6 signalling. Increased circulating concentration of sIL-6R disrupts glucose homeostasis and correlates with the development of the metabolic syndrome (Zuliani, Galvani et al. 2010; Clementi, Gaudy et al. 2011). To address the possibility that PKR promotes the cleavage of IL-6 receptors to induce inflammation in the liver, I assessed hepatic IL-6 trans-signalling.

Densitometry analysis of hepatic protein levels of the cleaved soluble IL-6 receptor suggest that IL-6 trans-signalling is activated to a similar extent in both PKR WT and knockout mice (Fig.4.18A and B). Correspondingly, protein levels of the soluble IL-6 receptor and metalloproteinase ADAM17 are similar in apoE:PKR and apoE knockout mice (Fig.4.18C and D). Hence, IL-6 trans-signalling does not play an important role in hepatic inflammation and so is not a potential mechanism for PKR-dependent diet induced metabolic dysregulation in the liver.

4.4.15 PKR regulates inflammasome mediated signalling.

Activation of the inflammasome results in the secretion of the inflammatory cytokines IL-1β and IL-18. IL-1β. Importantly IL-1β has been demonstrated to be a driver of

obesity and related pathologies. Figure 4.19A shows that expression of components of the inflammasome, NALP3 and caspase-1, in white adipose tissue and IL-1β in liver (Fig.4.19B) is similar in PKR knockout and WT mice. However, hepatic IL-18 mRNA is significantly (*p=0.016) decreased in the liver of mice ablated for PKR (Fig.4.19B). This result is in accordance with preceding reports that show PKR to augment the primary TLR-dependent response to induce NF-κB dependent transcription. The secondary, critical, step of inflammasome activation is inflammasome complex assembly, activation of Caspase-1 and subsequent processing of the pro-form of IL-1β and IL-18 to enable secretion of the active cytokines.

I assessed activation of the inflammasome in response to nigericin, or ATP in LPS primed RAW and primary spleen and peritoneal macrophage cells, however I was unable to detect caspase-1 cleavage (appendix IX-XI). This work was continued by Dr. Howard Lim in our laboratory who has demonstrated PKR to modulate the inflammasome.

To test a possible function for PKR in inflammasome activation *in vivo* I assessed secretion of IL-1β from *ex vivo* tissue explants. PKR WT and knockout mice fed were fed a high fat diet for 5 weeks after which the liver, pancreas and white adipose tissue was isolated and cultured overnight in DMEM. Figures 4.20A and B demonstrate that levels of IL-1β detected in the media collected from *ex vivo* liver and WAT tissue cultures was similar between PKR knockout and WT mice. However, pancreas isolated from mice ablated for PKR secreted significantly more IL-1β compared to the WT pancreas (Fig.4.20C). These findings are confirmed in another experiment shown in appendix IX. Fitting with this result, mRNA levels of pancreatic IL-1β (but not ASC) were significantly greater in the PKR ablated mice compared to WT (Fig.4.20G and H). Importantly, concentration of IL-6 secreted from WT and PKR ablated WAT, liver and pancreas was equivalent (Fig.4.20D-G). These findings suggest that loss of PKR promotes IL-1β production, without inducing a concurrent increase in the concentration of classic cytokines. In addition to being interpreted as a readout of inflammasome activation, secretion of IL-1β may also be indicative of other signalling impairments, principally cell death.

Given that inflammasome activation is linked to obesity and insulin resistance, and given the specificity of the response in the pancreas, this is likely to be an important potential mechanism for diet induced metabolic dysfunction in PKR knockout mice. However seeing as the results presented in this section are not conclusive on their own this concept requires further examination. To investigate whether increased secretion of IL-1β may be due to activation of apoptotic signalling cascades, the pancreas from both PKR knockout and wild type mice should be assessed for apoptotic cells via TUNEL staining.

4.5 DISCUSSION

This study was undertaken to define the PKR-dependent molecular mechanisms that modulate metabolic disease. In this chapter I demonstrate that PKR regulates a number of metabolic and innate immune signalling networks to protect against the pathophysiology of the metabolic syndrome. Preliminary findings from chapter three show that mice ablated for PKR have a minor but statistically non-significant reduction in BAT temperature compared to wild type mice. Comparisons of thermogenic activation of BAT in other studies suggest that small changes in temperature might account for weight gain. In conjunction with these findings, results garnered in this chapter show that mice ablated for PKR have significantly reduced expression of the thermogenic protein UCP1 in WAT. Repressed expression of UCP1 is linked to suppressed energy expenditure and diet induced obesity although some reports have suggested that BAT specific deletion of UCP1 does not associate with weight gain because mitochondrial proton leak in skeletal muscle compensates for UCP1 deficiency in BAT (Kopecky, Clarke et al. 1995; Kopecky, Hodny et al. 1996). (Enerback, Jacobsson et al. 1997; Monemdjou, Hofmann et al. 2000).

The applicability of a putative role for PKR in BAT thermogenesis for humans is uncertain. Until recently it was believed that BAT depots in adult humans were not physiologically relevant. However, a number of studies have now confirmed the presence of metabolically functional BAT in adult humans and that a lower metabolic rate increases the susceptibility to obesity related pathologies (Rising, Keys et al. 1992; Nedergaard, Bengtsson

et al. 2007; Cypess, Lehman et al. 2009; Cypess and Kahn 2010). Regardless of the role of BAT, the observed change in UCP1 in PKR ablated mice may have broader relevance because uncoupling protein 2, which is the human homologue of murine UCP1, is widely expressed in human tissues, especially WAT, and is implicated in regulating body composition and energy expenditure in humans (Fleury, Neverova et al. 1997).

A function for PKR in modulating energy expenditure is alternately substantiated by *in vitro* mitochondrial studies. I demonstrated that spleen macrophages and 3T3 MEF cell lines lacking PKR have significantly increased basal oxygen consumption likely due to the observed increase in ATP synthesis. Heightened ATP synthesis can be suggestive of enhanced OXPHOS activity. Additionally, cells devoid of functional PKR have decreased mitochondrial proton leak. Correspondingly, these measures showing increased ATP synthesis and mitochondrial proton leak, in humans correlate with obesity (Hallgren, Sjostrom et al. 1989). However it is plausible that the observed increase in ATP synthesis in mice lacking PKR is due to an increase in cellular energy demand. Accordingly a recent publication from our laboratory suggests that PKR-dependent regulation of the actin modifying protein gelsolin is critical in cytoskeletal remodelling (Irving et al., 2012). Hence, an increase in ATP synthesis in mice ablated for PKR could be explained by this phenomenon.

Based on previous knowledge that increased mitochondrial biogenesis correlates with enhanced ATP synthesis, I hypothesized that mRNA and protein expression of electron transport chain enzymes would be increased in mice ablated for PKR to explain for greater ATP synthesis. However, mRNA expression of ATP synthase and NADH dehydrogenase and mitochondrial protein levels of cytochrome C oxidase IV is equivalent in WT and PKR knockout mice. To garner more insight into mitochondrial bioenergetics future studies should measure the enzymatic activity of OXPHOS complexes and assess expression of PGC1α, a transcription factor involved in mitochondrial biogenesis. The data harnessed from the mitochondrial experiments suggest an involvement of PKR in energy expenditure however the results from BAT temperature studies are not conclusive enough on their own to account for the weight gain and adiposity in mice ablated for PKR.

The process of thermogenesis in addition to having an important role in energy expenditure is also beneficial in protecting against oxidative stress. Excess calorie intake combined with a lower capacity for energy expenditure is known to increase the proton motive force and results in the production of reactive oxygen species. This is of consequence, because if mice deficient for PKR have reduced mitochondrial proton leak this could associate with greater oxidative stress caused by increased generation of ROS. Oxidative stress is detrimental to the cell because it causes mitochondrial dysfunction and results in the development of type 2 diabetes. Therefore, further investigation of mitochondrial ROS production could provide important insight toward mechanisms that govern glucose intolerance and diabetes in PKR knockout mice. Future studies should measure ROS production and the enzymatic activity of complex I and III, which are responsible for generating a large amount of cellular ROS.

Consistent with increased weight gain, I also demonstrate that mice ablated for PKR are glucose intolerant and I identify impairments in gluconeogenesis. Assessment of hepatic gluconeogenic gene expression revealed that G6pase is significantly elevated in PKR knockout mice. G6pase plays a major role in glucose homeostasis by catalysing the final step of gluconeogenesis as it converts glucose-6-phosphate to glucose. Over expression of G6pase in hepatocytes has been shown to increase hepatic glucose output and concurrently suppress glycolysis and glycogen synthesis (Aiston, Trinh et al. 1999). Although not experimentally tested as part of this thesis, the increase in G6pase expression could account for fasting hyperglycemia in mice ablated for PKR because of reduced ability to store glycogen. Alternatively, deletion of PKR could impair glucose clearance from the blood, by either reducing expression of the glucose transporter GLUT4 or by sequestering it in the cytoplasm and preventing its translocation to the plasma membrane for glucose transport activity. To elucidate this, future studies should quantify hepatic glycogen content and assess high fat diet induced glucose clearance in PKR knockout and wild type mice. In conjunction with these findings, expression of glycolytic enzyme HK1, HK3 and PFK1 in the liver is similar in WT and PKR knockout mice, suggesting that glycolysis-mediated breakdown of glucose is equivalent in both animal cohorts. As a consequence, enhanced expression of

G6pase in mice deleted for PKR most likely accounts for elevated blood glucose concentrations.

The identification of defects in glucose homeostasis prompted me to assess glucose output by measuring the conversion of pyruvate to glucose. Ablation of PKR significantly enhanced glucose output in response to a pyruvate challenge, indicating a heightened rate of conversion to glucose. Opposing this finding, I detected an increased expression of the rate-limiting enzyme of the pentose phosphate pathway, glucose-6-phosphatedehydrogenase in PKR knockout mice. G6PD plays a key role in glucose oxidation by converting 6-phosphogluconate to ribulose-5-phosphate and counteracts the role of G6pase in glucose production. I speculate that the identified fold increase in transcription of G6PD is not high enough to sufficiently increase its enzymatic activity and to effectively neutralize elevated glucose concentrations in PKR knockout mice. Collectively these findings suggest that increased expression of G6pase dominates the phenotype.

G6PD is also a principal generator of the cofactor NADPH that is an essential intermediate for biosynthetic pathways of lipid and cholesterol metabolism as well as OXPHOS. In conjunction with enhanced expression of G6PD in PKR knockout mice, the expression of other NADPH producing enzymes, IDH2 and ME1 is also induced, suggesting that ablation of PKR may increase concentration of the NADPH molecule. A consequence of elevated NADPH is augmented triglyceride biosynthesis resulting in adiposity and weight gain. Although the cellular concentration of NADPH appeared similar in WT and PKR knockout MEFs it was observed that the PKR null cells had heightened ATP synthesis and so NADPH is likely rapidly consumed by OXPHOS. It would be more appropriate to measure NADPH *in vivo*.

In addition to the aforementioned mechanisms that could account for impairments in glucose homeostasis, data compiled from this chapter suggests that a high fat diet does not induce the UPR or activate PERK, confirming that the PKR dependent regulation of pancreatic islet size, identified in the preceding chapter, is independent of PERK activity. Importantly, the morphology of the pancreas from a PKR ablated mouse did not reflect that of a mouse deficient for PERK (Harding, Zeng et al. 2001).

I speculated that mice lacking PKR could have reduced islet size because of decreased expression of IRS2 (Withers, Gutierrez et al. 1998; Kubota, Tobe et al. 2000). Accordingly, expression of the critical signal transducer protein IRS2 is significantly reduced in PKR ablated primary and 3T3 MEFs. Importantly, suppressed expression of IRS2 correlates with reduced insulin-mediated phosphorylation of its downstream target p70S6K in PKR ablated MEFs. Despite reduced activation of p70S6K, phosphorylation of the PI3K downstream target 4EBP1 is comparable. Recent reports have established that PI3K facilitates the phosphorylation of 4EBP1 in a rapamycin sensitive manner, and that PI3K could therefore mediate 4EBP1 phosphorylation in an mTOR dependent manner. Opposing the expected consequence of suppressed IRS2 expression, cells deficient for PKR had persistently increased phosphorylation of Akt. These findings are conflicting because attenuated insulin signalling should correlate with decreased phosphorylation of Akt. There are a number of feedback control mechanisms that regulate insulin signalling that could potentially explain the enhanced activation of Akt. Recently, PP2A was identified as a negative regulator of insulin signalling by dephosphorylating and inhibiting the activity of Akt and as a consequence contributing to insulin resistance. Since protein levels of PP2A are significantly lower in the liver of mice ablated for PKR in comparison to wild type mice I speculated that PKR-mediated regulation of PP2A may be critical in modulating activation of Akt, however more experiments need to be performed to establish this (Xu and Williams 2000). In addition to the aforementioned mechanism, PKR modulates the activity of the PTEN phosphatase, which also dephosphorylates Akt rendering it inactive (Mounir, Krishnamoorthy et al. 2009). Hence, different potential mechanisms exist that might explain the unexpected phosphorylation status of Akt.

AMPK is a central energy sensor and a critical modulator of cellular metabolism. Our findings suggest that AMPK and its downstream target ACC are not differentially activated in response to a high fat diet in the liver of WT or PKR knockout mice, which is fitting with the observation showing that hepatic and muscle mRNA levels of LKB1, ACC and FASN is equivalent in all animal cohorts. However, evaluation of protein and gene expression of the AMPK cascade in the murine model for atherosclerosis suggests that unlike single PKR

knockout mice, loss of PKR on the apoE deficient background modulates activation of AMPK in a tissue specific manner. The AMPK cascade is notably activated in WAT of apoE:PKR ablated mice, as reflected by increased phosphorylation of ACC and enhanced expression of FASN. These findings appear to deviate from that expected, given the increased weight gain in the absence of PKR, because phosphorylation of ACC inhibits fatty acid synthesis whilst co-ordinately promoting mitochondrial fatty acid oxidation. One regulatory mechanism that could account for ACC activation, again, involves the PP2A phosphatase (Kowluru, Chen et al. 2001). PKR-dependent regulation of PP2A expression could reduce phosphorylation of ACC in WT mice. Even though fatty acid oxidation is a potential therapeutic strategy to improving insulin sensitivity in obesity, it is not entirely protective to the cell because it creates NADH which is an essential cofactor used by OXPHOS to synthesise ATP. Therefore, ACC-mediated oxidation of fatty acids in WAT of PKR ablated mice could contribute to an unfavourable increase in ATP synthesis, thereby supporting my earlier findings that show that loss of PKR impairs mitochondrial processes.

Despite the increased phosphorylation of ACC in WAT of chow and high fat diet fed apoE:PKR knockout mice, expression of FASN is markedly increased, constituting a potential mechanism for increased adiposity and weight gain in these mice. The contribution of FASN to WAT specific fatty acid synthesis implicates PKR in a tissue specific translational and transcription regulation of lipogenic genes in response to high fat diets. Previous studies have demonstrated that long chain fatty acids such as palmitate increase the phosphorylation of AMPK and ACC in skeletal muscle (Fediuc, Gaidhu et al. 2006). Therefore, I speculated that FASN-mediated production of fatty acids in WAT could contribute to increased concentration of circulating FFA in apoE:PKR knockout mice, which would in turn induce a similar phosphorylation event to promote ACC activation and fatty acid oxidation. In conclusion, the disposition of PKR knockout mice toward fatty acid synthesis appears to constitute the phenotype because simultaneous activation of ACC-mediated fatty acid oxidation does not appear to counteract diet induced weight gain. However, β-oxidation could provide some protection against weight gain because of the reduced weight of apoE:PKR ablated mice in comparison to single PKR knockout mice. It is

important to note that western blots assessing activation of AMPK signalling in apoE:PKR and apoE knockout mice are n=1, therefore the discussion above is speculative and I cannot make any final assumptions about PKR-dependent effects on AMPK signalling.

Although mRNA levels of hepatic ACC and FASN are similar in WT and PKR ablated mice, expression of their transcriptional activator SREBP1C is significantly decreased in PKR knockout mice. This finding is difficult to equate with the phenotype of the animal, as suppression of SREB1C associates with improved metabolic syndrome (Shimomura, Shimano et al. 1998; Horton, Goldstein et al. 2002; Knebel, Haas et al. 2012). However, the observed changes in SREBP1C mRNA levels between WT and PKR ablated mice may not be physiologically relevant to significantly alter induction of downstream targets ACC and FASN. The family of C/EBP transcription factors have recently come to light as important positive regulators of SREBP1C transcription (Payne, Au et al. 2010). PKR is demonstrated to control the ratio of C/EBPβ and C/EBPα isoforms by modulating translational repression via eIF2α. Loss of PKR associates with decreased expression of C/EBPβ, which provides a plausible mechanism by which PKR could suppress induction of SREBP1C.

Although PKR is generally considered to be pro-inflammatory and inflammation has a strong link to obesity, it is the PKR knockout mouse that accumulates the greater weight. Accordingly, I found no evidence that PKR advances production of the pro-inflammatory cytokines IL-6, TNFα, and CRP in response to diet. Neither does it affect hepatic or skeletal muscle mRNA expression of a wide array of pro-inflammatory mediators IL-6, IL-1β, IL-12, CXCL10 and IL-10. Furthermore, protein levels of the soluble IL-6 receptor and metalloproteinase ADAM17 were comparable in WT, PKR knockout, apoE and apoE:PKR knockout animals, indicating that PKR does not play a role in IL-6 trans-signalling to regulate hepatic inflammation.

Rather than advancing the production of the classic inflammatory cytokines, I made the novel discovery that PKR suppressed pancreas specific secretion of IL-1β. I postulated that production of IL-1β was associated with inflammasome activation, however as I did not measure inflammasome activity it is difficult to make such conclusions. An alternate mechanism that could account for enhanced production of IL-1β would involve activation of

NF-kB. Previous studies have reported that ablation of PKR in mice creates a small transcript that is capable of signalling through protein-protein interactions. Therefore the observed increase in levels of Il-1beta in mice ablated for PKR may be the result of PKRs capacity to signal and activate NF-kb resulting in transcription of pro-inflammatory cytokines. However in saying this, I did not observe an increase in one of the primary targets of NF-kB, TNF-a which suggests that NF-kB is likely not activated. Alternatively mice lacking PKR may retain their capacity to participate in cell-signalling through protein-protein interactions with other yet unknown adapter molecules to modulate expression of IL-1β. Nevertheless it is highly likely that PKR represses the activity of the inflammasome because preliminary experiments performed by Dr.Lim from our laboratory suggest that PKR regulates inflammasome activation. Additionally, palmitic acid, which has been demonstrated to activate the inflammasome, has also been shown to inhibit PKR (Yang, Badeanlou et al. 2009; Cho, Mukherjee et al. 2011; Wen, Gris et al. 2011).

During the course of this study two papers were published that contradict the findings of my study. The first by Nakamura et al (2010) reported that PKR promoted, rather than reduced, weight gain and ensuing pathologies by promoting inflammation and disrupting insulin signalling (Nakamura, Furuhashi et al. 2010). They also demonstrated that in response to palmitic acid and ER stress PKR mediates phosphorylation of IRS1 at serine residue 307, which is a conflicting observation because as suggested above palmitate ppears to inhibit PKR. Also, there is currently conflicting data on the consequence of serine 307 phosphorylation of IRS1 on insulin signalling with *in vitro* data suggesting phosphorylation of the serine 307 residue of IRS1 blocks insulin signalling and associates with insulin resistance, while *in vivo* data suggests this phosphorylation is protective (Sykiotis and Papavassiliou 2001; Copps, Hancer et al. 2010). The second report that contrasts my findings was by Lu et al (2012), whom demonstrated that PKR promotes, rather than inhibits, inflammasome activation (Lu, Nakamura et al. 2012). The reason for the variance in the role for PKR is not certain however some minor technical differences are identifiable between studies. The likely significant difference is the use of separate transgenic mice. Support for this comes from recently reported conflicts in the role for PKR in colitis, induced by treatment with

dextran sodium sulphate (DSS) using the different PKR knockout mice. A study by Cao et al (Cao, Song et al. 2012), like ourselves, used the PKR knockout animal produced in Charles Weissmann's laboratory (Yang, Reis et al. 1995), while a study by Rath et al (Rath, Berger et al. 2011) like Nakamura et al, used a PKR knockout animal produced in John Bell's laboratory. Ours and Cao et al's. study report that PKR is protective, while Rath and Nakamura et al. report that PKR exacerbates colitis and weight gain. The cause of this discrepancy between these transgenic mice has not been established. It has been claimed both mice produce, different, truncated PKR products. Hence, it seems plausible that the reported discrepancies in the studies are due to catalytic activity retained by the separate truncated peptides expressed in one or both animals. This is particularly interesting in light of the contrasting phenotypes of the K271R heterozygous and homozygous mice in my study.

Significantly, the inflammasome has been demonstrated to be a major modulator of colitis in the models used (dextran sodium sulfate-induced colitis). Therefore, there is the potential that the effects of PKR, in colitis and high fat feeding, could be mediated through inflammasome activation (Bauer, Duewell et al. 2010; Vandanmagsar, Youm et al. 2011). Hence, the report by Lu et al, suggesting a role for PKR in inflammasome activation is highly relevant, despite it appearing to contradict our findings on PKR (Lu, Nakamura et al. 2012). Independent preliminary studies in our laboratory have demonstrated PKR can play different roles in control of the inflammasome and that this is highly dependent on the stimulus. Therefore, I contend that PKR is able to repress activation of the inflammasome and that is relevant to stimulus generated by high fat feeding, because of the observed increased IL-1β production in the pancreas of PKR ablated mice. As PKR is constitutively expressed in all tissues, this tissue specific response suggests a particular stimulus. To date two reports have been published describing a role for the inflammasome in pancreatic homeostasis (Masters, Dunne et al. 2010; Youm, Adijiang et al. 2011). The conclusive experiment to validate PKR-dependent repression of diet activated inflammasome, by blocking IL-1β signalling with a receptor agonist, has not been completed in time to be included in this thesis.

Notably, the effects we identified for PKR reproduce those previously found for the other eIF2α kinases, GCN2 and PERK. Mice ablated for both GCN2 and PERK demonstrate exacerbated diet induced weight gain, as we demonstrate for PKR. This would appear to demonstrate that this pathway is generally protective in obesity, and encourages us to believe the responses we have measured in transgenic PKR knockout mouse used in this study faithfully demonstrate true loss of PKR. However, the reported mechanism by which each kinase functions differ between the different eIF2α kinases. We also demonstrate, using the homozygous K271R mouse, that the kinase activity for PKR is apparently dispensable for the protective effect. This seems at odds with common protective effect of eIF2α kinases and clarification awaits further analysis of the K271R transgenic mouse.

4.6 CONCLUSION

In summary our results have demonstrated that genetic deletion of PKR induces weight gain, adiposity and glucose intolerance by dysregulating vital gluconeogenic and lipogenic metabolic signalling pathways. PKR mediates protection against diet-induced pathologies by inducing a number metabolic gene networks that together alleviate metabolic disease. Ablation of functional PKR is shown to augment processes that govern energy expenditure, ATP production and lipid biosynthesis to promote weight gain, glucose intolerance and fatty liver disease. In contrast to other reports, we do not detect any role for PKR in promoting the inflammatory cytokines, TNFα or IL-6, previously associated with obesity but rather demonstrate PKR reduces the secretion of IL-1β, specifically from the pancreases.

4.7 REFERENCES

Aiston, S., K. Y. Trinh, et al. (1999). "Glucose-6-phosphatase overexpression lowers glucose 6-phosphate and inhibits glycogen synthesis and glycolysis in hepatocytes without affecting glucokinase translocation. Evidence against feedback inhibition of glucokinase." J Biol Chem **274**(35): 24559-24566.

Bastard, J. P., M. Maachi, et al. (2006). "Recent advances in the relationship between obesity, inflammation, and insulin resistance." Eur Cytokine Netw **17**(1): 4-12.

Bauer, C., P. Duewell, et al. (2010). "Colitis induced in mice with dextran sulfate sodium (DSS) is mediated by the NLRP3 inflammasome." Gut **59**(9): 1192-1199.

Cao, S. S., B. Song, et al. (2012). "PKR protects colonic epithelium against colitis through the unfolded protein response and prosurvival signaling." Inflamm Bowel Dis.

Chakrabarti, A., A. J. Sadler, et al. (2008). "Protein kinase R-dependent regulation of interleukin-10 in response to double-stranded RNA." J Biol Chem **283**(37): 25132-25139.

Cho, H., S. Mukherjee, et al. (2011). "Molecular mechanism by which palmitate inhibits PKR autophosphorylation." Biochemistry **50**(6): 1110-1119.

Chopra, I., H. F. Li, et al. (2012). "Phosphorylation of the insulin receptor by AMP-activated protein kinase (AMPK) promotes ligand-independent activation of the insulin signalling pathway in rodent muscle." Diabetologia **55**(3): 783-794.

Clementi, A. H., A. M. Gaudy, et al. (2011). "Deletion of interleukin-6 improves pyruvate tolerance without altering hepatic insulin signaling in the leptin receptor-deficient mouse." Metabolism **60**(11): 1610-1619.

Copps, K. D., N. J. Hancer, et al. (2010). "Irs1 serine 307 promotes insulin sensitivity in mice." Cell Metab **11**(1): 84-92.

Cypess, A. M. and C. R. Kahn (2010). "The role and importance of brown adipose tissue in energy homeostasis." Curr Opin Pediatr **22**(4): 478-484.

Cypess, A. M., S. Lehman, et al. (2009). "Identification and importance of brown adipose tissue in adult humans." N Engl J Med **360**(15): 1509-1517.

de Heredia, F. P., S. Gomez-Martinez, et al. (2012). "Obesity, inflammation and the immune system." Proc Nutr Soc **71**(2): 332-338.

Deb, A., S. J. Haque, et al. (2001). "RNA-dependent protein kinase PKR is required for activation of NF-kappa B by IFN-gamma in a STAT1-independent pathway." J Immunol **166**(10): 6170-6180.

Deiuliis, J. A., L. F. Liu, et al. (2010). "Beta(3)-adrenergic signaling acutely down regulates adipose triglyceride lipase in brown adipocytes." Lipids **45**(6): 479-489.

Enerback, S., A. Jacobsson, et al. (1997). "Mice lacking mitochondrial uncoupling protein are cold-sensitive but not obese." Nature **387**(6628): 90-94.

Fediuc, S., M. P. Gaidhu, et al. (2006). "Regulation of AMP-activated protein kinase and acetyl-CoA carboxylase phosphorylation by palmitate in skeletal muscle cells." J Lipid Res **47**(2): 412-420.

Fleury, C., M. Neverova, et al. (1997). "Uncoupling protein-2: a novel gene linked to obesity and hyperinsulinemia." Nat Genet **15**(3): 269-272.

Galve-de Rochemonteix, B., K. Wiktorowicz, et al. (1993). "C-reactive protein increases production of IL-1 alpha, IL-1 beta, and TNF-alpha, and expression of mRNA by human alveolar macrophages." J Leukoc Biol **53**(4): 439-445.

Garvey, W. T., J. M. Olefsky, et al. (1986). "Insulin induces progressive insulin resistance in cultured rat adipocytes. Sequential effects at receptor and multiple postreceptor sites." Diabetes **35**(3): 258-267.

Gingras, A. C., S. G. Kennedy, et al. (1998). "4E-BP1, a repressor of mRNA translation, is phosphorylated and inactivated by the Akt(PKB) signaling pathway." Genes Dev **12**(4): 502-513.

Goh, K. C., M. J. deVeer, et al. (2000). "The protein kinase PKR is required for p38 MAPK activation and the innate immune response to bacterial endotoxin." EMBO J **19**(16): 4292-4297.

Grujic, D., V. S. Susulic, et al. (1997). "Beta3-adrenergic receptors on white and brown adipocytes mediate beta3-selective agonist-induced effects on energy expenditure, insulin secretion, and food intake. A study using transgenic and gene knockout mice." J Biol Chem **272**(28): 17686-17693.

Hallgren, P., L. Sjostrom, et al. (1989). "Influence of age, fat cell weight, and obesity on O2 consumption of human adipose tissue." Am J Physiol **256**(4 Pt 1): E467-474.

Horton, J. D., J. L. Goldstein, et al. (2002). "SREBPs: activators of the complete program of cholesterol and fatty acid synthesis in the liver." J Clin Invest **109**(9): 1125-1131.

Hotamisligil, G. S., P. Peraldi, et al. (1996). "IRS-1-mediated inhibition of insulin receptor tyrosine kinase activity in TNF-alpha- and obesity-induced insulin resistance." Science **271**(5249): 665-668.

Hotamisligil, G. S., N. S. Shargill, et al. (1993). "Adipose expression of tumor necrosis factor-alpha: direct role in obesity-linked insulin resistance." Science **259**(5091): 87-91.

Iordanov, M. S., J. M. Paranjape, et al. (2000). "Activation of p38 mitogen-activated protein kinase and c-Jun NH(2)-terminal kinase by double-stranded RNA and encephalomyocarditis virus: involvement of RNase L, protein kinase R, and alternative pathways." Mol Cell Biol **20**(2): 617-627.

Jung, R. T., P. S. Shetty, et al. (1979). "Reduced thermogenesis in obesity." Nature **279**(5711): 322-323.

Katta, A., S. K. Kakarla, et al. (2012). "Diminished muscle growth in the obese Zucker rat following overload is associated with hyperphosphorylation of AMPK and dsRNA-dependent protein kinase." J Appl Physiol **113**(3): 377-384.

Kazemi, S., Z. Mounir, et al. (2007). "A novel function of eIF2alpha kinases as inducers of the phosphoinositide-3 kinase signaling pathway." Mol Biol Cell **18**(9): 3635-3644.

Killick, R., G. Scales, et al. (2009). "Deletion of Irs2 reduces amyloid deposition and rescues behavioural deficits in APP transgenic mice." Biochem Biophys Res Commun **386**(1): 257-262.

Klingenberg, M. and S. G. Huang (1999). "Structure and function of the uncoupling protein from brown adipose tissue." Biochim Biophys Acta **1415**(2): 271-296.

Knebel, B., J. Haas, et al. (2012). "Liver-specific expression of transcriptionally active SREBP-1c is associated with fatty liver and increased visceral fat mass." PLoS One **7**(2): e31812.

Kopecky, J., G. Clarke, et al. (1995). "Expression of the mitochondrial uncoupling protein gene from the aP2 gene promoter prevents genetic obesity." J Clin Invest **96**(6): 2914-2923.

Kopecky, J., Z. Hodny, et al. (1996). "Reduction of dietary obesity in aP2-Ucp transgenic mice: physiology and adipose tissue distribution." Am J Physiol **270**(5 Pt 1): E768-775.

Kopf, M., H. Baumann, et al. (1994). "Impaired immune and acute-phase responses in interleukin-6-deficient mice." Nature **368**(6469): 339-342.

Kowluru, A., H. Q. Chen, et al. (2001). "Activation of acetyl-CoA carboxylase by a glutamate- and magnesium-sensitive protein phosphatase in the islet beta-cell." Diabetes **50**(7): 1580-1587.

Kubota, N., K. Tobe, et al. (2000). "Disruption of insulin receptor substrate 2 causes type 2 diabetes because of liver insulin resistance and lack of compensatory beta-cell hyperplasia." Diabetes **49**(11): 1880-1889.

Li, S., W. Ogawa, et al. (2011). "Role of S6K1 in regulation of SREBP1c expression in the liver." Biochem Biophys Res Commun **412**(2): 197-202.

Liu, Q., M. S. Gauthier, et al. (2010). "Activation of AMP-activated protein kinase signaling pathway by adiponectin and insulin in mouse adipocytes: requirement of acyl-CoA synthetases FATP1 and Acsl1 and association with an elevation in AMP/ATP ratio." FASEB J **24**(11): 4229-4239.

Lu, B., T. Nakamura, et al. (2012). "Novel role of PKR in inflammasome activation and HMGB1 release." Nature.

Masters, S. L., A. Dunne, et al. (2010). "Activation of the NLRP3 inflammasome by islet amyloid polypeptide provides a mechanism for enhanced IL-1beta in type 2 diabetes." Nat Immunol **11**(10): 897-904.

Meusel, T. R., K. E. Kehoe, et al. (2002). "Protein kinase R regulates double-stranded RNA induction of TNF-alpha but not IL-1 beta mRNA in human epithelial cells." J Immunol **168**(12): 6429-6435.

Monemdjou, S., W. E. Hofmann, et al. (2000). "Increased mitochondrial proton leak in skeletal muscle mitochondria of UCP1-deficient mice." Am J Physiol Endocrinol Metab **279**(4): E941-946.

Montague, C. T., I. S. Farooqi, et al. (1997). "Congenital leptin deficiency is associated with severe early-onset obesity in humans." Nature **387**(6636): 903-908.

Morel, M., J. Couturier, et al. (2009). "Evidence of molecular links between PKR and mTOR signalling pathways in Abeta neurotoxicity: role of p53, Redd1 and TSC2." Neurobiol Dis **36**(1): 151-161.

Mounir, Z., J. L. Krishnamoorthy, et al. (2009). "Tumor suppression by PTEN requires the activation of the PKR-eIF2alpha phosphorylation pathway." Sci Signal **2**(102): ra85.

Nakamura, T., M. Furuhashi, et al. (2010). "Double-stranded RNA-dependent protein kinase links pathogen sensing with stress and metabolic homeostasis." Cell **140**(3): 338-348.

Nawroth, R., F. Stellwagen, et al. (2011). "S6K1 and 4E-BP1 are independent regulated and control cellular growth in bladder cancer." PLoS One **6**(11): e27509.

Nedergaard, J., T. Bengtsson, et al. (2007). "Unexpected evidence for active brown adipose tissue in adult humans." Am J Physiol Endocrinol Metab **293**(2): E444-452.

Park, J., H. K. Rho, et al. (2005). "Overexpression of glucose-6-phosphate dehydrogenase is associated with lipid dysregulation and insulin resistance in obesity." Mol Cell Biol **25**(12): 5146-5157.

Payne, V. A., W. S. Au, et al. (2010). "C/EBP transcription factors regulate SREBP1c gene expression during adipogenesis." Biochem J **425**(1): 215-223.

Pindel, A. and A. Sadler (2011). "The role of protein kinase R in the interferon response." J Interferon Cytokine Res **31**(1): 59-70.

Rath, E., E. Berger, et al. (2011). "Induction of dsRNA-activated protein kinase links mitochondrial unfolded protein response to the pathogenesis of intestinal inflammation." Gut.

Rising, R., A. Keys, et al. (1992). "Concomitant interindividual variation in body temperature and metabolic rate." Am J Physiol **263**(4 Pt 1): E730-734.

Scheller, J., N. Ohnesorge, et al. (2006). "Interleukin-6 trans-signalling in chronic inflammation and cancer." Scand J Immunol **63**(5): 321-329.

Shimomura, I., H. Shimano, et al. (1998). "Nuclear sterol regulatory element-binding proteins activate genes responsible for the entire program of unsaturated fatty acid biosynthesis in transgenic mouse liver." J Biol Chem **273**(52): 35299-35306.

Sun, S. Y., L. M. Rosenberg, et al. (2005). "Activation of Akt and eIF4E survival pathways by rapamycin-mediated mammalian target of rapamycin inhibition." Cancer Res **65**(16): 7052-7058.

Sykiotis, G. P. and A. G. Papavassiliou (2001). "Serine phosphorylation of insulin receptor substrate-1: a novel target for the reversal of insulin resistance." Mol Endocrinol **15**(11): 1864-1869.

Tiwari, S., V. K. Halagappa, et al. (2007). "Reduced expression of insulin receptors in the kidneys of insulin-resistant rats." J Am Soc Nephrol **18**(10): 2661-2671.

Ueno, M., J. B. Carvalheira, et al. (2005). "Regulation of insulin signalling by hyperinsulinaemia: role of IRS-1/2 serine phosphorylation and the mTOR/p70 S6K pathway." Diabetologia **48**(3): 506-518.

Ugi, S., T. Imamura, et al. (2004). "Protein phosphatase 2A negatively regulates insulin's metabolic signaling pathway by inhibiting Akt (protein kinase B) activity in 3T3-L1 adipocytes." Mol Cell Biol **24**(19): 8778-8789.

van der Poll, T. and S. J. van Deventer (1998). "The role of interleukin 6 in endotoxin-induced inflammatory responses." Prog Clin Biol Res **397**: 365-377.

Vandanmagsar, B., Y. H. Youm, et al. (2011). "The NLRP3 inflammasome instigates obesity-induced inflammation and insulin resistance." Nat Med **17**(2): 179-188.

Wang, F., Y. Zhao, et al. (2012). "Activated Glucose-6-phosphate Dehydrogenase is Associated with Insulin Resistance by Upregulating Pentose and Pentosidine in Diet-induced Obesity of Rats." Horm Metab Res.

Wei, L. H., M. L. Kuo, et al. (2001). "The anti-apoptotic role of interleukin-6 in human cervical cancer is mediated by up-regulation of Mcl-1 through a PI 3-K/Akt pathway." Oncogene **20**(41): 5799-5809.

Wen, H., D. Gris, et al. (2011). "Fatty acid-induced NLRP3-ASC inflammasome activation interferes with insulin signaling." Nat Immunol **12**(5): 408-415.

Winkler, E. and M. Klingenberg (1994). "Effect of fatty acids on H+ transport activity of the reconstituted uncoupling protein." J Biol Chem **269**(4): 2508-2515.

Withers, D. J., J. S. Gutierrez, et al. (1998). "Disruption of IRS-2 causes type 2 diabetes in mice." Nature **391**(6670): 900-904.

Xiao, F., Z. Huang, et al. (2011). "Leucine deprivation increases hepatic insulin sensitivity via GCN2/mTOR/S6K1 and AMPK pathways." Diabetes **60**(3): 746-756.

Xu, Z. and B. R. Williams (2000). "The B56alpha regulatory subunit of protein phosphatase 2A is a target for regulation by double-stranded RNA-dependent protein kinase PKR." Mol Cell Biol **20**(14): 5285-5299.

Yang, G., L. Badeanlou, et al. (2009). "Central role of ceramide biosynthesis in body weight regulation, energy metabolism, and the metabolic syndrome." Am J Physiol Endocrinol Metab **297**(1): E211-224.

Yang, S. I., R. L. Lickteig, et al. (1991). "Control of protein phosphatase 2A by simian virus 40 small-t antigen." Mol Cell Biol **11**(4): 1988-1995.

Yang, Y. L., L. F. Reis, et al. (1995). "Deficient signaling in mice devoid of double-stranded RNA-dependent protein kinase." EMBO J **14**(24): 6095-6106.

Youm, Y. H., A. Adijiang, et al. (2011). "Elimination of the NLRP3-ASC inflammasome protects against chronic obesity-induced pancreatic damage." Endocrinology **152**(11): 4039-4045.

Zhou, L., J. Zhang, et al. (2009). "Autophagy-mediated insulin receptor down-regulation contributes to endoplasmic reticulum stress-induced insulin resistance." Mol Pharmacol **76**(3): 596-603.

Zuliani, G., M. Galvani, et al. (2010). "Plasma soluble gp130 levels are increased in older subjects with metabolic syndrome. The role of insulin resistance." Atherosclerosis **213**(1): 319-324.

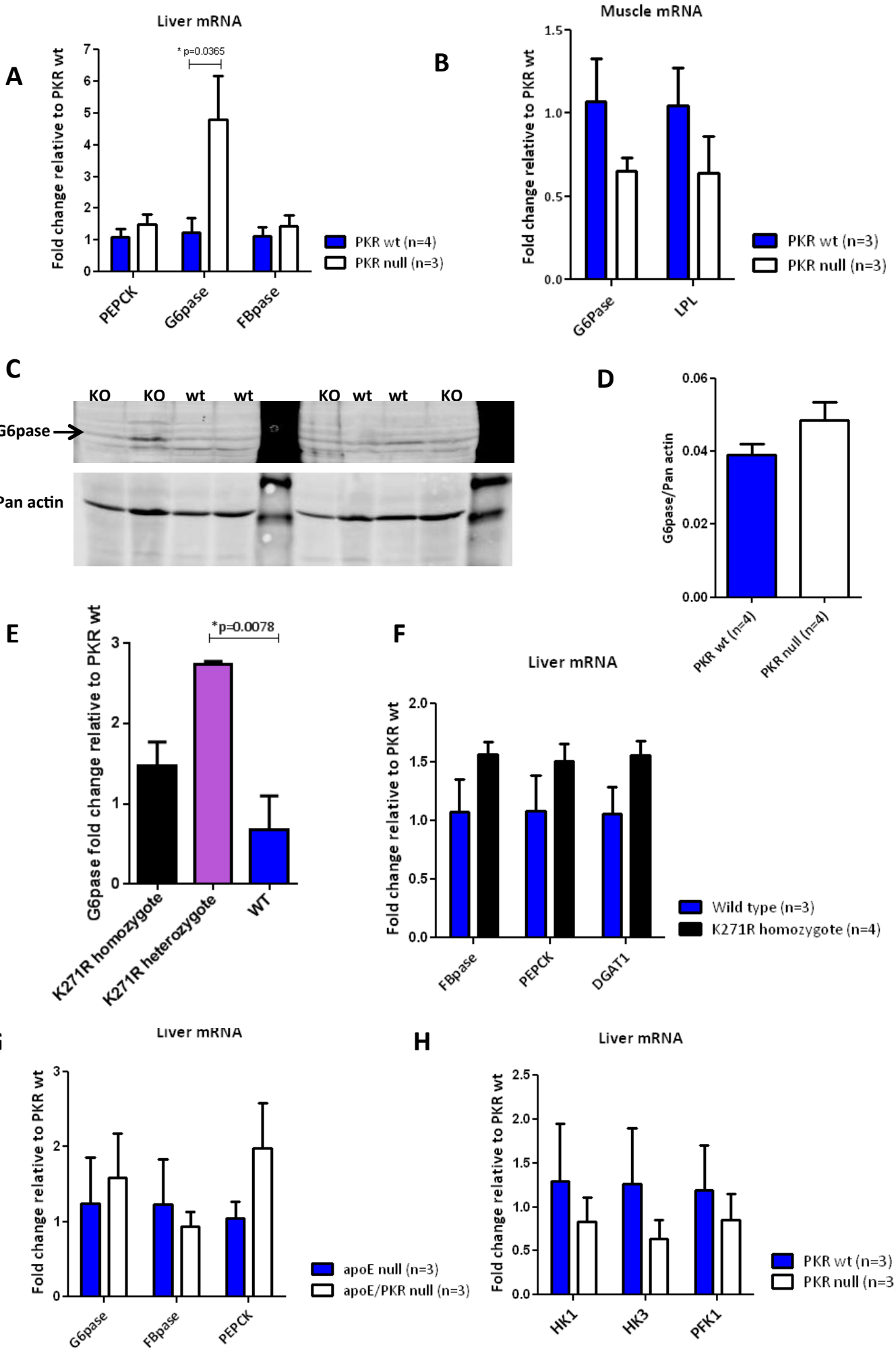
A
Liver mRNA
Fold change relative to PKR wt
* p=0.0365
PEPCK
G6pase
FBpase
PKR wt (n=4)
PKR null (n=3)
B
Muscle mRNA
Fold change relative to PKR wt
G6Pase
LPL
PKR wt (n=3)
PKR null (n=3)
C
KO KO wt wt KO wt wt KO
G6pase
Pan actin
D
G6pase/Pan actin
PKR wt (n=4)
PKR null (n=4)
E
*p=0.0078
G6pase fold change relative to PKR wt
K271R homozygote
K271R heterozygote
WT
F
Liver mRNA
Fold change relative to PKR wt
FBpase
PEPCK
DGAT1
Wild type (n=3)
K271R homozygote (n=4)
G
Liver mRNA
Fold change relative to PKR wt
G6pase
FBpase
PEPCK
apoE null (n=3)
apoE/PKR null (n=3)
H
Liver mRNA
Fold change relative to PKR wt
HK1
HK3
PFK1
PKR wt (n=3)
PKR null (n=3)

Figure 4.1 Expression of gluconeogenic enzymes in response to high fat diet.

mRNA levels of gluconeogenic and glycolytic enzymes analysed by QRT-PCR and expressed as fold change relative to PKR wt. Expression of target genes was compared to the internal control 18s. **A** mRNA levels of PEPCK, G6pase and FBPase analyzed by QRT-PCR in liver of PKR wt (n=4) and PKR null (n=3) mice fed a high fat diet, **B** mRNA levels of G6pase and LPL analysed by QRT-PCR in muscle of PKR wt (n=3) and PKR null (n=3) mice fed a high fat diet, **C** western blot analysis of G6pase protein expression in liver lysates from PKR wt (n=4) and PKR null (n=4) mice fed a high fat diet. KO - PKR knockout **D** Relative band intensity of G6pase protein calculated by densitometry and normalized to the loading control pan actin. Densitometry results are expressed as G6pase/pan actin ratio, **E** mRNA extracted levels of G6pase in the liver of K271R homozygote (n=3), K271R heterozygote (n=3) and WT (n=3) mice fed a high fat diet, **F** mRNA levels of FBPase and DGAT1 analyzed by QRT-PCR in the liver of wild type (n=3) and K271R homozygote (n=4) mice fed a high fat diet for 10 weeks, **G** mRNA levels of G6pase, FBpase and PEPCK analyzed by QRT-PCR in the liver of apoE:PKR knockout (n=3) and apoE knockout (n=3) mice fed a high fat diet, **H** mRNA levels of glycolytic enzymes HK1, HK2 and PFK1 analyzed by QRT-PCR in liver of PKR knockout (n=3) and PKR wt (n=3) mice fed a high fat diet assess for expression of glycolytic enzymes by QRT-PC. Statistical analysis: unpaired T-test, mean ± SEM. * Statistically significant.

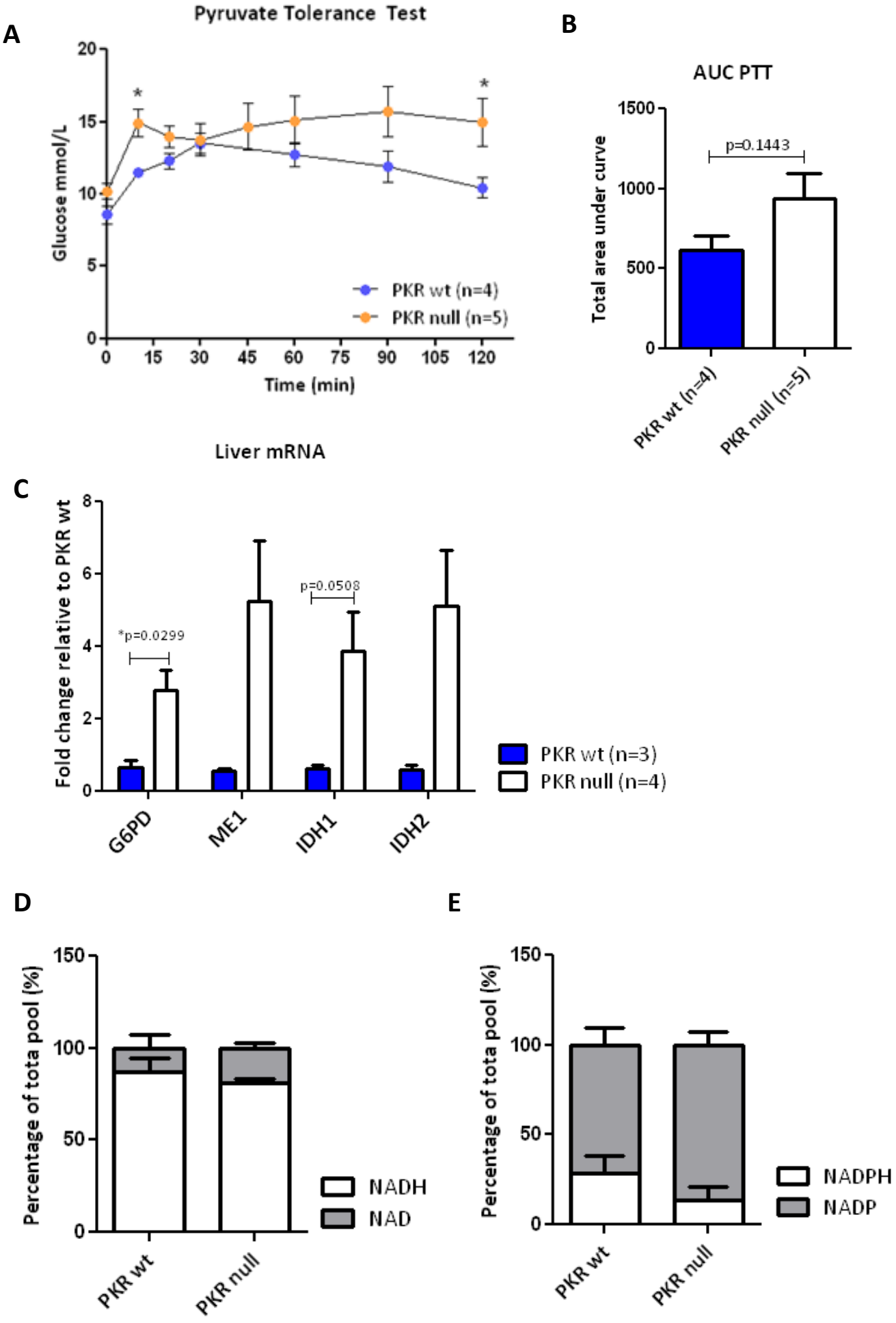
A
Pyruvate Tolerance Test
Glucose mmol/L
Time (min)
PKR wt (n=4)
PKR null (n=5)
B
AUC PTT
Total area under curve
p=0.1443
PKR wt (n=4)
PKR null (n=5)
C
Liver mRNA
Fold change relative to PKR wt
*p=0.0299
p=0.0508
G6PD
ME1
IDH1
IDH2
PKR wt (n=3)
PKR null (n=4)
D
Percentage of tota pool (%)
NADH
NAD
PKR wt
PKR null
E
Percentage of tota pool (%)
NADPH
NADP
PKR wt
PKR null

Figure 4.2 Assessment of the pentose phosphate pathway.

A Pyruvate tolerance test in PKR wt (n=4) and knockout (n=5) mice fed a HFD. Statistical analysis of time points between PKR wt compared to PKR knockout mice: 0min p=0.0903, *10min p=0.0159, 20min p=0.1905 30min p=0.9048, 60min p=0.3893, 90min p=0.0635 and *120min p=0.0317, **B** bar graph representing total area under curve for PTT, **C** mRNA levels of G6PD, ME1, IDH1 and IDH2 in liver tissue of PKR wt (n=3) and PKR null (n=4) mice fed a high fat diet for 10 weeks. Expression levels of genes was analysed by QRT-PCR and expressed as fold change relative to PKR wt. Expression of target genes was compared to the internal control 18s. **D** Bar graph representing the percentage (%) of NAD and NADH that makes up the total NAD pool in BAC7 and BAc10 MEFs and the **E** percentage of NADPH and NADP in total NDAP pool in BAC cells. Statistical analysis: unpaired T-test, mean ± SEM. * Statistically significant.

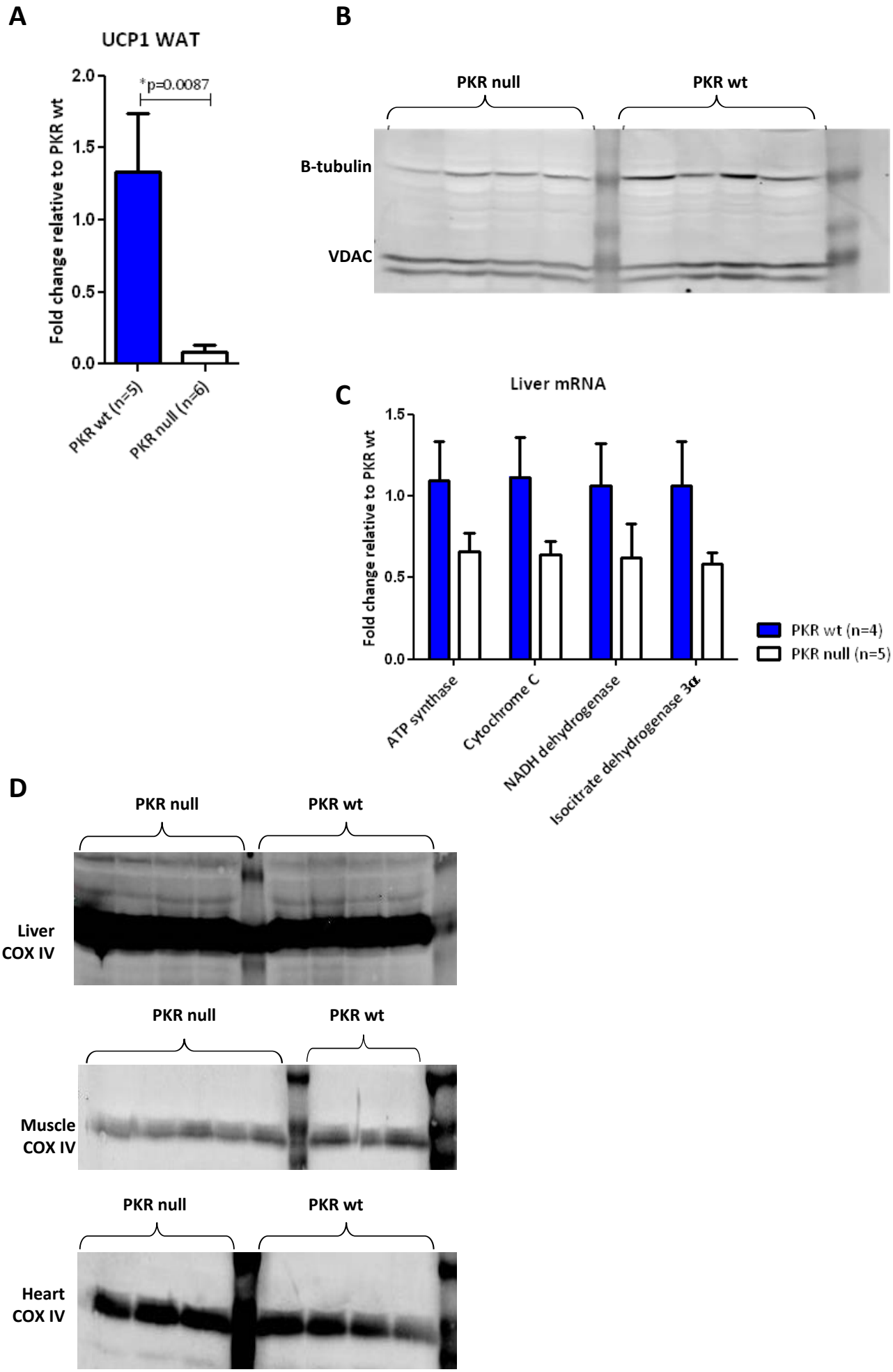
A
UCP1 WAT
*p=0.0087
Fold change relative to PKR wt
2.0
1.5
1.0
0.5
0.0
PKR wt (n=5)
PKR null (n=6)
B
PKR null
PKR wt
B-tubulin
VDAC
C
Liver mRNA
Fold change relative to PKR wt
1.5
1.0
0.5
0.0
ATP synthase
Cytochrome C
NADH dehydrogenase
Isocitrate dehydrogenase 3α
PKR wt (n=4)
PKR null (n=5)
D
PKR null
PKR wt
Liver
COX IV
PKR null
PKR wt
Muscle
COX IV
PKR null
PKR wt
Heart
COX IV

Figure 4.3 Expression of genes required for OXPHOS and thermogenesis in response to high fat diet.

A mRNA levels of UCP1 in white adipose tissue of PKR wt (n=5) and PKR null (n=6) mice fed a high fat diet. Expression levels of genes analysed by QRT-PCR and expressed as fold change relative to PKR wt. Expression of target genes was compared to the internal control RPL27. **B** Western blot analysis of mitochondrial liver lysates from PKR null (n=4) and PKR wt(n=) mice fed a high fat diet for protein expression of VDAC and β-tubulin, **C** mRNA levels of ATP synthase, cytochrome C, NADH dehydrogenase, isocitrate dehydrogenase 3α in liver of PKR wt (n=4) and PKR null (n=5) mice fed a high fat diet. Expression levels of genes analysed by QRT-PCR and expressed as fold change relative to PKR wt. Expression of target genes was compared to the internal control 18s. **D** Western blot analysis for protein expression of COX IV in mitochondrial cell lysates collected from PKR wt and null liver, muscle and heart. Statistical analysis: Unpaired T- test, mean±SEM. *Statistically significant.

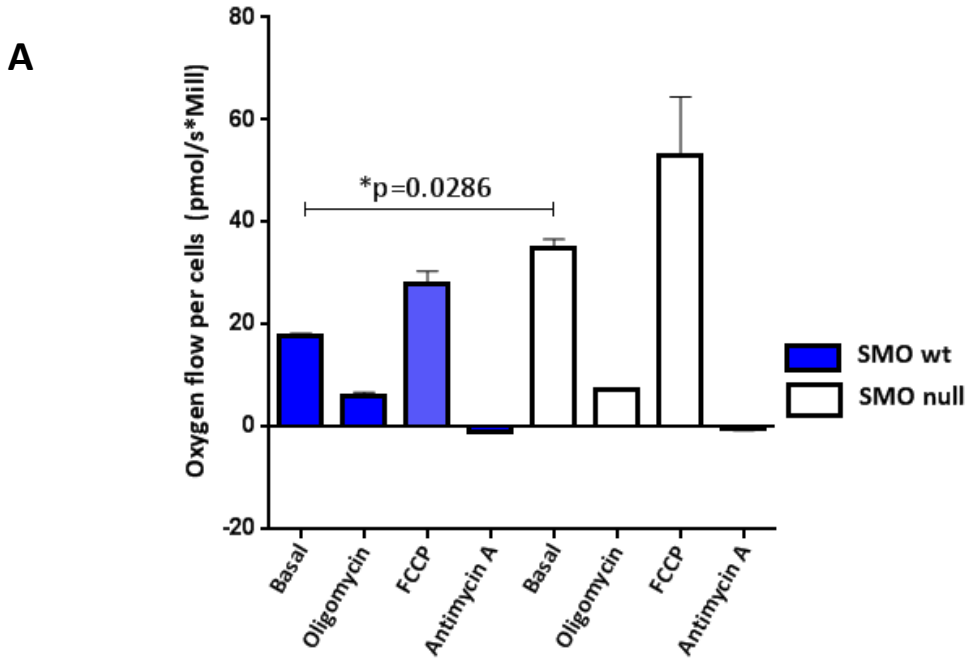
A
Oxygen flow per cells (pmol/s*Mill)
80
60
40
20
0
-20
*p=0.0286
SMO wt
SMO null
Basal
Oligomycin
FCCP
Antimycin A
Basal
Oligomycin
FCCP
Antimycin A

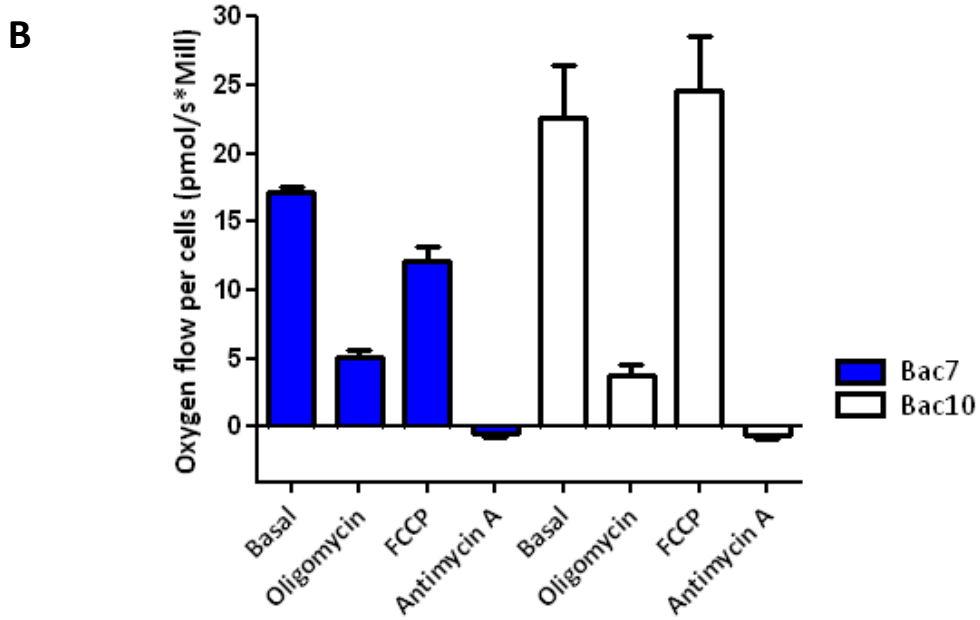
B
Oxygen flow per cells (pmol/s*Mill)
30
25
20
15
10
5
0
Bac7
Bac10
Basal
Oligomycin
FCCP
Antimycin A
Basal
Oligomycin
FCCP
Antimycin A

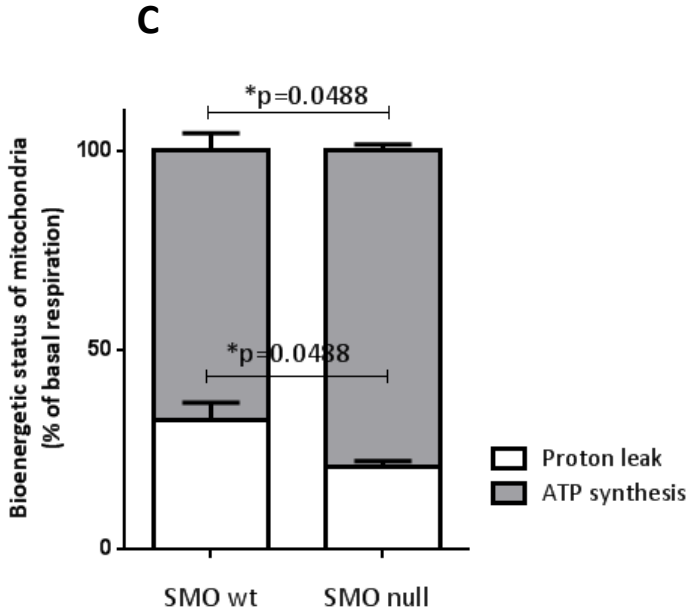
C
*p=0.0488
*p=0.0488
Bioenergetic status of mitochondria (% of basal respiration)
100
50
0
Proton leak
ATP synthesis
SMO wt
SMO null

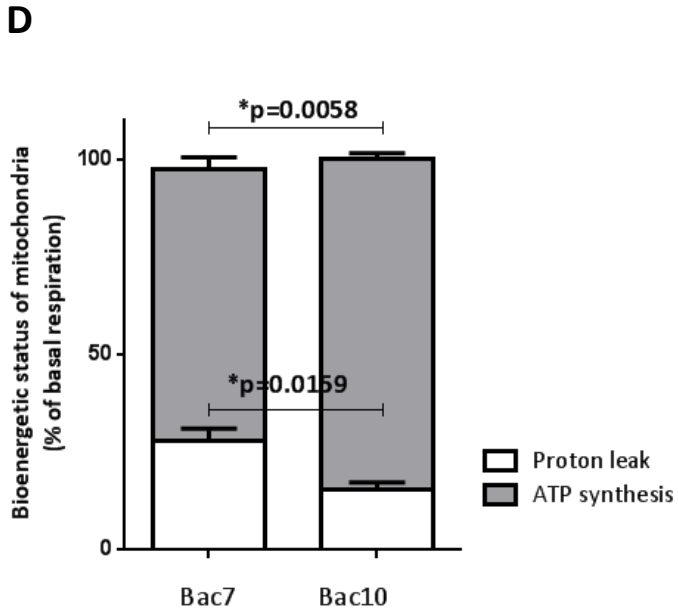
D
*p=0.0058
*p=0.0159
Bioenergetic status of mitochondria (% of basal respiration)
100
50
0
Proton leak
ATP synthesis
Bac7
Bac10

Figure 4.4 Oxygen consumption *in vitro.*

A Oxygen flow per million cells in PKR null and wt spleen macrophages treated with oligomycin, FCCP, and antimycin A, **B** oxygen flow per million cells in PKR null and wt 3T3 MEFs, **C** bioenergetic status of the mitochondria in spleen macrophages and **D** in 3T3 MEFs. All experiments were repeated four times. Statistical analysis: Unpaired T- test, mean±SEM. *Statistically significant.

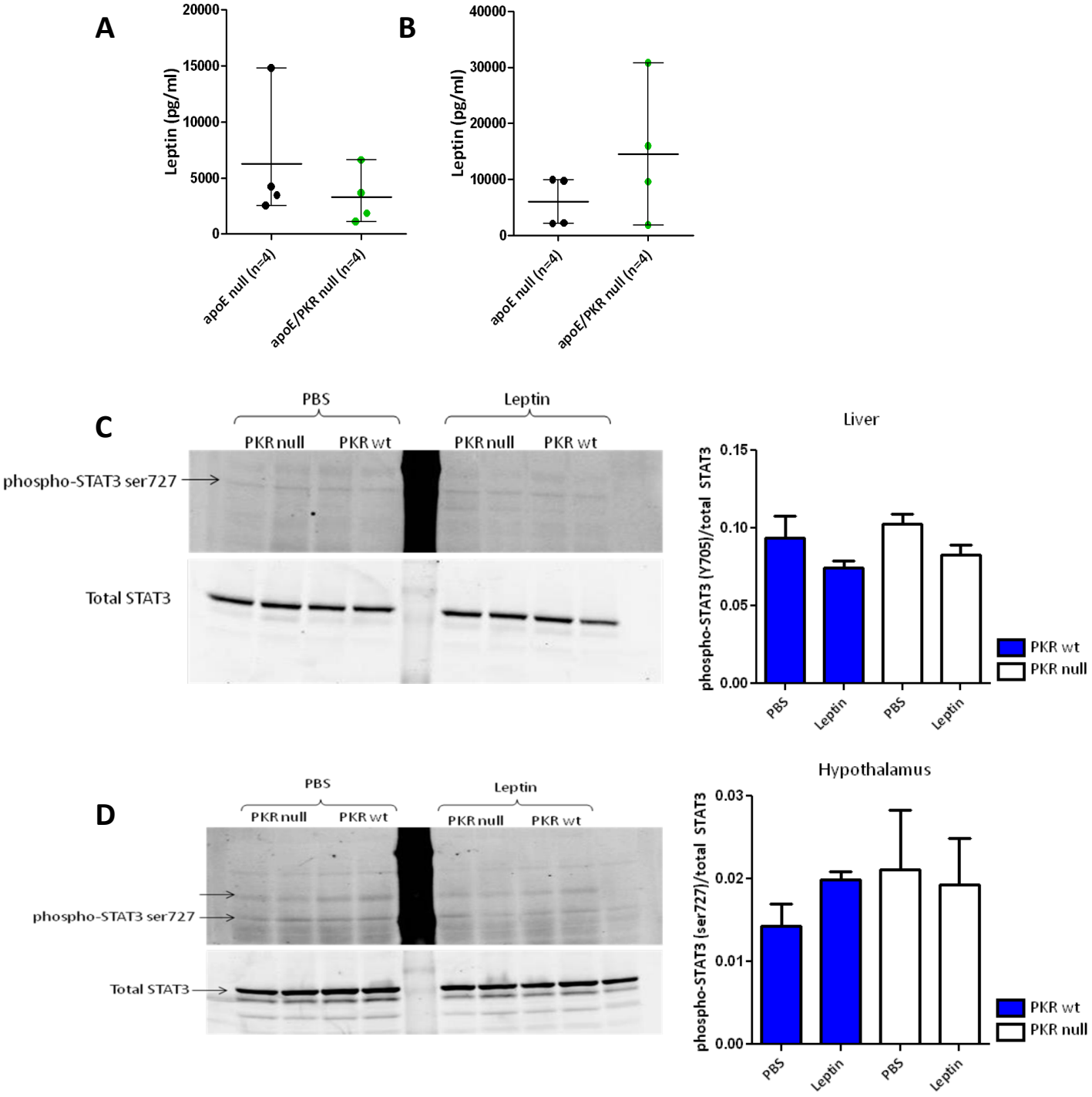

Figure 4.5 Circulating concentration of leptin and phosphorylation of STAT3 at serine residue 727 in the liver and hypothalamus post leptin injection.

Concentration of circulating leptin measured after a **A** 40 week chow diet, **B** 10 week high fat diet. Western blot analysis of **C** liver lysates and **D** hypothalamic lysates from PKR wt (n=2) and null (n=2) mice collected 45minutes post intraperitoneal injection with PBS or 1mg/kg body weight of human leptin. Relative band intensities of phospho-STAT3 were calculated by densitometry and normalized to the loading control total STAT3.

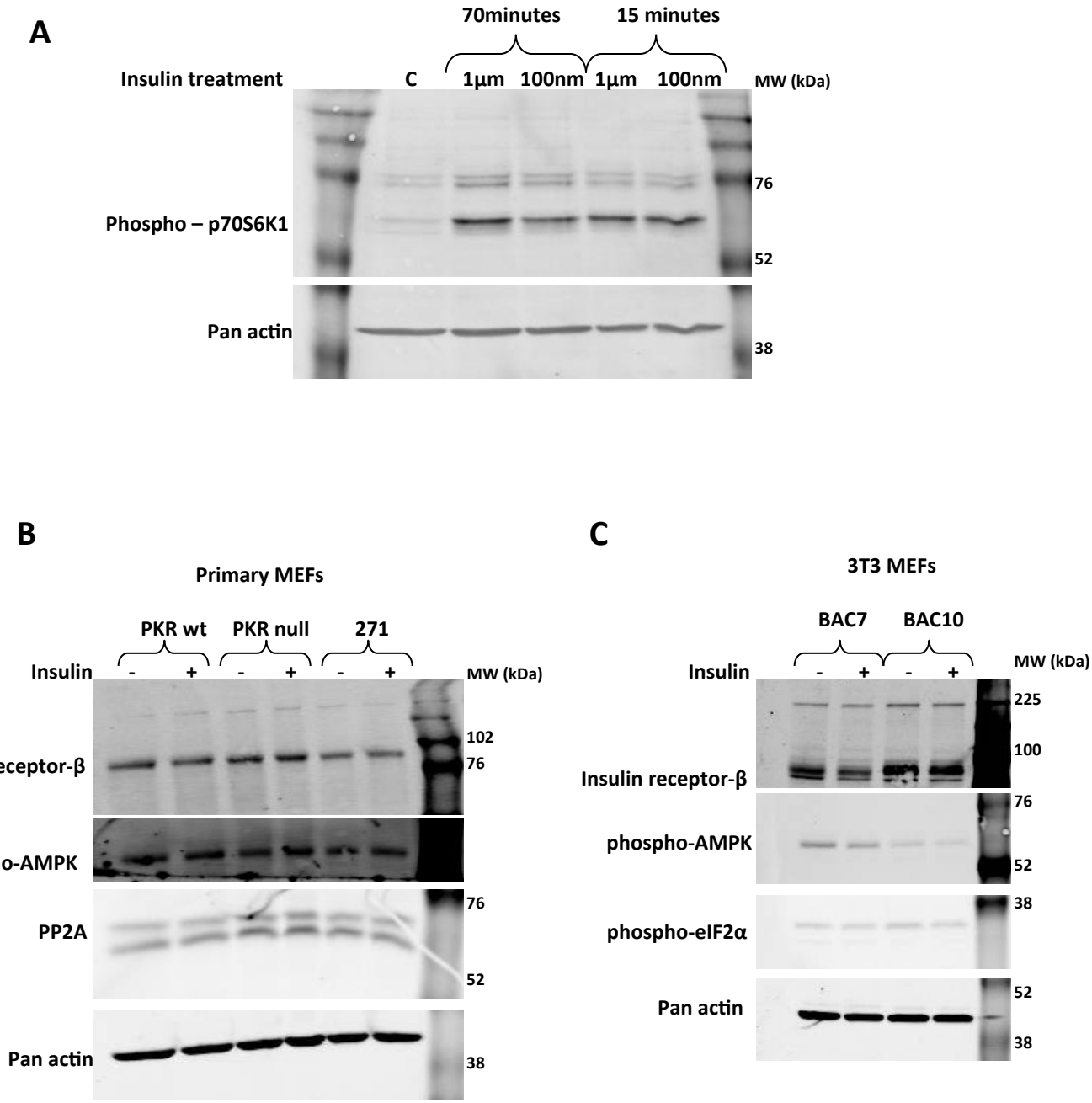

Figure 4.6 Western blot analysis for phosphorylation of p70S6K in MEFs after insulin stimulation.

Western blot analysis of **A** cell lysates collected from BAC7 3T3 MEFs after insulin (1µM or 100nm) treatment following overnight serum starvation (C=no treatment control). **B** western blot analysis of cell lysates collected fromm primary MEFs after10 minutes of insulin treatment (1nM) following overnight serum starvation. **C** western blot analysis of cell lysates collected from 3T3 MEFs after 10 minutes of insulin treatment (1nM) following overnight serum starvation.

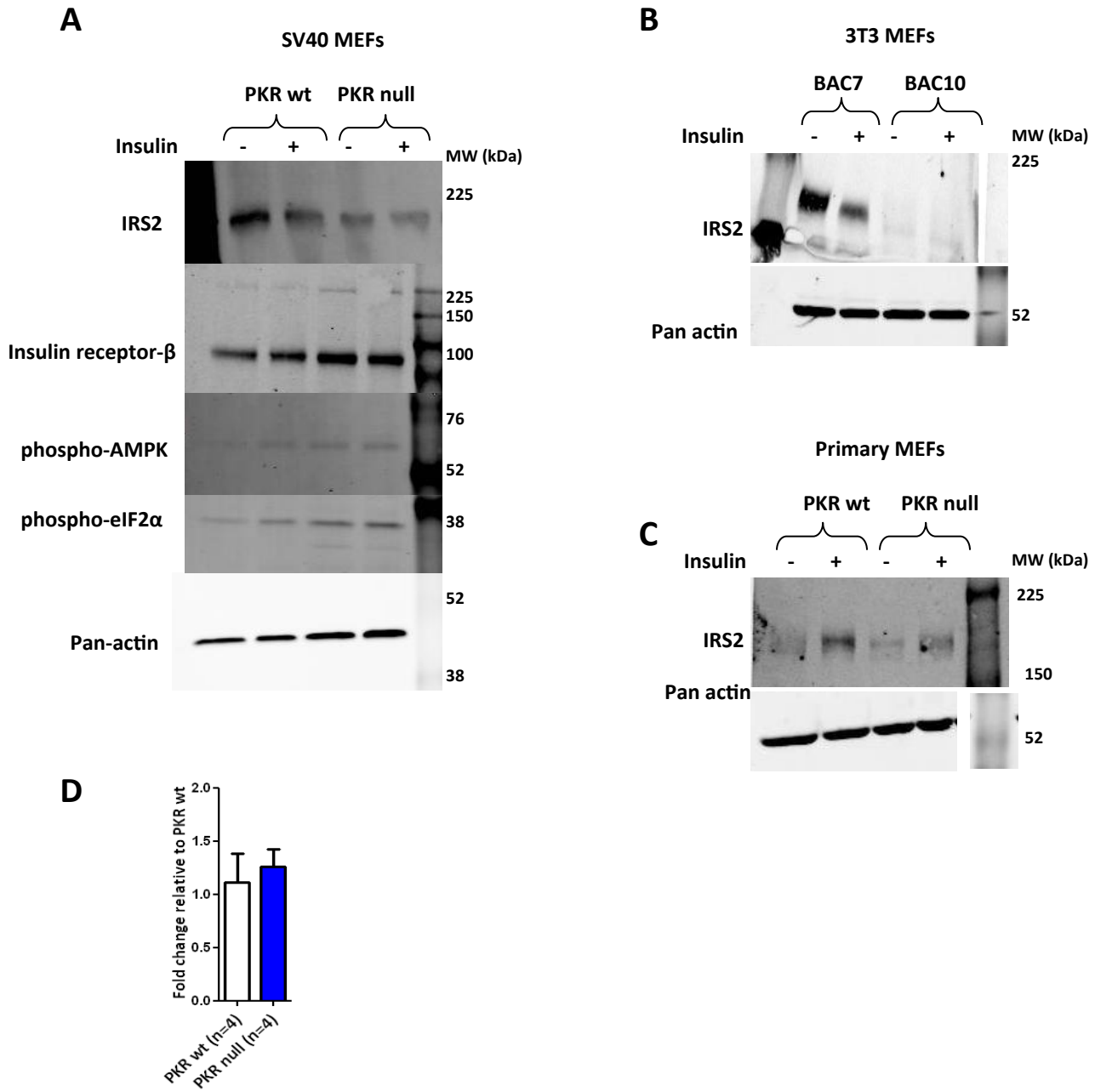

Figure 4.7 Activation of the PI3K/p70S6K/Akt signalling cascade phosphorylation after insulin stimulation.

Western blot analysis of **A** SV40 MEF cell lysates and **B** 3T3 MEF cell lysates and **C** primary MEF cell lysates collected following 10 minutes of insulin treatment (1nM) after overnight serum starvation. Membrane was probed for pro-insulin receptor, IRβ, phospho-AMPK, phospho-eIF2α and PP2A. **D** RNA extracted from muscle of PKR wt (n=2) and PKR null (n=4) mice fed a high fat diet for 10 weeks. Expression levels of IRS2 were analysed by QRT-PCR and expressed as fold change relative to PKR wt. Expression of target genes was compared to the internal control RPL30.

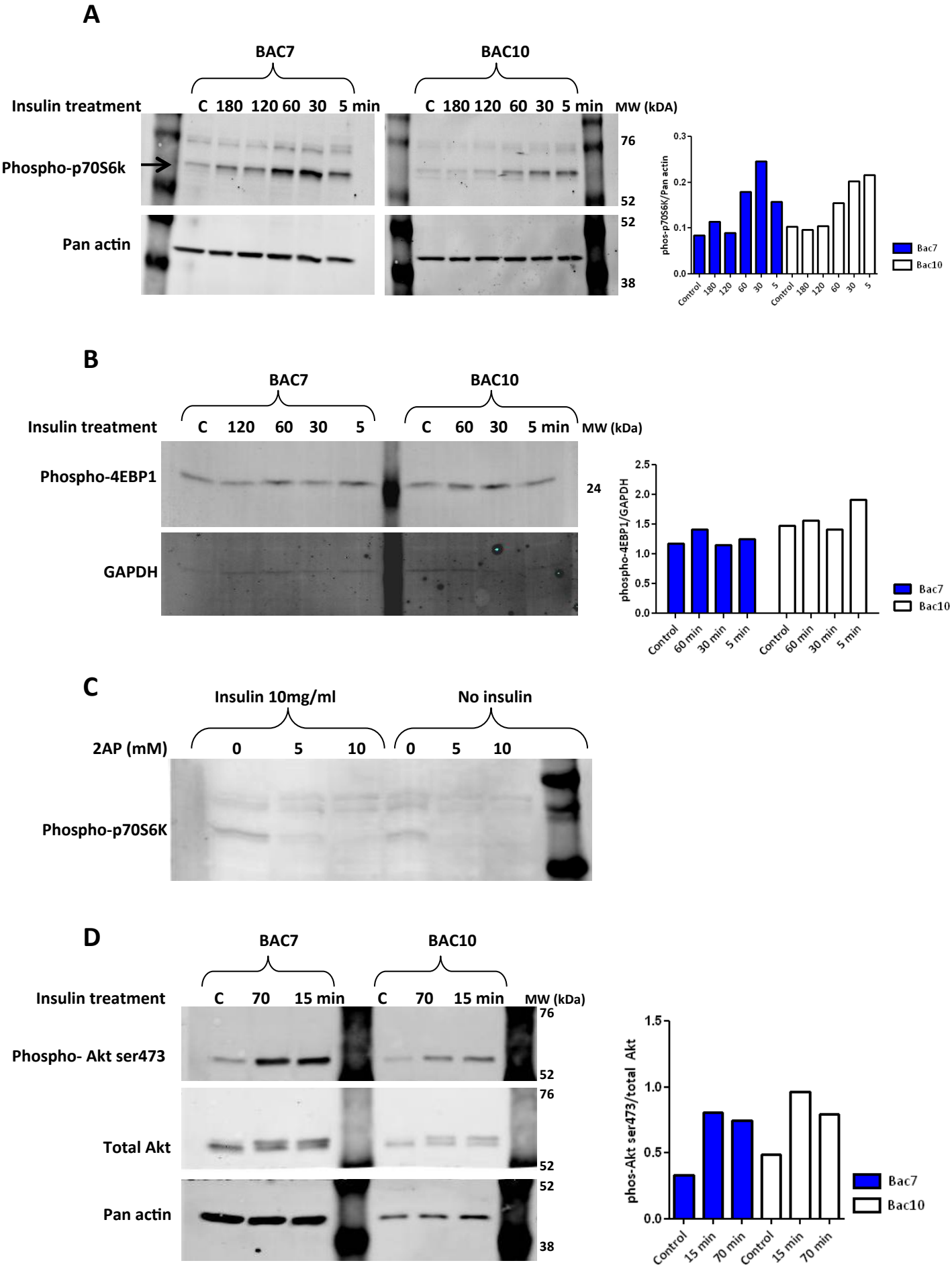
A
BAC7
BAC10
Insulin treatment
C 180 120 60 30 5 min
C 180 120 60 30 5 min
MW (kDA)
Phospho-p70S6k
Pan actin
76
52
52
38
phos-p70S6k/Pan actin
0.3
0.2
0.1
0.0
Control 180 120 60 30 5 Control 180 120 60 30 5
Bac7
Bac10
B
BAC7
BAC10
Insulin treatment
C 120 60 30 5
C 60 30 5 min
MW (kDa)
Phospho-4EBP1
GAPDH
24
phospho-4EBP1/GAPDH
2.5
2.0
1.5
1.0
0.5
0.0
Control 60 min 30 min 5 min Control 60 min 30 min 5 min
Bac7
Bac10
C
Insulin 10mg/ml
No insulin
2AP (mM)
0 5 10 0 5 10
Phospho-p70S6K
D
BAC7
BAC10
Insulin treatment
C 70 15 min C 70 15 min
MW (kDa)
Phospho- Akt ser473
Total Akt
Pan actin
76
52
76
52
52
38
phos-Akt ser473/total Akt
1.5
1.0
0.5
0.0
Control 15 min 70 min Control 15 min 70 min
Bac7
Bac10

Figure 4.8 Effects of insulin on the activation of the PI3K/p70S6K/Akt signalling cascade.

Western blot analysis of **A** p70S6K phosphorylation following the indicated time of insulin treatment (1nM) after overnight serum starvation. **B** 4EBP1 phosphorylation in BAC7 and BAC10 3T3 MEF cell lysates following the indicated time of insulin treatment (1μM) after overnight serum starvation. **C** p70S6K phosphorylation in MNuMNG cells treated with 0, 5 or 10mM 2amino-purine followed by insulin treatment. **D** Akt phosphorylation in BAC7 and BAC10 3T3 MEF cell lysates following the indicated time of insulin treatment (1μM) after overnight serum starvation. C-control, no treatment. Relative band intensities were calculated by densitometry and normalized to the loading control pan-actin, total Akt or GAPDH.

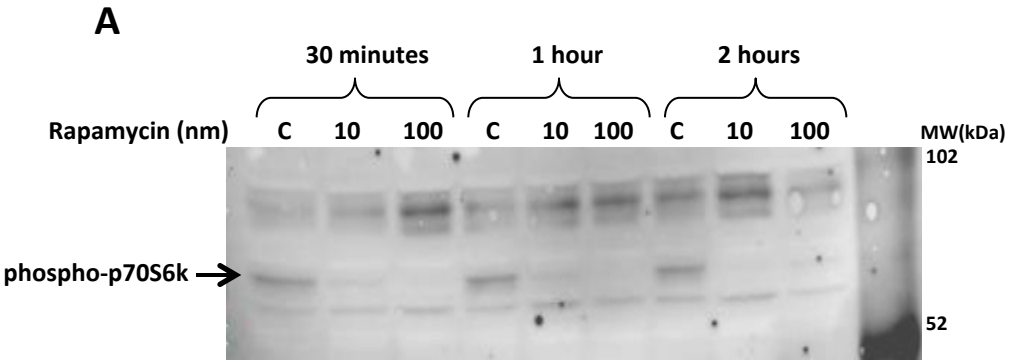
A
30 minutes
1 hour
2 hours
Rapamycin (nm)
C
10
100
C
10
100
C
10
100
MW(kDa)
102
phospho-p70S6k
52

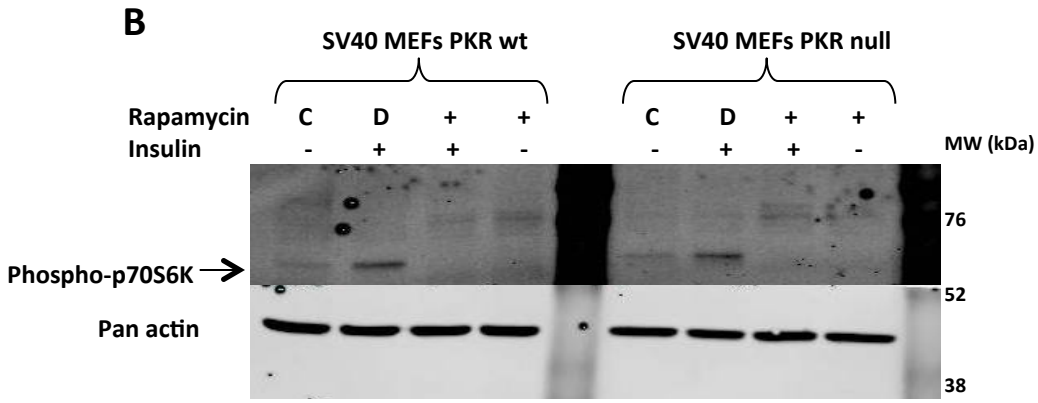
B
SV40 MEFs PKR wt
SV40 MEFs PKR null
Rapamycin
Insulin
C
D
+
+
C
D
+
+
MW (kDa)
Phospho-p70S6K
Pan actin
76
52
38

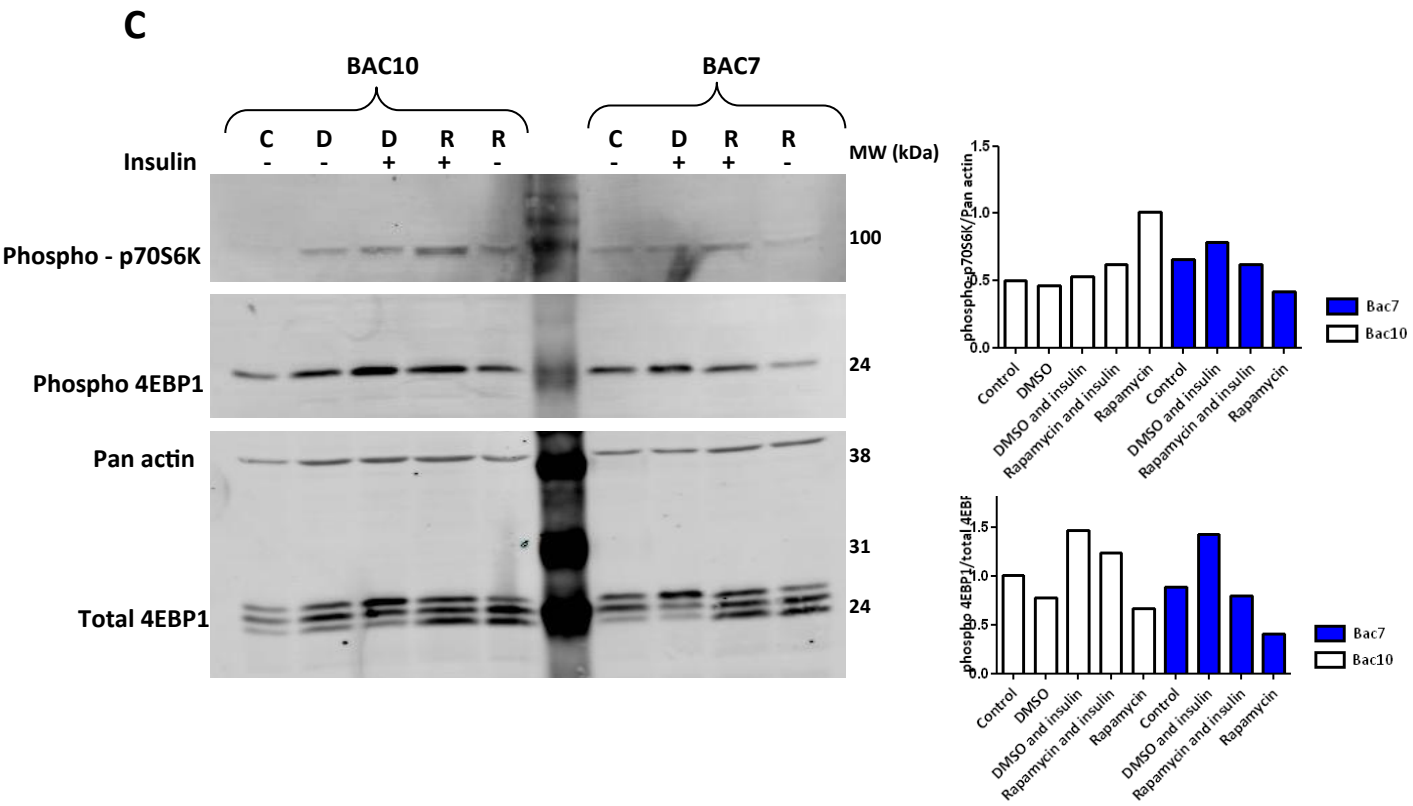
C
BAC10
BAC7
Insulin
C
D
D
R
R
C
D
R
R
MW (kDa)
Phospho - p70S6K
Phospho 4EBP1
Pan actin
Total 4EBP1
100
24
38
31
24
phospho-p70S6K/Pan actin
1.5
1.0
0.5
0.0
Control
DMSO
DMSO and insulin
Rapamycin and insulin
Rapamycin
Control
DMSO and insulin
Rapamycin and insulin
Rapamycin
Bac7
Bac10
phospho 4EBP1/total 4EBP
1.5
1.0
0.5
0.0
Control
DMSO
DMSO and insulin
Rapamycin and insulin
Rapamycin
Control
DMSO and insulin
Rapamycin and insulin
Rapamycin
Bac7
Bac10

Figure 4.9 Activation of the PI3K insulin signalling cascade following rapamycin treatment.

Western blot analysis for **A** p70S6K phosphorylation in PKR WT spleen macrophages treated with 10nm or 100nm of rapamycin for 30, 60 or 120 minutes, followed by insulin (1μM) stimulation. **B** phosphorylation of p70S6K in SV40 MEFs treated with rapamycin and insulin following overnight serum starvation. **C** phosphorylation of p70S6K and 4EBP1 in protein lysates from MEFs treated with rapamycin and insulin following overnight serum starvation. D-DMSO, C-no treatment control.

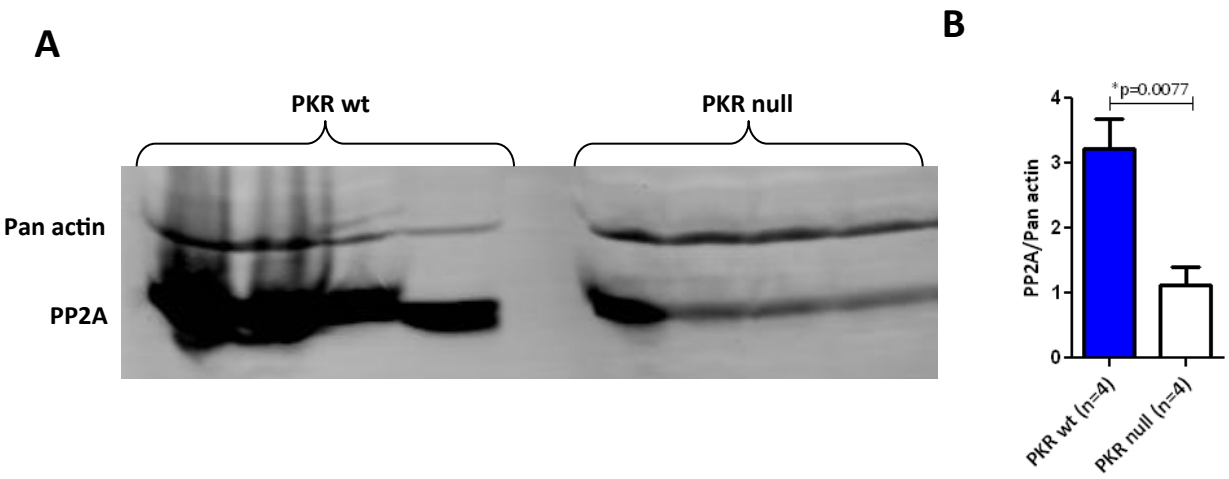

Figure 4.10 Western blot analysis of insulin signalling in SV40 MEFs after insulin stimulation and expression of PP2A in the liver.

Western blot analysis of **A** liver lysates from PKR wt (n=4) and null (n=4) mice fed a high fat diet for 10 weeks. Relative band intensities were calculated by densitometry and normalized to the loading control pan actin. **B** Densitometry results from band analysis expressed as PP2A/pan actin ratio. Statistical analysis: Unpaired T- test, mean±SEM. *Statistically significant.

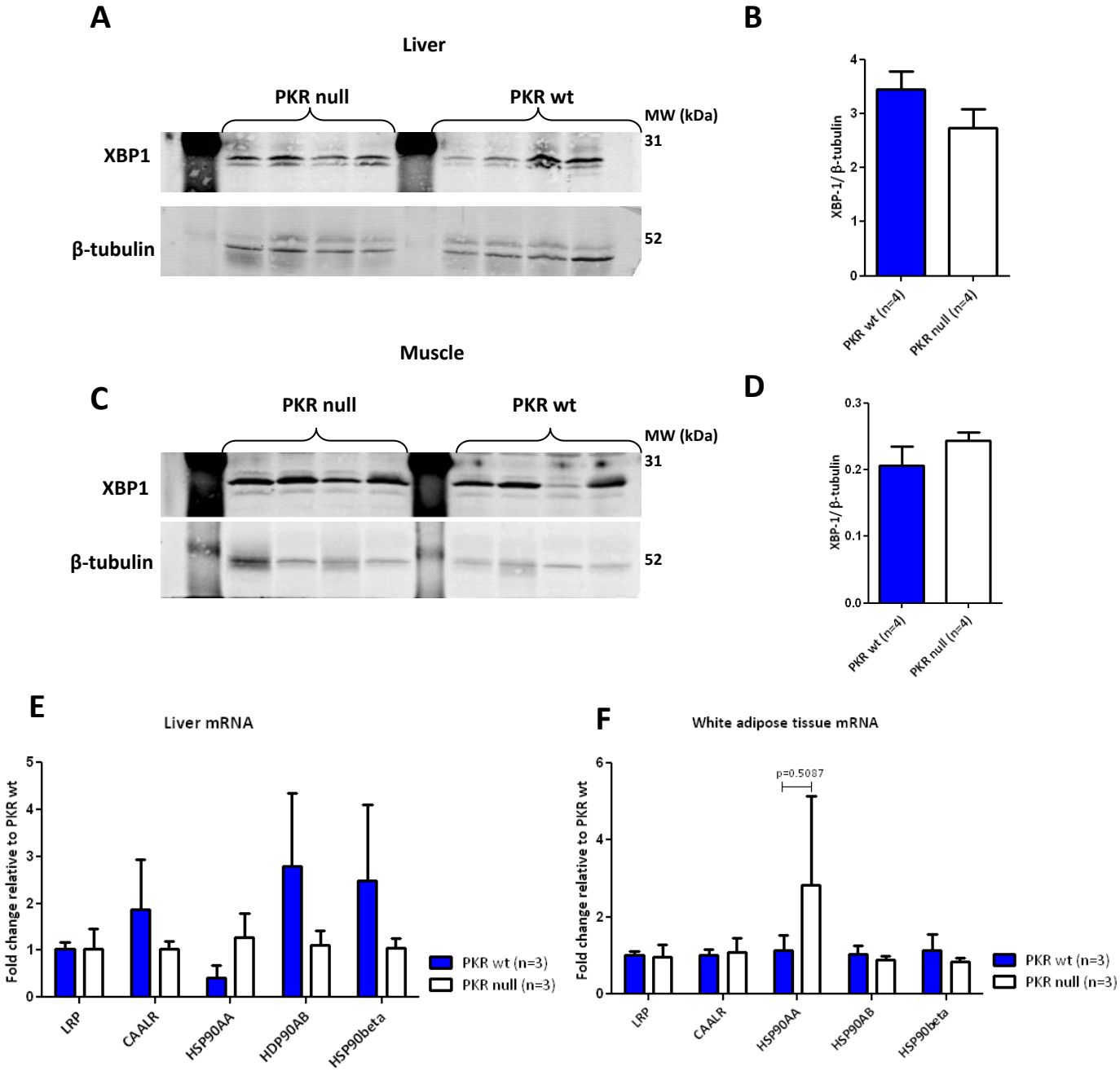

Figure 4.11 Protein and gene expression of molecules involved in UPR.

Western blot analysis of **A** liver lysates and **C** muscle lysates from PKR wt (n=4) and null (n=4) mice fed a high fat diet for 10 weeks for protein expression of XBP-1. Relative band intensities of XBP1 were calculated by densitometry and normalized to the loading control β-tubulin. **C-D** Densitometry results from band analysis expressed as XBP1/β-tubulin ratio.. mRNA levels of LRP, CAALR, HSP90AA, HSP90AB analysed by QRT-PCR in **E** liver of PKR wt (n=3) and PKR null (n=3) **F** white adipose tissue of PKR wt (n=3) and PKR null (n=3) mice fed a high fat diet. QRT-PCR and expressed as fold change relative to PKR wt. Expression of target genes was compared to the internal control 18s. Statistical analysis: Unpaired T- test, mean±SEM. *Statistically significant.

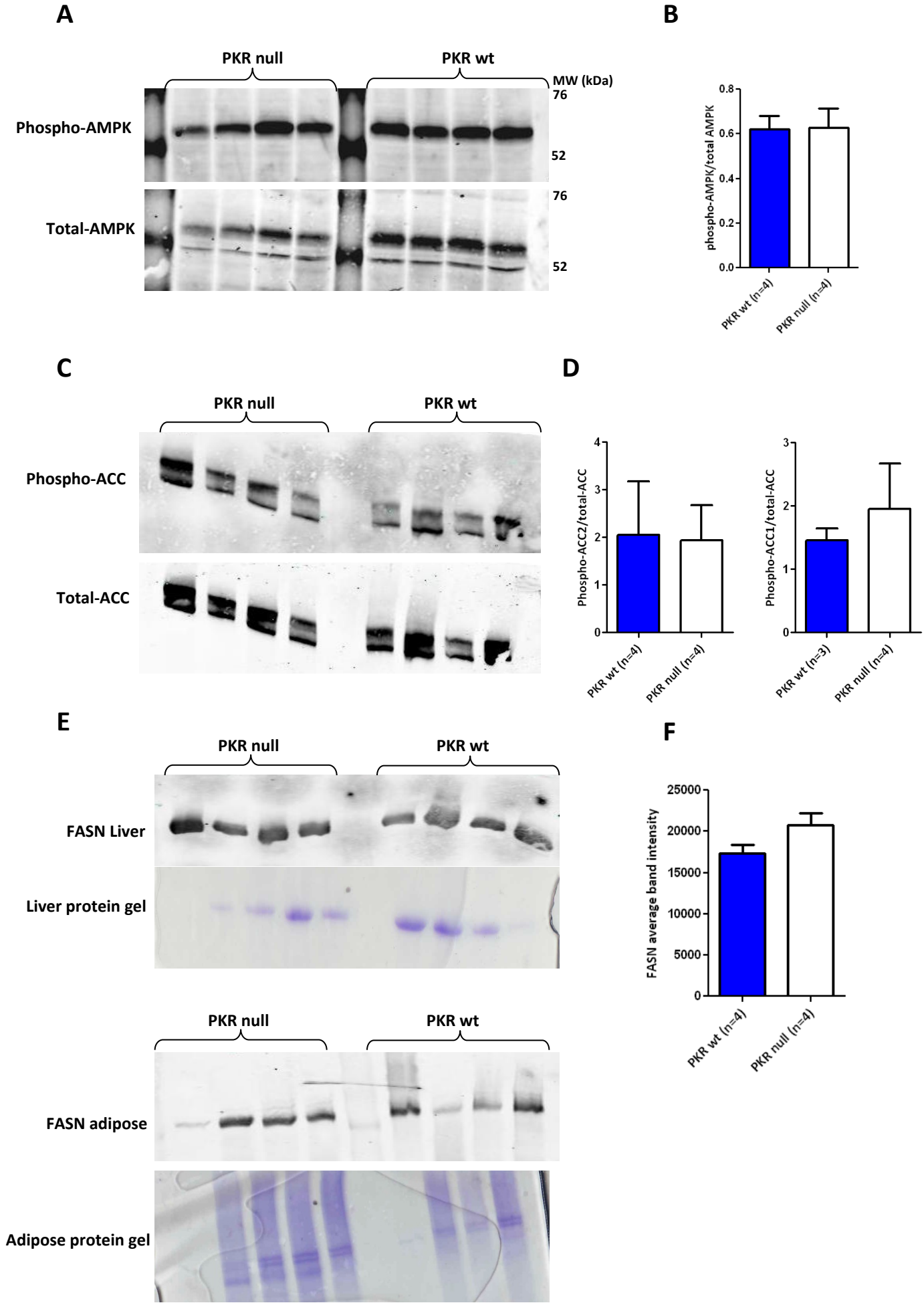
A
PKR null
PKR wt
MW (kDa)
76
52
Phospho-AMPK
76
52
Total-AMPK
B
phospho-AMPK/total AMPK
0.8
0.6
0.4
0.2
0.0
PKR wt (n=4)
PKR null (n=4)
C
PKR null
PKR wt
Phospho-ACC
Total-ACC
D
Phospho-ACC2/total-ACC
4
3
2
1
0
PKR wt (n=4)
PKR null (n=4)
Phospho-ACC1/total-ACC
3
2
1
0
PKR wt (n=3)
PKR null (n=4)
E
PKR null
PKR wt
FASN Liver
Liver protein gel
PKR null
PKR wt
FASN adipose
Adipose protein gel
F
FASN average band intensity
25000
20000
15000
10000
5000
0
PKR wt (n=4)
PKR null (n=4)

Figure 4.12 Western blot analysis of activation of the AMPK signalling cascade in liver and muscle.

A Western blot analysis of liver lysates from PKR wt (n=4) and null (n=4) mice fed a high fat diet for protein expression of phospho-AMPK. **B** densitometry results from band analysis expressed as phospho-AMPK/total AMPK ratio. **C** Western blot analysis of liver lysates from PKR wt (n=4) and null (n=4) mice fed a high fat diet for protein expression of phospho-ACC. **D** densitometry results from band analysis expressed as phospho-ACC/total ACC ratio. **E** western blot analysis of liver or white adipose tissue lysates from PKR wt (n=4) and null (n=4) mice fed a high fat diet for protein expression of FASN, scans of the protein gels are included to show sample loading, **E** relative band intensity of FASN calculated by densitometry, not normalized to the loading control, **F** densitometry analysis demonstrating the average intensity of the FASN band detected in liver lysates.

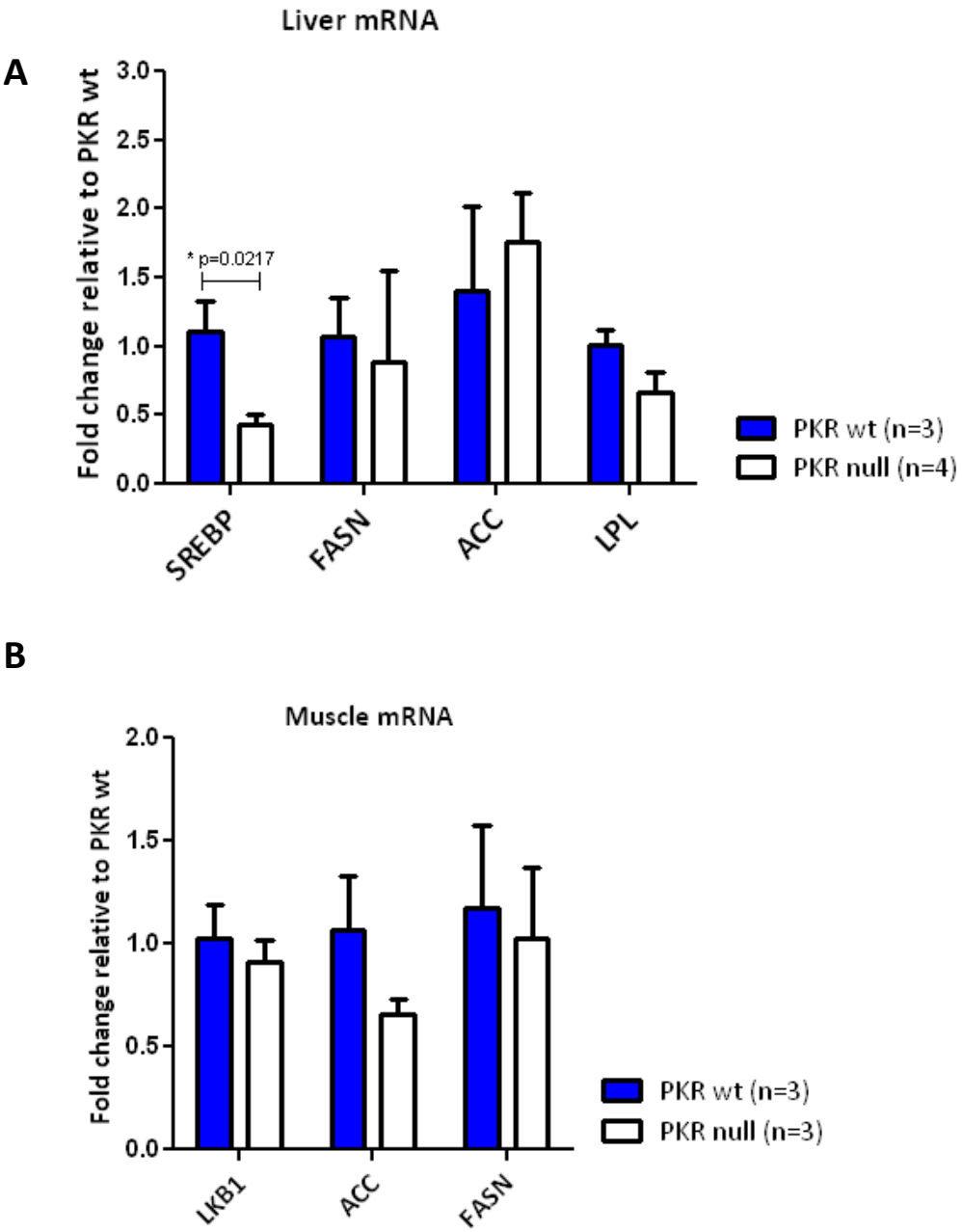

Figure 4.13 Hepatic expression of fatty acid synthesis and lipid transport genes in response to high fat diet.

A mRNA levels of SREBP1C, FASN, ACC and LPL analysed by QRT-PCR in liver of PKR wt (n=3) and PKR null (n=4) mice fed a high fat diet. Note: To detect SREBP mRNA 5 PKR wt and 5 PKR null samples were used. **B m**RNA levels of LKB1, ACC and FASN analysed by QRT-PCR in muscle of PKR wt (n=3) and PKR null (n=3) mice fed a high fat diet for 10 weeks. Expression levels of target genes was analysed by QRT-PCR and expressed as fold change relative to PKR wt. Expression of target genes was compared to the internal control 18s. Statistical analysis: unpaired T-test, mean ± SEM. * Statistically significant.

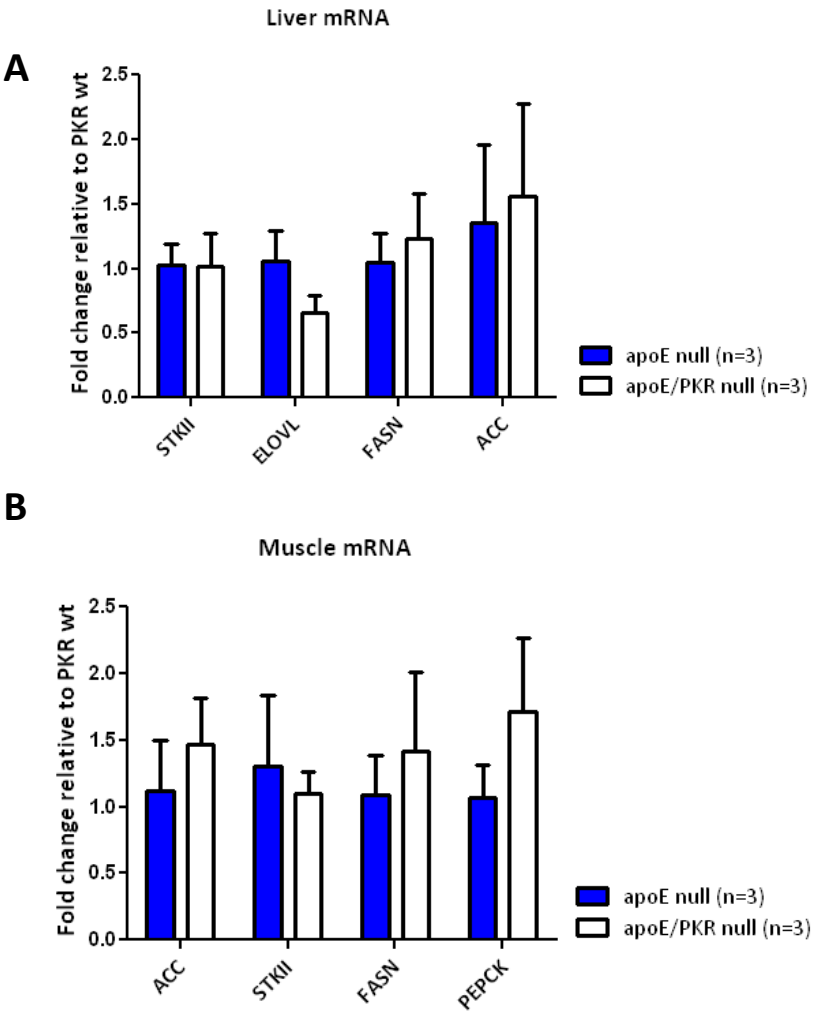

Figure 4.14 Muscle and hepatic gene expression in response to high fat diet.

Expression levels of target genes was analysed by QRT-PCR and expressed as fold change relative to PKR wt. **A** RNA extracted from liver, of apoE null (n=3) and apoE:PKR null (n=3) mice fed a high fat diet, expression of target genes was compared to the internal control 18s. **B** RNA extracted from muscle tissue of apoE null (n=3) and apoE:PKR null (n=3) mice fed a high fat diet, expression of target genes was compared to the internal control β-actin.. Statistical analysis: unpaired T-test, mean±SEM.

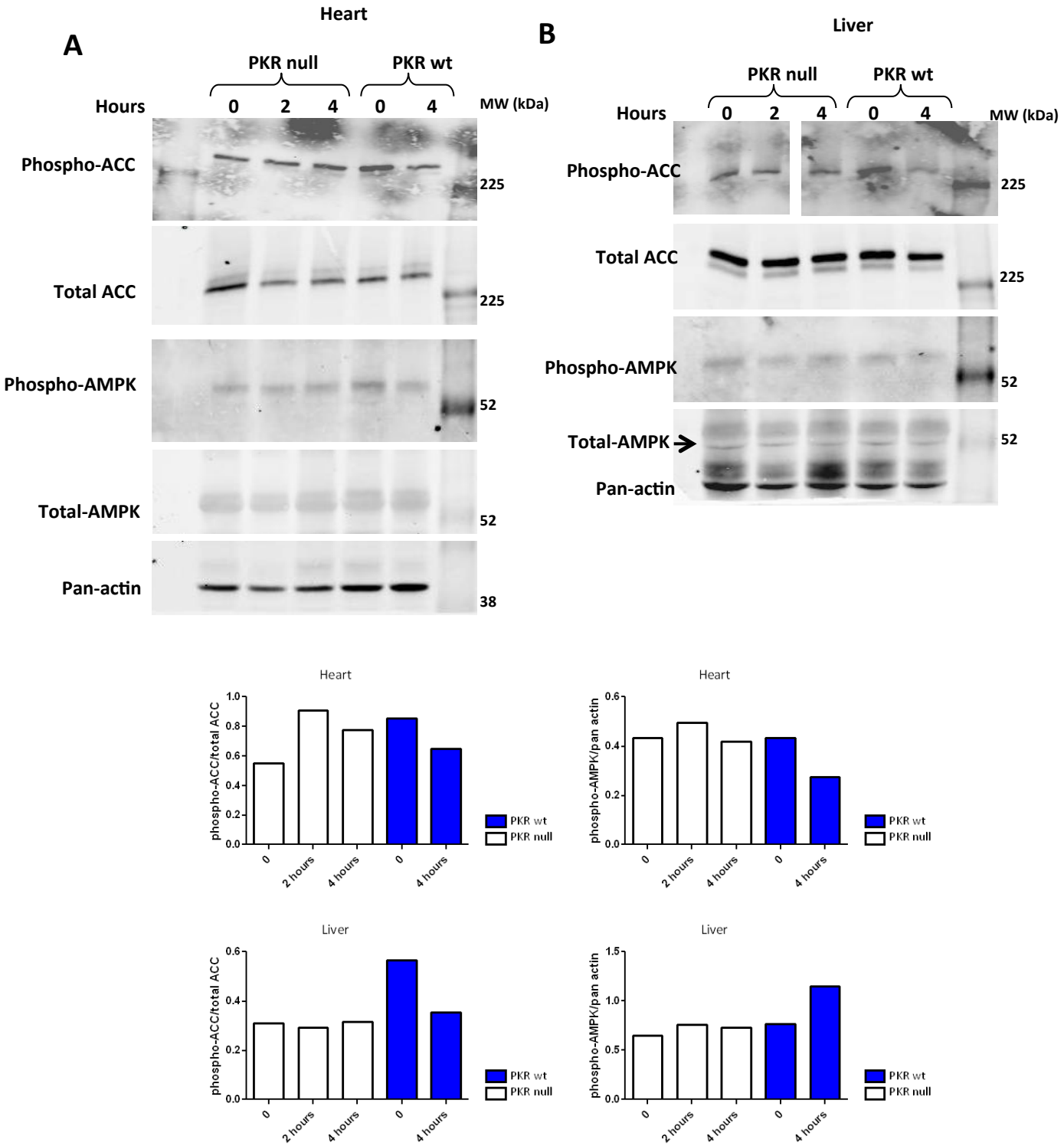

Figure 4.15 Western blot analysis of AMPK and ACC phosphorylation in liver and heart of fasted and re-fed mice.

Western blot analysis of **A** heart, or **B** liver lysates from PKR wt and null mice fed a high fat diet for 5 weeks. Mice were starved overnight and allowed to feed for 2 or 4 hours post starvation. Relative band intensities were calculated by densitometry and normalized to the loading control total AMPK, total ACC and pan actin (shown below the western blots).

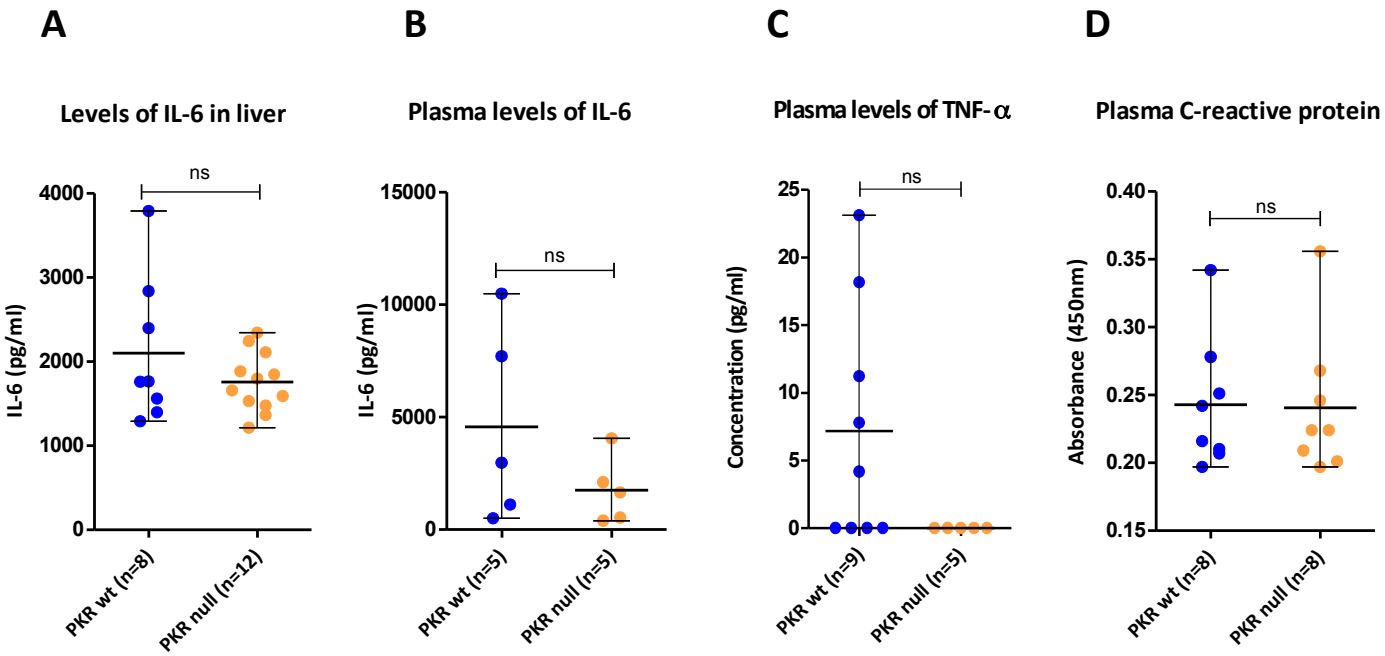

Figure 4.16 Levels of inflammatory cytokines in response to high fat diet.

Levels of inflammatory cytokines from PKR wt and PKR null mice fed a HFD. **A** Protein levels of IL-6 in the liver. **B** blood concentrations of IL-6. **C** Blood concentration of TNFα. **D** blood concentration of CRP. Statistical analysis Unpaired T-test, mean±SEM.

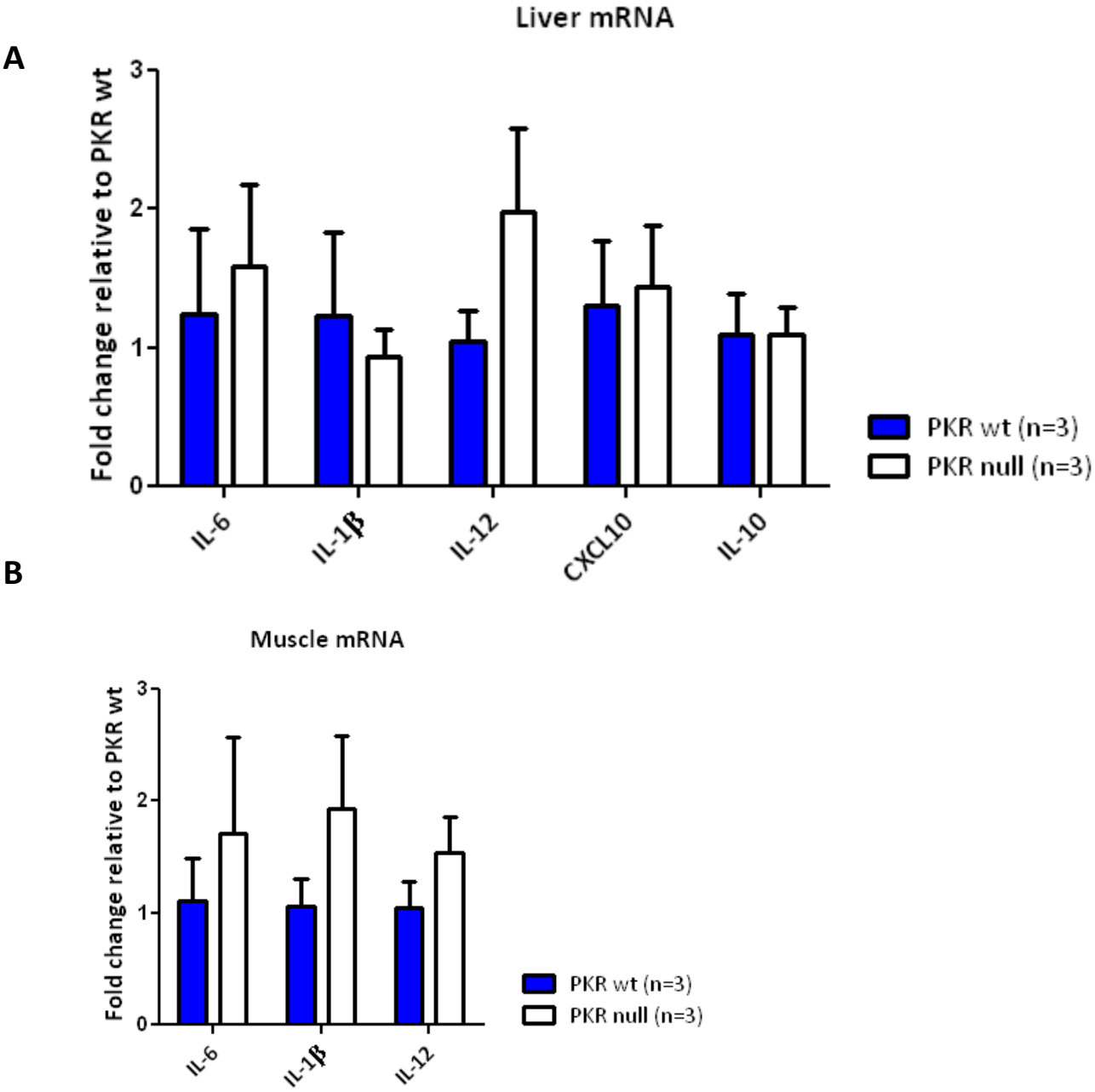

Figure 4.17 Hepatic and muscle expression of cytokines in response to high fat diet.

A mRNA levels of IL-6, IL-1β, IL-12, CXCL10 and IL-10 analyzed by QRT-PCR in liver of PKR wt (n=3) and PKR null (n=3) mice fed a high fat diet. **B** mRNA levels of IL-6, IL-1β, IL-12 analyzed by QRT-PCR in muscle of PKR wt (n=3) and PKR null (n=3) mice fed a high fat diet for 10 weeks. Expression levels of target genes was analysed by QRT-PCR and expressed as fold change relative to PKR wt. Expression of target genes were compared to the internal control 18s. Statistical analysis:Unpaired T-test, Mean±SEM.

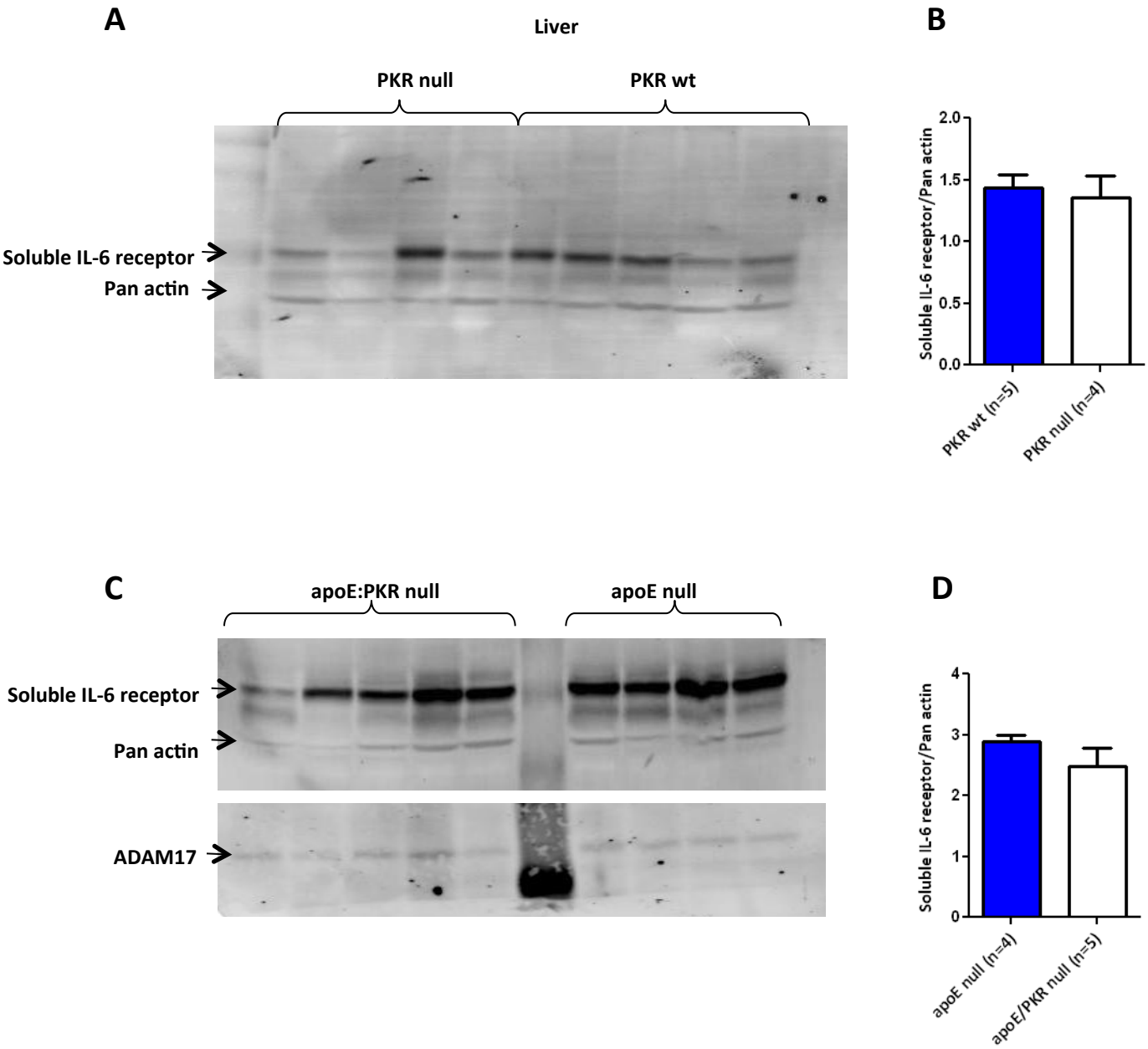

Figure 4.18 Western blot analysis of IL-6 transignalling in the liver.

A Western blot analysis of liver lysates from PKR null (n=4) and PKR wt (n=5) mice fed a high fat diet for 10 weeks for protein expression of IL-6 receptor and ADAM17. **B** Relative band intensities were calculated by densitometry and normalized to the loading control pan-actin. **C** Western blot analysis of liver lysates from apoE:PKR null (n=5) and apoE null (n=4) mice fed a high fat diet for 10 weeks for protein expression of IL-6 receptor and ADAM17. **D** Relative band intensities were calculated by densitometry and normalized to the loading control pan actin.

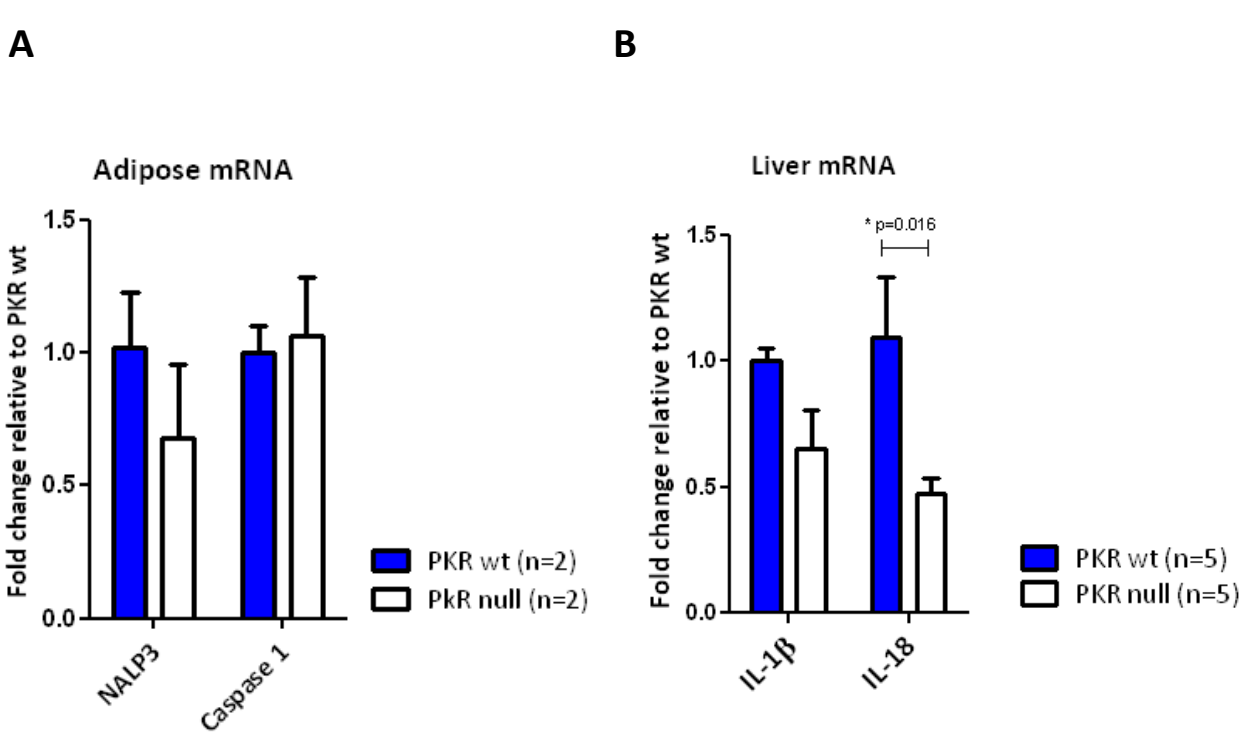

Figure 4.19 Expression of genes encoding for inflammasome components, IL-1β and IL-18 in response to high fat diet.

A mRNA levels of NALP3 and caspase-1 analysed by QRT-PCR in adipose tissue of PKR wt (n=2) and PKR null (n=2) mice fed a high fat diet. Results are expressed as fold change relative to PKR wt. Expression of target genes were compared to the internal control β-actin. **B** mRNA levels of IL-1β and IL-18 analysed by QRT-PCR in liver tissue of PKR wt (n=5) and PKR null (n=5) mice fed a high fat diet for 10 weeks. Results are expressed as fold change relative to PKR wt. Expression of target genes were compared to the internal control 18s. Statistical analysis:Unpaired T-test, Mean±SEM.

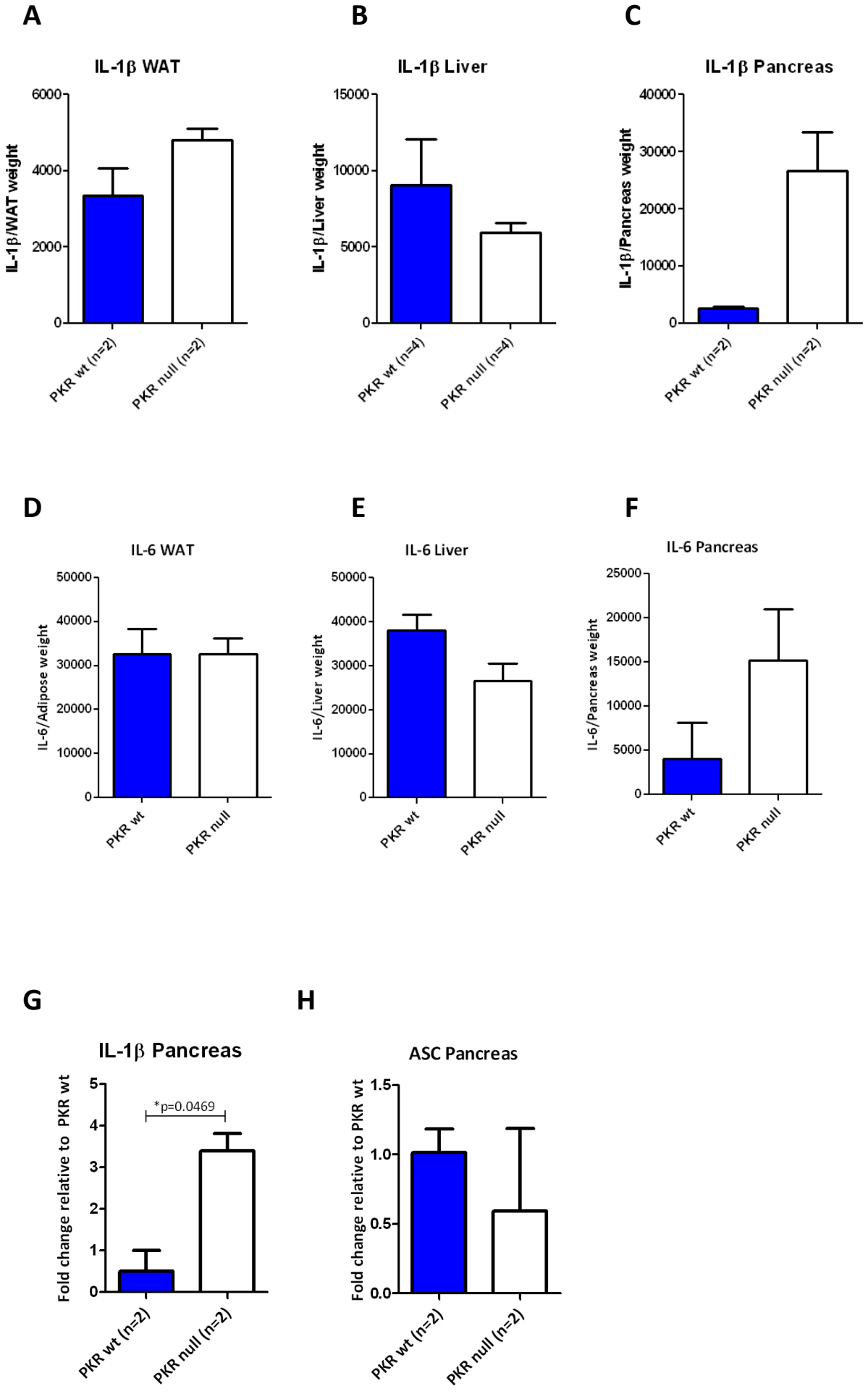
A
IL-1β WAT
IL-1β/WAT weight
6000
4000
2000
0
PKR wt (n=2)
PKR null (n=2)
B
IL-1β Liver
IL-1β/Liver weight
15000
10000
5000
0
PKR wt (n=4)
PKR null (n=4)
C
IL-1β Pancreas
IL-1β/Pancreas weight
40000
30000
20000
10000
0
PKR wt (n=2)
PKR null (n=2)
D
IL-6 WAT
IL-6/Adipose weight
50000
40000
30000
20000
10000
0
PKR wt
PKR null
E
IL-6 Liver
IL-6/Liver weight
50000
40000
30000
20000
10000
0
PKR wt
PKR null
F
IL-6 Pancreas
IL-6/Pancreas weight
25000
20000
15000
10000
5000
0
PKR wt
PKR null
G
IL-1β Pancreas
Fold change relative to PKR wt
*p=0.0469
5
4
3
2
1
0
PKR wt (n=2)
PKR null (n=2)
H
ASC Pancreas
Fold change relative to PKR wt
1.5
1.0
0.5
0.0
PKR wt (n=2)
PKR null (n=2)

Figure 4.20 Secretion of IL-1β from *ex vivo* tissue culture.

Concentration of IL-1β protein secreted from **A** WAT, **B** Liver and **C** Pancreas of PKR wt (n=2) and PKR null (n=2) mice fed a high fat diet for 5 weeks. Protein levels of IL-1β are normalised to weight of tissue. Concentration of IL-6 protein secretion from **D** WAT, **E** liver and **F** pancreas. Protein levels of IL-6 are normalised to weight of tissue. RNA extracted from pancreas tissue of PKR wt (n=2) and PKR null (n=2) mice fed a high fat diet 5 weeks. Expression levels of **G** IL-1β and **H** ASC were analysed by QRT-PCR and expressed as fold change relative to PKR wt. Expression of target genes were compared to the internal control 18S. Statistical analysis: Unpaired T-test, Mean±SEM.

CHAPTER 5 DISCUSSION

CHAPTER 5 DISCUSSION 137
5.1 GENERAL DISCUSSION 138
5.2 CONCLUSION 144
5.3 REFERENCES 145

5.1 GENERAL DISCUSSION

Obesity is currently one of the largest health concerns of our era with Australians being ranked as one of the fattest nations globally. The mission statement of the Obesity Prevention Australia organisation is: *"To reduce the incidence of obesity and metabolic syndrome in Australia while raising awareness of healthy lifestyle practices through preventative initiatives."* They believe that a straightforward approach of eating healthier and exercising will tackle the obesity epidemic. However, lifestyle intervention has not been proven to be an effective treatment for all obese individuals and often fails to alleviate the burden of co-morbidities that associate with obesity. Therefore pharmacological therapy must be considered. This requires a greater understanding of the mechanisms that regulate of body weight and the pathogenesis of obesity-related disorders.

The major objective of this investigation was to test a role for the innate immune protein PKR in diet induced obesity and ensuing metabolic pathologies. The findings here show that PKR plays a biologically significant function in suppressing weight gain and metabolic disease in response to high fat diets. This role for PKR in metabolic disease is supported in high fat diet fed apoE:PKR ablated mice, which like the single PKR knockout mice, are susceptible to weight gain but have worsened atherosclerosis. Our findings demonstrate that PKR modulates metabolic signalling pathways specifically in response to diets high in fats.

To evaluate the mechanism by which PKR regulates responses to high fat diets, I screened a number of signalling pathways that have been demonstrated to regulate metabolic homeostasis. I did not identify a single prevailing pathway but, rather, discovered PKR coordinates a number of metabolic and energy-sensing pathways that modulate weight gain. Our findings are somewhat analogous to the protective effects previously reported for two other eIF2α kinases, GCN2 and PERK, in diet-induced obesity, which suggests that the mechanism underlying metabolic disease would involve eIF2α (Harding, Zeng et al. 2001; Guo and Cavener 2007). However, the mechanisms of action differ between the separate eIF2α kinases. Unlike the PERK ablated mice, we show that mice ablated for PKR, although

they have diminished islet mass, have healthy insulin producing β-cells and a normal exocrine pancreas. We also ruled out the possibility of PERK being activated in our model of diet-induced obesity by demonstrating that the UPR (measured by assessing XBP1 splicing) is equivalent between WT and PKR knockout mice. In conjunction with the GCN2 knockout mouse, we show that apoE:PKR ablated mice have increased expression of FASN. However, the expression pattern of FASN differs significantly between the animal models, as loss of GCN2 upregulates FASN expression in liver, whilst apoE:PKR deficient mice have increased expression of FASN in WAT. These findings suggest that GCN2 and PKR regulate separate signalling pathways to modulate the development of metabolic disease. This may be a reflection of the different expression patterns and activation stimuli of each kinase, as GCN2 is activated by amino acid deprivation, an event that is unlikely to occur during high fat diet feeding. Intriguingly there was no change in expression of FASN in single PKR knockout mice suggesting that unlike the responses of GCN2 deficient mice, FASN mediated *de novo* lipid synthesis does not contribute to fatty liver disease or adiposity seen in these animals.

To test the requirement for PKR-dependent substrate phosphorylation in modulating obesity and ensuing disease, I used a kinase dead (K271R) mutant PKR mouse generated in our laboratory. Unexpectedly, this revealed that the kinase function of PKR is not required to modulate responses to high fat diet. Intriguingly, however, the K271R heterozygote mouse gained weight to a comparable magnitude as mice ablated for PKR. We can't currently explain this difference between the heterozygote and homozygote mice, but speculate that there may be a gene dosage effect. This conjecture is based on work performed by others in the laboratory showing that the K271R homozygous mouse expresses very high levels of the PKR protein. Hence, we speculate that the very high concentration of kinase dead PKR may, in some way, compensate for the loss of kinase activity as it has previously been reported that the equivalently mutated human PKR (K296R) participates in signalling, although to a reduced extent. Previous reports have also established that PKR associates with the TNF-receptor-associated factor (TRAF) via its RBM, to regulate downstream signalling events such as activation of NF-κB and other transcription factors (Gil, Garcia et al. 2004). NF-κB plays a critical role in transcription of genes regulating

a diverse range of biological processes, some of which directly impact inflammation, adiposity and metabolic homeostasis. Although the role of NF-κB in inflammation is largely believed to be pro-inflammatory, it has also been shown to modulate expression of anti-inflammatory genes. Therefore we speculate that the tentative interaction of the K271R mutant protein could be protective by modulating NF-κB responses.

Chronic low-grade inflammation is part of the pathogenesis of obesity. However we demonstrate that PKR does not regulate classical inflammatory responses upon exposure to dietary fats as systemic levels of inflammatory cytokines are similar between WT and PKR knockout mice. Instead our results suggest that PKR activates the inflammasome to induce sterile inflammation. We show in an *ex vivo* tissue explant experiment that loss of PKR promotes pancreas specific secretion of IL-1β. Previous evidence reports that activation of NLRP3 and increased expression of IL-1β in the pancreas induces β-cell death, islet deficiency and subsequent insulin resistance (Youm, Adijiang et al. 2011). Given that the primary consequence of diminished islet cell mass is insulin insufficiency and type 2 diabetes, it was possible that pancreas specific inflammasome activity could explain the reduced size of the islet size in mice ablated for PKR and affect glucose homeostasis. However, islets of Langerhans were also reduced in the homozygous K271R mouse, which unlike the PKR knockout mouse, was protected from diet induced weight gain and had sufficient insulin signalling. Hence these findings indicate that islet deficiency is unlikely to account for the disrupted glucose homeostasis in the PKR null mouse. We speculate however, that inflammasome-dependent inflammation identified in the PKR null mouse, could account for the disruption of insulin signalling. This conjecture should be proven by determining whether antagonism of the IL-1β receptor improves disease outcome and blood glucose concentration. Time restrictions have prevented these experiments being completed for this study.

Further investigation revealed that loss of PKR affects a number of additional pathways involved in glucose homeostasis. Firstly, loss of PKR enhanced glucose output due to increased expression of G6Pase and a higher rate of conversion of pyruvate to glucose. Contrasting this, we establish that PKR deficiency also results in increased expression of the rate-limiting enzyme of the pentose phosphate pathway, G6PD in the liver. This increased

expression of G6PD does not appear to rescue the effect of high glucose blood concentration, as mice ablated for PKR remain glucose intolerant. However, we did find evidence, at least *in vitro*, that PKR null cells have increased ATP production, which would be an expected consequence of increased G6PD and the ensuing product of NADPH.

This study also identified that MEFs devoid of PKR have an attenuated insulin response, as demonstrated by decreased phosphorylation of p70S6K. We speculate that this is due to reduced expression of the insulin signalling protein IRS2. IRS2 is critical for the maintenance of β-cell mass and loss of this adaptor protein disturbs cellular insulin signal transduction and causes type 2 diabetes. This suggests a molecular mechanism that could account for the glucose intolerance in mice ablated for PKR. Opposing the expected consequence of suppressed insulin signalling we demonstrate that loss of PKR enhances basal phosphorylation of Akt at ser347 in MEFs. To provide a potential explanation for this, we suggest that PKR-mediated regulation of PP2A protein expression prevents phosphatase-mediated dephosphorylation of Akt. Although we did not assess enzymatic activity of PP2A, we speculate that decreased expression of PP2A in the liver of mice ablated for PKR could correlate with reduced enzymatic activity.

Interestingly, our findings suggest that inflammasome induced secretion of IL-1β from WAT or liver is comparable in WT and PKR knockout mice and is therefore not a likely explanation for increased adiposity or liver disease seen in mice deficient for PKR. In addition, there is no difference in circulating and mRNA levels of inflammatory mediators TNFα or IL-6 between WT and PKR knockout mice suggesting that neither sterile nor classic inflammatory responses play a role in adiposity. Instead we show that mechanism involved in lipid metabolism and energy homeostasis have a greater impact on weight gain in mice deficient for PKR. Part of the adverse effects of high fat diet fed mice ablated for apoE:PKR can be explained for by increased expression of FASN in WAT, which acts to induce *de novo* fatty acid synthesis and could lead to increased adipocyte size. We also demonstrate that PKR induces the expression of DGAT2 in WAT, although the difference in expression is not statistically significant (Shi and Cheng 2009). We believe that adipose specific secretion of free fatty acids into the circulation disturbs the serum lipid profile and promotes

dyslipidemia that, in mice ablated for PKR, is characterised by increased triglyceride concentration. Furthermore, we speculate that adipocyte hypertrophy and consequent dyslipidemia may be the cause of non-alcoholic fatty liver disease in mice ablated for PKR by encouraging ectopic lipid deposition and causing tissue lipotoxicity. This speculation is supported by the observation that fatty liver disease is caused independent of changes in *de novo* fatty acid synthesis because hepatic expression of DGAT2 and FASN is similar in both mice, suggesting that either deposition of circulating triglycerides, or failure to induce β-oxidation account for liver steatosis.

A role for PKR in lipid synthesis is further substantiated by the observation that PKR regulates hepatic expression enzymes IDH1 and IDH2, which along with DGAT2 play a key role in fatty acid synthesis by increasing cellular concentration of the NADPH cofactor. Although we did not detect a difference in the levels of NADH and NADPH between MEFs expressing or lacking PKR, we speculate that the energy harnessed from NADH is consumed by ATP synthesis.

Also supporting a role for PKR in lipid metabolism, this thesis establishes that loss of PKR modulates cellular energy homeostasis by decreasing the expression of UCP1 in WAT, which is linked to suppressed energy expenditure. The role for PKR in energy homeostasis is emphasised by *in vitro* studies, which demonstrate that 3T3 MEFs and SMO cell lines lacking PKR have impaired mitochondrial bioenergetics. MEFs deficient for PKR have increased basal oxygen consumption, reduced mitochondrial proton leak and increased oxidative ATP synthesis that are hallmark features of metabolic disease. These findings support the hypothesis that in mice ablated for PKR the NADH cofactor may be consumed by the process of oxidative ATP synthesis and consequently prevent the detection of a difference in NADH levels between WT and PKR knockout mice. We also establish that PKR regulates mitochondrial function independent of translational or transcriptional control of genes encoding for mitochondrial electron transport chain enzymes. Alternatively, disturbances in OXPHOS function may be due to impaired enzymatic activity of OXPHOS complexes. However, this notion warrants further investigation. Collectively these findings suggest that mice ablated for PKR accumulate energy as a consequence of increased oxidative ATP

synthesis and *de novo* fatty acid synthesis. Without impeding BAT thermogenesis and physical activity to suppress energy expenditure.

In addition to mitochondrial specific processes that contribute to energy homeostasis, we establish that PKR modulates activation of the AMPK signalling network *in vivo*. AMPK is induced upon nutrient deprivation. In line with this finding we observed that fasting increased phosphorylation of the AMPK target ACC in the liver of wild type mice and re-feeding suppressed this activation. Activation of this pathway was lost in mice ablated for PKR. The expected consequence of ACC phosphorylation is reduced fatty acid synthesis and increased fatty acid oxidation, therefore these findings provide a tentative molecular mechanism for PKR mediated protection from lipid storage and adiposity. These findings are consistent with a previous report that phosphorylation and activation of AMPK was associated with increased phosphorylation of PKR and eIF2α (Katta, Kakarla et al. 2012).

To investigate whether loss of PKR has a consequence on development of cardiovascular disease, we created the double apoE:PKR knockout mice. Interestingly we observed a number of key differences between the metabolic phenotype of mice ablated for apoE:PKR and single PKR ablated mice which is most likely explained for by the protective effects and altered lipid transport caused by apoE deficiency. Notably, apoE:PKR ablated mice fed a high fat diet have significantly reduced levels of plasma triglycerides and increased LDL concentration. This lipoprotein profile contrasts that of single PKR knockout mice, which have decreased levels of TG and increased LDL. In spite of these discrepancies, we demonstrate that loss of PKR on the apoE background has a significant consequence on disease outcomes because these mice develop atherosclerotic plaques greater than mice deficient for apoE.

Interestingly, reports by others suggest a mechanism by which PKR could affect circulating lipid by regulating apoE gene dosage (Van Eck, Herijgers et al. 1997; Segev, Michaelson et al. 2013). The gene encoding apoE protein contains regulatory sequences in its promoter region that would suggest regulation by PKR-dependent phosphorylation of eIF2α. Indeed, other evidence suggests that translation of apoE is associated with increased

eIF2α phosphorylation. Hence, PKR could regulate translation of apoE, in an eIF2α dependent manner, to modulate lipoprotein composition.

5.2 CONCLUSION

The central proposition of this thesis is that PKR influences major metabolic, inflammatory and energy sensing networks, independent of its kinase function, to regulate whole body homeostasis and to protect against high fat diet induced metabolic disease. A variety of physiological, metabolic and immune alterations are identified in mice ablated for PKR. The findings from this thesis are summarised in figure 5.1. The relative significance of each of these PKR-dependent effects to diet induced obesity remains to be established. Nevertheless, deterioration of the metabolic system in mice deficient for PKR has significant implications for cardiovascular disease and diabetes. These results validate the PKR knockout mouse as an informative model for understanding the pathogenesis of metabolic disease, because unlike mutations in the *Ob* or *Db* genes, PKR links both inflammatory and metabolic aspects underlying obesity and associated diseases.

5.3 REFERENCES

Gil, J., M. A. Garcia, et al. (2004). "TRAF family proteins link PKR with NF-kappa B activation." Mol Cell Biol **24**(10): 4502-4512.
Guo, F. and D. R. Cavener (2007). "The GCN2 eIF2alpha kinase regulates fatty-acid homeostasis in the liver during deprivation of an essential amino acid." Cell Metab **5**(2): 103-114.
Harding, H. P., H. Zeng, et al. (2001). "Diabetes mellitus and exocrine pancreatic dysfunction in perk-/- mice reveals a role for translational control in secretory cell survival." Mol Cell **7**(6): 1153-1163.
Katta, A., S. K. Kakarla, et al. (2012). "Diminished muscle growth in the obese Zucker rat following overload is associated with hyperphosphorylation of AMPK and dsRNA-dependent protein kinase." J Appl Physiol **113**(3): 377-384.
Segev, Y., D. M. Michaelson, et al. (2013). "apoE epsilon4 is associated with eIF2alpha phosphorylation and impaired learning in young mice." Neurobiol Aging **34**(3): 863-872.
Shi, Y. and D. Cheng (2009). "Beyond triglyceride synthesis: the dynamic functional roles of MGAT and DGAT enzymes in energy metabolism." Am J Physiol Endocrinol Metab **297**(1): E10-18.
Van Eck, M., N. Herijgers, et al. (1997). "Bone marrow transplantation in apolipoprotein E-deficient mice. Effect of apoE gene dosage on serum lipid concentrations, (beta)VLDL catabolism, and atherosclerosis." Arterioscler Thromb Vasc Biol **17**(11): 3117-3126.
Youm, Y. H., A. Adijiang, et al. (2011). "Elimination of the NLRP3-ASC inflammasome protects against chronic obesity-induced pancreatic damage." Endocrinology **152**(11): 4039-4045.

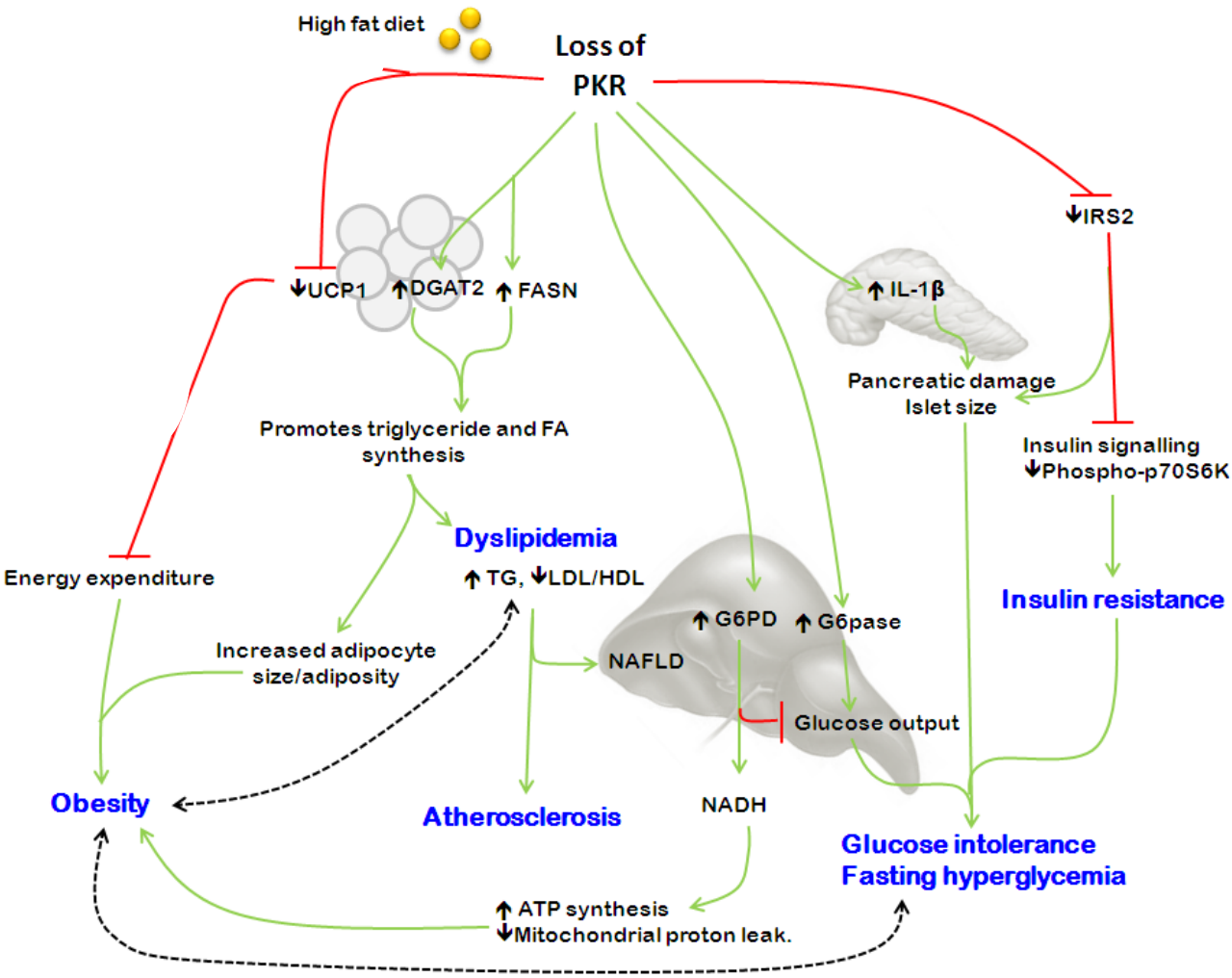
High fat diet
Loss of PKR
↓IRS2
↓UCP1
↑DGAT2
↑FASN
↑IL-1β
Pancreatic damage
Islet size
Promotes triglyceride and FA synthesis
Insulin signalling
↓Phospho-p70S6K
Dyslipidemia
↑TG, ↓LDL/HDL
Energy expenditure
Insulin resistance
↑G6PD
↑G6pase
Increased adipocyte size/adiposity
NAFLD
Glucose output
Obesity
Atherosclerosis
NADH
Glucose intolerance
Fasting hyperglycemia
↑ATP synthesis
↓Mitochondrial proton leak.

Figure 5.1 Ablation of PKR is detrimental in response to high fat diets.

Ablation of PKR decreases expression of UCP1 in WAT thereby suppressing BAT temperature and the ability to expend energy through thermogenesis. Loss of PKR also suppresses locomotor activity and disturbs energy balance by promoting ATP synthesis. Hepatic expression of G6PD is increased in mice ablated for PKR, which is speculated to increase production of NADH, required for ATP synthesis. In WAT loss of PKR induces expression of DGAT2 and FASN to promote triglyceride and fatty acid synthesis. This phenotype likely accounts for increased adipocyte size and dyslipidemia and the consequent development of atherosclerosis and obesity, respectively. PKR deficiency also promotes the development of glucose intolerance by increasing expression of G6pase in the liver thereby enhancing glucose output and by inhibiting expression of IRS1 to dampen insulin signalling. We also show that PKR regulates the expression of pancreatic IL-1β and islet size providing another mechanism that could account for impaired glucose homeostasis.

APPENDICIES

APPENDIX I

ACCEPTED MANUSCRIPTS GENERATED FROM THIS THESIS

Review publication:

Pindel, A. and A. Sadler (2011). "The role of protein kinase R in the interferon response." J Interferon Cytokine Res **31**(1): 59-70.

APPENDIX II
RESULTS FROM HONOURS THESIS

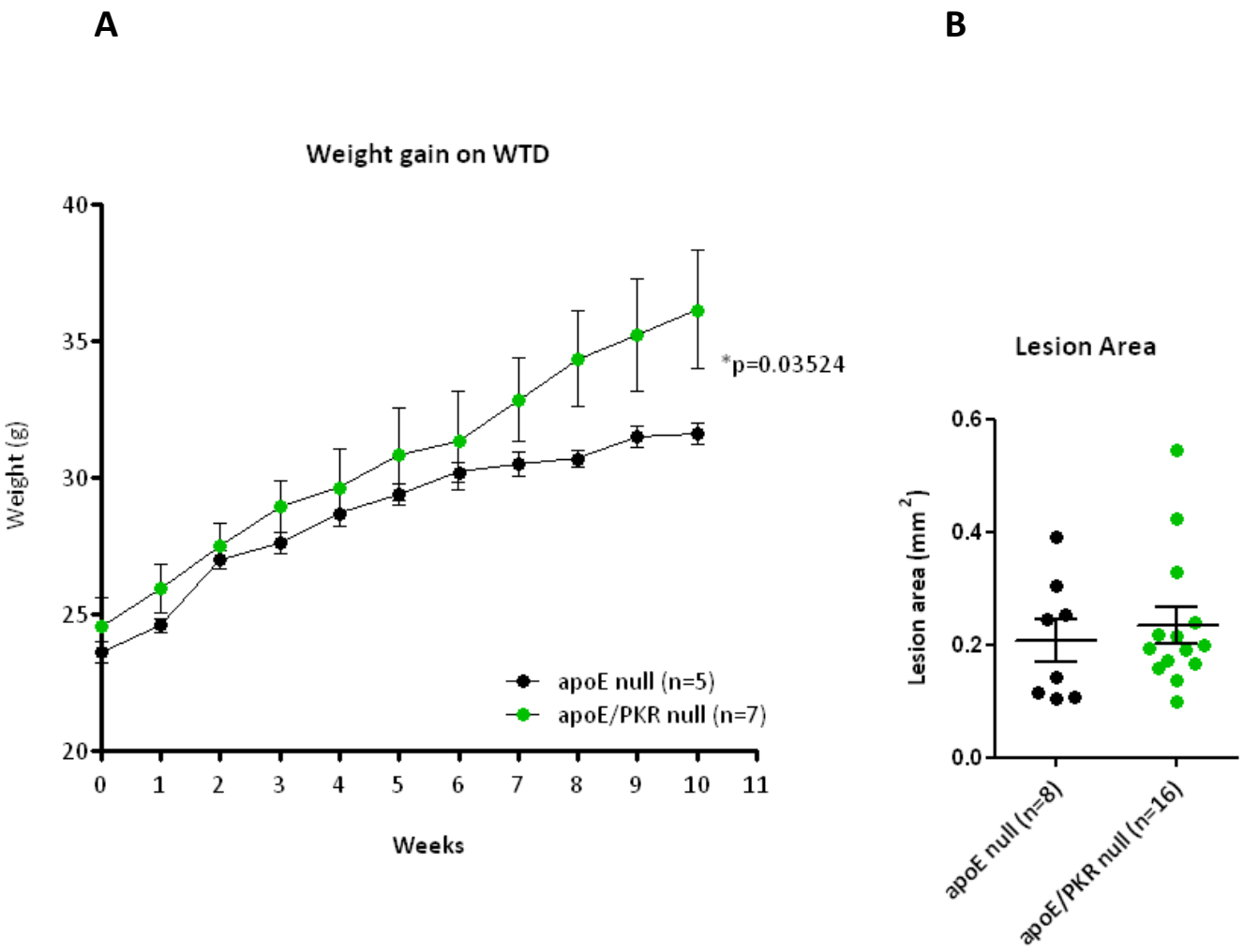

Appendix II. Weight gain and atherosclerotic plaque build up after high fat diet feeding. Data obtained as part of my honours thesis in 2008. **A** Weight gain of apoE knockout and apoE:PKR knockout mice fed a high fat diet for ten weeks and **B** quantification of atherosclerotic plaque build at the aortic root of the heart (mm^2). Weight was recorded weekly. Statistical analysis: linear regression, mean±SEM and unpaired T-test, mean±SEM. *Statistically significant.

APPENDIX III
RESULTS FROM HONOURS THESIS

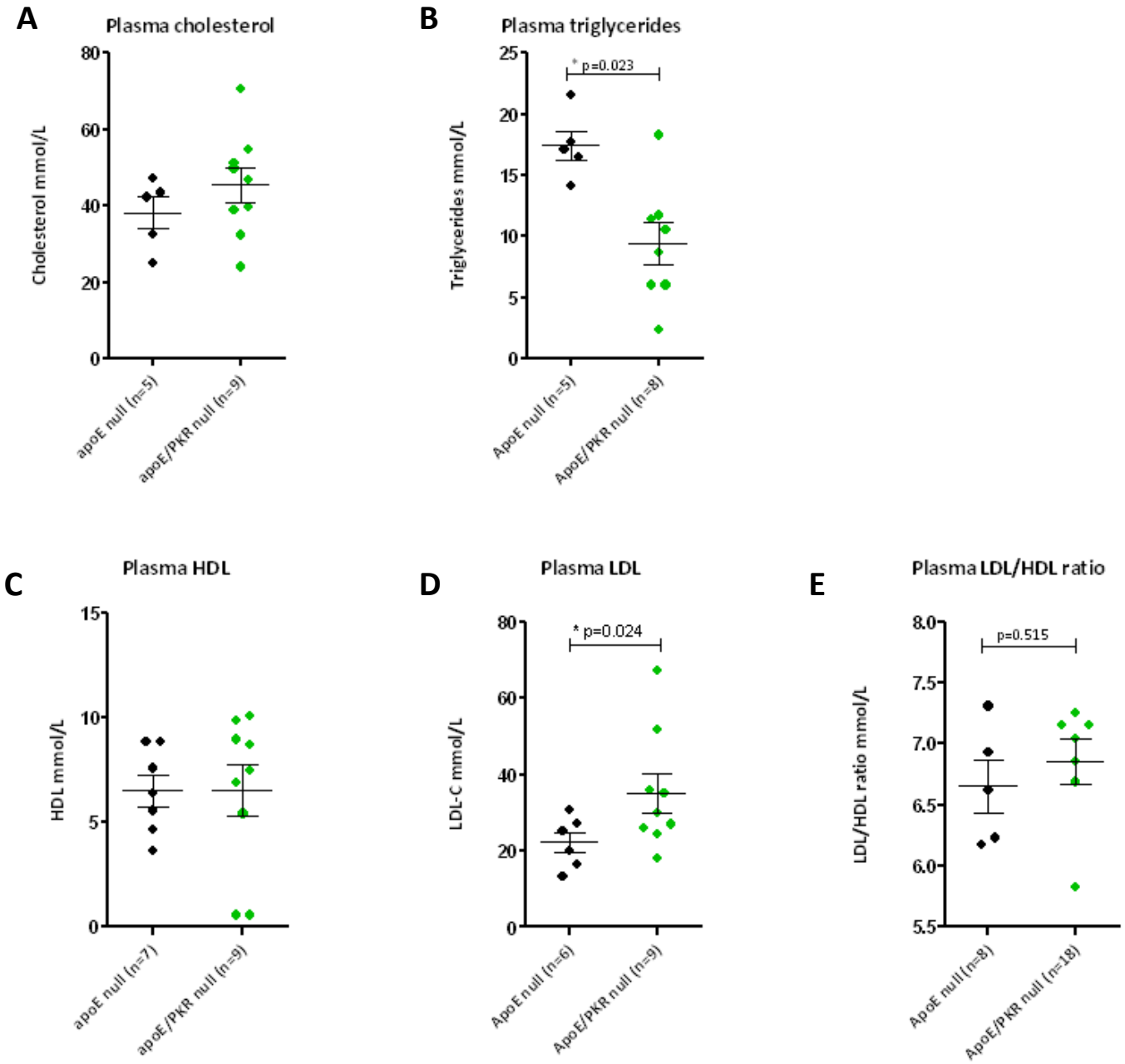

Appendix III. Blood lipid and lipoprotein composition of apoE knockout and apoE:PKR knockout mice fed a high fat diet.

Data obtained as part of my honours thesis in 2008. **A** Plasma cholesterol levels **B** plasma triglyceride levels, **C** plasma HDL levels were **D** plasma LDL levels and **E** plasma HDL/LDL ratio. Statistical analysis: unpaired T-test, Mean±SD. *Statistically significant.

APPENDIX IV
WESTERN BLOT ANALYSIS OF AMPK ACTIVATION

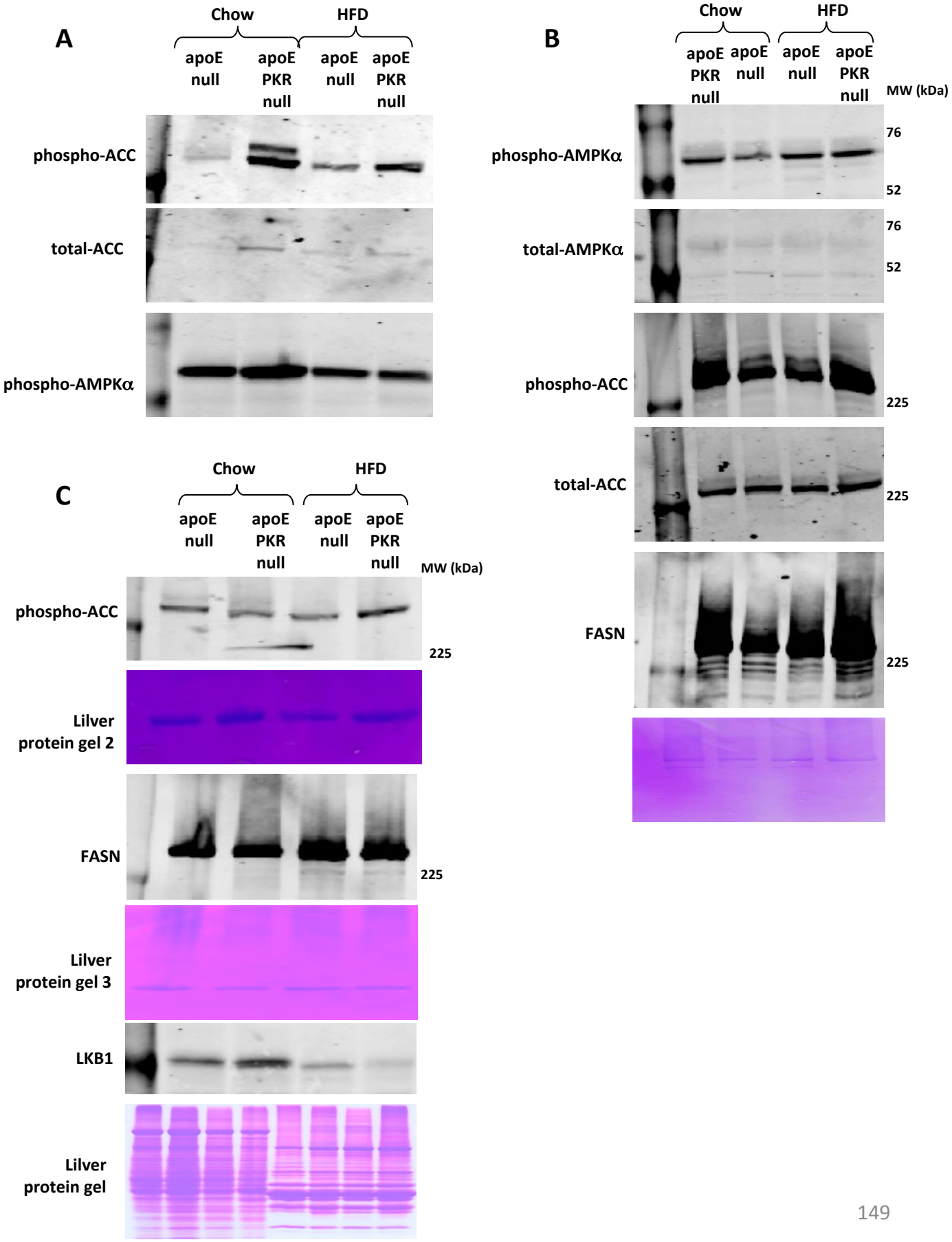

Appendix IVA. Western blot analysis of AMPK activation.

Western blot analysis of phospho-AMPK and phospho-ACC in liver lysates from apoE and apoE:PKR null mice fed either a chow or HFD . **A** liver tissue lysates collected following a chow or HFD and **B** white adipose tissue lysates collected following a chow or HFD and C liver tissue lysates collected following a chow or HFD. All western blots performed by O.Latchoumanin.

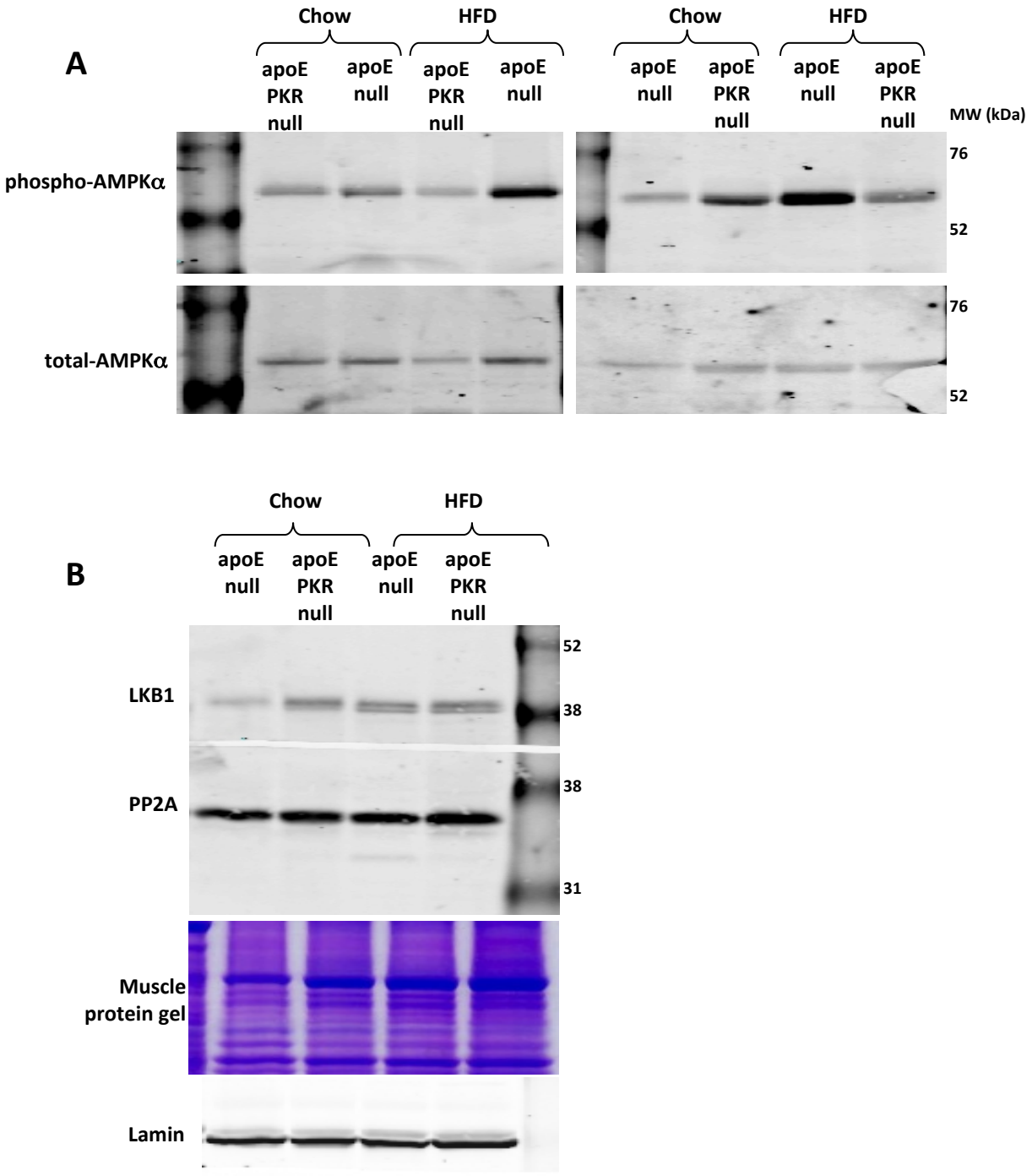

Figure IVB. Western blot analysis of AMPK cascade activation in muscle response to chow or HFD.

Western blot analysis of muscle tissue lysates (**A** and **B**) collected following a chow or HFD. All western blots performed by O.Latchoumanin.

APPENDIX V
WESTERN BLOT ANALYSIS OF INSULIN SIGNALLING *IN VITRO*

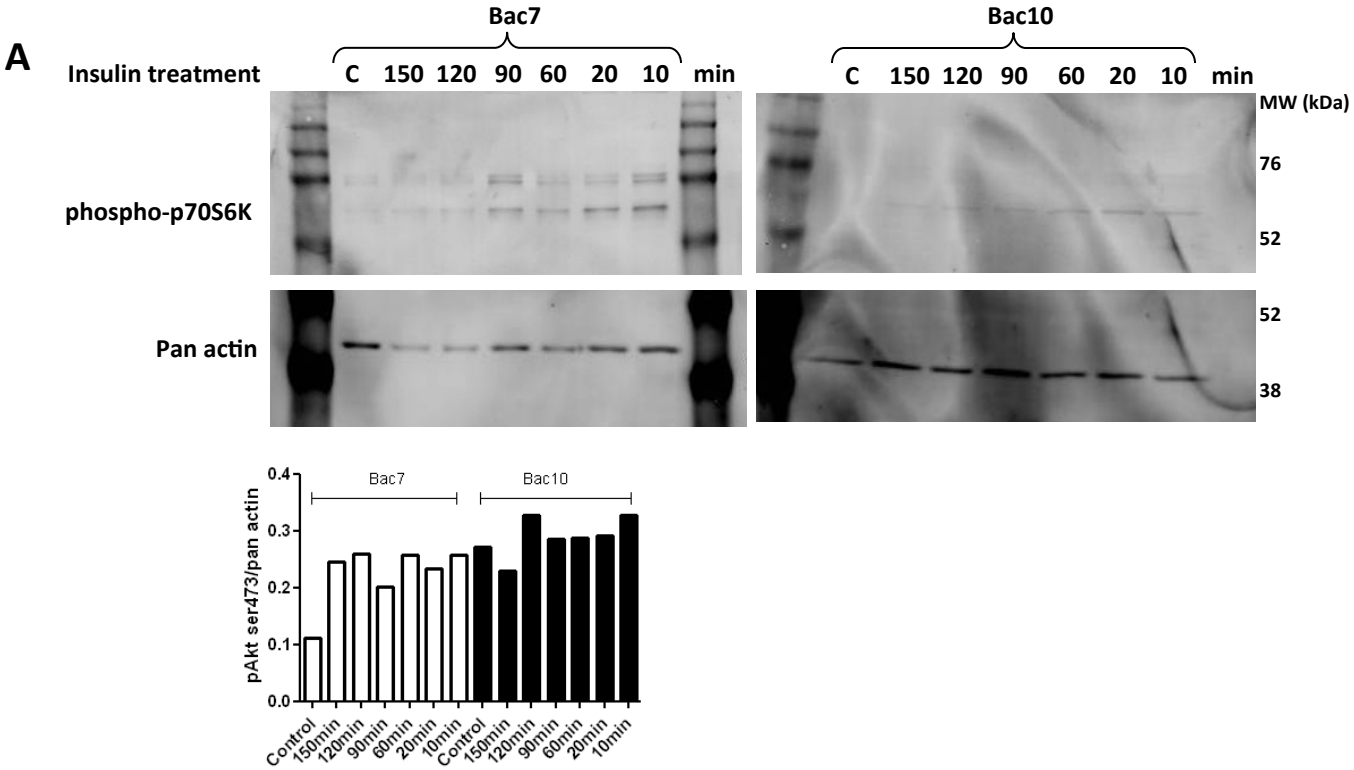

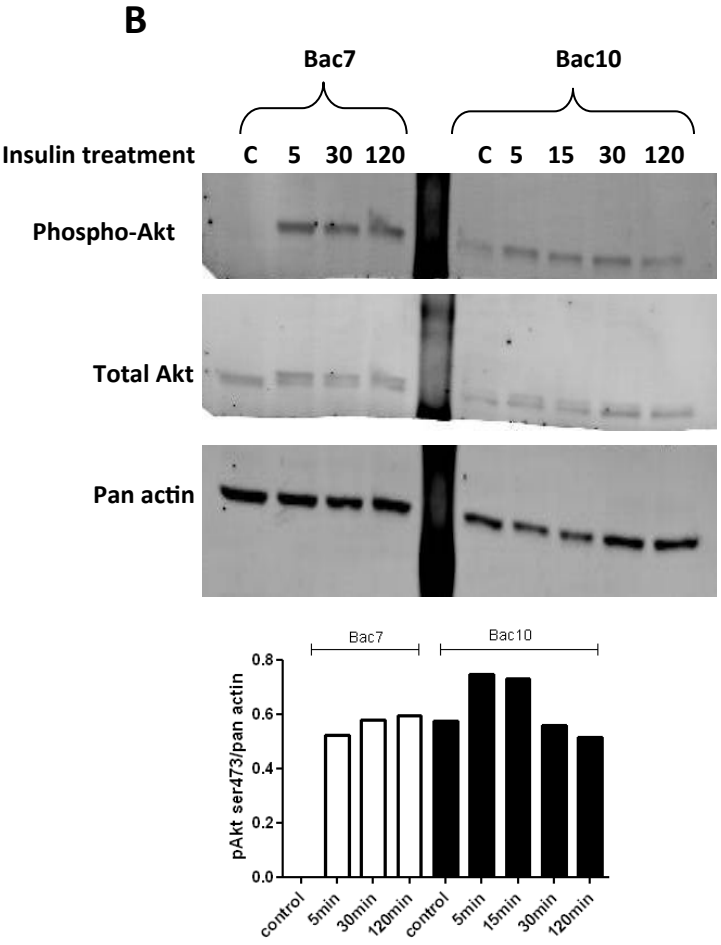

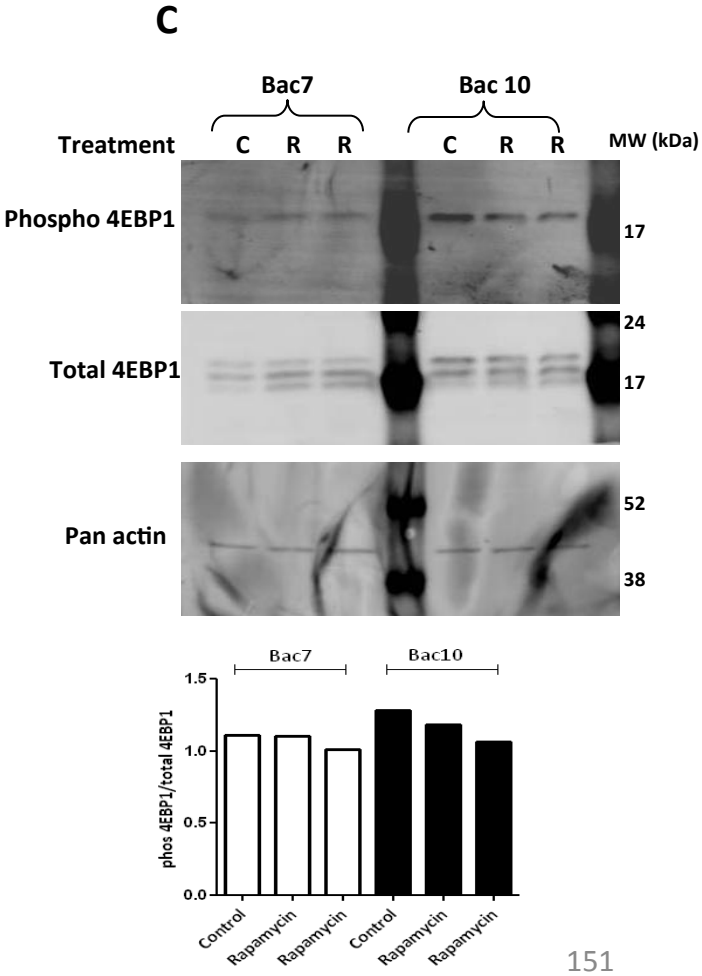

Appendix V. Western blot analysis of p70S6k, Akt and 4EBP1 phosphorylation in 3T3 MEFs after insulin treatment.

Western blot analysis of **A** p70S6k phosphorylation in Bac7 and Bac10 3T3 MEF cell lysates following the indicated period of insulin treatment. Relative band intensity of phospho-p70S6K was normalized to pan actin, **B** Akt phosphorylation following the indicated period of insulin treatment, relative band intensity of phospho-Akt was normalized to pan actin and **C** phosphorylation of 4EBP1 following rapamycin treatment (1µM) after overnight serum starvation, relative band intensity of phospho-4EBP1normalized to total 4EBP1. C-control, no treatment, R-rapamycin.

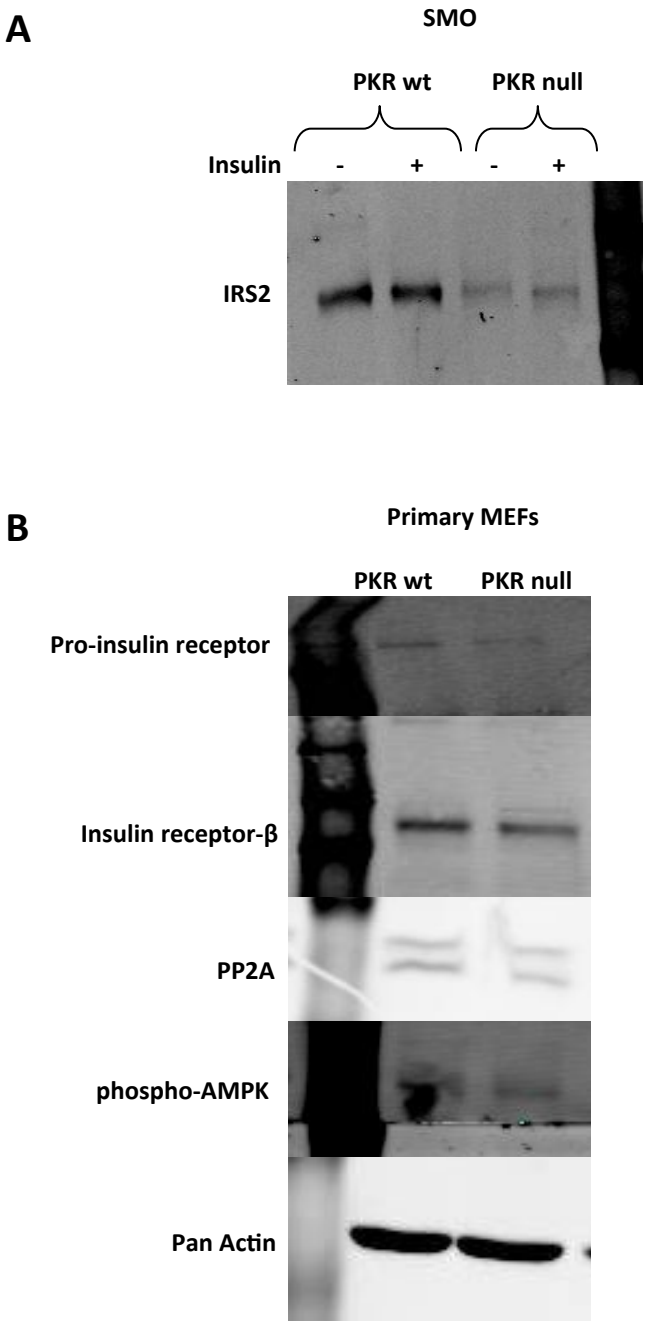

Appendix VI. Western blot analysis of the insulin signalling cascade.

Western blot analysis of **A** SMO and MEF cell lysates for IRS2 protein expression following insulin treatment and **B** unstimulated primary MEF cell lysates.

APPENDIX VII
GENOTYPING OF CELL LINES

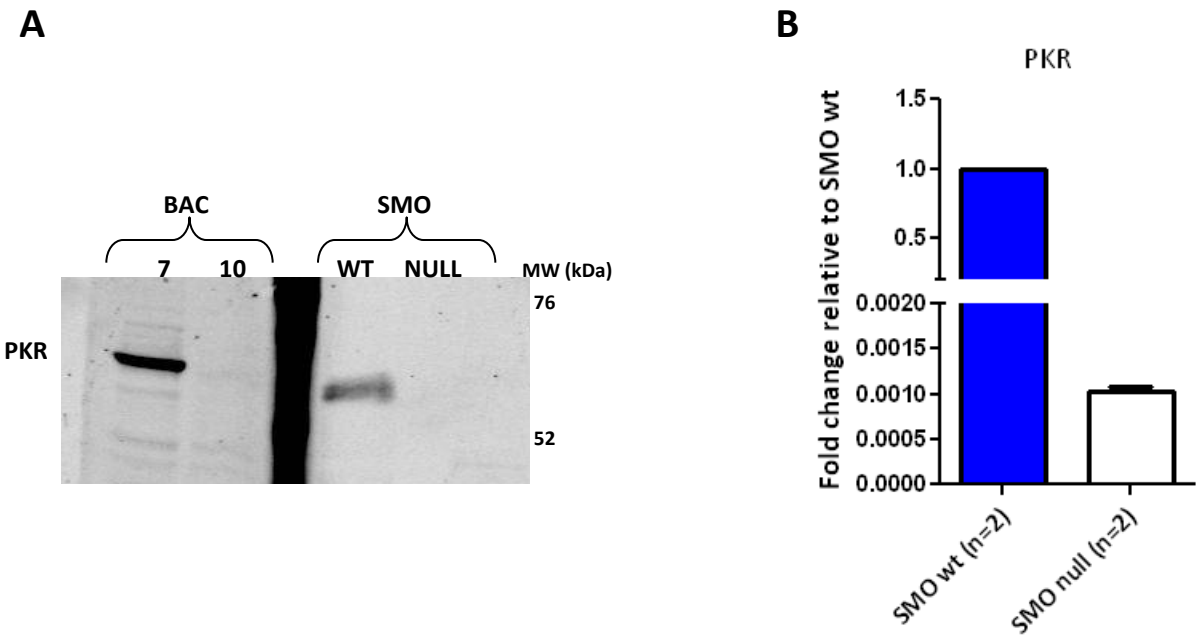

Appendix VII. Genotyping of cell lines.

A Western blot analysis of cell lysates collected from PKR wt and knockout spleen macrophages and MEFs. Probed with PKR B10 antibody. **B** RNA extracted from spleen macrophages of PKR wt (n=2) and PKR knockout (n=2) mice fed a high fat diet for 10 weeks. Expression levels of PKR were analysed by QRT-PCR and expressed as fold change relative to PKR wt. Expression of target genes was compared to the internal control RPL30.

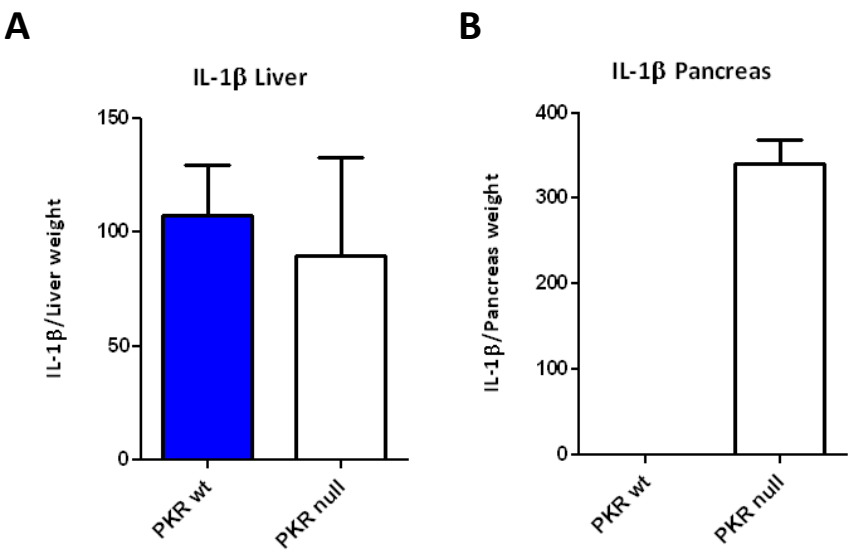

Appendix VIII. Secretion of IL-1β from *in vivo* tissue culture.

Concentration of IL-1β protein secreted from **A** liver and **B** pancreas of PKR wt (n=2) and PKR null (n=2) mice fed a high fat diet for 5 weeks. Protein levels of IL-1β are normalised to weight of tissue.

APPENDIX IX
INFLAMMASOME ACTIVATION IN SMO CELL LINES

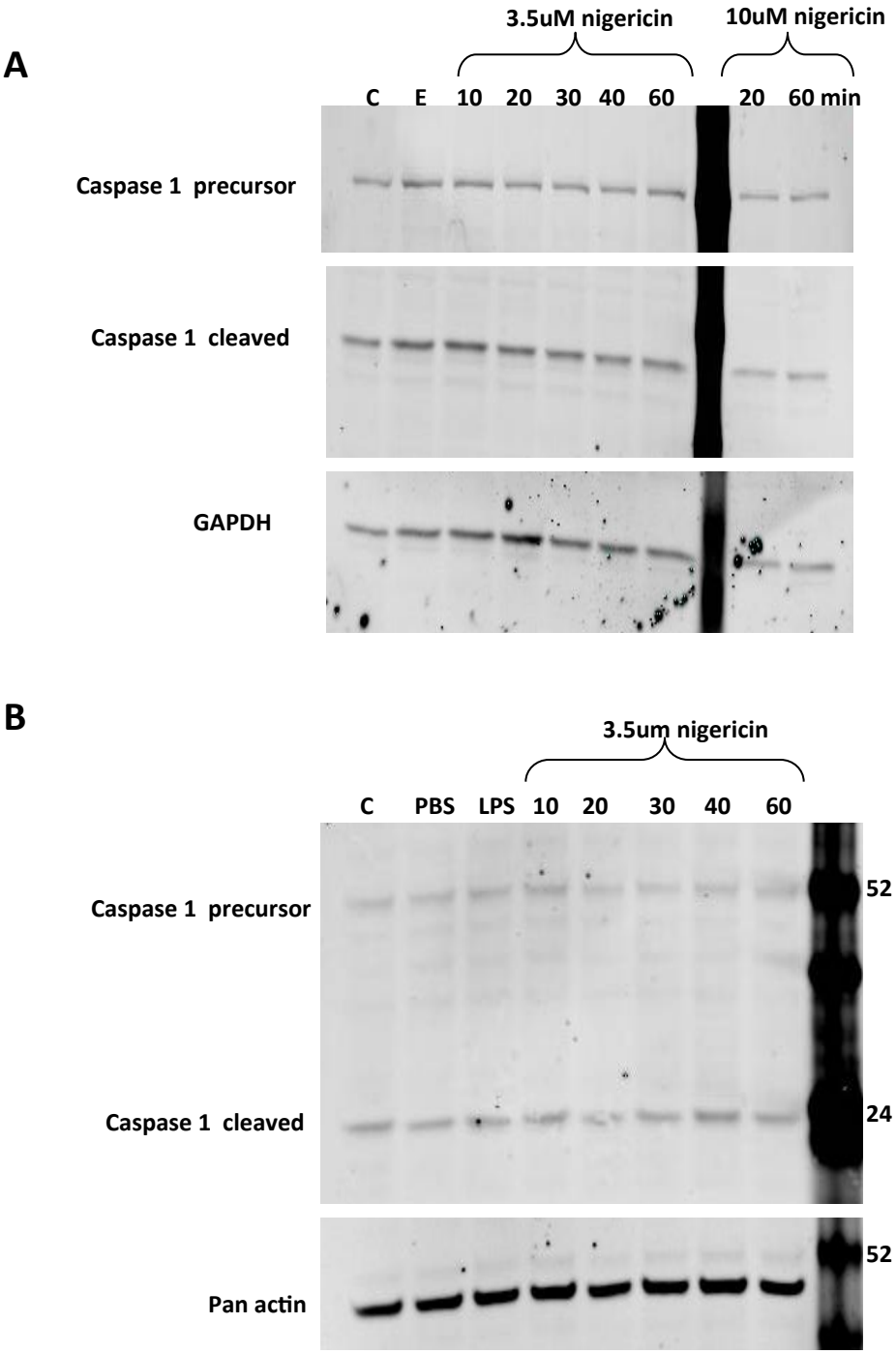

Appendix IX. Inflammasome activation in SMO cells.

Western blot analysis of caspase-1 cleavage **A** in serum starved smo wt treated with 3.5 um or 10um of nigericin for specified amount of time and **B** in serum starved WT SMO cells primed with 10ng/ml LPS followed by 3.5uM nigericin for specified amount of time.

APPENDIX X
INFLAMMASOME ACTIVATION IN RAW CELL LINES

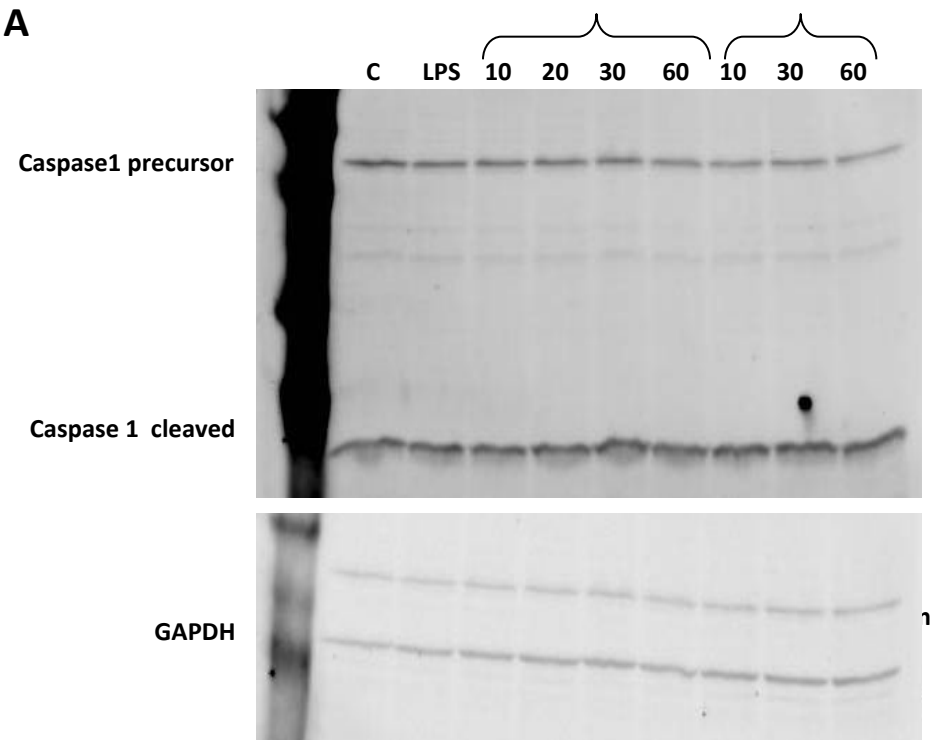

Appendix X. Inflammasome activation in RAW cells.

Western blot analysis of caspase-1 cleavage in serum starved RAW cells, primed with 10ng/ml LPS for 2 hours followed by treatment with nigericin 3.5um or 10um for specified amount of time .

APPENDIX XI
INFLAMMASOME ACTIVATION IN RAW CELL LINES

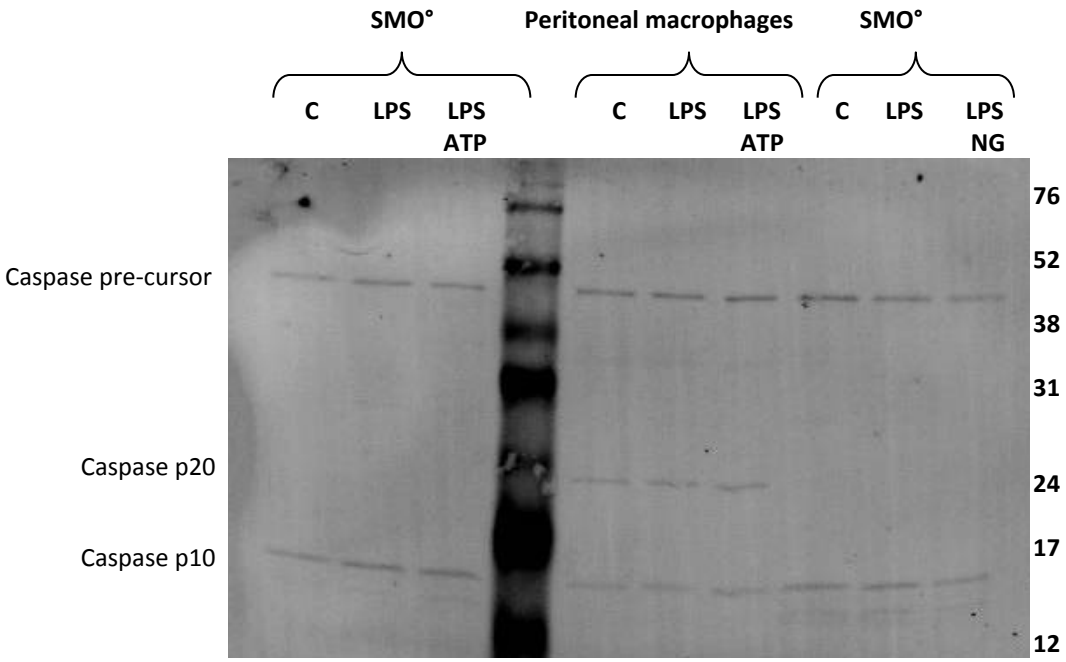

Appendix XI. Inflammasome activation in RAW cells.

Western blot analysis of caspase-1 cleavage in primary spleen macrophage and peritoneal macrophage cells, primed with 1mg/ml LPS for 4 hours followed by treatment with 1mM ATP or 3.5uMnigericin for 15 minutes.

Appendix XII. High fat and chow diet composition

The specification sheets for the high fat 'atherogenic' diet and the chow diet were obtained from the specialty feeds website www.specialtyfeeds.com.

JOURNAL OF INTERFERON & CYTOKINE RESEARCH
Volume 31, Number 1, 2011

DOI: 10.1089/jir.2010.0099

The Role of Protein Kinase R in the Interferon Response

Agnieszka Pindel and Anthony Sadler

The effects of interferons (IFNs) are mediated through the induction of around 2,000 IFN-stimulated gene (ISG) products. However, the majority of these ISGs do not directly instigate IFN-mediated states, such as the defining resistance to viral infection. Rather, most ISGs encode cell signaling molecules that enhance the responsiveness to pathogens, and systemically disseminate signals from localized sites of infection. Relatively few IFN effector proteins have been well characterized. The protein kinase R (PKR) is one of the first and best characterized of these effector molecules. PKR mediates responses via phosphorylation of protein substrates and promotes signal transduction pathways to maintain homeostasis, mediate immune responses, and, upon sustained activation, promote apoptosis. As a number of reviews have dealt with PKR-dependent resistance to virus, this review will cover broader roles ascribed to PKR and the mechanism(s) by which PKR exerts its effects.

Introduction

Protein kinase R (PKR) belongs to the eukaryotic initiation factor 2α (eIF2α) phosphorylating family of kinases. The other members of this family in mammals are the haem-regulated inhibitor (HRI), PKR-like endoplasmic reticulum kinase (PERK), and the general control nonderepressible-2 (GCN2) protein (Proud 2005). The members of this protein family are constitutively expressed, but their activity is repressed by inhibitory ligands, with haem and chaperone proteins inhibiting HRI and PERK, respectively, or through autoinhibition, for GCN2 and PKR. Relief of inhibition and subsequent activation occurs by intradomain movement that allows binding of ATP and subsequent autophosphorylation to form a competent dimeric kinase. Relief of inhibition of each kinase is either by disassociation of inhibitory ligands, for HRI and PERK, or displacement of inhibitory domains by binding of activators, for GCN2 and PKR. Each kinase is activated by distinct signals: low haem levels for HRI, accumulation of unfolded proteins in the endoplasmic reticulum for PERK, accumulation of uncharged transfer RNA for GCN2, and double-stranded RNA (dsRNA) for PKR. In addition to these specific activating ligands that enable coordination of distinct stimuli in the cell, each kinase has been found to respond to broader stress responses such that there is a degree of redundancy between the family members. PKR is the only member of the eIF2α kinase family that is induced by interferon (IFN), accenting its part in the immune response.

PKR's Induction and Response to IFN

The *eif2ak2* gene, which encodes PKR, is constitutively expressed in all differentiated tissues at low levels, and then further induced by a variety of stress-associated responses (Ank and others 2006). Expression of *eif2ak2* is coordinately regulated by an IFN-stimulated response element (ISRE), a kinase-conserved sequence (KCS), as well as the transcription factors Sp-1 and -3, and the tumor suppressor protein p53 (Fig. 1) (Kuhen and Samuel 1997, 1999; Ward and Samuel 2002, 2003; Das and others 2004, 2006; Yoon and others 2009). Putative roles for Ets, Myb, myogenic differentiation antigen (MyoD), E2F, and the nuclear factor-κB (NF-κB) have also been proposed based upon identification of regulatory elements for these transcription factors in the gene promoter (Tanaka and Samuel 1994). In addition, an IFN-γ activation site-like element has been identified in the promoters of the human and mouse *eif2ak2* gene, although this element does not appear to be functional (Tanaka and Samuel 1994, 2000; Xu and Williams 1998).

PKR expression is also regulated post-transcriptionally. At heightened protein levels, activated PKR autoregulates expression of its own mRNA via the inhibition of global translational initiation (Thomis and Samuel 1992). As was identified by Garaigorta and Chisari (2009) this mechanism is applicable to other IFN-stimulated genes (ISGs) (Garaigorta and Chisari 2009). This apparent paradox, in which IFN-induced PKR represses ISG translation, occurs in cells with activated PKR, while cells in which PKR is inactive remain permissive to translation of ISGs. In this way, PKR tailors the IFN response, so that it can be partitioned to elevate immune surveillance in uninfected cells but is constrained in cells already infected. The significance of this PKR-dependent adaptation of the IFN response is largely unexplored but is likely to have considerable significance. In light of this conjecture, it would be interesting to know if any of the ISGs

Centre for Cancer Research, Monash Institute of Medical Research, Monash University, Melbourne, Australia.

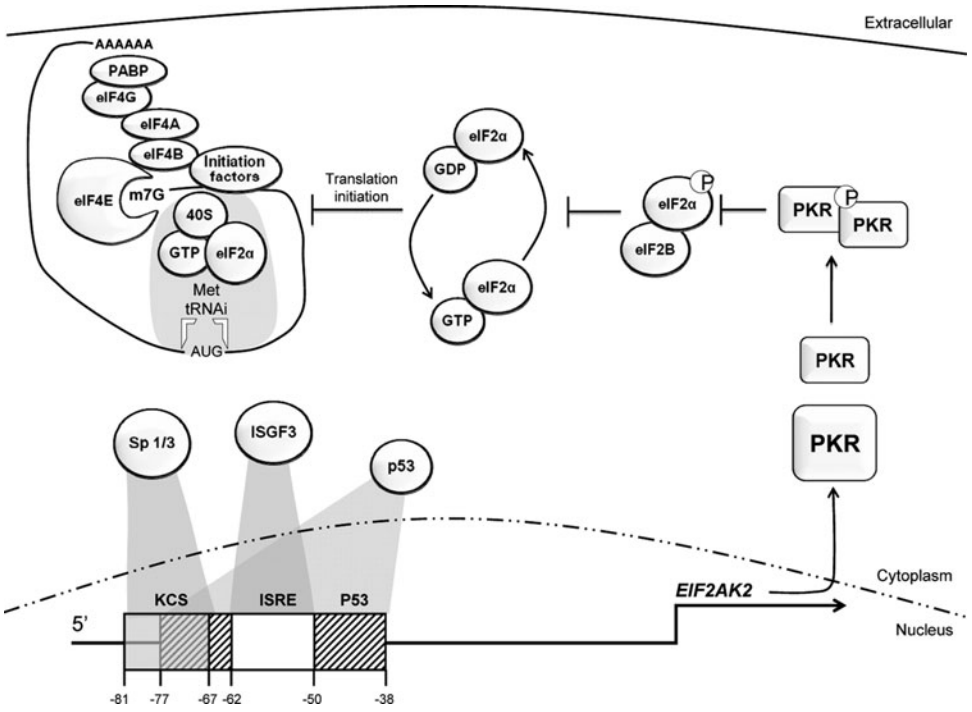

FIG. 1. Transcriptional regulation of the human *eif2ak2* gene and subsequent translational control. Transcription factor-binding sites in the 5′-untranslated regions of the *eif2ak2* gene include the KCS (shown as a gray box), ISRE (white box), and p53 (patterned box) responsive elements. The p53 responsive element is split by the ISRE, and overlaps with the KCS element. The Sp-1 and -3, ISGF-3, and p53 transcription factors bind to the KCS, ISRE, and p53, respectively, for constitutive expression and subsequent induction of the *eif2ak2* gene. Induced PKR must then be activated before it phosphorylates eIF2α to impose global translation regulation. Phosphorylated eIF2α sequesters the guanine nucleotide exchange factor, eIF2B. This inhibits replacement of the inactive eIF2-GDP with eIF2-GTP to enable formation of an active 43S preinitiation complex and subsequent recruitment to the mRNA via eIF4 factors that are attached to the mRNA cap structure (m^7G). eIF2α, eukaryotic initiation factor 2α; IFN, interferon; ISRE, IFN-stimulated response element; ISGF-3, IFN-stimulated gene factor 3; KCS, kinase conserved sequence; PKR, protein kinase R.

contain structures in their 5′-untranslated regions (UTRs) that permit escape from PKR-dependent translational control.

The identification of PKR as a p53-regulated gene was significant for our understanding of PKR expression (Yoon and others 2009). It was demonstrated that p53 directly induces the *eif2ak2* promoter via a response element that is split by the ISRE (Fig. 1). Accordingly, PKR was shown to play a role in p53-mediated inhibition of translation, apoptosis, and tumor growth by phosphorylation of eIF2α in response to DNA damage (Yoon and others 2009). The IFN response has subsequently been demonstrated to be modulated by p53 regulation of the IFN-regulated factor-9 (IRF-9) (Munoz-Fontela and others 2008). Moreover, p53 itself is an ISG (Takaoka and others 2003). This supports previous studies that demonstrate a role for IFNs in growth control and apoptosis. Not only does p53 induce *eif2ak2* expression, but it has also been shown to associate with PKR. Pull-down experiments using glutathione S-transferase fusion proteins demonstrated that p53 associates with PKR through its C-terminal domain. Additionally, it is proposed that PKR phosphorylates p53 at serine residue 392 (Cuddihy and others 1999). Together, these observations describe partly redundant functions for p53, PKR, and the IFN response that may account for the previous inability to confirm an anticipated role of PKR as a tumor suppressor, as will be discussed later.

Activation of PKR by dsRNA

As stated, PKR is constitutively expressed but is not functional until activated. A variety of activating stimuli have been characterized. The classical activator of PKR is dsRNA. The mechanism by which dsRNA activates PKR has been extensively covered by others, so it will not be discussed here in detail. Briefly, dsRNA is cooperatively bound by tandem RNA-binding motifs (RBMs) at the N-terminus of PKR. Binding of RNA relieves steric inhibition of the kinase domain. Although there is excellent data supporting regulation by autoinhibition, this is challenged by some who contend the sole role of the RBMs is to colocalize PKR monomers to a dsRNA molecule (reviewed by Cole 2007). Colocalization of PKR monomers enables transautophosphorylation to stabilize the active dimeric enzyme (Cosentino and others 1995; Nanduri and others 2000; Vattem and others 2001; Sadler and Williams 2007). In keeping with this model, it had been established that activating RNA must be double stranded and of a minimum length (30 bp) to accommodate 2 PKR monomers (Manche and others 1992). This convention was overturned by Nallagatla and others (2007), who showed that RNAs with limited duplexed regions could activate PKR if these molecules contained a 5′-triphosphate moiety. This feature distinguishes host-capped mRNAs from viral uncapped RNAs. Significantly, PKR could only be activated by 5′-triphosphate-RNAs when

induced by IFNs. This may be due to elevated levels of PKR obviating the requirement for colocalization. Alternatively, PKR activated in this manner may be functionally different, as has been shown for PKR activated by select other processes (as will be discussed below). This modification of the faculty of PKR to detect alternative forms of viral RNA is a remarkable feature of the IFN response.

In addition to activation by viral RNAs, endogenous transcripts can activate PKR. The best characterized instance of this is the IFN-γ mRNA (Osman and others 1999; Ben-Asouli and others 2002). It has been demonstrated that PKR binds to a pseudoknot structure in the gene's 5′UTR, which subsequently activates PKR to then inhibit translation of the transcript via phosphorylation of eIF2α. PKR only binds to the pseudoknot structure at induced levels due to competitive exclusion by the ribosome. Hence, this delineates a mechanism by which type I IFNs regulate the production of toxic gene products. Also, this mechanism may provide an explanation for the observed suppression of IFN-γ by IFN-α/-β (Rayamajhi and others 2010).

Activation of PKR by Polyanionic Molecules

PKR is activated by the polyanionic molecules dextran sulfate, chondroitin sulfate, poly L-glutamine, and heparin (Hovanessian and Galabru 1987; Bergeron and others 2000). No general mechanism accounts for the activation of PKR by polyanionic molecules. It might be assumed that, like charged RNA, polyanionic molecules would bind the protein's RBMs. However, at least for heparin, this is not the case (George and others 1996; Fasciano and others 2005). In contrast to dsRNA, PKR activated by heparin is reported to function as a monomer. Heparin binding, within the kinase domain, likely sterically blocks interdomain interactions. This atypical form of the active enzyme still binds and phosphorylates eIF2α.

Activation of PKR by heparin is intriguing. The distribution of heparin in the body is restricted largely to secretory basophil and mast cells. Consequently, it is believed to function in wound and antimicrobial responses. Therefore, heparin-mediated effects would seem to indicate a PKR-dependent immune function in the skin, mucosa of the lungs, gut, mouth, nose, and eyes. Little has been done to gauge the function of PKR in mucosal immunity. The closely related proteoglycan heparin sulfate has a broader expression than heparin, occurring on the surface of most, if not all, cells as well as extracellularly. Accordingly, heparin sulfate has been purported to have a wide variety of biological activities. It has been identified as a receptor for some viruses (Spear and others 1992; Hallak and others 2000a, 2000b). Intracytoplasmic heparin sulfate could indicate viral entry into a cell, and might present an early warning to the innate immune system. Therefore, it would be interesting to test if PKR is also activated by heparin sulfate and if this is relevant to PKR's established role in the antiviral response.

Activation of PKR by Caspases

Activation of PKR by caspases involves proteolytic cleavage of PKR at asparagine residue 251 by the apoptotic initiator caspase-8 and effectors caspase-3 and -7 (Saelens and others 2001). Removal of the autoinhibitory N-terminus of PKR by caspase cleavage generates a constitutively active kinase. As with heparin activation, the cleaved kinase is described to function as a monomer (Wu and Kaufman 2004). However, it is not clear what would prevent the truncated PKR from dimerizing. PKR monomers associate via residues in the kinase domain, which are present in the truncated protein. Similar truncated kinase constructs have been demonstrated to dimerize (Dey and others 2005). Presumably, the removal of the RBM prevents colocalization of PKR monomers. It seems possible that the truncated PKR protein might dimerize at higher concentrations during, for instance, induction with IFNs.

The promoter of the gene encoding caspase-8 has been shown to contain an ISRE and so is induced as part of the type I IFN response (Casciano and others 2004; De Ambrosis and others 2007). Caspase-8 has been demonstrated to be part of the innate immune response to virus and dsRNA. Moreover, mouse embryonic fibroblasts that are null for caspase-8 have an attenuated inflammatory response (Takahashi and others 2006). Hence, the IFN regulation of caspase-8 parallels the nucleotide-binding oligomerization domain-like receptor induction of caspase-1 and -5 and assembly of inflammasomes.

PKR's Activity

Once activated PKR has 2 roles: first, to directly affect protein function by phosphorylation; second, to activate transcription factors by modulating cellular signaling networks. It has been established that, at least in the instance of NF-κB activation, PKR functions in signaling pathways as an adaptor protein, without phosphorylating substrates.

As a kinase, PKR phosphorylates serine and threonine residues in protein substrates (Table 1). It has also been reported that PKR phosphorylates tyrosine residues (Su and others 2006). Moreover, it is claimed that autophosphorylation of tyrosines is essential for RNA-binding and subsequent kinase activity (Su and others 2006). Structures of PKR's kinase domain may provide support for this (Dar and others 2005). The structure of the kinase domain shows that the sub-element of the activation segment, termed the $p+1$ loop, adopts a conformation that is intermediary between that expected of serine/threonine and tyrosine kinases. However, the autophosphorylated tyrosine residues identified as being essential for PKR's activity are either in regions that are not previously associated with activity (Y101, Y162), or that would appear to disrupt catalytic function (Y293). Also, autophosphorylation is triggered after binding of dsRNA, and so the claimed requirement for phosphorylation of tyrosine residues within the N-terminus of PKR to enable dsRNA binding seems unlikely. Rather, phosphorylation within the RBMs is more consistent with ejection of dsRNA after activation (Jammi and Beal 2001).

No substrate motif has been recognized that dictates PKR phosphorylation specificity. Although no definitive sequence is apparent, there may be a bias in the residues encoded at phosphorylated sites (Table 1). This speculative bias shows a preference for lysine and arginine residues proximal to phosphorylated amino acids. Analysis of kinase substrate preference, using short randomly assorted peptides from yeast, showed that another eIF2α kinase, GCN2, has low specificity but clustered, by weak association, with kinases that had a preference for arginine residues proximal to the phosphophorylated serine/threonine (Mok and others 2010). A qualification to the low specificity for short peptide substrates demonstrated for GCN2, and extrapolated for PKR, is that a crystal structure of PKR's kinase domain in

Table 1. Protein Substrates of Protein Kinase R

Substrate	*Region phosphorylated*	*Residue*
eIF2α	L S E L **S** R R R I	S51
B56α	D G F T R K **S** V R K A Q R	S28
ILF-3	L G M D P L P S K M P K K P K N E N P V D Y T V Q I P P S T T Y A I T P M K R P M E E K S P S K K K K K K I Q	Unknown
RHA	Residues 1–263	Unknown
PKR	F Q V I I **T** F Q V I I	S33
PKR	E K K A V **S** P L L L **T T** T N **S S** E G L **S** M G N	S83, S88, S89, S92, S93, S97
PKR	R K A K R **S** L A P R F	S242
PKR	P D M K E **T** K Y **T** V D K R	T255, T258
PKR	D Y D P E **T S** D D S L E **S** S D Y D P E N **S** K N **S** S R **S** K **T** K C L F I	T336, S337, S343, S354, S357, T359
PKR	N D G K R **T** R S K G **T** L R Y M S	T446, T451
PKR[a]	A A K L A **Y** L Q I L S	Y162
PKR[a]	L S M G N **Y** I G L I N	Y101
PKR[a]	I D G K T **Y** V I K R V	Y293
P53[a]	K K L M F K T E G P D **S** D	S392
MKK6[a]	Unknown	Unknown
IRS-1[a,b]	Mouse: S I T A T **S** P A S M V Human: R R S R T E S I T A T S P	S307
HIV TAT[a]	A H Q N **S** Q **T** H Q A **S** L S K Q	S62, T64, S68

Reported serine (S), threonine (T), and tyrosine (Y) residues phosphorylated by PKR in protein substrates (indicated by bold and underlined text).

[a]Conditions for an *in vitro* kinase assay for PKR were established that recommended the inclusion of manganese in the reaction buffer (Galabru and Hovanessian 1987). As we have observed a consequence of manganese for kinase specificity, we have indicated PKR substrates identified without manganese in the buffer.

[b]The serine residue 307 within IRS-1 was not validated as a PKR phosphorylation site but is assumed from Western blot analysis of mouse cell lysates.

Citations for PKR's peptide substrates are Romano and others 1998, Taylor and others 1996, Zhang and others 2001, MKK6 Silva and others 2004 and HIV TAT Endo-Munoz and others 2005. Citations for others substrates are listed in the text.

eIF2α, eukaryotic initiation factor 2α; ILF-3, interleukin factor-3; IRS-1, insulin receptor substrate-1; MKK6, mitogen-activated protein kinase kinase 6; PKR, protein kinase R; RHA, RNA helicase A.

association with eIF2α shows specificity is mediated by protein contacts outside of the catalytically active pocket of the enzyme. Hence, although there may be little specificity, for short peptides, substrate specificity is increased by restricting access to the catalytic pocket of PKR (Dar and others 2005).

Phosphorylational Control of eIF2α

The best-characterized substrate of PKR is eIF2α. Through this activity PKR controls translation. The mechanism of this translational control is well established, so this will be only briefly covered here (Fig. 1). However, many mRNAs have evolved mechanisms that allow them to escape this translational repression through features encoded in their 5′UTR regions, such as internal-ribosomal entry sites and multiple upstream open reading frames (Petryshyn and others 1996; Wek and others 2006). Transcripts regulated in this manner assuage stress responses. In addition, a number of transcripts that are resistant to this translational repression, such as the CCAAT/enhancer binding protein-α and -β, mediate cellular differentiation (Calkhoven and others 2000). PKR has been ascribed a role in cellular differentiation (Salzberg and others 1995). Appropriately, PKR is not expressed in undifferentiated cells, but its expression increases as cells differentiate (Wang and others 2002). However, as PKR-null mice do not have developmental defects, there cannot be a strong dependence on PKR for cellular differentiation.

It had previously been demonstrated that defects in the regulation of eIF2α by phosphorylation caused malignant transformation (Donze and others 1995; Perkins and Barber 2004). Hence it was presumed that PKR would act as a tumor suppressor. Although this was supported by data showing that expression of kinase-dead PKR in NIH-3T3 cells results in malignant transformation, mice lacking PKR do not develop tumors at an increased rate (Chong and others 1992; Koromilas and others 1992; Meurs and others 1993; Yang and others 1995; Abraham and others 1999). An explanation for this variance in PKR-dependent effects, in cell lines compared to *in vivo*, has been attributed to IFN-priming in murine models. The regulatory network identified between IFN, p53, and PKR suggests that each gene may partially compensate for each other in this network. Correspondingly, Yoon and others (2009) demonstrated, using a tumor xenograft model in nude mice, that deletion of p53 with simultaneous knockdown of PKR promoted tumor development.

PKR has subsequently been shown to participate in the activity of one of the most commonly mutated tumor suppressive genes, the phosphatase and tensin homolog deleted from chromosome 10 (PTEN). Mutations of PTEN have been identified in a large fraction of tumors, notably prostate cancers and glioblastomas. Mounir and others (2009) demonstrated that cell lines expressing PTEN showed enhanced PKR and eIF2α phosphorylation and impaired colony formation. Consequently, the antiproliferative and pro-apototic effects of PTEN were reduced in cells ablated for PKR.

Phosphorylation of B56α

PKR was shown to physically interact with the B56α regulatory subunit of the phosphatase 2A (PP2A) proteins. PP2A

consists of a family of heterotrimeric enzymes, composed of a structural and catalytic subunit, which associates with one of several regulatory B subunits. PP2A is the major serine and threonine phosphatase in the cell and as such regulates a wide array of processes. PKR was shown to phosphorylate B56α at serine residue 28 (Xu and Williams 2000). As a result, PKR was shown to block B56α-mediated inhibition of PP2A and, thus, enhances PP2A activity. PKR was demonstrated to regulate dephosphorylation and, consequentially, the activity of the eIF4E via activity of PP2A (Joshi and others 1995; Xu and Williams 2000). In addition, PKR was shown to regulate PP2A-mediated dephosphorylation of BCL2 to mediate apoptotic processes (Ruvolo and others 2008).

PP2A regulates the activity of a range of potent kinases, such as the mammalian target of rapamycin (mTOR). The mTOR kinase pathway transduces stress signals, from mitogens, growth factors, sensors of cellular energy stasis, and the redox state of cells. This is particularly interesting in light of the recent identification of a role for PKR in obesity-related conditions (Nakamura and others 2010). This study proposed a role for PKR in regulating a diet-induced inflammatory response, predominantly through the c-jun N-terminal kinase (JNK), and by phosphorylation of the insulin receptor substrate-1. Relevant to these responses, mTOR has been demonstrated to regulate the nutrient response via insulin and has been demonstrated to phosphorylate insulin receptor substrate-1 (Ueno and others 2005; Tzatsos and Kandror 2006). A recent analysis of the protein kinase networks in yeast demonstrated interactions between the yeast PP2A regulatory subunit RTS1 and the GCN2 regulator GCN1. Further, GCN2 was linked into the TORC1 nutrient-sensing kinase network (Breitkreutz and others 2010).

Coordinate Regulation of Proteins That Encode the RBM

PKR has also been demonstrated to phosphorylate a number of proteins that share the RBM, including the RNA helicase A and interleukin factor-3 (ILF-3) (Parker and others 2001; Sadler and others 2009). A number of additional proteins with RBMs interact with PKR, but have not been shown to be substrates. These include the spermatid perinuclear RNA and transactivating (SPNR) and (TAR)-RNA binding (TRBP2) proteins, adenosine deaminase acting on RNA-1 (ADAR-1), the protein coded DRBP-120, and dihydrouridine synthase 2-like proteins (DUS2L) (Park and others 1994; Coolidge and Patton 2000; Toth and others 2006; Mittelstadt and others 2008; Wang and Samuel 2009). As is evident from this catalog, the RBM mediates protein–protein interactions. Through these interactions the activity of different proteins that encode the RBM are coordinated, predominantly by suppression of their function. In this way, the RBM acts like the caspase recruitment domain and toll/IL-1 receptor domain to mediate protein interactions to coordinate enzyme activity in protein networks. As a number of these proteins have been associated with virus replication, the interaction with PKR has a consequence for the host antiviral response (Fujii and others 2001; Isken and others 2003; Hartman and others 2006; Jeang and Yedavalli 2006; Toth and others 2006; Li and others 2010).

Activation of PKR in Cell Signaling Networks

In addition to the direct binding of activating ligands that triggers phosphorylation of protein substrates, PKR is also activated indirectly and subsequently modulates cellular signaling networks (Fig. 2).

PKR responds indirectly to IL-1, IFN-γ, tumor necrosis factor (TNF)-α, platelet-derived growth factor, as well as a variety of pathogen-associated molecules and general stress stimuli (Mundschau and Faller 1995; Yang and others 1995; Kumar and others 1997; Cheshire and others 1999; Goh and others 2000; Ramana and others 2000; Deb and others 2001; Ichikawa and others 2002; Tam and others 2007; Zheng and others 2008). Responses to these molecules are initiated via the cognate receptors: IL-1 receptor, IFN-γ receptor-1 with -2, TNF receptor (TNFR) -1 and -2, and either platelet-derived growth factor receptor-α or -β, and the innate immune toll-like receptors and retinoic acid-inducible gene (RIG)-like helicases, and by undefined pathways. Association between each ligand and the cognate receptors triggers signal transduction pathways that activate latent cytoplasmic transcription factors. The transcription factors that have been demonstrated to be regulated by PKR are NF-κB, c-jun, the signal transducers and activators of transcription (STAT) -1 and -3, IRF-1, and the activating transcription factors (ATF) -3 and -4 (Wong and others 1997; Gil and others 2000; Deb and others 2001; Guerra and others 2006; Lee and others 2007). Of these transcription factors, only regulation of the ATFs by PKR has a clearly established mechanism. ATF-3 and -4 mRNA contain multiple upstream translational start sites. This feature of mRNAs promotes translation upon phosphorylation of eIF2α. Consequently, PKR-dependent induction of ATF-3 and -4 is via control of eIF2α. Consistent with this mechanism, the other eIF2α kinases also induce ATFs (Guerra and others 2006).

PKR-dependent activation of the other transcription factors listed above is independent of phosphorylation of eIF2α. At least in the instance of NF-κB, PKR-dependent activation appears to be independent of phosphorylation of any protein substrate. It has been shown that a kinase-dead mutant of PKR was competent to activate NF-κB (Chu and others 1999; Bonnet and others 2000; Gil and others 2000; Zamanian-Daryoush and others 2000). Activation of NF-κB requires phosphorylation and ubiquitin-dependent proteolysis of the inhibitor-κB (IκB). Under normal circumstances NF-κB exists in a latent state in the cytoplasm bound to its inhibitor IκB. Phosphorylation of IκB renders it susceptible to proteolysis via the ubiquitin-proteosome pathway, which results in the release and translocation of NF-κB to the nucleus, where it binds to DNA and induces gene transcription (Brown and others 1993; Kumar and others 1994). PKR affects NF-κB activity by association with the IκB kinase complex to regulate levels of IκB (Kumar and others 1994). A plausible mechanism for PKR's activation of NF-κB, and likely other transcription factors, has emerged that involves the protein activator of the IFN-inducible protein kinase (PACT) and TNFR-associated factors (TRAFs).

PKR's Association with TRAFs

Gil and others (2004) identified a mechanism by which PKR might mediate indirect phosphorylation and ubiquination of IκB. Human PKR was shown to encode 2 functional binding motifs for TRAF proteins. TRAFs dock with activated cell signaling complexes to then regulate the subcellular location and, as E3-ubiquitin ligases, promote the degradation of key signaling components. Seven TRAF proteins have been identified (TRAF-1 to -7). The relevant

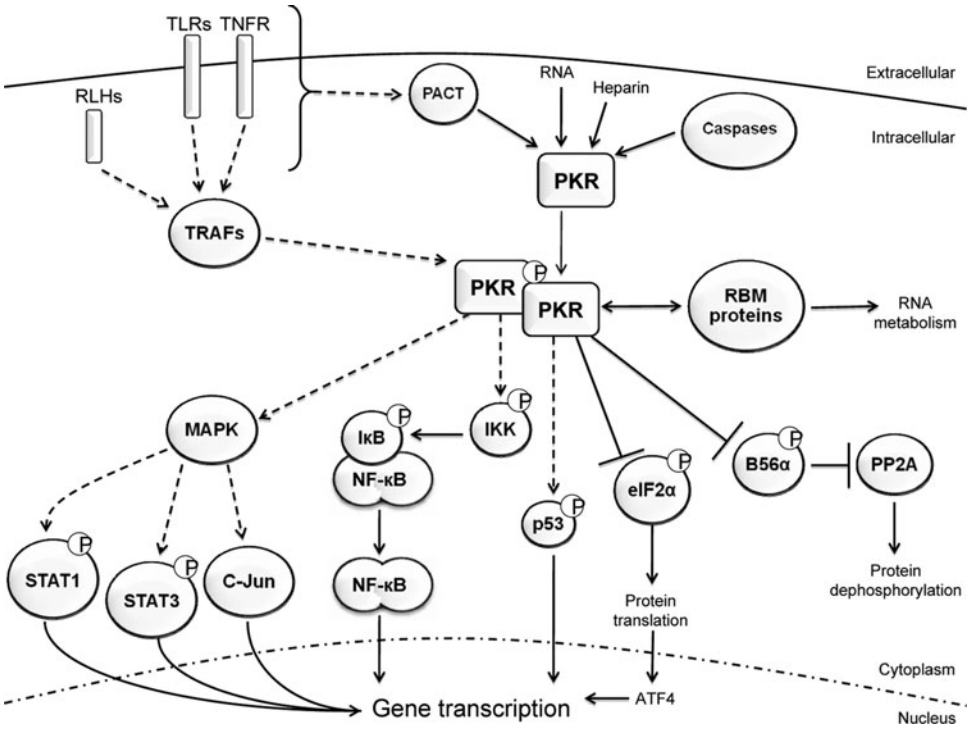

FIG. 2. Cellular activities of PKR. PKR is activated by ligand-induced dimerization and transautophosphorylation. Although it is also reported that heparin and caspase generate an active monomeric PKR. Once activated, PKR functions directly by protein phosphorylation, or indirectly by integrating signaling networks to promote the activation of transcription factors and ensuing gene induction. In this figure, direct interactions are indicated as *solid lines*, whereas indirect actions, or speculative interactions, are drawn with *dashed lines*. Although PKR has been shown to directly interact with STAT-1 and -3, the kinase does not phosphorylate these proteins. Instead, this is predicted to be mediated by the MAPK family. Therefore, PKR's effect upon STAT-1 and -3 is drawn as being via this signaling cascade. This figure is representative of PKR function and does not include all protein substrates and pathways affected by the kinase. MAPK, mitogen-activated protein kinase; STAT-1, signal transducers and activators of transcription.

residues in PKR, within the N-terminus (TKQE) and kinase domain (PEQIS) of human PKR, appear most similar to consensus motifs that bind TRAF-2 and -3. Correspondingly, PKR was shown to associate with TRAF-2 and also with TRAF-5 and -6. The consensus binding motif for TRAF-6 (KXXPXE) is different from those identified in PKR. However, the various TRAF proteins associate with each other through their TRAF domains. TRAF-2 has been demonstrated to interact with TRAF-6 (Davies and others 2005). Similarly, TRAF-3 interacts with TRAF-5 (Pullen and others 1998). Hence the observed interactions with TRAF-5 and -6 may be indirect. Characterization of truncated constructs of PKR showed that the kinase domain binds TRAF proteins to a greater extent than the N-terminus of PKR. However, a challenge to the consequence of the C-terminal TRAF-binding motif in human PKR is that this motif is not conserved in the mouse kinase. As the same signaling pathways function in mice, the altered motif (PEQLF) may still bind TRAFs, a different TRAF-binding may exist (none is apparent), or this association is mediated by the motif at the N-terminus.

Contrary to the mouse PKR, the C-terminal TRAF-binding motif is otherwise generally preserved (occurring in PKR from rat, pig, cow, and hamster). Indeed, the residues within this region of PKR are highly conserved as they encode part of the activation segment of the kinase domain, which regulates catalytic function of the kinase. The consensus residue in the TRAF-binding motif overlaps with residues that define a feature termed the $p+1$ loop within the activating segment. This feature acts as a phospho-acceptor during substrate phosphorylation. Despite the required functional conservation of this feature, the TRAF-binding motif in PKR's kinase domain does not occur in the other eIF2α kinases.

The TRAF-binding motif at PKR's N-terminus occurs at the C-terminal end of the second RBM. The equivalent amino acids are conserved within PKR from different species (including human, mouse, rat, hamster, cat, pig, and cow). However, the motif does not occur in PKR's first RBM, or on RBMs from other human proteins (including TRBP2, PACT, DiGeorge syndrome critical region 8, Dicer, ADAR-1, -2, -3, ILF-3, and SPNR). Amino acid residues on either side of the TRAF-binding motif in RBM-2 (96 to 118 and 162 to 171) interact with the kinase domain (within residues 328 to 335) to instigate autoinhibition (Gelev and others 2006; Li and others 2006). Binding of dsRNA relieves autoinhibition. Indeed, the equivalent location in RBMs from other proteins that constitute the RBM-2 TRAF-binding motif in PKR have been demonstrated to mediate hydrogen bonding to nucleotides in the major groove of dsRNA (Ryter and Schultz 1998). As the association between RBM-2 and the kinase domain is mediated by residues close to both TRAF-binding motifs, it predicts that autoinhibition would prevent an association with TRAFs. Accordingly, it was shown that PKR interacted with TRAFs only after activation.

There is an interesting consequence to this conjecture. The kinase-dead PKR, with a point mutant at the lysine residue 296, is still able to activate NF-κB. This would appear to contradict data that showed PKR had to be activated to interact with TRAFs. However, this mutation (K296R) disrupts the interaction between RBM-2 and the kinase domain. Hence, the TRAF-binding motifs in the kinase-dead PKR would be exposed and able to constitutively interact with TRAFs. Therefore, the functionality of kinase-dead PKR as a signaling molecule may be an artefact of the protein's altered shape.

TRAFs play a major role in signal transduction downstream of pattern recognition receptors. Significantly, the consensus TRAF motif recognized in PKR has been associated with signals triggered by toll-like receptors and RIG-like helicases that then recruit TRAFs to activate NF-κB, via TRAF-2 and -6 (Takada and others 2007; Yamashita and others 2008; Sondarva and others 2010). Consequently, the association between PKR and TRAFs correlates with the observed responsiveness of PKR (Horng and others 2001; Hsu and others 2004; Kalali and others 2008; Zhang and Samuel 2008; Zhang and others 2009). Experiments reported by Takada and others (2007) exploring TNF-α activation of NF-κB corroborated this association with TRAFs in PKR-dependent signaling. A defect in NF-κB activation in PKR-null cells could be rescued by expressing p65, IκB kinase-β, or the NF-κB-inducing kinase, but not TRAF-2, TNFR-1-associated protein, or TNF-α. This delineates the point within the network at which PKR functions as the recruiter of TRAFs to the signaling complexes.

TRAF-2, -3, and -6 have also been shown to trigger activation of JNK and p38 (Dadgostar and others 2003). Hence, PKR's association with TRAFs could also be evoked as a mechanism by which the kinase regulates these 2 mitogen-activated protein kinases (MAPK) (Goh and others 2000; Iordanov and others 2000; Silva and others 2004).

Perturbation of the MAPK cascade also partly accounts for the PKR-dependent effects toward STAT proteins. There is a defect in activation of STAT-1 and -3 in PKR-null cells (Deb and others 2001; Lee and others 2005). Dimerization of STATs is partially instigated through tyrosine phosphorylation of the proteins by the janus kinases. Full transcriptional activity also requires serine phosphorylation at residue 727, at least for human STAT-1 and -3. Although, significantly, serine phosphorylation is not required for transcriptional activity of the ISG factor-3. The identification of the serine kinase has not been confirmed, but the phosphorylated motif (PMSP) in STAT-1 is characteristic of a phosphorylation site for MAPKs, particularly JNK, p38, and extracellular signal-regulated kinase.

Activation of PKR by PACT

It is generally accepted that the PKR-dependent response to stress stimuli that include the sphingolipid ceramide, arsenite, thapsigargin, and hydrogen peroxide is mediated by PACT (also called RAX in mice) (Ito and others 1999; Ruvolo and others 2001). As well as responding to general stress, it is also claimed that PACT mediates many other PKR-dependent activities. PKR-mediated activation of NF-κB, IRF-1, and STAT-1 are reportedly all attenuated in cells in which PACT is knocked down by RNA interference, or that express a mutant PACT that does not activate PKR (Bennett and others 2006). A requirement for PACT in the activation of these transcription factors may not be at odds with signaling mediated by TRAFs. PACT could provide the activating signal that then enables PKR to associate with TRAFs to trigger subsequent activation of the various transcription factors.

PACT encodes 3 RBMs that mediate the interaction with PKR (Patel and Sen 1998; Peters and others 2001; Huang and others 2002). Although PACT encodes 3 RBMs and binds dsRNA, it can activate PKR independently of dsRNA (Patel and Sen 1998; Peters and others 2001). Stress signals result in phosphorylation of PACT (at serine residue 18), followed by its interaction with PKR (Bennett and others 2004). The kinase that phosphorylates PACT has not been identified. Residues around the phosphorylated serine (REDSGTF) form a putative phosphorylation motif for the MAPK family (Blom and others 1999; Xue and others 2008).

The biological significance of PACT-mediated regulation of PKR is not entirely clear, as different transgenic mutant PACT mice have been reported that have markedly different phenotypes (Rowe and others 2006; Bennett and others 2008; Peters and others 2009). In one instance a PACT-null mouse is viable but has developmental defects (Rowe and others 2006). Subsequently, a second heterozygous PACT mutant was reported that was embryonically lethal in homozygous PACT-null mice (Bennett and others 2008). This same group knocked out the equivalent gene in *Drosophila* (dRAX). Flies homozygous for the mutant allele were viable but died prematurely and had a number of additional defects. These mutant flies demonstrated neurological defects and had impaired locomotion. This phenotype mimics the dystonia and gait abnormalities observed in humans with mutations in the gene encoding PACT (Camargos and others 2008). In any case, these observed phenotypes are not seen in the PKR-null mice, so it raises the question of how these effects are mediated. Generation of PACT and PKR double-knockout mice is required to elucidate the role of each protein in this interaction.

Future Perspectives

PKR is unique among the eIF2α kinases as it is induced by IFNs and plays a more significant role in immune responses as a cell signaling molecule. In this capacity PKR has been categorized to promote inflammation. However, the emphasis to date has been on deciphering PKR's role as an antiviral protein. Viral infection models induce an acute stress event where viral RNAs directly activate PKR. It is now clear that PKR can be activated by other more general stress stimuli. Hence, PKR is likely to play a role in diseases that have chronic stress stimuli. Correspondingly, a recent study has shown that PKR influences obesity-related conditions (Nakamura and others 2010). This study suggests that PKR promotes inflammation caused by diet, thereby compounding metabolic disease. This is consistent with considerable *in vitro* cell-based studies but far more limited *in vivo* experiments that have assessed PKR-dependent responses to pathogen-associated molecules and inflammatory cytokines. Pertinently, the transcription factors activated by PKR do not exclusively promote inflammation. It has been demonstrated that PKR induces the anti-inflammatory IL-10 via activation of NF-κB (Cheung and others 2005; Chakrabarti and others 2008). Further, it has been demonstrated that, at least *in vitro*, expression of the potent inflammatory cytokines TNF-α and

IFN-γ is limited by PKR. Also, other functions of PKR are inconsistent with a narrow role in advancing inflammation. PKR-dependent phosphorylation of eIF2α is generally perceived to be protective, rather than pro-inflammatory. In relation to obesity-mediated etiologies, the other eIF2α kinases and phosphorylation control of eIF2α itself have been demonstrated to be protective (Harding and others 2001; Guo and Cavener 2007; Oyadomari and others 2008). Therefore, it will be important to assess the *in vivo* role of PKR in different diseases that have varying inflammatory states. Similarly, the role of PKR in different cells and tissue types has not been well addressed. PKR activity is generally assessed *in vitro* using mouse embryonic fibroblast or macrophage cells. Investigation of PKR's role in other immune cells, such as mast cells, or different specialist cells or tissues requires additional analysis. The function of PKR in neurons, for instance, is of relevance given the proposition that PKR regulates diseases associated with the brain to affect the development of dementia (Hugon and others 2009). This is particularly intriguing as the brain is an immune privileged organ and so does not elicit the usual inflammatory responses.

The recent demonstration of PKR as a p53-induced gene supports a previous presumed involvement of PKR in stress-induced growth arrest. The recognition that deletion of PKR in combination with loss of the tumor suppressor p53 advanced tumorigenesis is exciting. A double-knockout murine model, in which both p53 and PKR are ablated, would be informative to test the significance of PKR in tumorigenesis, and the consequences for therapy. Similarly, the dependence of TRAFs for PKR-mediated cell signaling should be addressed with suitable knockout animal models. As the association between the different TRAF proteins complicates these experiments, this could be addressed with animal models that have targeted mutations of PKR. However, unequivocal evidence of precisely which residues are essential to mediate the different functions of PKR is still lacking. Related to this, transgenic mice that have ablated kinase activity are essential to distinguish kinase from merely scaffold functions of PKR. Similarly, a better understanding of the consequence of phosphorylation of PKR's substrates is necessary. Given the broad activity of the PP2A family of phosphatases, it would be anticipated that phosphorylation of B56α by PKR will be shown to have significant effects on the cell. This seemingly counterproductive induction of a phosphatase by a kinase requires a better understanding of the function of the PP2A proteins. Finally, although it was initially thought that much of PKR's effects were mediated through the induction of IFN, the signaling networks that PKR affects have more recently been shown to induce IFN relatively modestly. Studies that assess the activity of PKR in the IFNAR-null mouse are required to gauge the reliance upon IFN in PKR-dependent responses.

Acknowledgments

The authors are grateful to Drs. Frances Cribbin and Claire McCoy for their editorial assistance in the preparation of this article.

Author Disclosure Statement

No competing financial interests exist.

References

Abraham N, Stojdl DF, Duncan PI, Methot N, Ishii T, Dube M, Vanderhyden BC, Atkins HL, Gray DA, McBurney MW, Koromilas AE, Brown EG, Sonenberg N, Bell JC. 1999. Characterization of transgenic mice with targeted disruption of the catalytic domain of the double-stranded RNA-dependent protein kinase, PKR. J Biol Chem 274(9):5953–5962.

Ank N, West H, Bartholdy C, Eriksson K, Thomsen AR, Paludan SR. 2006. Lambda interferon (IFN-lambda), a type III IFN, is induced by viruses and IFNs and displays potent antiviral activity against select virus infections *in vivo*. J Virol 80(9): 4501–4509.

Ben-Asouli Y, Banai Y, Pel-Or Y, Shir A, Kaempfer R. 2002. Human interferon-gamma mRNA autoregulates its translation through a pseudoknot that activates the interferon-inducible protein kinase PKR. Cell 108(2):221–232.

Bennett RL, Blalock WL, Abtahi DM, Pan Y, Moyer SA, May WS. 2006. RAX, the PKR activator, sensitizes cells to inflammatory cytokines, serum withdrawal, chemotherapy, and viral infection. Blood 108(3):821–829.

Bennett RL, Blalock WL, Choi EJ, Lee YJ, Zhang Y, Zhou L, Oh SP, May WS. 2008. RAX is required for fly neuronal development and mouse embryogenesis. Mech Dev 125(9–10): 777–785.

Bennett RL, Blalock WL, May WS. 2004. Serine 18 phosphorylation of RAX, the PKR activator, is required for PKR activation and consequent translation inhibition. J Biol Chem 279(41):42687–42693.

Bergeron J, Benlimame N, Zeng-Rong N, Xiao D, Scrivens PJ, Koromilas AE, Alaoui-Jamali MA. 2000. Identification of the interferon-inducible double-stranded RNA-dependent protein kinase as a regulator of cellular response to bulky adducts. Cancer Res 60(24):6800–6804.

Blom N, Gammeltoft S, Brunak S. 1999. Sequence and structure-based prediction of eukaryotic protein phosphorylation sites. J Mol Biol 294(5):1351–1362.

Bonnet MC, Weil R, Dam E, Hovanessian AG, Meurs EF. 2000. PKR stimulates NF-kappaB irrespective of its kinase function by interacting with the IkappaB kinase complex. Mol Cell Biol 20(13):4532–4542.

Breitkreutz A, Choi H, Sharom JR, Boucher L, Neduva V, Larsen B, Lin ZY, Breitkreutz BJ, Stark C, Liu G, Ahn J, Dewar-Darch D, Reguly T, Tang X, Almeida R, Qin ZS, Pawson T, Gingras AC, Nesvizhskii AI, Tyers M. 2010. A global protein kinase and phosphatase interaction network in yeast. Science 328(5981):1043–1046.

Brown K, Park S, Kanno T, Franzoso G, Siebenlist U. 1993. Mutual regulation of the transcriptional activator NF-kappa B and its inhibitor, I kappa B-alpha. Proc Natl Acad Sci U S A 90(6):2532–2536.

Calkhoven CF, Muller C, Leutz A. 2000. Translational control of C/EBPalpha and C/EBPbeta isoform expression. Genes Dev 14(15):1920–1932.

Camargos S, Scholz S, Simon-Sanchez J, Paisan-Ruiz C, Lewis P, Hernandez D, Ding J, Gibbs JR, Cookson MR, Bras J, Guerreiro R, Oliveira CR, Lees A, Hardy J, Cardoso F, Singleton AB. 2008. DYT16, a novel young-onset dystonia-parkinsonism disorder: identification of a segregating mutation in the stress-response protein PRKRA. Lancet Neurol 7(3):207–215.

Casciano I, De Ambrosis A, Croce M, Pagnan G, Di Vinci A, Allemanni G, Banelli B, Ponzoni M, Romani M, Ferrini S. 2004. Expression of the caspase-8 gene in neuroblastoma cells is regulated through an essential interferon-sensitive response element (ISRE). Cell Death Differ 11(1):131–134.

Chakrabarti A, Sadler AJ, Kar N, Young HA, Silverman RH, Williams BR. 2008. Protein kinase R-dependent regulation of interleukin-10 in response to double-stranded RNA. J Biol Chem 283(37):25132–25139.

Cheshire JL, Williams BR, Baldwin AS, Jr. 1999. Involvement of double-stranded RNA-activated protein kinase in the synergistic activation of nuclear factor-kappaB by tumor necrosis factor-alpha and gamma-interferon in preneuronal cells. J Biol Chem 274(8):4801–4806.

Cheung BK, Lee DC, Li JC, Lau YL, Lau AS. 2005. A role for double-stranded RNA-activated protein kinase PKR in Mycobacterium-induced cytokine expression. J Immunol 175(11): 7218–7225.

Chong KL, Feng L, Schappert K, Meurs E, Donahue TF, Friesen JD, Hovanessian AG, Williams BR. 1992. Human p68 kinase exhibits growth suppression in yeast and homology to the translational regulator GCN2. EMBO J 11(4):1553–1562.

Chu WM, Ostertag D, Li ZW, Chang L, Chen Y, Hu Y, Williams B, Perrault J, Karin M. 1999. JNK2 and IKKbeta are required for activating the innate response to viral infection. Immunity 11(6):721–731.

Cole JL. 2007. Activation of PKR: an open and shut case? Trends Biochem Sci 32(2):57–62.

Coolidge CJ, Patton JG. 2000. A new double-stranded RNA-binding protein that interacts with PKR. Nucleic Acids Res 28(6):1407–1417.

Cosentino GP, Venkatesan S, Serluca FC, Green SR, Mathews MB, Sonenberg N. 1995. Double-stranded-RNA-dependent protein kinase and TAR RNA-binding protein form homo- and heterodimers *in vivo*. Proc Natl Acad Sci U S A 92(21): 9445–9449.

Cuddihy AR, Wong AH, Tam NW, Li S, Koromilas AE. 1999. The double-stranded RNA activated protein kinase PKR physically associates with the tumor suppressor p53 protein and phosphorylates human p53 on serine 392 *in vitro*. Oncogene 18(17):2690–2702.

Dadgostar H, Doyle SE, Shahangian A, Garcia DE, Cheng G. 2003. T3JAM, a novel protein that specifically interacts with TRAF3 and promotes the activation of JNK(1). FEBS Lett 553(3):403–407.

Dar AC, Dever TE, Sicheri F. 2005. Higher-order substrate recognition of eIF2alpha by the RNA-dependent protein kinase PKR. Cell 122(6):887–900.

Das S, Ward SV, Markle D, Samuel CE. 2004. DNA damage-binding proteins and heterogeneous nuclear ribonucleoprotein A1 function as constitutive KCS element components of the interferon-inducible RNA-dependent protein kinase promoter. J Biol Chem 279(8):7313–7321.

Das S, Ward SV, Tacke RS, Suske G, Samuel CE. 2006. Activation of the RNA-dependent protein kinase PKR promoter in the absence of interferon is dependent upon Sp proteins. J Biol Chem 281(6):3244–3253.

Davies CC, Mak TW, Young LS, Eliopoulos AG. 2005. TRAF6 is required for TRAF2-dependent CD40 signal transduction in nonhemopoietic cells. Mol Cell Biol 25(22):9806–9819.

De Ambrosis A, Casciano I, Croce M, Pagnan G, Radic L, Banelli B, Di Vinci A, Allemanni G, Tonini GP, Ponzoni M, Romani M, Ferrini S. 2007. An interferon-sensitive response element is involved in constitutive caspase-8 gene expression in neuroblastoma cells. Int J Cancer 120(1):39–47.

Deb A, Zamanian-Daryoush M, Xu Z, Kadereit S, Williams BR. 2001. Protein kinase PKR is required for platelet-derived growth factor signaling of c-fos gene expression via Erks and Stat3. EMBO J 20(10):2487–2496.

Dey M, Cao C, Dar AC, Tamura T, Ozato K, Sicheri F, Dever TE. 2005. Mechanistic link between PKR dimerization, autophosphorylation, and eIF2alpha substrate recognition. Cell 122(6):901–913.

Donze O, Jagus R, Koromilas AE, Hershey JW, Sonenberg N. 1995. Abrogation of translation initiation factor eIF-2 phosphorylation causes malignant transformation of NIH 3T3 cells. EMBO J 14(15):3828–3834.

Endo-Munoz L, Warby T, Harrich D, McMillan NA. 2005. Phosphorylation of HIV Tat by PKR increases interaction with TAR RNA and enhances transcription. Virol J 2:17.

Fasciano S, Hutchins B, Handy I, Patel RC. 2005. Identification of the heparin-binding domains of the interferon-induced protein kinase, PKR. FEBS J 272(6):1425–1439.

Fujii R, Okamoto M, Aratani S, Oishi T, Ohshima T, Taira K, Baba M, Fukamizu A, Nakajima T. 2001. A role of RNA helicase A in cis-acting transactivation response element-mediated transcriptional regulation of human immunodeficiency virus type 1. J Biol Chem 276(8):5445–5451.

Galabru J, Hovanessian A. 1987. Autophosphorylation of the protein kinase dependent on double-stranded RNA. J Biol Chem 262(32):15538–15544.

Garaigorta U, Chisari FV. 2009. Hepatitis C virus blocks interferon effector function by inducing protein kinase R phosphorylation. Cell Host Microbe 6(6):513–522.

Gelev V, Aktas H, Marintchev A, Ito T, Frueh D, Hemond M, Rovnyak D, Debus M, Hyberts S, Usheva A, Halperin J, Wagner G. 2006. Mapping of the auto-inhibitory interactions of protein kinase R by nuclear magnetic resonance. J Mol Biol 364(3):352–363.

George CX, Thomis DC, McCormack SJ, Svahn CM, Samuel CE. 1996. Characterization of the heparin-mediated activation of PKR, the interferon-inducible RNA-dependent protein kinase. Virology 221(1):180–188.

Gil J, Alcami J, Esteban M. 2000. Activation of NF-kappa B by the dsRNA-dependent protein kinase, PKR involves the I kappa B kinase complex. Oncogene 19(11):1369–1378.

Gil J, Garcia MA, Gomez-Puertas P, Guerra S, Rullas J, Nakano H, Alcami J, Esteban M. 2004. TRAF family proteins link PKR with NF-kappa B activation. Mol Cell Biol 24(10):4502–4512.

Goh KC, deVeer MJ, Williams BR. 2000. The protein kinase PKR is required for p38 MAPK activation and the innate immune response to bacterial endotoxin. EMBO J 19(16):4292–4297.

Guerra S, Lopez-Fernandez LA, Garcia MA, Zaballos A, Esteban M. 2006. Human gene profiling in response to the active protein kinase, interferon-induced serine/threonine protein kinase (PKR), in infected cells. Involvement of the transcription factor ATF-3 IN PKR-induced apoptosis. J Biol Chem 281(27):18734–18745.

Guo F, Cavener DR. 2007. The GCN2 eIF2alpha kinase regulates fatty-acid homeostasis in the liver during deprivation of an essential amino acid. Cell Metab 5(2):103–114.

Hallak LK, Collins PL, Knudson W, Peeples ME. 2000a. Iduronic acid-containing glycosaminoglycans on target cells are required for efficient respiratory syncytial virus infection. Virology 271(2):264–275.

Hallak LK, Spillmann D, Collins PL, Peeples ME. 2000b. Glycosaminoglycan sulfation requirements for respiratory syncytial virus infection. J Virol 74(22):10508–10513.

Harding HP, Zeng H, Zhang Y, Jungries R, Chung P, Plesken H, Sabatini DD, Ron D. 2001. Diabetes mellitus and exocrine pancreatic dysfunction in perk −/− mice reveals a role for translational control in secretory cell survival. Mol Cell 7(6): 1153–1163.

Hartman TR, Qian S, Bolinger C, Fernandez S, Schoenberg DR, Boris-Lawrie K. 2006. RNA helicase A is necessary for translation of selected messenger RNAs. Nat Struct Mol Biol 13(6):509–516.

Horng T, Barton GM, Medzhitov R. 2001. TIRAP: an adapter molecule in the Toll signaling pathway. Nat Immunol 2(9): 835–841.

Hovanessian AG, Galabru J. 1987. The double-stranded RNA-dependent protein kinase is also activated by heparin. Eur J Biochem 167(3):467–473.

Hsu LC, Park JM, Zhang K, Luo JL, Maeda S, Kaufman RJ, Eckmann L, Guiney DG, Karin M. 2004. The protein kinase PKR is required for macrophage apoptosis after activation of toll-like receptor 4. Nature 428(6980):341–345.

Huang X, Hutchins B, Patel RC. 2002. The C-terminal, third conserved motif of the protein activator PACT plays an essential role in the activation of double-stranded-RNA-dependent protein kinase (PKR). Biochem J 366(Pt 1):175–186.

Hugon J, Paquet C, Chang RC. 2009. Could PKR inhibition modulate human neurodegeneration? Expert Rev Neurother 9(10):1455–1457.

Ichikawa T, Nakao K, Nakata K, Yamashita M, Hamasaki K, Shigeno M, Abiru S, Ishikawa H, Ishii N, Eguchi K. 2002. Involvement of IL-1beta and IL-10 in IFN-alpha-mediated antiviral gene induction in human hepatoma cells. Biochem Biophys Res Commun 294(2):414–422.

Iordanov MS, Paranjape JM, Zhou A, Wong J, Williams BR, Meurs EF, Silverman RH, Magun BE. 2000. Activation of p38 mitogen-activated protein kinase and c-Jun NH(2)-terminal kinase by double-stranded RNA and encephalomyocarditis virus: involvement of RNase L, protein kinase R, and alternative pathways. Mol Cell Biol 20(2):617–627.

Isken O, Grassmann CW, Sarisky RT, Kann M, Zhang S, Grosse F, Kao PN, Behrens SE. 2003. Members of the NF90/NFAR protein group are involved in the life cycle of a positive-strand RNA virus. EMBO J 22(21):5655–5665.

Ito T, Yang M, May WS. 1999. RAX, a cellular activator for double-stranded RNA-dependent protein kinase during stress signaling. J Biol Chem 274(22):15427–15432.

Jammi NV, Beal PA. 2001. Phosphorylation of the RNA-dependent protein kinase regulates its RNA-binding activity. Nucleic Acids Res 29(14):3020–3029.

Jeang KT, Yedavalli V. 2006. Role of RNA helicases in HIV-1 replication. Nucleic Acids Res 34(15):4198–4205.

Joshi B, Cai AL, Keiper BD, Minich WB, Mendez R, Beach CM, Stepinski J, Stolarski R, Darzynkiewicz E, Rhoads RE. 1995. Phosphorylation of eukaryotic protein synthesis initiation factor 4E at Ser-209. J Biol Chem 270(24):14597–14603.

Kalali BN, Kollisch G, Mages J, Muller T, Bauer S, Wagner H, Ring J, Lang R, Mempel M, Ollert M. 2008. Double-stranded RNA induces an antiviral defense status in epidermal keratinocytes through TLR3-, PKR-, and MDA5/RIG-I-mediated differential signaling. J Immunol 181(4):2694–2704.

Koromilas AE, Roy S, Barber GN, Katze MG, Sonenberg N. 1992. Malignant transformation by a mutant of the IFN-inducible dsRNA-dependent protein kinase. Science 257(5077):1685–1689.

Kuhen KL, Samuel CE. 1997. Isolation of the interferon-inducible RNA-dependent protein kinase Pkr promoter and identification of a novel DNA element within the 5′-flanking region of human and mouse Pkr genes. Virology 227(1): 119–130.

Kuhen KL, Samuel CE. 1999. Mechanism of interferon action: functional characterization of positive and negative regulatory domains that modulate transcriptional activation of the human RNA-dependent protein kinase Pkr promoter. Virology 254(1):182–195.

Kumar A, Haque J, Lacoste J, Hiscott J, Williams BR. 1994. Double-stranded RNA-dependent protein kinase activates transcription factor NF-kappa B by phosphorylating I kappa B. Proc Natl Acad Sci U S A 91(14):6288–6292.

Kumar A, Yang YL, Flati V, Der S, Kadereit S, Deb A, Haque J, Reis L, Weissmann C, Williams BR. 1997. Deficient cytokine signaling in mouse embryo fibroblasts with a targeted deletion in the PKR gene: role of IRF-1 and NF-kappaB. EMBO J 16(2):406–416.

Lee E-S, Yoon C-H, Kim Y-S, Bae Y-S. 2007. The double-strand RNA-dependent protein kinase PKR plays a significant role in a sustained ER stress-induced apoptosis. FEBS Lett 581(22): 4325–4332.

Lee JH, Park EJ, Kim OS, Kim HY, Joe EH, Jou I. 2005. Double-stranded RNA-activated protein kinase is required for the LPS-induced activation of STAT1 inflammatory signaling in rat brain glial cells. Glia 50(1):66–79.

Li S, Peters GA, Ding K, Zhang X, Qin J, Sen GC. 2006. Molecular basis for PKR activation by PACT or dsRNA. Proc Natl Acad Sci U S A 103(26):10005–10010.

Li Z, Wolff KC, Samuel CE. 2010. RNA adenosine deaminase ADAR1 deficiency leads to increased activation of protein kinase PKR and reduced vesicular stomatitis virus growth following interferon treatment. Virology 396(2):316–322.

Manche L, Green SR, Schmedt C, Mathews MB. 1992. Interactions between double-stranded RNA regulators and the protein kinase DAI. Mol Cell Biol 12(11):5238–5248.

Meurs EF, Galabru J, Barber GN, Katze MG, Hovanessian AG. 1993. Tumor suppressor function of the interferon-induced double-stranded RNA-activated protein kinase. Proc Natl Acad Sci U S A 90(1):232–236.

Mittelstadt M, Frump A, Khuu T, Fowlkes V, Handy I, Patel CV, Patel RC. 2008. Interaction of human tRNA-dihydrouridine synthase-2 with interferon-induced protein kinase PKR. Nucleic Acids Res 36(3):998–1008.

Mok J, Kim PM, Lam HY, Piccirillo S, Zhou X, Jeschke GR, Sheridan DL, Parker SA, Desai V, Jwa M, Cameroni E, Niu H, Good M, Remenyi A, Ma JL, Sheu YJ, Sassi HE, Sopko R, Chan CS, De Virgilio C, Hollingsworth NM, Lim WA, Stern DF, Stillman B, Andrews BJ, Gerstein MB, Snyder M, Turk BE. 2010. Deciphering protein kinase specificity through large-scale analysis of yeast phosphorylation site motifs. Sci Signal 3(109):ra12.

Mounir Z, Krishnamoorthy JL, Robertson GP, Scheuner D, Kaufman RJ, Georgescu MM, Koromilas AE. 2009. Tumor suppression by PTEN requires the activation of the PKR-eIF2alpha phosphorylation pathway. Sci Signal 2(102):ra85.

Mundschau LJ, Faller DV. 1995. Platelet-derived growth factor signal transduction through the interferon-inducible kinase PKR. Immediate early gene induction. J Biol Chem 270(7): 3100–3106.

Munoz-Fontela C, Macip S, Martinez-Sobrido L, Brown L, Ashour J, Garcia-Sastre A, Lee SW, Aaronson SA. 2008. Transcriptional role of p53 in interferon-mediated antiviral immunity. J Exp Med 205(8):1929–1938.

Nakamura T, Furuhashi M, Li P, Cao H, Tuncman G, Sonenberg N, Gorgun CZ, Hotamisligil GS. 2010. Double-stranded RNA-dependent protein kinase links pathogen sensing with stress and metabolic homeostasis. Cell 140(3):338–348.

Nallagatla SR, Hwang J, Toroney R, Zheng X, Cameron CE, Bevilacqua PC. 2007. 5′-Triphosphate-dependent activation of PKR by RNAs with short stem-loops. Science 318(5855): 1455–1458.

Nanduri S, Rahman F, Williams BRG, Qin J. 2000. A dynamically tuned double-stranded RNA binding mechanism for the activation of antiviral kinase PKR. EMBO J 19(20):5567–5574.

Osman F, Jarrous N, Ben-Asouli Y, Kaempfer R. 1999. A cis-acting element in the 3′-untranslated region of human TNF-alpha mRNA renders splicing dependent on the activation of protein kinase PKR. Genes Dev 13(24):3280–3293.

Oyadomari S, Harding HP, Zhang Y, Oyadomari M, Ron D. 2008. Dephosphorylation of translation initiation factor 2alpha enhances glucose tolerance and attenuates hepatosteatosis in mice. Cell Metab 7(6):520–532.

Park H, Davies MV, Langland JO, Chang HW, Nam YS, Tartaglia J, Paoletti E, Jacobs BL, Kaufman RJ, Venkatesan S. 1994. TAR RNA-binding protein is an inhibitor of the interferon-induced protein kinase PKR. Proc Natl Acad Sci U S A 91(11): 4713–4717.

Parker LM, Fierro-Monti I, Mathews MB. 2001. Nuclear factor 90 is a substrate and regulator of the eukaryotic initiation factor 2 kinase double-stranded RNA-activated protein kinase. J Biol Chem 276(35):32522–32530.

Patel RC, Sen GC. 1998. PACT, a protein activator of the interferon-induced protein kinase, PKR. EMBO J 17(15):4379–4390.

Perkins DJ, Barber GN. 2004. Defects in translational regulation mediated by the alpha subunit of eukaryotic initiation factor 2 inhibit antiviral activity and facilitate the malignant transformation of human fibroblasts. Mol Cell Biol 24(5):2025–2040.

Peters GA, Hartmann R, Qin J, Sen GC. 2001. Modular structure of PACT: distinct domains for binding and activating PKR. Mol Cell Biol 21(6):1908–1920.

Peters GA, Seachrist DD, Keri RA, Sen GC. 2009. The double-stranded RNA-binding protein, PACT, is required for postnatal anterior pituitary proliferation. Proc Natl Acad Sci U S A 106(26):10696–10701.

Petryshyn R, Chen JJ, Danley L, Matts RL. 1996. Effect of interferon on protein translation during growth stages of 3T3 cells. Arch Biochem Biophys 326(2):290–297.

Proud CG. 2005. eIF2 and the control of cell physiology. Semin Cell Dev Biol 16(1):3–12.

Pullen SS, Miller HG, Everdeen DS, Dang TT, Crute JJ, Kehry MR. 1998. CD40-tumor necrosis factor receptor-associated factor (TRAF) interactions: regulation of CD40 signaling through multiple TRAF binding sites and TRAF hetero-oligomerization. Biochemistry 37(34):11836–11845.

Ramana CV, Grammatikakis N, Chernov M, Nguyen H, Goh KC, Williams BR, Stark GR. 2000. Regulation of c-myc expression by IFN-gamma through Stat1-dependent and -independent pathways. EMBO J 19(2):263–272.

Rayamajhi M, Humann J, Penheiter K, Andreasen K, Lenz LL. 2010. Induction of IFN-alphabeta enables Listeria monocytogenes to suppress macrophage activation by IFN-gamma. J Exp Med 207(2):327–337.

Romano PR, Garcia-Barrio MT, Zhang X, Wang Q, Taylor DR, Zhang F, Herring C, Mathews MB, Qin J, Hinnebusch AG. 1998. Autophosphorylation in the activation loop is required for full kinase activity *in vivo* of human and yeast eukaryotic initiation factor 2alpha kinases PKR and GCN2. Mol Cell Biol 18(4):2282–2297.

Rowe TM, Rizzi M, Hirose K, Peters GA, Sen GC. 2006. A role of the double-stranded RNA-binding protein PACT in mouse ear development and hearing. Proc Natl Acad Sci U S A 103(15):5823–5828.

Ruvolo PP, Gao F, Blalock WL, Deng X, May WS. 2001. Ceramide regulates protein synthesis by a novel mechanism involving the cellular PKR activator RAX. J Biol Chem 276(15): 11754–11758.

Ruvolo VR, Kurinna SM, Karanjeet KB, Schuster TF, Martelli AM, McCubrey JA, Ruvolo PP. 2008. PKR regulates B56 (alpha)-mediated BCL2 phosphatase activity in acute lymphoblastic leukemia-derived REH cells. J Biol Chem 283(51): 35474–35485.

Ryter JM, Schultz SC. 1998. Molecular basis of double-stranded RNA-protein interactions: structure of a dsRNA-binding domain complexed with dsRNA. EMBO J 17(24):7505–7513.

Sadler AJ, Latchoumanin O, Hawkes D, Mak J, Williams BR. 2009. An antiviral response directed by PKR phosphorylation of the RNA helicase A. PLoS Pathog 5(2):e1000311.

Sadler AJ, Williams BR. 2007. Structure and function of the protein kinase R. Curr Top Microbiol Immunol 316:253–292.

Saelens X, Kalai M, Vandenabeele P. 2001. Translation inhibition in apoptosis: caspase-dependent PKR activation and eIF2-alpha phosphorylation. J Biol Chem 276(45):41620–41628.

Salzberg S, Mandelboim M, Zalcberg M, Shainberg A, Mandelbaum M. 1995. Interruption of myogenesis by transforming growth factor beta 1 or EGTA inhibits expression and activity of the myogenic-associated (2′-5′) oligoadenylate synthetase and PKR. Exp Cell Res 219(1):223–232.

Silva AM, Whitmore M, Xu Z, Jiang Z, Li X, Williams BR. 2004. Protein kinase R (PKR) interacts with and activates mitogen-activated protein kinase kinase 6 (MKK6) in response to double-stranded RNA stimulation. J Biol Chem 279(36): 37670–37676.

Sondarva G, Kundu CN, Mehrotra S, Mishra R, Rangasamy V, Sathyanarayana P, Ray RS, Rana B, Rana A. 2010. TRAF2-MLK3 interaction is essential for TNF-alpha-induced MLK3 activation. Cell Res 20(1):89–98.

Spear PG, Shieh MT, Herold BC, WuDunn D, Koshy TI. 1992. Heparan sulfate glycosaminoglycans as primary cell surface receptors for herpes simplex virus. Adv Exp Med Biol 313: 341–353.

Su Q, Wang S, Baltzis D, Qu LK, Wong AH, Koromilas AE. 2006. Tyrosine phosphorylation acts as a molecular switch to full-scale activation of the eIF2alpha RNA-dependent protein kinase. Proc Natl Acad Sci U S A 103(1):63–68.

Takada Y, Ichikawa H, Pataer A, Swisher S, Aggarwal BB. 2007. Genetic deletion of PKR abrogates TNF-induced activation of IkappaBalpha kinase, JNK, Akt and cell proliferation but potentiates p44/p42 MAPK and p38 MAPK activation. Oncogene 26(8):1201–1212.

Takahashi K, Kawai T, Kumar H, Sato S, Yonehara S, Akira S. 2006. Roles of caspase-8 and caspase-10 in innate immune responses to double-stranded RNA. J Immunol 176(8):4520–4524.

Takaoka A, Hayakawa S, Yanai H, Stoiber D, Negishi H, Kikuchi H, Sasaki S, Imai K, Shibue T, Honda K, Taniguchi T. 2003. Integration of interferon-alpha/beta signalling to p53 responses in tumor suppression and antiviral defence. Nature 424(6948):516–523.

Tam CL, Hofbauer M, Towle CA. 2007. Requirement for protein kinase R in interleukin-1alpha-stimulated effects in cartilage. Biochem Pharmacol 74(11):1636–1641.

Tanaka H, Samuel CE. 1994. Mechanism of interferon action: structure of the mouse PKR gene encoding the interferon-inducible RNA-dependent protein kinase. Proc Natl Acad Sci U S A 91(17):7995–7999.

Tanaka H, Samuel CE. 2000. Mouse interferon-inducible RNA-dependent protein kinase Pkr gene: cloning and sequence of the 5′-flanking region and functional identification of the minimal inducible promoter. Gene 246(1–2):373–382.

Taylor DR, Lee SB, Romano PR, Marshak DR, Hinnebusch AG, Esteban M, Mathews MB. 1996. Autophosphorylation sites

participate in the activation of the double-stranded-RNA-activated protein kinase PKR. Mol Cell Biol 16(11):6295–6302.
Thomis DC, Samuel CE. 1992. Mechanism of interferon action: autoregulation of RNA-dependent P1/eIF-2 alpha protein kinase (PKR) expression in transfected mammalian cells. Proc Natl Acad Sci U S A 89(22):10837–10841.
Toth AM, Zhang P, Das S, George CX, Samuel CE. 2006. Interferon action and the double-stranded RNA-dependent enzymes ADAR1 adenosine deaminase and PKR protein kinase. Prog Nucleic Acid Res Mol Biol 81:369–434.
Tzatsos A, Kandror KV. 2006. Nutrients suppress phosphatidylinositol 3-kinase/Akt signaling via raptor-dependent mTOR-mediated insulin receptor substrate 1 phosphorylation. Mol Cell Biol 26(1):63–76.
Ueno M, Carvalheira JB, Tambascia RC, Bezerra RM, Amaral ME, Carneiro EM, Folli F, Franchini KG, Saad MJ. 2005. Regulation of insulin signalling by hyperinsulinaemia: role of IRS-1/2 serine phosphorylation and the mTOR/p70 S6K pathway. Diabetologia 48(3):506–518.
Vattem KM, Staschke KA, Wek RC. 2001. Mechanism of activation of the double-stranded-RNA-dependent protein kinase PKR: role of dimerization and cellular localization in the stimulation of PKR phosphorylation of eukaryotic initiation factor-2 (eIF2). Eur J Biochem 268(13):3674–3684.
Wang H, Ding B, Liu CJ, Ma XY, Deschamps S, Roe BA, Lengyel P. 2002. The increase in levels of interferon-inducible proteins p202a and p202b and RNA-dependent protein kinase (PKR) during myoblast differentiation is due to transactivation by MyoD: their tissue distribution in uninfected mice does not depend on interferons. J Interferon Cytokine Res 22(6):729–737.
Wang Y, Samuel CE. 2009. Adenosine deaminase ADAR1 increases gene expression at the translational level by decreasing protein kinase PKR-dependent eIF-2alpha phosphorylation. J Mol Biol 393(4):777–787.
Ward SV, Samuel CE. 2002. Regulation of the interferon-inducible PKR kinase gene: the KCS element is a constitutive promoter element that functions in concert with the interferon-stimulated response element. Virology 296(1):136–146.
Ward SV, Samuel CE. 2003. The PKR kinase promoter binds both Sp1 and Sp3, but only Sp3 functions as part of the interferon-inducible complex with ISGF-3 proteins. Virology 313(2):553–566.
Wek RC, Jiang HY, Anthony TG. 2006. Coping with stress: eIF2 kinases and translational control. Biochem Soc Trans 34(Pt 1):7–11.
Wong AH, Tam NW, Yang YL, Cuddihy AR, Li S, Kirchhoff S, Hauser H, Decker T, Koromilas AE. 1997. Physical association between STAT1 and the interferon-inducible protein kinase PKR and implications for interferon and double-stranded RNA signaling pathways. EMBO J 16(6):1291–1304.
Wu S, Kaufman RJ. 2004. trans-Autophosphorylation by the isolated kinase domain is not sufficient for dimerization or activation of the dsRNA-activated protein kinase PKR. Biochemistry 43(34):11027–11034.
Xu Z, Williams BR. 1998. Genomic features of human PKR: alternative splicing and a polymorphic CGG repeat in the 5′-untranslated region. J Interferon Cytokine Res 18(8):609–616.
Xu Z, Williams BR. 2000. The B56alpha regulatory subunit of protein phosphatase 2A is a target for regulation by double-stranded RNA-dependent protein kinase PKR. Mol Cell Biol 20(14):5285–5299.
Xue Y, Ren J, Gao X, Jin C, Wen L, Yao X. 2008. GPS 2.0, a tool to predict kinase-specific phosphorylation sites in hierarchy. Mol Cell Proteomics 7(9):1598–1608.
Yamashita M, Fatyol K, Jin C, Wang X, Liu Z, Zhang YE. 2008. TRAF6 mediates Smad-independent activation of JNK and p38 by TGF-beta. Mol Cell 31(6):918–924.
Yang YL, Reis LF, Pavlovic J, Aguzzi A, Schafer R, Kumar A, Williams BR, Aguet M, Weissmann C. 1995. Deficient signaling in mice devoid of double-stranded RNA-dependent protein kinase. EMBO J 14(24):6095–6106.
Yoon CH, Lee ES, Lim DS, Bae YS. 2009. PKR, a p53 target gene, plays a crucial role in the tumor-suppressor function of p53. Proc Natl Acad Sci U S A 106(19):7852–7857.
Zamanian-Daryoush M, Mogensen TH, DiDonato JA, Williams BR. 2000. NF-kappaB activation by double-stranded-RNA-activated protein kinase (PKR) is mediated through NF-kappaB-inducing kinase and IkappaB kinase. Mol Cell Biol 20(4):1278–1290.
Zhang F, Romano PR, Nagamura-Inoue T, Tian B, Dever TE, Mathews MB, Ozato K, Hinnebusch AG. 2001. Binding of double-stranded RNA to protein kinase PKR is required for dimerization and promotes critical autophosphorylation events in the activation loop. J Biol Chem 276(27):24946–24958.
Zhang P, Langland JO, Jacobs BL, Samuel CE. 2009. Protein kinase PKR-dependent activation of mitogen-activated protein kinases occurs through mitochondrial adapter IPS-1 and is antagonized by vaccinia virus E3L. J Virol 83(11):5718–5725.
Zhang P, Samuel CE. 2008. Induction of protein kinase PKR-dependent activation of interferon regulatory factor 3 by vaccinia virus occurs through adapter IPS-1 signaling. J Biol Chem 283(50):34580–34587.
Zheng JC, Huang Y, Tang K, Cui M, Niemann D, Lopez A, Morgello S, Chen S. 2008. HIV-1-infected and/or immune-activated macrophages regulate astrocyte CXCL8 production through IL-1beta and TNF-alpha: involvement of mitogen-activated protein kinases and protein kinase R. J Neuroimmunol 200(1–2):100–110.

Address correspondence to:
Dr. Anthony Sadler
Centre for Cancer Research
Monash Institute of Medical Research
P.O. Box 5418
Clayton 3168
Australia

Received 6 August 2010/Accepted 6 August 2010

Specialty Feeds

3150 Great Eastern Hwy
Glen Forrest
Western Australia 6071
p: +61 8 9298 8111
F: +61 8 9298 8700
Email: info@specialtyfeeds.com

Diet

Meat Free Rat and Mouse Diet

A fixed formulation diet for Laboratory Rats and Mice fortified with vitamins and minerals to meet the requirements of breeding animals after the diet is autoclaved or irradiated.

- Minor modifications were made to this fixed formulation on 27 Jan 2009. Please contact us for details.
- All nutritional parameters of this diet meet or exceed the NRC guidelines for Rats and Mice.
- The diet has been designed as a general ration for breeding and early growth in all rat and mouse strains. The total fat content has been deliberately kept low at around 5%, to maximise the long term breeding performance of most strains.
- The formulation is designed to be fed ad-lib to rodents of all ages. There is some indication that growth performance in a minority of strains can be improved by increasing dietary energy (fat content). BalbC mice, DA rats and some of the modified strains appear to be most susceptible to this problem. Please contact us if you are concerned about this issue.
- Mammalian meals have been excluded from the diet, however the diet does contain fish meal. We have formulated totally vegetarian diets, and maintained colonies for some time on these diets. Please contact us if you require such a diet.
- The feed is manufactured in a cylindrical form with a diameter of around 12 mm, length is variable from 10 mm to 30 mm. We have found that this form is ideal for overhead hopper feeding, maximising the ease of handling whilst minimising fines formation and the risk of bridging in the feed hopper. Pellet strength has been kept lower than conventional pelletised diets. While this leads to a slight increase in transit and storage damage to the diet (fines generation), we have found that juvenile mice often have a lower feed intake on harder pellets.
- The diet is packed in permeable bags suitable for direct loading into an autoclave. It is recommended that the diet be autoclaved at 120^{O} C for 20 minutes with a post autoclaving vacuum drying cycle. Some clumping of the diet can be expected, but the diet clumps can usually be easily broken. Modifying the drying time to leave some residual moisture in the diet can minimise the clumping. Do not autoclave at 135^{0} C as this will result in significant clumping that will be difficult to break.

Calculated Nutritional Parameters

Protein	20.00%
Total Fat	4.80%
Crude Fibre	4.80%
Acid Detergent Fibre	7.60%
Neutral Detergent Fibre	16.40%
Total Carbohydrate	59.40%
Digestible Energy	14.0 MJ / Kg
% Total Calculated Energy From Protein	23.00%
% Total Calculated Energy From Lipids	12.00%

Ingredients

A Fixed formula ration using the following ingredients:
Wheat, barley, Lupins, Soya meal, Fish meal, Mixed vegetable oils, Canola oil, Salt, Calcium carbonate, Dicalcium phosphate, Magnesium oxide, and a Vitamin and trace mineral premix.

Added Vitamins

Vitamin A (Retinol)	10 000 IU/Kg
Vitamin D (Cholecalciferol)	2 000 IU/Kg
Vitamin E (a Tocopherol acetate)	100 mg/Kg
Vitamin K (Menadione)	20 mg/Kg
Vitamin B1 (Thiamine)	80 mg/Kg
Vitamin B2 (Riboflavin)	30 mg/Kg
Niacin (Nicotinic acid)	100 mg/Kg
Vitamin B6 (Pryridoxine)	25 mg/Kg
Calcium Pantothenate	50 mg/Kg
Biotin	300 ug/Kg
Folic Acid	5.0 mg/Kg
Vitamin B12 (Cyancobalamin)	150 ug/Kg

Diet Form and Features

- Cereal grain base diet. 12 mm diameter pellets.
- Pack size 10 and 20 Kg Bags.
- Diet suitable for irradiation, also suitable for autoclave.
- Lead time 2 weeks

Added Trace Minerals

Magnesium	100 mg/Kg
Iron	70 mg/Kg
Copper	16 mg/Kg
Iodine	0.5 mg/Kg
Manganese	70 mg/Kg
Zinc	60 mg/Kg
Molybdenum	0.5 mg/Kg
Selenium	0.1 mg/Kg

Calculated Amino Acids

Valine	0.87%
Leucine	1.40%
Isoleucine	0.80%
Threonine	0.70%
Methionine	0.30%
Cystine	0.30%
Lysine	0.90%
Phenylanine	0.90%
Tyrosine	0.50%
Tryptophan	0.20%
Histidine	0.53%

Calculated Total Minerals	
Calcium	0.80%
Phosphorous	0.70%
Magnesium	0.20%
Sodium	0.18%
Potassium	0.82%
Sulphur	0.20%
Iron	200 mg/Kg
Copper	23 mg/Kg
Iodine	0.5 mg/Kg
Manganese	104 mg/Kg
Cobalt	0.7 mg/Kg
Zinc	90 mg/Kg
Molybdenum	1.2 mg/Kg
Selenium	0.4 mg/Kg
Cadmium	0.05 mg/Kg

Calculated Total Vitamins	
Vitamin A (Retinol)	10 950 IU/Kg
Vitamin D (Cholecalciferol)	2 000 IU/Kg
Vitamin E (a Tocopherol acetate)	110 mg/Kg
Vitamin K (Menadione)	20 mg/Kg
Vitamin C (Ascorbic acid)	No data
Vitamin B1 (Thiamine)	80 mg/Kg
Vitamin B2 (Riboflavin)	30 mg/Kg
Niacin (Nicotinic acid)	145 mg/Kg
Vitamin B6 (Pryridoxine)	28 mg/Kg
Pantothenic Acid	60 mg/Kg
Biotin	410 ug/Kg
Folic Acid	5 mg/Kg
Inositol	No data
Vitamin B12 (Cyancobalamin)	150 ug/Kg
Choline	1 640 mg/Kg

Calculated Fatty Acid Composition	
Myristic Acid 14:0	0.03%
Palmitic Acid 16:0	0.50%
Stearic Acid 18:0	0.14%
Palmitoleic Acid 16:1	0.01%
Oleic Acid 18:1	1.90%
Gadoleic Acid 20:1	0.03%
Linoleic Acid 18:2 n6	1.30%
a Linolenic Acid 18:3 n3	0.30%
Arachadonic Acid 20:4 n6	0.01%
EPA 20:5 n3	0.02%
DHA 22:6 n3	0.05%
Total n3	0.37%
Total n6	1.31%
Total Mono Unsaturated Fats	2.00%
Total Polyunsaturated Fats	1.77%
Total Saturated Fats	0.74%

Calculated data uses information from typical raw material composition. It could be expected that individual batches of diet will vary from this figure. **Diet post treatment by irradiation or auto clave could change these parameters**.

We are happy to provide full calculated nutritional information for all of our products, however we would like to emphasise that these diets have been specifically designed for manufacture by Specialty Feeds.

Specialty Feeds

3150 Great Eastern Hwy
Glen Forrest
Western Australia 6071
p: +61 8 9298 8111
F: +61 8 9298 8700
Email: info@specialtyfeeds.com

Diet SF00-219 — 22% Fat, 0.15% Cholesterol Semi-Pure Rodent Diet

A semi-pure high fat diet formulation for laboratory rats and mice based formulated to mimic a ”Western fast food diet”. This diet was originally formulated to be equivalent to *Harlan Teklad* TD88137 or *Research Diets* Western Diet D12079B. Some modifications have been made to the original formulation to suit locally available raw materials.

- This Diet was developed to generate arteriosclerotic lesions in a range of susceptible mice strains.

Calculated Nutritional Parameters

Protein	19.0%
Total Fat	21.0%
Crude Fibre	4.7%
AD Fibre	4.7%
Digestible Energy	19.4 MJ / Kg
% Total calculated digestible energy from lipids	40.0%
% Total calculated digestible energy from protein	17.0%

Diet Form and Features

- Semi pure high fat diet. 12 mm diameter pellets.
- Pack size 1.5 Kg trays, vacuum packed in oxygen impermeable plastic bags, under nitrogen. Bags are packed into cardboard cartons to protect them during transit. Smaller pack quantity on request.
- Diet suitable for irradiation but not suitable for autoclave.
- Lead time 2 weeks for non-irradiation or 4 weeks for irradiation.

Ingredients

Casein (Acid)	195 g/Kg
Sucrose	341 g/Kg
Clarified Butter (Ghee)	210 g/Kg
Cellulose	50 g/Kg
Wheat Starch	154 g/Kg
DL Methionine	3.0 g/Kg
Calcium Carbonate	17.1 g/Kg
Sodium Chloride	2.6 g/Kg
AIN93 Trace Minerals	1.4 g/Kg
Potassium Citrate	2.6 g/Kg
Potassium Dihydrogen Phosphate	6.9 g/Kg
Potassium Sulphate	1.6 g/Kg
Choline Chloride (75%)	2.5 g/Kg
SF00-219 Vitamins	10 g/Kg
Cholesterol	1.5 g/Kg
Oxicap E2	0.04 g/Kg

Calculated Amino Acids	
Valine	1.20%
Leucine	1.80%
Isoleucine	0.80%
Threonine	0.80%
Methionine	0.80%
Cystine	0.06%
Lysine	1.50%
Phenylanine	1.00%
Tyrosine	1.00%
Tryptophan	0.30%
Histidine	0.59%

Calculated Total Minerals	
Calcium	0.60%
Phosphorous	0.30%
Magnesium	0.10%
Sodium	0.12%
Chloride	0.16%
Potassium	0.40%
Sulphur	0.23%
Iron	80 mg/Kg
Copper	7.0 mg/Kg
Iodine	0.2 mg/Kg
Manganese	20 mg/Kg
Cobalt	No data
Zinc	52 mg/Kg
Molybdenum	0.15 mg/Kg
Selenium	0.3 mg/Kg
Cadmium	No data
Chromium	1.0 mg/Kg
Fluoride	1.0 mg/Kg
Lithium	0.1 mg/Kg
Boron	2.3 mg/Kg
Nickel	0.5 mg/Kg
Vanadium	0.1 mg/Kg

Calculated Total Vitamins	
Vitamin A (Retinol)	11 650 IU/Kg
Vitamin D (Cholecalciferol)	1 100 IU/Kg
Vitamin E (a Tocopherol acetate)	64 mg/Kg
Vitamin K (Menadione)	12.5 mg/Kg
Vitamin C (Ascorbic acid)	700 mg/Kg
Vitamin B1 (Thiamine)	11 mg/Kg
Vitamin B2 (Riboflavin)	11 mg/Kg
Niacin (Nicotinic acid)	50 mg/Kg
Vitamin B6 (Pryridoxine)	11 mg/Kg
Pantothenic Acid	34 mg/Kg
Biotin	200 ug/Kg
Folic Acid	1 mg/Kg
Inositol	55 mg/Kg
Vitamin B12 (Cyancobalamin)	18 ug/Kg
Choline	3 860 mg/Kg

Calculated Fatty Acid Composition	
Saturated Fats C12:0 or less	1.80%
Myristic Acid 14:0	2.60%
Palmitic Acid 16:0	7.00%
Stearic Acid 18:0	2.40%
Palmitoleic Acid 16:1	0.40%
Oleic Acid 18:1	5.50%
Gadoleic Acid 20:1	No data
Linoleic Acid 18:2 n6	0.40%
a Linolenic Acid 18:3 n3	0.20%
Arachadonic Acid 20:4 n6	Trace
Total n3	0.35%
Total n6	0.41%
Cholesterol	0.15%
Total Mono Unsaturated Fats	6.23%
Total Polyunsaturated Fats	0.77%
Total Saturated Fats	13.99%

Calculated data uses information from typical raw material composition. **Diet post treatment by irradiation or auto clave could change these parameters**. It could be expected that individual batches of diet will vary from this figure. We are happy to provide full calculated nutritional information for all of our products, however we would like to emphasise that these diets have been specifically designed for manufacture by Specialty Feeds.